Hull York Medical School (HYMS)

Deposit of Thesis in University libraries (PhD, MD, MPhil, MSc by Thesis) for examination

Name	Benjamin Spurgeon	Degree	PhD Medical Sciences

Department/ Centre	HYMS Centre for Cardiovascular and Metabolic Research

Thesis Title	Phosphoproteomic Analysis of Platelet Signalling Cascades by Flow Cytometry

I hereby give consent that copies of my thesis, if accepted for the degree specified above by The Hull York Medical School, will be deposited in libraries and digital repositories of the University of Hull and the University of York. I understand that copies of my thesis will at the discretion of the Universities be made available for public access as follows:

1. the paper copy shall be available for consultation, interlibrary loans and photocopying
2. the electronic copy shall be made available for access by any person or institution via the world wide web.

Signature (please type your full name in the signature box for electronic submission)	Benjamin Spurgeon	Date	27/02/15

If in special circumstances, the author wishes to withhold consent for a period of not more than five years from the date of the degree being awarded, and if for similar reasons he or she does not wish details of the thesis to be presented via the University Library's catalogues or repository or forwarded to any indexing or abstracting organisation, he or she should complete and sign sections 1 and 2 below, as appropriate.

Section 1

I wish the thesis to be withheld until:	
Please specify the reason why the thesis should be withheld:	

Signature (please type your full name in the signature box for electronic submission)		Date	

Section 2

I further wish that full details of the title and subject of my thesis are not to be presented via the University Library's catalogue or repository or forwarded to any indexing or abstracting organisation until:	
Please specify the reason why the thesis should be withheld:	

Signature (please type your full name in the signature box for electronic submission)		Date	

Please return this form to elaine.brookes@hyms.ac.uk. If this form is not returned to HYMS with the thesis, it will be assumed that the author consents to the thesis being made available, fully catalogued and details noted to any appropriate indexing or abstracting organisations.

Phosphoproteomic Analysis of Platelet Signalling Cascades by Flow Cytometry

Benjamin E.J. Spurgeon

PhD Medical Sciences

The University of Hull and The University of York

Hull York Medical School

October 2014

Abstract

The activation of blood platelets is a critical haemostatic response that serves to prevent haemorrhage, but unregulated platelet activation is associated with arterial thrombosis. Endothelial-derived inhibitors prostacyclin (PGI_2) and nitric oxide (NO) activate protein kinase-mediated signalling cascades to regulate platelet function and prevent vascular thrombosis. These signalling cascades involve a number of complex protein phosphorylation reactions, which regulate different aspects of platelet function. Dissecting the signalling events that regulate platelet function could facilitate the development of novel antiplatelet agents. Intraplatelet protein phosphorylation is commonly measured by immunoblotting, which is not conducive to whole blood analysis and therefore may not provide an accurate representation of signalling events in a (patho)physiological context. Therefore, the major aim of this thesis was to develop methodologies that could examine platelet signalling events in a more physiological context. In particular, we wanted to develop methodologies that could evaluate the ability of PGI_2 to modulate blood platelet activity. Using whole blood flow cytometry, PGI_2 was found to inhibit platelet fibrinogen binding and P-selectin expression, two independent markers of platelet activation. The inhibition of platelet function by PGI_2 corresponded with increased phosphorylation of proteins known to be targeted by PGI_2-mediated signalling cascades including vasodilator-stimulated phosphoprotein (VASP). In the next series of experiments, we developed an assay to evaluate these signalling events in whole blood. This phosphoflow assay was sensitive enough to accurately and reproducibly detect subtle dose- and time-dependent changes in protein

phosphorylation in whole blood that were consistent with immunoblotting protocols with washed platelets. The application of fluorescent barcoding protocols to this assay enabled the simultaneous staining and acquisition of 24-96 samples in a single analysis tube. To exploit the high-throughput nature of the method and demonstrate its value as a drug discovery platform, we screened a library of 70 prostaglandins for their ability to stimulate intraplatelet VASP phosphorylation. The screen revealed three previously uncharacterised molecules that stimulated cAMP formation, induced VASP phosphorylation, and inhibited platelet aggregation. Because whole blood samples could be processed after cold storage, the method could be performed on samples obtained at remote locations such as clinical sites. To this end, we showed that the method could be used to measure signalling events in patients with polycystic ovary syndrome (PCOS), an endocrine disorder associated with platelet dysfunction. We envisage that the method will be useful for basic scientists, clinicians, and pharmacologists seeking novel therapies.

Publications

AYE, M. M., KILPATRICK, E. S., ABURIMA, A., WRAITH, K. S., MAGWENZI, S., SPURGEON, B., RIGBY, A. S., SANDEMAN, D., NASEEM, K. M. & ATKIN, S. L. 2014. Acute Hypertriglyceridemia Induces Platelet Hyperactivity That is Not Attenuated by Insulin in Polycystic Ovary Syndrome. *Journal of the American Heart Association,* 3**,** e000706.

SPURGEON, B. E., ABURIMA, A., OBERPRIELER, N. G., TASKÉN, K. & NASEEM, K. M. 2014. Multiplexed Phosphospecific Flow Cytometry Enables Large-scale Signaling Profiling and Drug Screening in Blood Platelets. *Journal of Thrombosis and Haemostasis,* 12**,** 1733-1743.

Oral Presentations

SPURGEON, B. 2013. *Phosphospecific flow cytometry enables large-scale signalling profiling and compound screening in human platelets*. 15th UK Platelet Group Meeting, 13 September, Birmingham, UK.

Poster Presentations

SPURGEON, B. 2013. *Phosphospecific flow cytometry enables large-scale signalling profiling and compound screening in human platelets*. XXIV Congress of the International Society on Thrombosis and Haemostasis, 3 July, Amsterdam, Netherlands.

Contents

Figures

General Introduction

Methods

Analysis of Platelet Function

Flow Cytometric Analysis of Platelet Signalling Events

Pharmacological and Clinical Applications of Phosphoflow Cytometry

Appendix

Tables

General Introduction

Flow Cytometric Analysis of Platelet Signalling Events

Pharmacological and Clinical Applications of Phosphoflow Cytometry

Appendix

Abbreviations

ABP _____Actin-binding protein

AC _____ Adenylyl cyclase

ADP _____ Adenosine diphosphate

AKAP_____A kinase anchoring protein

AMPK _____ AMP-activated protein kinase

ATP _____ Adenosine triphosphate

BSA _____Bovine serum albumin

CaM _____ Calmodulin

cAMP_____Cyclic adenosine monophosphate

cGMP_____Cyclic guanosine monophosphate

COX_____Cyclooxygenase

CRP _____ Collagen-related peptide

DAG_____Diacylglycerol

DTS _____ Dense tubular system

EC$_{50}$_____Half-maximal effective concentration

ECL _____Enhanced chemiluminescence

EDTA_____ Ethylenediaminetetraacetic acid

EIA_____Enzyme immunoassay

eNOS _____ Endothelial nitric oxide synthase

FACS _____ Fluorescence-activated cell sorter

FCB _____ Fluorescent cell barcoding

GAP _____ GTPase activating protein

GP _____ Glycoprotein

GPCR _____ G protein-coupled receptor

GDP _____ Guanosine diphosphate

GEF _____ Guanine nucleotide exchange factor

GKIP _____ G kinase interacting protein

GSK-3 _____ Glycogen synthase kinase-3

GSNO _____ S-nitrosoglutathione

GTP _____ Guanosine triphosphate

HRP _____ Horseradish peroxidase

HSP _____ Heat shock protein

IC$_{50}$ _____ Half-maximal inhibitory concentration

IP$_3$ _____ Inositol triphosphate

IRAG _____ IP$_3$ receptor-associated cGMP kinase substrate

ITAM _____ Immunoreceptor tyrosine-based activation motif

MFI _____ Median fluorescence intensity

MLC	Myosin light chain
MLCP	Myosin light chain phosphatase
NO	Nitric oxide
OCS	Open canalicular system
PAGE	Polyacrylamide gel electrophoresis
PAR	Protease-activated receptor
PBS	Phosphate buffered saline
PCOS	Polycystic ovary syndrome
PDE	Phosphodiesterase
PFA	Paraformaldehyde
PG	Prostaglandin
PGI_2	Prostacyclin
PI3-K	Phosphoinositide 3-kinase
PKA	Protein kinase A
PKB	Protein kinase B
PKC	Protein kinase C
PKG	Protein kinase G
PLC	Phospholipase C
PSGL-1	P-selectin glycoprotein ligand-1

PVDF _____ Polyvinylidene fluoride

RIAM _____ Rap 1-B interacting adapter molecule

RGS2 _____ Regulator of G-protein signalling 2

SDS _____Sodium dodecyl sulfate

sGC _____Soluble guanylyl cyclase

TRAP _____ Thrombin receptor activating peptide

TRPC _____ Transient receptor potential canonical

TXA$_2$ _____ Thromboxane A$_2$

VASP _____ Vasodilator-stimulated phosphoprotein

VEGF _____ Vascular endothelial growth factor

vWF _____ von Willebrand factor

Author's Declaration

I confirm that this work is original and that if any passage(s) or diagram(s) have been copied from academic papers, books, the internet or any other sources these are clearly identified by the use of quotation marks and the reference(s) is fully cited. I certify that, other than where indicated, this is my own work and does not breach the regulations of HYMS, the University of Hull or the University of York regarding plagiarism or academic conduct in examinations. I have read the HYMS Code of Practice on Academic Misconduct, and state that this piece of work is my own and does not contain any unacknowledged work from any other sources. I confirm that any patient information obtained to produce this piece of work has been appropriately anonymised.

Acknowledgements

First and foremost, I would like to thank Prof. Khalid Naseem for giving me the opportunity to work on this project and for providing excellent supervision throughout. I would like to acknowledge my co-supervisor Prof. Stephen Atkin and the funding provided by HYMS. I also acknowledge colleagues past and present including Dr. Thozhukat Sathyapalan and his research team at Hull Royal Infirmary for supporting the clinical work and the many members of the Naseem lab who have offered invaluable guidance throughout my project including the post-docs Dr. Simba Magwenzi, Dr. Ahmed Aburima, Dr. Zaher Raslan, and Dr. Katie Wraith, and the PhD students Jonathan Wake, Sreemoti Banerjee, Casey Woodward, Arti Trivedi, and Berto Law. Last but not least, I would like to thank the blood donors without whom this work would not have been possible.

General Introduction

1.1 Introduction

Haemostasis is an important physiological process that maintains the fluidity of blood within the vascular system. A number of mechanisms have evolved to maintain haemostasis in healthy vasculature. Vascular endothelium lines the entire cardiovascular system and separates blood from thrombogenic factors that lie within the vascular wall. Circulating blood platelets are central to the haemostasis. They circulate in close contact with the endothelium, but do not adhere to the vessel or to one another under normal physiological conditions. Damage to the vasculature exposes the subendothelium to flowing blood and stimulates a rapid haemostatic response that serves to prevent haemorrhage. This begins with the adherence and activation of platelets, although effective haemostasis also requires the concerted actions of plasma coagulation factors to form a haemostatic plug that prevents blood loss (Heemskerk et al., 2002).

The shear stress induced by flowing blood pushes small platelets into close proximity with the vascular endothelium to ensure the rapid recruitment of platelets to sites of damage and allow the efficient regulation of platelet function by the vessel wall. Indeed, the vascular endothelium is an active antithrombotic surface that secretes protective factors such as prostacyclin (PGI_2) and nitric oxide (NO), which inhibit platelet activation through distinct biochemical mechanisms (Schwarz et al., 2001). Pathological conditions can attenuate the antithrombotic properties of the vasculature endothelium (Ruggeri, 2002) while platelets themselves can become resistant to the

endothelial-derived inhibitors PGI_2 and NO (Van Geet et al., 2009, Chirkov and Horowitz, 2007). Endothelial and/or platelet defects can alter the balance of normal haemostasis and cause thrombosis, which describes the process of pathological clot formation. Since unregulated platelet activation can predispose serious clinical events such as myocardial infarction and stroke (Ruggeri, 2002), it is critical to increase our understanding of the mechanisms that drive platelet function.

1.2 The formation of blood platelets

Platelets are small anucleate cells (2-4 µM diameter) that circulate for approximately 10 days in the normal bloodstream (Kaushansky, 2005). Low platelet counts, or thrombocytopenias, are associated with pathological bleeding while high platelet counts can cause adverse cardiovascular events (Thaulow et al., 1991). To maintain a normal platelet count (150000-400000 cells/µL), an adult must produce approximately 10^{11} platelets per day (Kaushansky, 2005). The acidic peptide thrombopoietin stimulates platelet formation from precursor cells called megakaryocytes, which reside in the bone marrow (Kaushansky, 1995).

During megakaryocyte maturation, platelet-specific proteins such as von Willebrand factor (vWF) and P-selectin are synthesised and sent to the cell surface while plasma proteins such as fibrinogen are internalised and packaged into platelet-specific granules (Heijnen et al., 1998, Handagama et al., 1987). Mature megakaryocytes contain an expansive demarcation membrane that results from invagination of the plasma membrane (Patel et

al., 2005). Demarcation membranes are laden with essential organelles and platelet-specific glycoproteins (Debili et al., 1990). These membranes elongate to form pseudopodial extensions called proplatelets (Patel et al., 2005). Motor proteins transport organelles and platelet-specific granules along cytoskeletal tracks to proplatelet tips where nascent platelets assemble (Richardson et al., 2005). These proplatelet tips extend through vascular membranes and release platelets into the bloodstream (Patel et al., 2005). The exact mechanism by which platelets are liberated from proplatelets remains undetermined.

1.3 The structure of blood platelets

Platelets circulate as quiescent discoid cells but undergo radical shape change in response to haemostatic agonists such as collagen and vWF (Yuan et al., 1999). Activated platelets emit irregular membrane protrusions called filopodia and lamellipodia, which facilitate adhesion and aggregation at the site of haemorrhage (Figure 1.1) (Jackson, 2007).
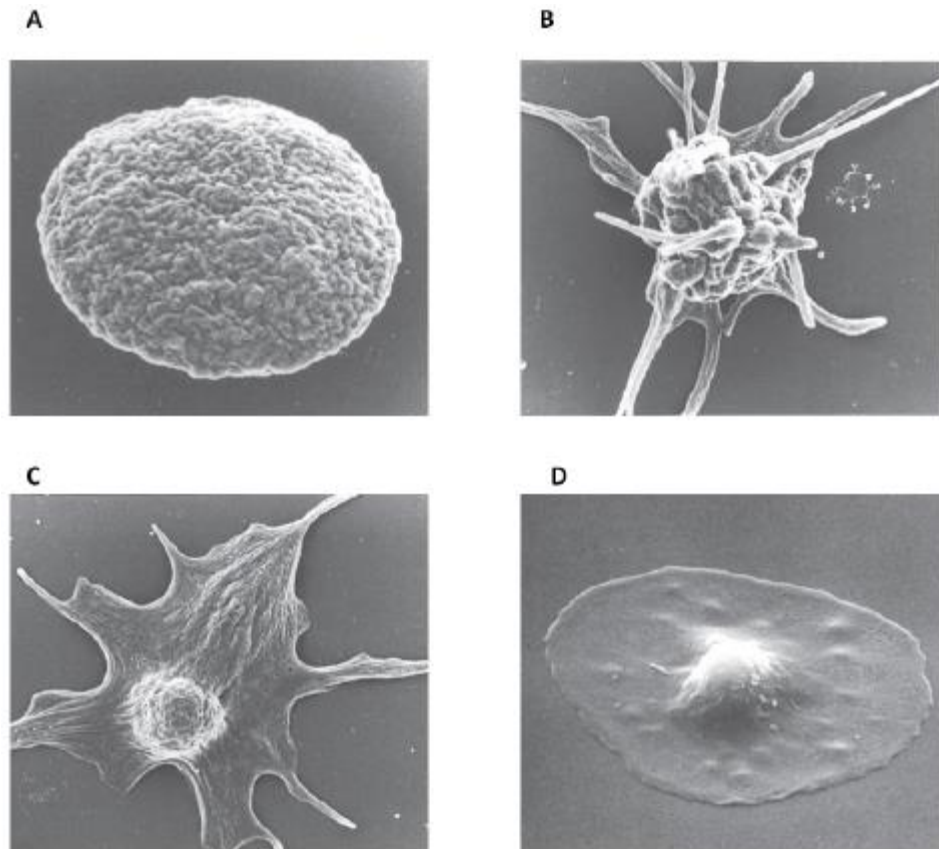
Figure 1.1. Electron microscope images of platelet structure. (**A**) Quiescent platelets circulate as discoid cells with wrinkled surfaces that result from complex membrane invaginations. (**B**) Platelets extend filopodia and lamellipodia in the early stages of activation. (**C**) The wrinkled surface disappears as the cell spreads among its lamellipodia into (**D**) a fully spread platelet (White, 2012).

1.3.1 Platelet membrane

The outermost layer of the platelet surface, called the glycocalyx, contains receptors that facilitate adhesion, aggregation, and coagulation (Hartwig, 2006). The glycocalyx sits on a lipid bilayer, which contains an extensive network of membrane invaginations known as the open canalicular system (OCS). The OCS serves as a conduit for the uptake and transfer of particles

to platelet storage granules (White, 1970) and represents a membrane reservoir that evaginates to facilitate platelet spreading and filopodia formation (Hartwig, 2002). The cytoplasmic side of the platelet membrane associates with filamentous proteins. These proteins are thought to interact with the cytoplasmic domains of transmembrane receptors and regulate the biochemical signalling processes that drive platelet activation (White, 2012). These filamentous proteins comprise the platelet cytoskeleton, which maintains the discoid shape of quiescent platelets and drives the morphologic changes that are required for adhesion and aggregation (Hartwig and DeSisto, 1991).

1.3.2 Platelet cytoskeleton

The cytoplasmic side of the platelet membrane is supported by a series of interconnecting spectrin filaments, which bind actin to form an expansive cross-linked structure that regulates platelet function (Hartwig, 2012). Actin filaments bind myosin to create an arrowhead structure with membrane-oriented barbed ends, which elongate by addition of actin monomers and actin-profilin complexes (Pollard et al., 2000). Actin polymerisation is limited by the availability of free barbed ends, which are capped by gelsolin in quiescent platelets. Gelsolin can be removed by phosphoinositides, which are synthesised in response to haemostatic agonists such as thrombin (Hartwig et al., 1995). In addition to gelsolin, actin-binding proteins such as Arp2/3, capZ, and thymosin-β4 interact with barbed ends and regulate actin filament elongation (Pollard et al., 2000). Importantly, this elongation process

provides a mechanical force required to extend lamellipodia (Tilney et al., 1981). While the cytoskeleton drives morphologic alterations, it can also sequester and localise kinases, phosphatases, and GTPases to regulate the magnitude of signalling events (Diviani and Scott, 2001, Kolch, 2005).

1.3.3 Platelet cytosol

The platelet cytosol is a glycogen-rich domain that contains mitochondria and a dense tubular system, which regulates platelet activation by sequestering and releasing calcium (Hartwig, 2002). In addition, the cytosol contains a number of distinct granular organelles, which contain membrane proteins and soluble cargo (Table 1.1). Upon platelet activation, these granules fuse with the platelet membrane and release their contents into the extracellular space (Flaumenhaft, 2003). Alpha granules release growth factors such as platelet-derived growth factor and chemokines such as platelet factor 4 that promote wound healing and angiogenesis as well as factors involved in coagulation such as factor V, fibrinogen, and vWF. By contrast, dense granules release substances such as adenine nucleotides that promote the recruitment and activation of additional platelets (Hartwig, 2002). While numerous kinases have been implicated in the platelet release reaction (Yoshioka et al., 2001), it is cytoskeletal reorganisation that facilitates the membrane fusion events that mediate granule secretion (Flaumenhaft et al., 2005). Indeed, the mechanical force that accompanies cytoskeletal rearrangement drives granules to the centre of the platelet where they are ideally positioned to fuse with the OCS (Stenberg et al., 1984).

Table 1.1. Important platelet granule contents.

Alpha granules	Dense granules
Factor V	ADP
Fibrinogen	ATP
Platelet-derived growth factor	Calcium
Platelet factor 4	GTP
P-selectin	Magnesium
Thrombospondin	Potassium
vWF	Serotonin

1.4 Role of platelet function in haemostasis

1.4.1 Platelet adhesion

Platelets express a variety of surface receptors that mediate their adhesion to the subendothelial matrix. The subendothelium is exposed by injury or the rupture of atherosclerotic plaques and contains proteins such as collagen that support the adhesion and activation of platelets. In the early phase of haemostasis, the plasma protein vWF binds to collagen and undergoes a conformational change that enables it to bind the GPIb receptor complex and initiate transient tethering and rolling on the subendothelium (Ruggeri and Mendolicchio, 2007). The transition from rolling to stable adhesion requires the cooperation of integrin $\alpha_2\beta_1$ and GPVI, which bind subendothelial collagen at the site of haemorrhage (Nieswandt and Watson, 2003). The subsequent activation of G protein-coupled receptors (GPCRs) and

interactions between fibrinogen and integrin αIIbβ3 result in platelet aggregation and the formation of a stable haemostatic plug (Figure 1.2) (Bennett and Vilaire, 1979). The complex and dynamic process of platelet activation is driven by intracellular protein kinases, which associate with platelet surface receptors and transmit phosphorylation-based signals to distinct cellular compartments. In platelets, kinase signalling cascades trigger a variety of functional responses including cytoskeletal reorganisation, spreading, and granule secretion (Gibbins, 2004).
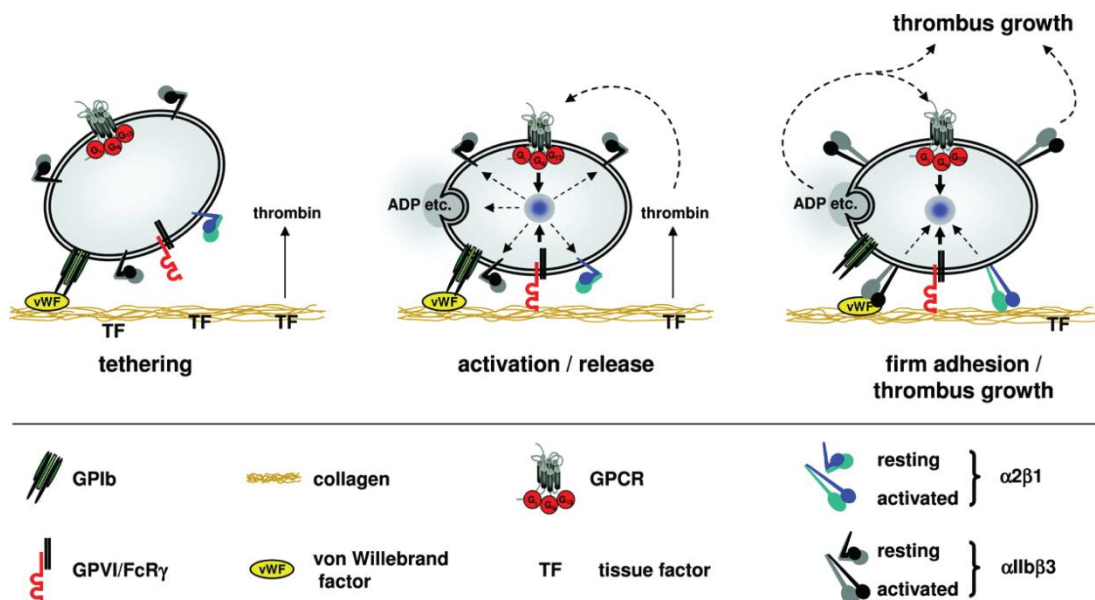
Figure 1.2. Platelet adhesion at sites of vascular injury. Initial adhesion (tethering) to the subendothelial matrix occurs when GPIb interacts with collagen-bound vWF. Adhesion is stabilised when $\alpha_2\beta_1$ and GPVI bind collagen resulting in αIIbβ3 activation and the release of soluble agonists while exposed tissue factor triggers the formation of thrombin, which potentiates platelet activation. Activated αIIbβ3 then binds fibrinogen resulting in platelet aggregation and formation of a stable haemostatic plug (Sachs and Nieswandt, 2007).

1.4.2 Initiation of platelet adhesion

1.4.2.1 GPIb signalling

The initial step in platelet adhesion involves interactions between GPIb and conformationally active vWF, which binds to subendothelial collagen at sites of vascular injury (Ruggeri and Mendolicchio, 2007). The interaction between GPIb and vWF stimulates actin polymerisation and cytoskeletal reorganisation through a shear-sensitive signalling cascade that is dependent on Src family kinases (Yuan et al., 1999, Asazuma et al., 1997). These kinases are essential for the phosphorylation and activation of PLCγ2, which mediates IP_3 production and calcium mobilisation in adherent platelets (Mangin et al., 2003). Calcium mobilisation is a critical signalling event that triggers a series of biochemical and morphological events such as shape change that contribute to platelet aggregation (Feinstein et al., 1985). Src kinase inhibition upon GPIb-vWF ligation abolishes PLCγ2 phosphorylation, calcium mobilisation, shape change, and adhesion, emphasising the importance of these signalling proteins downstream of the GPIb receptor complex (Wu et al., 2003).

1.4.3 Stabilisation of platelet adhesion

1.4.3.1 GPVI signalling

The initial capture of platelets on the subendothelium is stabilised by interactions between GPVI and collagen. The immunoglobulin receptor GPVI is expressed only on platelets and megakaryocytes and is important for

normal platelet-collagen adhesion. GPVI recognises a glycine-proline-hydroxyproline (GPO) amino acid sequence in collagen, which is mimicked by GPVI-selective agonists such as collagen-related peptide (CRP). Platelet-collagen interactions induce GPVI clustering and tyrosine kinase signalling, which mediates integrin activation and promotes stable adhesion (Figure 1.3) (Gibbins, 2004).
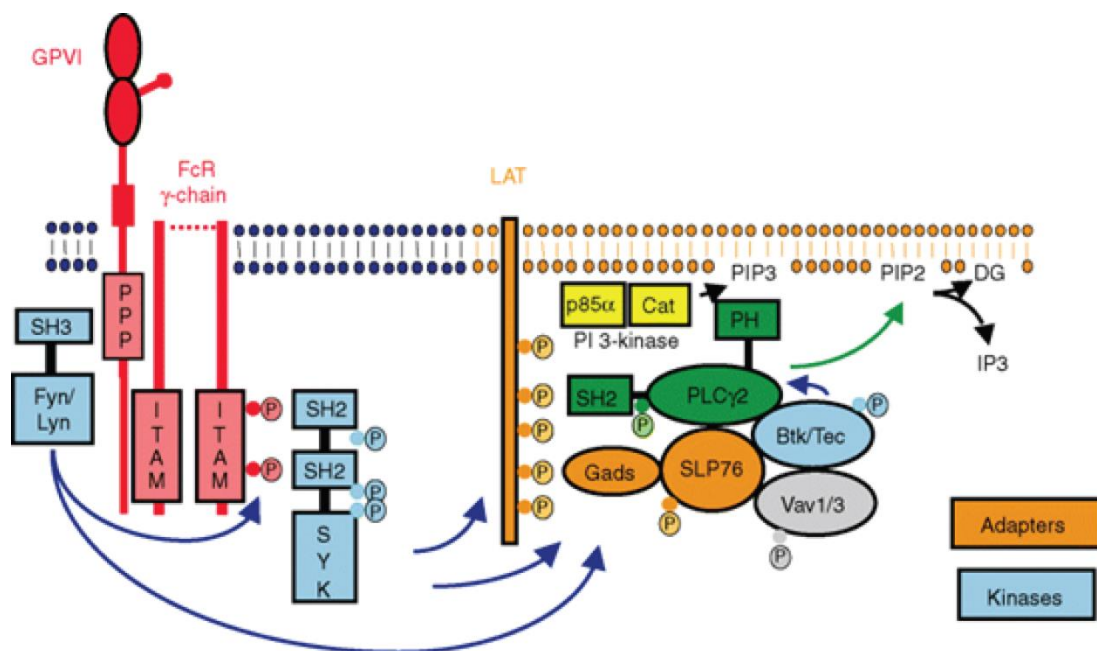
Figure 1.3. GPVI signalling cascade. GPVI ligation induces tyrosine phosphorylation of the FcRγ ITAM by Fyn and Lyn resulting in Syk activation and the physical association of various adapter proteins and kinases at the platelet membrane. PI3-K and PLCγ2 mediate the formation of IP_3, which stimulates calcium mobilisation and numerous functional responses that stabilise adhesion (Watson et al., 2005).

Collagen stimulates tyrosine phosphorylation of the FcRγ ITAM, leading to its association with Syk, and the subsequent phosphorylation of PLCγ2 (Farndale et al., 2004). FcRγ phosphorylation occurs rapidly after collagen stimulation (Gibbins et al., 1996) and is essential for the recruitment and activation of Syk (Poole et al., 1997). The cytoplasmic tail of GPVI contains an SH3-recognition motif that is essential for interaction with Fyn and Lyn kinases, which mediate the phosphorylation of FcRγ (Suzuki-Inoue et al., 2002). Fyn and Lyn are also required for the optimal phosphorylation of Syk, LAT, SLP-76, and PLCγ2, which form a signalling complex at the platelet membrane (Quek et al., 2000). PLCγ2 contains two catalytic regions enclosing two SH2 domains and one SH3 domain. The C-terminal SH2 domain associates directly with SLP-76 and LAT, but indirectly with Syk, Lyn, and FcRγ upon collagen stimulation (Gross et al., 1999). Once this complex is assembled, PLCγ2 generates IP_3 and DAG, resulting in calcium release and the activation of PKC, which phosphorylates additional proteins that are required for platelet activation (Gross et al., 1999). Another protein called PI3-K associates with FcRγ and LAT in this signalling complex and interacts indirectly with PLCγ2 to facilitate calcium mobilisation (Pasquet et al., 1999). Vav proteins and adapters such as Gads also assemble at the platelet membrane and contribute to the phosphorylation-based signalling events that mediate collagen-induced calcium mobilisation and platelet activation (Pearce et al., 2004, Asazuma et al., 2000).

1.4.3.2 Integrin $\alpha_2\beta_1$ signalling

Integrin $\alpha_2\beta_1$ mediates stable adhesion to collagen following the activation of GPIb and GPVI (Santoro, 1986, Staatz et al., 1989). $\alpha_2\beta_1$ is important but not essential for adhesion, and its requirement is largely determined by collagen structure since $\alpha_2\beta_1$-blocking antibodies abolish adhesion and aggregation on solubilised but not native collagen (Savage et al., 1999). Although collagens can undergo modification in pathological states, they are predominantly native (and insoluble) in normal blood vessels; and since $\alpha_2\beta_1$-inhibited platelets can adhere to native collagen, it seems that $\alpha_2\beta_1$ is dispensable for normal adhesion. Studies suggest that GPIb-dependent mechanisms can compensate for $\alpha_2\beta_1$ dysfunction since impaired adhesion of $\alpha_2\beta_1$-deficient washed platelets can be restored by addition of exogenous vWF (Chen et al., 2002).

While interactions between $\alpha_2\beta_1$ and collagen are enhanced by inside-out signals from GPIb and GPVI (Nieswandt and Watson, 2003), $\alpha_2\beta_1$ itself can generate signals that stabilise platelet-collagen adhesion. Suzuki-Inoue et al. (2001) found that $\alpha_2\beta_1$ ligation induced the Src and PI3-K-dependent activation of Rac and PAK. $\alpha_2\beta_1$ ligation also induces the tyrosine phosphorylation of Src, Syk, SLP-76, and PLCγ2, resulting in the release of intracellular calcium (Inoue et al., 2003). Since similar signalling events occur downstream of GPVI, it is conceivable that $\alpha_2\beta_1$ can compensate for GPVI dysfunction. Indeed, mice lacking the GPVI collagen receptor display only moderate increases in bleeding times (Nieswandt et al., 2001).

1.4.4 Platelet aggregation

1.4.4.1 Integrin αIIbβ3 signalling

Platelet aggregation and thrombus formation are dependent on the binding of soluble fibrinogen to αIIbβ3 (Bennett and Vilaire, 1979). In quiescent platelets, cytoskeletal proteins exert constraining effects on αIIbβ3 and decrease its affinity for soluble ligands. Haemostatic agonists relieve these constraints by activating an inside-out signalling cascade that allows the integrin to acquire a high affinity for fibrinogen (Bennett et al., 1999). Platelet agonists such as collagen induce calcium mobilisation, the production of DAG, and the subsequent activation of the calcium and DAG-regulated guanine nucleotide exchange factor I (CalDAG-GEFI) and Rap1-B, which promotes integrin activation through its adapter molecule RIAM and talin (Lee et al., 2009). Another protein that mediates inside-out signalling is kindlin-3. This protein binds directly to the β3 tail and triggers integrin activation (Moser et al., 2008). Kindlin-3 appears to be indispensable for normal platelet function since kindlin-3-deficient platelets do not bind fibrinogen or aggregate (Moser et al., 2008).
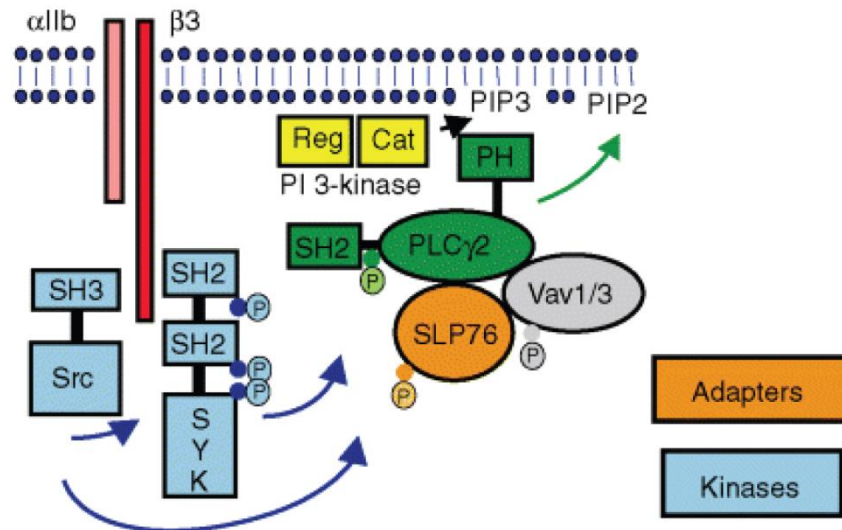
Figure 1.4. αIIbβ3 signalling cascade. Outside-in signalling stimulates the Src kinase-dependent phosphorylation and activation of Syk and the physical association of various signalling proteins at the platelet membrane. PI3-K and PLCγ2 stimulate intracellular calcium mobilisation resulting in numerous functional responses that promote stable adhesion (Watson et al., 2005).

αIIbβ3-fibrinogen binding, together with receptor clustering, triggers an outside-in signalling cascade that enhances platelet aggregation and thrombus formation (Figure 1.4) (Phillips et al., 2001). αIIbβ3 is a heterodimeric transmembrane receptor comprised of αIIb and β3 subunits, which associate with the adapter protein RACK1 and PKCβ (Buensuceso et al., 2005). In addition, the tyrosine kinase c-Src selectively associates with β3 subunits through its SH3 domain and is positively regulated by tyrosine autophosphorylation (Sun et al., 2002). αIIbβ3 clustering causes c-Src autophosphorylation and the phosphorylation and activation of Syk, which associates with the β3 subunit upon fibrinogen binding (Arias-Salgado et al., 2003, Woodside et al., 2001). Syk mediates the tyrosine phosphorylation of SLP-76, which associates with Vav1 and Gads in fibrinogen-adherent

platelets (Wonerow et al., 2002, Obergfell et al., 2001). SLP-76 also associates with the adapter protein SLAP-130 and the actin-binding protein VASP in fibrinogen-adherent platelets (Obergfell et al., 2001). The significance of this complex, which localises at the platelet membrane, has not been determined. However, it is thought that recruitment of VASP to integrin-based focal complexes enhances cytoskeletal reorganisation and platelet adhesion (Obergfell et al., 2001). PLCγ2 and PI3-K play an important role in calcium mobilisation downstream of αIIbβ3 (Wonerow et al., 2003, Nesbitt et al., 2002). PI3-K in particular appears to be important for cytoskeletal reorganisation, spreading, and aggregation. Indeed, its main substrate PIP2 associates with talin and regulates actin polymerisation *in vivo* (Fukami et al., 1994) but PI3-K inhibitors block their association and inhibit platelet adhesion, aggregation, and spreading on fibrinogen (Heraud et al., 1998).

1.4.5 Thrombus propagation

1.4.5.1 GPCR signalling

While the initial adhesion of platelets on the subendothelium requires GPIb, GPVI, and the integrins $\alpha_2\beta_1$ and αIIbβ3, the recruitment of additional platelets to the growing thrombus requires soluble mediators such as ADP, TXA_2, and thrombin, which signal through GPCRs (Figure 1.5) (Offermanns, 2006). These receptors possess seven transmembrane domains, which connect an extracellular N-terminus to an intracellular C-terminus. GPCR activation leads to the recruitment of heterotrimeric GTP-binding proteins, the

rapid formation of GDP, and the release of a highly-reactive Gα-subunit, which can modulate a variety of signalling cascades (Karnik et al., 2003).

Adherent platelets release dense granule contents such as ADP, which acts to potentiate secretion and aggregation. ADP-mediated platelet activation occurs through at least three distinct receptors: the $P2X_1$ ionotropic receptor, which mediates the rapid influx of extracellular calcium; the G_q-coupled $P2Y_1$ receptor, which mediates shape change and reversible aggregation through the mobilisation of intracellular calcium; and the G_i-linked $P2Y_{12}$ receptor, which mediates the inhibition of adenylyl cyclase (Daniel et al., 1998). Adherent platelets also release the arachidonic acid metabolite TXA_2, which signals through the $G_{12/13}$- and G_q-coupled TP receptor (Offermanns et al., 1994, Knezevic et al., 1993). Unlike ADP and TXA_2, thrombin is not released by activated platelets but is formed by the exposure of tissue factor to coagulation proteins at sites of vascular injury (Coughlin, 2005). Thrombin-mediated platelet activation occurs predominantly through PAR-1 (Andersen et al., 1999) which is activated when thrombin cleaves its N-terminal domain, unmasking a tethered ligand that self-activates the receptor (Vu et al., 1991). PAR-1 couples to $G_{12/13}$, G_q, and G_i proteins, which activate distinct signalling cascades (Coughlin, 2005). Thrombin-mediated platelet activation may also proceed through the $G_{12/13}$ and G_q-coupled PAR-4, but this receptor is thought to be largely redundant and only responds to high concentrations of thrombin (Coughlin, 2005).
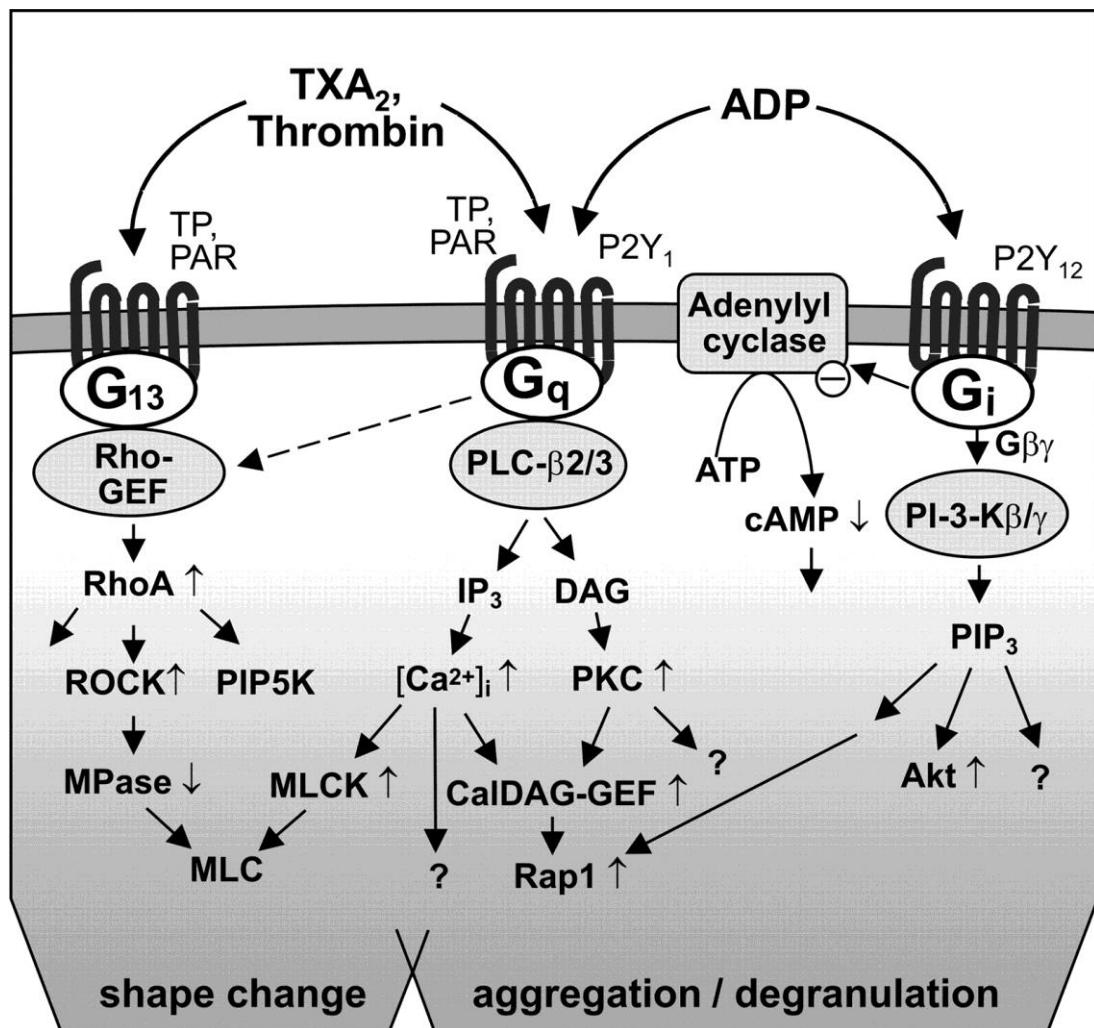
Figure 1.5. GPCR signalling cascades. The soluble agonists ADP, TXA_2, and thrombin bind $G_{12/13}$, G_q, or G_i protein-coupled receptors, which activate calcium-dependent (G_q and G_i) or calcium-independent ($G_{12/13}$) signalling cascades resulting in degranulation, shape change, and aggregation (Offermanns, 2006).

The central effector of GPCR-mediated platelet activation is PLCβ, which generates IP_3 and DAG, resulting in calcium mobilisation, granule secretion, and aggregation (Offermanns, 2006). Wild-type platelets, but not G_q-deficient platelets, secrete ATP and aggregate in response to ADP, thrombin, and the TP receptor agonist U46619. Wild-type platelets also activate PLCβ and

stimulate IP_3 formation and $[Ca^{2+}]_i$ release in response to these agonists (Offermanns et al., 1997). These results indicate that G_q-coupled receptors regulate PLCβ signalling and the degranulation and aggregation of adherent platelets.

Despite their functional abnormalities, G_q-deficient platelets still change shape in response to ADP, thrombin, and U46619 (Offermanns et al., 1997). By contrast, G_q-deficient platelets incubated with Rho kinase or Rho GTPase inhibitors show minimal shape change (Klages et al., 1999). Since TP receptors couple to $G_{12/13}$- and G_q-proteins, U46619-activated G_q-deficient platelets can be used to examine $G_{12/13}$-mediated signalling. U46619 induces the phosphorylation of c-Src, Syk, and MLC in G_q-deficient platelets. While MLC phosphorylation is maintained in the presence of tyrosine kinase inhibitors and calcium chelators, it is abolished by Rho kinase and Rho GTPase inhibitors (Klages et al., 1999). These results suggest that $G_{12/13}$-coupled receptors mediate platelet shape change through a Rho-dependent, tyrosine kinase/calcium-independent, signalling cascade. The activation of Rho is likely mediated by the GTP exchange factor p115 RhoGEF, which associates with G_{13} subunits and stimulates their intrinsic GTPase activity (Kozasa et al., 1998).

G_i-coupled receptors stimulate the recruitment and activation of PI3-K leading to calcium mobilisation and platelet activation (Rittenhouse, 1996). In addition, G_i-coupled receptors mediate the inhibition of adenylyl cyclase (Offermanns, 2006). In unstimulated platelets, the inhibition of adenylyl cyclase alone does not cause aggregation (Savi et al., 1996). Stimulation of $P2Y_{12}$ and PAR-1 activates G_i proteins and inhibits adenylyl cyclase-

mediated cAMP formation (Ohlmann et al., 1995). ADP and thrombin inhibit forskolin-stimulated cAMP accumulation in wild-type but not G_i-deficient platelets. Moreover, ADP- and thrombin-induced aggregation is impaired in G_i-deficient platelets (Jantzen et al., 2001). Together, these results suggest that platelet aggregation requires concomitant activation of G_q-coupled receptors and G_i-mediated inhibition of cAMP formation. The second messenger cAMP is an important regulator of platelet function that can inhibit many of the processes that drive adhesion and aggregation. The mechanism of action of cAMP and other inhibitors is discussed in detail in the following sections.

1.5 Regulation of platelet function

Although platelet activation is critical to haemostasis, it is subject to tight regulation in healthy vasculature to prevent spontaneous thrombosis. The vascular endothelium plays an important role in platelet regulation by neutralising platelet releasates and secreting vasoactive substances to prevent excessive platelet activation. CD39 is expressed on the endothelial cell surface and acts on the platelet releasate by hydrolysing ADP to limit platelet recruitment and aggregation (Gayle et al., 1998). Platelet function is also regulated by the endothelial-derived inhibitors PGI_2 and NO, which stimulate adenylyl cyclase (AC) and soluble guanylyl cyclase (sGC) leading to the elevation of intracellular cyclic nucleotides and the activation of cAMP and cGMP-dependent signalling cascades. The extent of platelet inhibition is dependent on the rates of cAMP and/or cGMP synthesis and their rates of degradation by cyclic nucleotide-dependent phosphodiesterases (PDEs).

The following sections describe the endothelial-derived mediators that regulate platelet function with a particular focus on the mechanisms that initiate, propagate, and terminate cyclic nucleotide signalling.

1.5.1 Prostacyclin

PGI_2 is a labile signalling molecule derived from the oxidation of fatty acids that inhibits platelet function through a cAMP-dependent signalling cascade (Tateson et al., 1977). In the bloodstream, albumin binds PGI_2 to protect it from rapid degradation (Tsai et al., 1991) and to enhance interactions with its

adenylyl cyclase-activating IP receptor (Tsai et al., 1991, Gorman et al., 1977). Vascular endothelial cells secrete PGI_2 in response to shear stress, which stimulates calcium mobilisation (James et al., 1995, Frangos et al., 1985). Calcium activates cytosolic phospholipase A_2 which liberates arachidonic acid from membrane phospholipids (Leslie, 1997). Thereafter, arachidonic acid undergoes a series of COX-mediated conversions to the unstable metabolites PGG_2 and PGH_2 (Moncada et al., 1976) with the latter being converted to PGI_2 by the enzyme PGI_2 synthase (Weksler et al., 1977).

1.5.2 Nitric oxide

The vascular endothelium secretes the gaseous free radical NO, which inhibits platelet function through a cGMP-dependent signalling cascade (Schwarz et al., 2001). NO synthesis is mediated by endothelial nitric oxide synthase (eNOS), which belongs to a family of enzymes that convert L-arginine to NO and L-citrulline. eNOS is constitutively expressed and can be activated by ATP, bradykinin, vascular endothelial growth factor (VEGF), and laminar shear stress and/or cyclic strain (Sessa, 2004). Mechanical stress or strain activates eNOS through calcium- and kinase-dependent mechanisms. Indeed, these forces cause mechanosensitive ion channels to open leading to rapid calcium influx; and they also induce the phosphorylation and activation of intracellular protein kinases such as PKB (Rizzo et al., 1998, Dimmeler et al., 1998). Under basal conditions, eNOS associates with caveolin-1; but in response to the mechanical force of flowing blood and subsequent calcium influx, eNOS dissociates from caveolin-1 and associates

with calmodulin (Rizzo et al., 1998). The association with calmodulin correlates with an increase in eNOS activity and this is further potentiated by intracellular calcium release (Rizzo et al., 1998). PKB stimulates NO synthesis by phosphorylating and activating eNOS (Fulton et al., 1999). AMPK, PKC, and CaM kinase II have also been implicated in the phosphorylation and regulation of eNOS, which contains at least five different phosphorylation sites (Mount et al., 2007).

1.5.3 Adenylyl cyclases

PGI_2 exerts its antiplatelet properties through receptor-mediated activation of adenylyl cyclases (ACs) (Armstrong, 1996). ACs are membrane-bound enzymes whose activity is regulated by G-protein coupled receptors. The enzymes contain two transmembrane domains, each linked to a cytosolic domain. The cytosolic domains, labelled C_1 and C_2, are subdivided into C_{1a} and C_{2a}, and C_{1b} and C_{2b} (Hurley, 1999). The conserved C_{1a} and C_{2a} domains dimerise and catalyse the formation of cAMP from ATP (Cooper, 2003) while the C_{1b} and C_{2b} domains contain regulatory sites whose functions are incompletely understood (Figure 1.6) (Hurley, 1999).

Nine membrane-bound AC isoforms and one soluble isoform have been identified. While early transcriptome studies suggested that platelets contained AC3, AC6, and AC7 (Rowley et al., 2011), recent proteome studies suggest only the presence of AC6 (Burkhart et al., 2012). All AC isoforms can be activated by G_s-coupled receptors (Tang and Hurley, 1998). The C_{1a} and C_{2a} domains contain negatively-charged binding sites for the

positively charged G_s protein. Upon platelet activation, It is thought that GTP-loaded G_s first binds to C_{2a} and promotes dimerisation with C_{1a} (Yan et al., 1997). The resultant C_{1a}/C_{2a} heterodimer contains an active catalytic site that hydrolyses ATP to form cAMP (Yan et al., 1997).
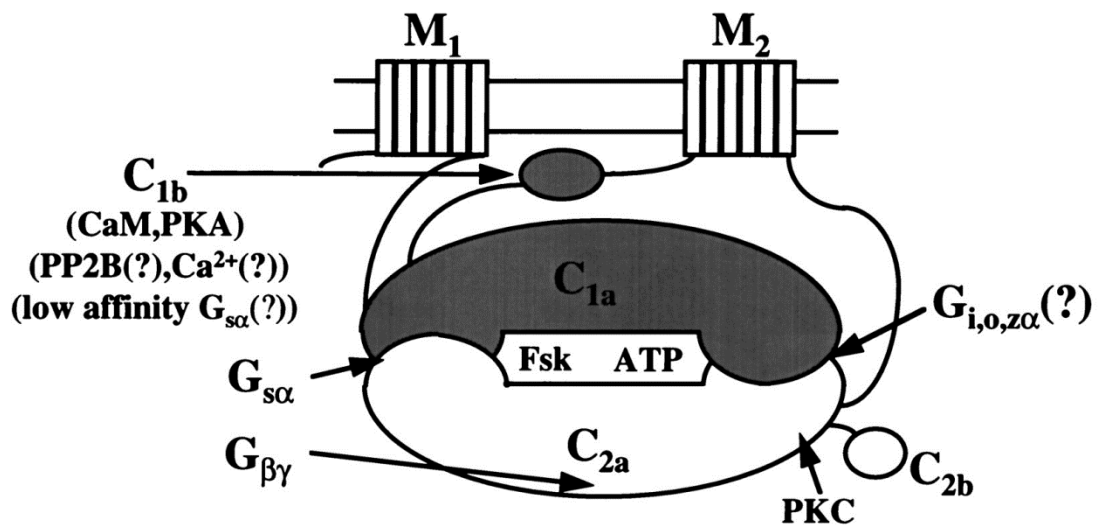
Figure 1.6. Structure of mammalian AC. AC contains two transmembrane domains (M_1 and M_2), linked to C_1 and C_2 cytosolic domains. The C_{1a} and C_{2a} domains dimerise and catalyse the formation of cAMP from ATP while the C_{1b} and C_{2b} domains contain regulatory sites for G-protein subunits, calcium, PKA, and PKC (Tang and Hurley, 1998).

G_i-coupled receptors such as $P2Y_{12}$ and PAR-1 can inhibit the activity of some AC isoforms (Offermanns, 2006). G_i proteins strongly inhibit AC1, AC5, and AC6 activity in the absence of G_s proteins, indicating that G_i-mediated inhibition is noncompetitive and that G_i- and G_s proteins bind to distinct sites on AC (Taussig et al., 1994). To a lesser extent, G_i can also inhibit AC3, AC8, and AC9 (Cooper, 2003). For AC6, which is found in platelets, G_i-

mediated inhibition is abolished by mutation of C_{1b}, but not C_{1a} or C_2 (Dessauer et al., 1998). It is thought that G_i binding to the C_{1b} domain, which lies close to the catalytic site, disturbs the optimal alignment of the C_{1a}/C_{2a} heterodimer and inhibits ATP hydrolysis (Tang and Hurley, 1998).

Almost all mammalian ACs are regulated either directly or indirectly by calcium-dependent signalling cascades (Halls and Cooper, 2011). For example, AC1 and AC8 are stimulated by calcium in a CaM-dependent manner (Fagan et al., 1996) while AC7 appears to be calcium insensitive (Cooper et al., 1995). By contrast, AC3 undergoes phosphorylation and inhibition in HEK-293 cells incubated with the calcium ionophore A23187 but not in cells incubated with CaM kinase inhibitors (Wei et al., 1996). The expression of constitutively active CaM kinase II completely inhibits AC3 activity suggesting that the cyclase is regulated through a calcium-dependent signalling cascade (Wayman et al., 1995). AC5 and AC6 are also subject to inhibition by calcium (Willoughby and Cooper, 2007). AC6, which exists in platelets, is inhibited by addition of submicromolar calcium in CaM-deficient NCB-20 cells suggesting that calcium regulates the cyclase through a direct mechanism (Yoshimura and Cooper, 1992). It has been suggested that calcium binds to the C_{1b} domain and inhibits AC6 independently of calcium-dependent protein kinases (Wu et al., 1993).

Like G_s-coupled receptors, AC isoforms undergo desensitisation within minutes of activation. G_s-stimulated AC6 is inhibited by PKA, which phosphorylates the C_{1b} domain (Chen et al., 1997). PKA-mediated phosphorylation of AC6 may contribute to desensitisation of the cAMP signalling cascade such that cAMP formation is transient and does not

increase to such an extent that platelet activation is compromised. By contrast, the ubiquitous kinase PKC phosphorylates and inactivates AC6 through a cAMP/calcium-independent mechanism since the suppression of AC6 during G_s-receptor desensitisation is blocked by PKC inhibition in EGTA-containing calcium-free buffers (Lai et al., 1997). In platelets, AC6 may be downregulated by regulator of G-protein signalling 2 (RGS2), which attenuates G_s activity by stimulating intrinsic GTPase activity (Noé et al., 2010).

1.5.4 Guanylyl cyclases

In platelets, the heterodimeric hemoprotein soluble guanylyl cyclase (sGC) is the principle receptor for NO (Hobbs, 1997). sGC contains α- and β-subunits, which dimerise and catalyse the formation of cGMP from GTP (Harteneck et al., 1990). The α- and β-subunits contain N-terminal ligand-binding domains and C-terminal catalytic domains. N-terminal truncation of the α- and β-subunits results in loss of sensitivity to the NO-releasing compound GSNO (Wedel et al., 1995) indicating that these domains are essential for enzyme activation. Truncated N-terminal domains of β-subunits do not contain heme and are insensitive to NO (Wedel et al., 1994); and while truncated N-terminal domains of α-subunits contain heme moieties, these mutants are still insensitive to NO (Koglin and Behrends, 2003). These results suggest that both subunits are required for NO stimulation, but that the β-subunit is critical for interactions between NO and heme. sGC activation occurs when NO binds to the heme group and disrupts interactions between heme and

histidine residues found on the β-subunit allowing GTP to bind and undergo conversion to cGMP.

The catalytic activity of sGC is rapid and peaks within seconds of NO stimulation. Thereafter, sGC undergoes rapid desensitisation, characterised by a decline in cGMP formation as NO dissociates from the heme domain (Friebe and Koesling, 2003). Neither the addition nor the removal of calcium affects NO-stimulated sGC, suggesting that desensitisation occurs through a calcium-independent mechanism (Bellamy et al., 2000). While sGC is thought to localise in the cytosol (Garbers, 1979), agonist-induced calcium elevations might drive its translocation to the platelet membrane, which is the preferred site of NO action (Zabel et al., 2002). There is no additional evidence that sGC undergoes spatial regulation in platelets. However, the effect of intracellular messengers on the subcellular distribution of sGC is a novel concept that requires further investigation. While the mechanism of sGC desensitisation is incompletely understood, the duration and intensity of the cGMP response appears to be largely dependent on PDEs since cGMP formation is prolonged in NO-stimulated platelets incubated with the PDE inhibitors sildenafil and EHNA (Bellamy et al., 2000, Mullershausen et al., 2001).

1.5.5 Phosphodiesterases

PDEs can terminate PGI_2- and NO-stimulated signalling events and are thus important regulators of cellular function in platelets and other cells (Schwarz et al., 2001). PDEs form a large group of enzymes that hydrolyse the 3'

cyclic phosphate bond of either cAMP or cGMP, yielding their inactive 5'
metabolites. While cyclic nucleotides can be transported across the platelet
membrane, the catalytic action of PDEs represents the only known
mechanism for rapidly lowering cellular cyclic nucleotide content and
regulating cAMP- and cGMP-mediated signalling events (Bender and Beavo,
2006).

Platelets contain three different PDE isozymes, including cGMP-stimulated
PDE2A, cGMP-inhibited PDE3A, and cGMP-specific PDE5 (Haslam et al.,
1999b). Binding of cGMP to allosteric binding sites induces the PDE2A-
catalysed degradation of both cAMP and cGMP. By contrast, binding of
cGMP to PDE3A inhibits the preferential hydrolysis of cAMP. PDE3A can be
phosphorylated and activated by PKA in a negative feedback loop to ensure
that cAMP levels do not increase to levels that might compromise platelet
activation (Hunter et al., 2009). PDE5 contains a high-affinity noncatalytic
binding site for cGMP. Binding of cGMP stimulates the phosphorylation and
activation of PDE5, either by PKA or PKG, leading to the rapid hydrolysis of
cGMP (Turko et al., 1998).

Since PDE activity is regulated by cGMP, the concentration of cAMP is
partially dependent on platelet sensitivity to NO and other activators of sGC.
Studies have demonstrated significant cross-talk between cAMP/cGMP-
dependent signalling cascades. Indeed, cAMP has been shown to play an
important role in NO/cGMP-mediated platelet inhibition due to cGMP-
mediated inhibition of PDE3A (Jensen et al., 2004). The relative contributions
of PDE isozymes to platelet function are incompletely understood. PDE2A is
likely the most important regulator of cAMP since PDE2A inhibition results in

higher levels of intraplatelet cAMP than PDE3A inhibition (Manns et al., 2002). However, inhibition of PDE3A but not PDE2A causes VASP phosphorylation and the inhibition of calcium mobilisation and aggregation (Manns et al., 2002). Accordingly, PDE5 inhibition blocks thrombin-induced secretion via cGMP-mediated inhibition of PDE3A and subsequent elevation of cAMP levels (Dunkern and Hatzelmann, 2005). Studies have shown that PDE3A can be phosphorylated and activated by PKB (Zhang and Colman, 2007) and/or PKC (Hunter et al., 2009) in thrombin-stimulated platelets. It is likely that platelet agonists downregulate cyclic nucleotide signalling in order to potentiate the platelet activation response.

1.5.6 Protein kinase A

The only known intracellular target for cAMP is protein kinase A (PKA), a tetrameric holoenzyme with two catalytic subunits and a dimeric regulatory subunit. Differential expression of these subunits gives rise to different isoforms with distinct biochemical properties in different cell types. PKA isoforms are classified by their regulatory subunits into type I (PKA-I) and type II (PKA-II), both of which are present in platelets (Burkhart et al., 2012). The regulatory subunits contain N-terminal dimerisation domains that bind to the catalytic subunits and C-terminal domains that bind free cAMP (Skålhegg and Tasken, 2000). Binding of four cAMP molecules to the C-terminal domains leads to a reversible conformational switch and the release of active catalytic subunits, which phosphorylate local protein substrates that contain

an arginine-arginine-X-serine/threonine sequence (RRXS/T), where X is a hydrophobic amino acid (Figure 1.7) (Skålhegg and Tasken, 2000).
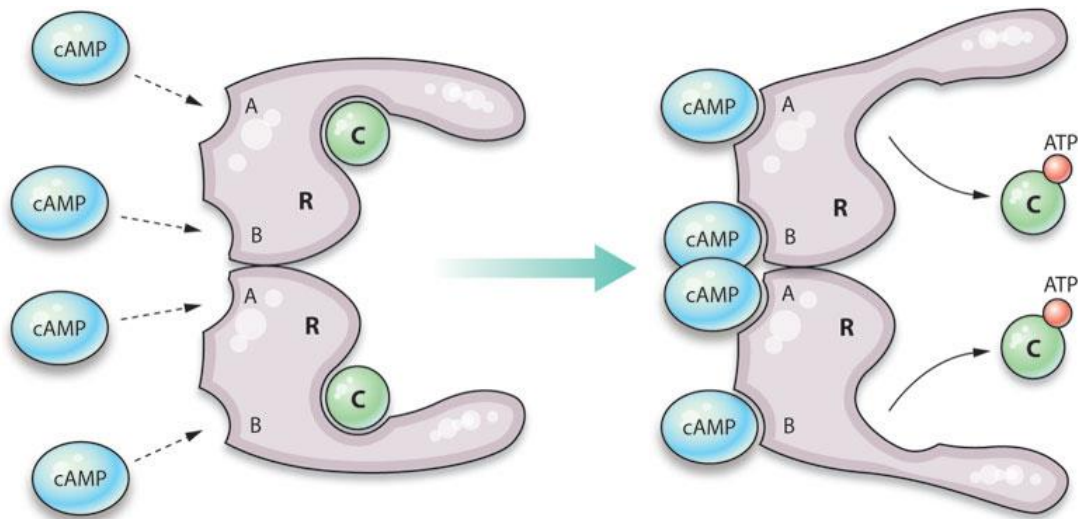
Figure 1.7. cAMP-mediated activation of PKA. Inactive PKA is a tetrameric protein containing two regulatory (R) and two catalytic (C) subunits. Binding of four cAMP molecules to the regulatory subunits leads to the release of ATP-bound catalytic subunits, which phosphorylate specific serine and threonine residues on a variety of protein substrates (Murray, 2008).

PKA isoforms show different subcellular localisation in different cell types. PKA-I is soluble (Meinkoth et al., 1990) whereas PKA-II associates with A kinase anchoring proteins (AKAPs), which sequester the inactive holoenzyme in distinct subcellular compartments (Skålhegg and Tasken, 2000). Spatiotemporal regulation of PKA isoforms has been demonstrated in human T cells where the subcellular localisation of PKA-II does not change but PKA-I translocates and associates with cellular substructures such as antigen-receptor complexes. In unstimulated T cells, PKA-I resides

homogenously in the cytosol while PKA-II localises at the nucleus. After TCR-CD3 stimulation, PKA-I colocalises with antigen-receptor complexes at the plasma membrane while PKA-II remains at the nucleus (Skålhegg et al., 1994). Active PKA-I was found in CD3 precipitates from stimulated, but not unstimulated, T cells (Skålhegg et al., 1994). These CD3-PKA-I coprecipitates were associated with cAMP formation and increased phosphotransferase activity suggesting that cellular substructures can activate PKA-I through physical interaction (Skålhegg et al., 1994). Similar interactions have been observed in B cells (Levy et al., 1996), but few PKA-I-specific anchoring proteins have been identified. By contrast, a substantial number of PKA-II-specific AKAPs have been characterised along with dual-specificity AKAPs, which can bind both PKA isoforms (Carnegie et al., 2009).

AKAPs contain a PKA binding domain that sequesters the holoenzyme to cellular substructures in order to localise kinase activity to relevant substrates. AKAPs often recruit additional enzymes such as PDEs in order to limit the cAMP signalling response (Wong and Scott, 2004). For example, muscle-selective AKAP (mAKAP) associates with PKA-II and PDE4 in rat myocytes (Dodge et al., 2001). In mAKAP precipitates, PKA activity is enhanced by PDE4 inhibition while PDE4 activity is diminished by PKA inhibition (Dodge et al., 2001). Since PKA phosphorylates and activates PDE4 (Sette and Conti, 1996), these results suggest that mAKAP assembles a signalling module that regulates PKA-mediated phosphorylation through feedback inhibition. Interactions between AKAPs, PKA, and PDEs have also been observed in leukocytes (Asirvatham et al., 2004) and Sertoli cells (Taskén et al., 2001). A number of potential AKAPs have been identified in

platelets but their roles in the regulation of cAMP signalling have not yet been established (Burkhart et al., 2012, Rowley et al., 2011). In platelets, PKA isoforms and their substrates are confined to distinct cellular compartments. For example, PKA and substrates including GPIb and VASP are almost exclusively associated with the plasma membrane, which reflects the ability of cAMP to target surface receptors and cytoskeleton-associated proteins (El-Daher et al., 1996). Other substrates including the IP_3 (type I) receptor associate with intracellular membranes, which may represent the sites where calcium mobilisation is regulated (Raslan and Naseem, 2014). It is reasonable to assume that PKA is also present in the platelet cytosol where substrates such as RhoA and PDE3 reside (Aburima et al., 2013, Hunter et al., 2009).

1.5.7 Protein kinase G

The main intracellular receptor for cGMP is protein kinase G (PKG), a homodimeric enzyme with three functional domains: an N-terminal dimerisation domain, a regulatory domain, and a catalytic domain (Hofmann et al., 2000). There are two PKG families: the soluble PKGI and the membrane-bound PKGII (Francis et al., 2010). PKGI exists as α- and β splice variants that have different N-terminal sequences and different affinities for cGMP (Francis et al., 2010). While PKGIα has a well-defined role in smooth muscle cells (Pfeifer et al., 1999), PKGIβ is the main effector of NO/cGMP signalling in platelets (Eigenthaler et al., 1992). Indeed, platelets lacking PKG show increased adhesion and aggregation *in vivo* and

loss of NO sensitivity *in vitro* (Massberg et al., 1999). PKG is homologous to PKA and has a similar mechanism of action. Binding of four cGMP molecules to its regulatory domain stimulates N-terminal autophosphorylation, elongation, and the release of active catalytic subunits, which phosphorylate serine and threonine sites on local protein substrates (Wall et al., 2003). PKG regulates platelet function by phosphorylating a variety of proteins including VASP (Halbrügge et al., 1990), PI3-K (Pigazzi et al., 1999), and the TXA_2 receptor (Reid and Kinsella, 2003).

Molecular scaffolds called G kinase interacting proteins (GKIPs) can regulate the scope and magnitude of cGMP signalling by sequestering PKG to cellular substructures. MLCP has been identified as a GKIP in smooth muscle cells (Surks et al., 1999). PKGIα and MLCP colocalise at the plasma membrane, where NO/cGMP is abundant; and at actin-myosin fibres, which regulate contraction (Surks et al., 1999). Since MLCP targets PKGIα to actin-myosin fibres and since PKGIα activation increases MLCP activity (Nakamura et al., 1999), their association is thought to be important for the coordinated regulation of smooth muscle contraction. By contrast, PKGIβ interacts with actin-binding proteins (Casteel et al., 2013, Schwappacher et al., 2013) and associates with the transcription regulator TFII-I in cGMP-stimulated BHK cells (Casteel et al., 2002). In unstimulated BHK cells, PKGIβ resides in the cytosol while TFII-I localises at the nucleus. After cGMP stimulation, PKGIβ colocalises with TFII-I at the nucleus where PKGIβ phosphorylates TFII-I and enhances its transcriptional activity (Casteel et al., 2002). PKG may undergo similar spatial regulation in platelets. Indeed, PKGIβ associates with the IP_3 (type I) receptor and the IP_3 receptor-associated cGMP kinase substrate

(IRAG) in platelet membranes. PKG phosphorylates IRAG and inhibits IP_3-mediated calcium release but mutant IRAG causes defective inhibition of calcium mobilisation in NO/cGMP-stimulated platelets (Antl et al., 2007). PDE5 can also regulate PKGIβ activity by forming an intraplatelet complex with the IP_3 (type I) receptor and IRAG (Wilson et al., 2008). Since interactions between PKG and GKIPs appear to play an important role in platelet inhibition, loss of these spatiotemporal interactions may contribute to atherothrombotic-related disease. The importance of PKG in regulating platelet function has been recognised and therapeutic agents have been developed to stimulate cGMP signalling in the absence of NO, which platelets themselves may become resistant to in certain disease states (Stasch et al., 2011). Interestingly, recent studies have demonstrated weak sGC activation in platelets stimulated with vWF (Gambaryan et al., 2008) and collagen (Riba et al., 2008). These NO-independent mechanisms of sGC activation are incompletely understood but may contribute to feedback platelet inhibition.

1.5.8 PKA/PKG substrates and platelet function

Unless selectivity for cAMP versus cGMP is high, there will be cross-talk between cyclic nucleotide signalling cascades where cAMP cross-activates PKG and/or cGMP cross-activates PKA (Jiang et al., 1992, Francis et al., 2010). The activation of PKA and/or PKG leads to the phosphorylation of proteins that contain RRXS/T consensus motifs (Pearson and Kemp, 1991). Although some of these proteins are targets for both kinases, others are

differentially regulated by cyclic nucleotide signalling molecules (Figure 1.8, Table 1.1). The following section describes the various substrates for PKA and/or PKG and explores their roles in platelet function.
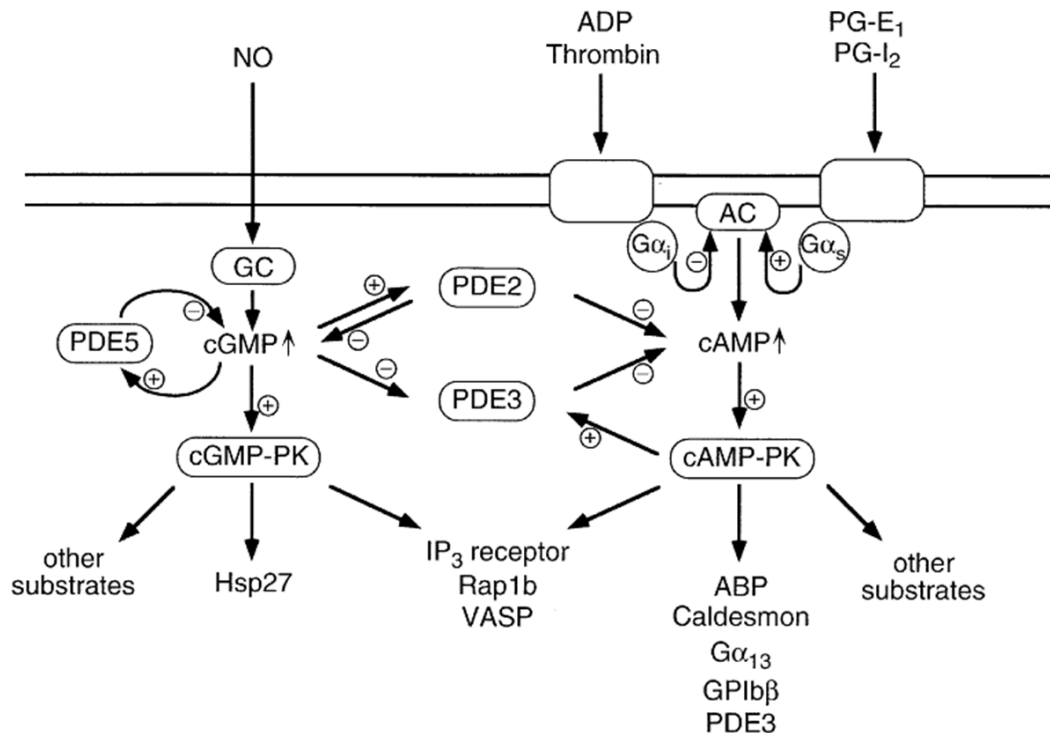
Figure 1.8. Regulation of cyclic nucleotide signalling cascades. Cyclic nucleotide signalling can be activated by PGI_2 and NO or inhibited by ADP and thrombin. The phosphorylation of downstream targets results from complex interplay between cyclic nucleotide-dependent phosphodiesterases and protein kinases, which may have overlapping substrate specificities (Schwarz et al., 2001).

Table 1.2. PKA and/or PKG substrates in human platelets.

Phosphoprotein	PKA	PKG	Function	Reference
ABP	✓		Inhibition of actin polymerisation	(Chen and Stracher, 1989)
Caldesmon	✓		Unknown	(Hettasch and Sellers, 1991)
G_{13}	✓		Inhibition of Rho kinase signalling	(Manganello et al., 1999)
GPIbβ	✓		Inhibition of actin polymerisation	(Fox and Berndt, 1989)
GSK-3α	✓		Unknown	(Beck et al., 2014)
HSP27		✓	Inhibition of actin polymerisation	(Butt et al., 2001)
IP_3 Receptor	✓	✓	Inhibition of calcium mobilisation	(Cavallini et al., 1996)
PDE3	✓		Enhanced cAMP degradation	(Macphee et al., 1988)
Rap1-B	✓	✓	Unknown	(Siess et al., 1990)
RhoA	✓		Inhibition of Rho kinase signalling	(Aburima et al., 2013)
VASP	✓	✓	Inhibition of GPIIb-IIIa	(Butt et al., 1994)

1.5.8.1 Actin polymerisation

Platelet activation is driven by reorganisation of the actin cytoskeleton, which is required for shape change and stable interactions between αIIbβ3 and fibrinogen (Fox et al., 1996). Cytoskeletal reorganisation is regulated through the phosphorylation of numerous protein substrates. One of the best characterised substrates is VASP, which plays an important role in cytoskeletal reorganisation by regulating actin bundling and polymerisation (Harbeck et al., 2000). VASP is a microfilament-associated protein that contains two Ena/VASP homology domains, which mediate interactions with specific cytoskeletal proteins; and one proline-rich domain, which facilitates actin polymerisation through recruitment of the G-actin binding protein, profilin (Reinhard et al., 2001). Intraplatelet VASP is a major substrate for both PKA and PKG (Butt et al., 1994). It appears to play an important role in platelet inhibition since VASP-deficient mice are unresponsive to NO and show enhanced adhesion to the subendothelium (Massberg et al., 2004). It is well established that PKA preferentially phosphorylates serine 157 while PKG preferentially phosphorylates serine 239 (Butt et al., 1994). Phosphorylation on serine 157, in the proline-rich domain, alters the binding properties of VASP and inhibits actin polymerisation. Additional phosphorylation on serine 239, an F-actin binding site, further inhibits filament formation (Harbeck et al., 2000). These post-translational modifications are significant because phosphorylation, particularly on serine 157, correlates with the inhibition of fibrinogen binding to αIIbβ3 and the inhibition of platelet aggregation (Horstrup et al., 1994). Thus, VASP phosphorylation can be used as a marker of platelet inhibition. Since VASP

is sensitive to cAMP/cGMP-elevating agents, it can provide important information about endothelial function and the bioavailability of PGI_2 and NO (Schäfer et al., 2004). In addition, it can be used to assess the *in vivo* response to antiplatelet drugs that target the $P2Y_{12}$ receptor such as clopidogrel (Hollopeter et al., 2001). The cAMP-elevating agent PGE_1 and ADP are commonly used to evaluate $P2Y_{12}$ inhibition by clopidogrel (Glenn et al., 2014, Schwarz et al., 1999b). PGE_1 binds to its AC-coupled receptor and stimulates VASP phosphorylation while ADP binds to its $P2Y_{12}$ receptor and inhibits AC-mediated signalling events. Thus; in platelets co-stimulated with PGE_1 and ADP, the level of VASP phosphorylation is directly proportional to the level of $P2Y_{12}$ inhibition.

Actin-binding protein (ABP) is an important component of the cytoskeleton that stabilises the platelet membrane against the mechanical forces of flowing blood (Cranmer et al., 2011). Upon platelet activation, ABP undergoes calpain-mediated proteolytic cleavage leading to cytoskeletal reorganisation and shape change (Hartwig and DeSisto, 1991). PKA can phosphorylate ABP to inhibit cleavage and maintain the stability of the cytoskeleton (Chen and Stracher, 1989). In addition, ABP anchors membrane proteins such as GPIb to the cytoskeleton to promote adhesion and downstream signalling (Feng et al., 2003). PKA can phosphorylate GPIbβ and inhibit actin polymerisation (Wardell et al., 1989) and adhesion on vWF (Bodnar et al., 2002). Although GPIbβ phosphorylation can be detected in unstimulated platelets (Zahedi et al., 2007), the receptor undergoes substantial phosphorylation in response to cAMP-elevating agents (Bodnar et al., 2002). Another actin-binding protein called caldesmon facilitates actin-

myosin interactions. Caldesmon undergoes phosphorylation in PGI$_2$-stimulated platelets, but the functional significance of this modification has not been determined (Hettasch and Sellers, 1991). Heat shock proteins are important regulatory components of the platelet cytoskeleton (Zhu et al., 1994). Heat shock protein 27 (HSP27) has been identified as a substrate for PKG, which phosphorylates threonine residues and inhibits actin polymerisation in platelets (Butt et al., 2001). In addition, PKA can phosphorylate other heat shock proteins but their roles in platelet function are unclear (Edwards et al., 2012).

Glycogen synthase kinase-3 (GSK-3) is an established regulator of glycogen metabolism and protein synthesis (Frame and Cohen, 2001) but recent studies have shown that the kinase plays an additional role in cytoskeletal reorganisation (Tang et al., 2011). GSK-3 regulates actin polymerisation by activating Rac and suppressing RhoGAP (Sun et al., 2009) while the kinase may also drive the protrusion of filopodia and lamellipodia (Etienne-Manneville and Hall, 2003). GSK-3 lies downstream of the GTPase Rap1-B (Arimura and Kaibuchi, 2007), which is a substrate for both PKA and PKG in human platelets (Lapetina et al., 1989). Another GTPase pathway involves RhoA, which is phosphorylated by PKA leading to inhibition of MLCP and likely inhibition of actin polymerisation and shape change (Aburima et al., 2013). Interestingly, RhoA has been shown to regulate the phosphorylation of GSK-3 in fibroblasts (Eng et al., 2006) but their relation in platelets is unclear. GSK-3 exists as constitutively active α and β isoforms that are negatively regulated by phosphorylation (Force and Woodgett, 2009). The phosphorylation and inhibition of GSK-3 can be induced by cAMP-elevating

agents or cAMP analogues (Fang et al., 2000, Oberprieler et al., 2010). Both GSK-3 isoforms are present in human platelets but their roles have not been defined (Barry et al., 2003). Some laboratories have shown that GSK-3 inhibition potentiates aggregation (Li et al., 2008) while others have shown that GSK-3 inhibition attenuates aggregation (Barry et al., 2003). Such discrepancies might be explained by the differential roles of GSK-3 isoforms. Indeed, one study measured aggregation in GSK-3β-deficient mice (Li et al., 2008) while the other measured aggregation in human platelets treated with nonselective compounds that could inhibit both isoforms (Barry et al., 2003).

1.5.8.2 Calcium mobilisation

Various aspects of platelet activation, including shape change, secretion, and integrin activation, are dependent on calcium mobilisation (Varga-Szabo et al., 2009). Platelet agonists stimulate the production of IP_3 and DAG, which mediate calcium mobilisation from internal and external sources. While IP_3 mediates calcium release from the DTS, DAG mediates calcium entry from the extracellular space. Extracellular calcium enters platelets through store-operated channels such as Orai1 (which is sensitive to IP_3), non-store-operated channels such as TRPC6 (which is sensitive to DAG), and membrane $P2X_1$ channels (which are sensitive to ATP) (Varga-Szabo et al., 2009). The endothelial-derived inhibitors PGI_2 and NO strongly inhibit agonist-induced calcium mobilisation from intracellular and extracellular sources (Geiger et al., 1994). The signalling mechanisms that inhibit calcium mobilisation are incompletely understood but likely involve the IP_3 receptor

since TRPC6 is insensitive to phosphorylation by PKA (Hassock et al., 2002) and P2X$_1$ is not affected by cAMP elevation (Fung et al., 2012). IP$_3$ receptors are known PKA substrates and their phosphorylation has been shown to inhibit calcium mobilisation (Quinton and Dean, 1992).

1.6 Aims of the study

Uncontrolled platelet activation can lead to arterial thrombosis and serious cardiovascular events such as myocardial infarction and stroke. Platelet activation is driven by a plethora of phosphorylation-based signalling events. A major challenge is to understand how signalling proteins and pathways integrate to drive different aspects of the platelet activation process. The phosphorylation of intraplatelet proteins is commonly measured by immunoblotting but this approach is cumbersome and does not facilitate large-scale analyses or provide the statistically-rich data that is required to obtain a detailed understanding of the molecular mechanisms that regulate platelet function.

Since flow cytometry can overcome the limitations of immunoblotting, the aim of this study was to develop a flow cytometric assay for high-throughput analyses of phosphorylation-based signalling events in platelets with a particular focus on cyclic nucleotide signalling cascades, which modulate platelet function and can be used to assess antiplatelet agents and antagonists of the ADP receptor P2Y$_{12}$. The aim will be achieved by:

1. Demonstrating that flow cytometry can detect the functional effects of platelet agonists and cyclic nucleotide-elevating agents such as PGI_2 in whole blood.

2. Optimising a flow cytometry protocol for the high-throughput analysis of phosphorylation-based signalling events in response to cyclic nucleotide-elevating agents in whole blood.

3. Demonstrating clinical and pharmacological application of the assay with a focus on drug screening in order to identify novel antiplatelet agents.

Methods

2.1 Materials

Antibodies against phosphoVASP-ser[157], phosphoVASP-ser[239], phosphoGSK-3α-ser[21], and phosphoPKA Substrate (RRXS/T) were from Cell Signaling Technology (Watford, UK). Anti-integrin β3 was from Santa Cruz (Wembley, UK). Anti-CD45-PE, anti-CD62P-PE, anti-CD42a-FITC, anti-CD42b-FITC, PE Mouse IgG$_1$, FITC Mouse IgG$_1$, BD CompBeads, BD Phosflow Lyse/Fix Buffer, BD Perm/Wash Buffer, BD Perm Buffer II, and BD Perm Buffer III were from BD Biosciences (Oxford, UK). Anti-fibrinogen-FITC was from Dako (Stockport, UK). Pacific Blue, Alexa Fluor 488- and Alexa Fluor 750 succinimidyl esters, and Alexa Fluor 647 anti-rabbit IgG were from Molecular Probes (Paisley, UK). DyLight 800 succinimidyl ester was from Thermo Scientific (Loughborough, UK). Paraformaldehyde (PFA) solution was from Electron Microscopy Sciences (Hatfield, PA). S-nitrosoglutathione (GSNO) and 1H-[1,2,4]oxadiazolo[4,3-a]quinoxalin-1-one (ODQ) were from Calbiochem (Feltham, UK). Milrinone and zaprinast were from Tocris Bioscience (Bristol, UK). BW A868C, erythro-9-(2-hydroxy-3-nonyl)adenine (EHNA), H89, 1-Methyl-3-isobutylxanthine (IBMX), Cyclic AMP EIA Kit, PGE$_1$, PGI$_2$, 16,16-dimethyl-6-keto PGE$_1$, 16-phenyl tetranor PGE$_1$, 5-*trans* PGD$_2$, Prostaglandin Screening Library II, and RO1138452 were from Cayman Chemical Company (Cambridge, UK). TRAP was from Anaspec (Cambridge, UK). Horm collagen (type I and III) was from Nycomed (Zurich, Switzerland). CRP-XL was obtained from Richard Farndale (Cambridge, UK). All other materials were from Sigma-Aldrich (Poole, UK).

2.2 Preparation of washed platelets

Unless otherwise stated, blood was drawn from healthy volunteers who had not taken medication known to affect platelet function for the previous 14 days. Experiments were conducted in accordance with the Declaration of Helsinki and approved by the Ethics Committee at the Hull York Medical School.

In this study, washed platelets were prepared by lowering the pH of platelet-rich plasma to 6.4, thereby preventing platelet activation during centrifugation (Mustard et al., 1989). Unlike prostaglandin-based techniques, pH-lowering methods maintain platelet sensitivity to cyclic nucleotide-elevating agents, which were used throughout this study. Blood was obtained from the median cubital vein using a 21-gauge butterfly needle. The initial 5 mL was discarded to exclude artifactually activated platelets. Blood was drawn into acid-citrate-dextrose (2.9 mM citric acid, 29.9 mM sodium citrate, 72.6 mM NaCl, 113.8 mM glucose, pH 6.4) and centrifuged for 20 min ($200g$, 20°C). Resultant platelet-rich plasma was treated with 0.3 mM citric acid and centrifuged for 12 min (800 g, 20°C). The supernatant was removed and platelet pellets were suspended in wash buffer (5 mM glucose, 5 mM KCl, 9 mM NaCl, 10 mM EDTA, 36 mM citric acid, pH 6.4), centrifuged for 12 min ($800g$, 20°C), and then resuspended in modified Tyrode's buffer (0.5 mM $MgCl_2$, 0.55 mM NaH_2PO_4, 2.7 mM KCl, 5 mM HEPES, 5.6 mM glucose, 7 mM $NaHCO_3$, 150 mM NaCl, pH 7.4).

2.3 Platelet count

Manual platelet counts were performed using a hemocytometer. Washed platelets were diluted (1:100) in 1% (w/v) ammonium oxalate to lyse contaminating red blood cells. The dilution was then loaded onto a hemocytometer. After 10 min, the hemocytometer was mounted onto a light microscope and platelets were counted using a 40× objective. After correcting for the initial dilution, counts were expressed as platelets/mL.

2.4 Electrophoresis and immunoblotting

Electrophoresis allows the separation of charged macromolecules in an electric field. When applied to a matrix such as a gel, it can be used to separate molecules based on their size and charge. SDS-polyacrylamide gel electrophoresis (SDS-PAGE) uses a combination of SDS and polyacrylamide gel to separate proteins according to their molecular mass by electrophoretic migration.

2.4.1 SDS-polyacrylamide gel electrophoresis

Prior to SDS-PAGE, samples are boiled in Laemmli buffer containing SDS and β-mercaptoethanol. While SDS intercalates with hydrophobic protein sites, β-mercaptoethanol breaks disulfide bonds. These interactions disrupt protein structure and impart a negative charge on polypeptide subunits. Since charge no longer affects electrophoretic mobility, proteins migrate toward the anode based on their molecular weight.

During SDS-PAGE, proteins are separated on a porous gel of polyacrylamide. The porosity of a gel is proportional to its acrylamide concentration, which can be tailored to the protein of interest. Gels that contain low concentrations of acrylamide enable better resolution of proteins with high molecular weights while gels that contain high concentrations of acrylamide enable better resolution of proteins with low molecular weights. Gradient gels, in which the concentration of acrylamide varies from low to high, allow excellent resolution to be obtained from lysates that contain proteins with diverse molecular weights. Gradients from 4-20% are routinely used to separate proteins in whole-platelet lysates (Gibbins and Mahaut-Smith, 2004).

2.4.2 Sample preparation for SDS-PAGE

Washed platelets (2.5×10^8 platelets/mL) were stimulated at 37°C in 96-well plates containing the appropriate agonists. This approach was used to replicate sample preparation for flow cytometry. In some cases, platelets were incubated with the PKA and sGC inhibitors H89 (10 µM, 20 min) and ODQ (20 µM, 20 min) before stimulation with PGI_2 (0-100 nM, 2 min) and NO (0-10 µM, 2 min). Platelets were lysed with 2x Laemmli sample buffer and boiled (5 min) before lysate proteins (30 µL) and biotinylated protein standards (5 µL) were loaded onto Bio-Rad Mini-PROTEAN TGX Precast Gels (either 10% or 4-20%) (Hemel Hempstead, UK) and run at 300 V for 15-20 min.

Samples underwent SDS-PAGE using a discontinuous buffer system in which chloride and glycinate ions form a tight mobile boundary around samples to yield stacked narrow bands that provide high resolution. Samples migrate through two regions: the stacking gel, which condenses samples into well-defined bands; and the resolving gel, which separates proteins based on their molecular weight.

2.4.3 Immunoblotting

Several techniques, including immunoblotting and *in vitro* kinase assays, require the proteins separated by electrophoresis to be transferred to a solid-phase membrane. Immunoblotting is frequently used to electrophoretically transfer proteins from polyacrylamide gels to nitrocellulose or polyvinylidene difluoride (PVDF) membranes. Electrotransfer occurs primarily through hydrophobic interactions between the protein and the membrane. While nitrocellulose membranes are relatively inexpensive, they are not suitable for repeated probing or fluorescent visualisation and proteins can completely traverse the membrane during prolonged electrotransfer. Conversely, PVDF membranes are mechanically stronger than nitrocellulose and have a higher protein binding affinity (Gibbins and Mahaut-Smith, 2004).

After SDS-PAGE, gels were sandwiched between an optimised buffer, membrane, and filter paper combination (Bio-Rad Tans-Blot Turbo PVDF Transfer Pack) and proteins were transferred to PVDF membranes (25 V, 7 min) using the Bio-Rad Trans-Blot Turbo Transfer System (Hemel Hempstead, UK).

2.4.4 Immunodetection of phosphorylated proteins

Platelet function is driven by a plethora of phosphorylation-based signalling events. Our challenge is to understand how these signalling events drive different aspects of the platelet activation process. Immunodetection is commonly used to visualise phosphorylated proteins on PVDF membranes. These protein-loaded membranes are incubated with primary phosphospecific antibodies and then with horseradish peroxidase (HRP)-conjugated secondary antibodies. Visualisation occurs through an enhanced chemiluminescent (ECL) system, where HRP reacts with H_2O_2 and luminol resulting in the emission of blue light (428 nm). This chemiluminescent light is captured on blue-sensitive x-ray film and used in the qualitative analysis of protein phosphorylation.

After transferring proteins from the gel to the membrane, membranes were washed for 5 min with Tris-buffered-saline-Tween (0.1%) and then blocked for 60 min with 5% non-fat milk in Tris-buffered-saline-Tween (0.1%) to prevent nonspecific antibody binding. These membranes were incubated overnight at 4°C with the indicated phosphospecific antibodies (diluted 1:1000 in Tris-buffered-saline containing 0.2% BSA and 0.1% Tween 20). Membranes were then washed for 5 min with Tris-buffered-saline-Tween (0.1%) and incubated for 45 min at room temperature with HRP-conjugated secondary antibodies (diluted 1:10000 in Tris-buffered-saline containing 0.1% Tween 20) and HRP-linked anti-biotin (1:2000). After 4 washes (15 min) with Tris-buffered-saline-Tween (0.1%), membranes were developed using an ECL detection system.

In some cases (to confirm equal loading), membranes were stripped for 15 min with Restore Western Blot Stripping Buffer (Thermo Scientific, UK), which contains SDS to dissociate antibody-antigen complexes. These membranes were washed for 5 min with Tris-buffered-saline-Tween (0.1%), blocked for 30 min with 5% non-fat milk in Tris-buffered-saline-Tween (0.1%), and then reprobed with anti-integrin β3 (diluted 1:1000 in Tris-buffered-saline containing 0.2% BSA and 0.1% Tween 20). Membranes were incubated overnight at 4°C, washed for 5 min with Tris-buffered-saline-Tween (0.1%) and incubated for 45 min at room temperature with HRP-conjugated secondary antibodies (diluted 1:10000 in Tris-buffered-saline containing 0.1% Tween 20) and HRP-linked anti-biotin (1:2000). After 4 washes (15 min) with Tris-buffered-saline-Tween (0.1%), membranes were developed by ECL.

2.5 Flow cytometry

Flow cytometry enables the rapid and quantitative analysis of individual cells as they pass through one or more laser beams. Resultant scattered and/or fluorescent laser light is converted into an electronic signal and used to interpret relative cell size and granularity. Specific cell populations with distinct morphologic properties can therefore be identified within heterogeneous samples such as whole blood. Prior to analysis, cells are normally stained with fluorescent-labelled antibodies that recognise cellular antigens. As they pass through the light source, bound antibodies emit fluorescence that is directly proportional to the amount of antigen present on or inside the cell. Through multiple detectors and emission filters, cytometers can selectively capture fluorescence across the entire visible and infared spectrum. Thus, antibodies coupled to fluorophores with different emission properties enable the simultaneous detection of multiple antigens on the same cell.

2.5.1 Sample preparation for flow cytometry

For the examination of platelet activation, samples were prepared according to a well-established method in which blood is diluted and incubated with appropriate antibodies, agonists, and/or inhibitors, and then fixed prior to analysis (Metcalfe et al., 1997). Freshly-obtained citrated blood (5 µL) was diluted in modified Tyrode's buffer (50 µL) containing anti-CD62P-PE (2 µL) and anti-fibrinogen-FITC (2 µL). Agonists (5 µL) were added, mixed by gentle vortexing, and left for 10 min. Samples were then fixed with 0.2% (v/v)

formylsaline (0.5 mL) and left for 10 min. Negative controls containing citrated blood (5 µL), modified Tyrode's buffer (50 µL), and either PE Mouse IgG$_1$ (2 µL) or anti-fibrinogen-FITC (2 µL) and 3 mM EDTA (to prevent fibrinogen binding to αIIbβ3) were also prepared.

For platelet-leukocyte aggregates, citrated blood (50 µL) was diluted in modified Tyrode's buffer (50 µL) containing anti-CD45-PE (5 µL) and anti-CD42a-FITC (5 µL). Agonists (5 µL) were added, mixed by gentle vortexing, and left for 10 min. Samples were then diluted with BD Phosflow Lyse/Fix Buffer (1 mL), vortexed, and left for 10 min. Negative controls containing citrated blood (50 µL), modified Tyrode's buffer (50 µL), and either PE Mouse IgG$_1$ (5 µL) and anti-CD42a-FITC (5 µL) or FITC Mouse IgG$_1$ (5 µL) and anti-CD45-PE (5 µL) were prepared as previously described (Li et al., 1999).

2.5.2 Flow cytometric analysis of platelet activation

Samples were analysed using a BD LSRFortessa. To correct for spectral overlap between PE- and FITC-labelled antibodies, automatic compensation was applied using BD CompBeads Anti-mouse IgG/Negative Control Compensation Particle Set. In brief, BD CompBeads Negative Control and Anti-mouse IgG were diluted in modified Tyrode's buffer (50 µL) containing either anti-CD62P-PE (2 µL) or anti-fibrinogen-FITC (2 µL) (for platelet activation), or anti-CD45-PE (5 µL) or anti-CD42a-FITC (5 µL) (for platelet-leukocyte aggregation). After 15 min, compensation controls were diluted in modified Tyrode's buffer (2 mL), pelleted (200g, 23°C, 10 min), decanted, and then suspended in modified Tyrode's buffer (0.5 mL). Samples were

subsequently acquired using the BD FACSDiva Compensation Setup feature, where compensation is automatically calculated and applied to the experiment file.

Platelet activation was examined using antibodies against CD62P and human fibrinogen. CD62P is expressed on the platelet surface after degranulation while fibrinogen binds to αIIbβ3. Activated platelets bind these antibodies and can be distinguished from inactive platelets according to their fluorescence intensity (Figure 2.1). For the determination of CD62P expression and fibrinogen binding, platelets were gated on their characteristic scatter properties and 10,000 events were analysed for median fluorescence. To ensure that data were representative of the entire platelet population, we confirmed the accuracy of gating in separate samples containing the platelet-specific marker CD42b. Gates were adjusted until >95% of the gated population stained positive for anti-CD42b-FITC versus FITC Mouse IgG$_1$ (Figure 2.2). CD62P expression and fibrinogen binding were analysed on gated cells and expressed as the percentage of positive cells above a predefined threshold, which was set at 2% to exclude negative fluorescence as previously described (Metcalfe et al., 1997).

(A) UNACTIVATED PLATELETS

LASER EXCITATION

FLUORESCENCE

(B) ACTIVATED PLATELETS

LASER EXCITATION
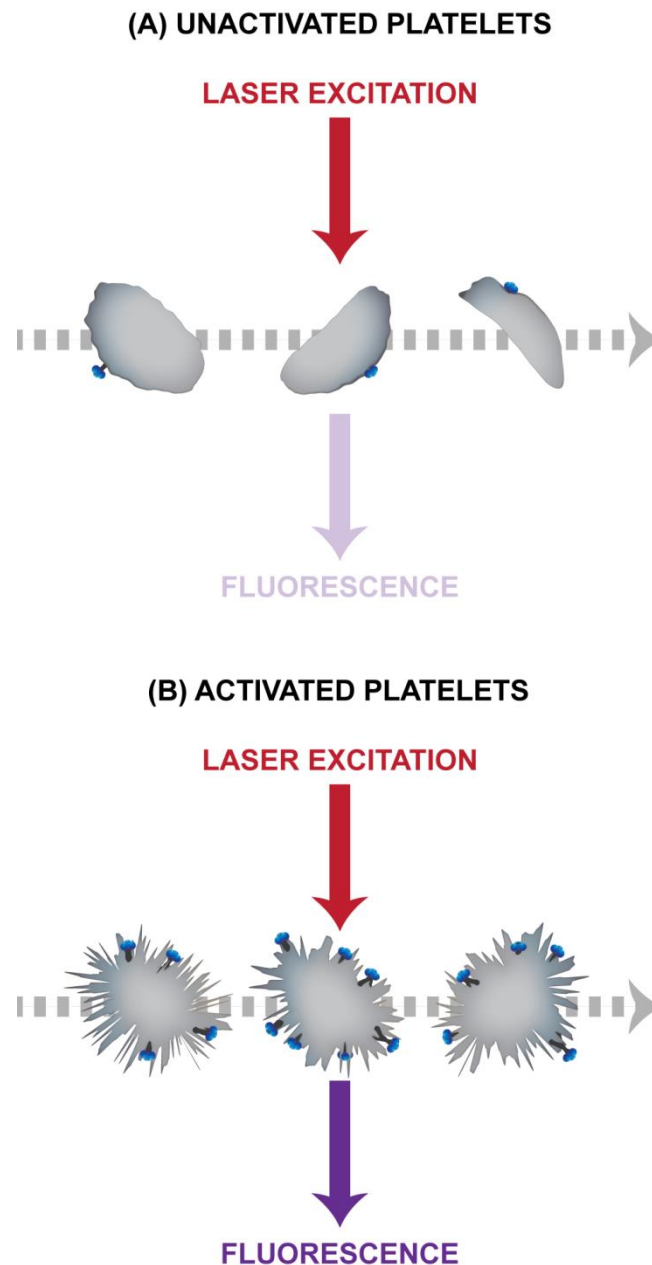
FLUORESCENCE

Figure 2.1. Flow cytometric analysis of platelet activation. (**A**) Inactive platelets bind few activation-dependent antibodies and generate little fluorescence whereas (**B**) activated platelets bind many activation-dependent antibodies and generate intense fluorescent signals.
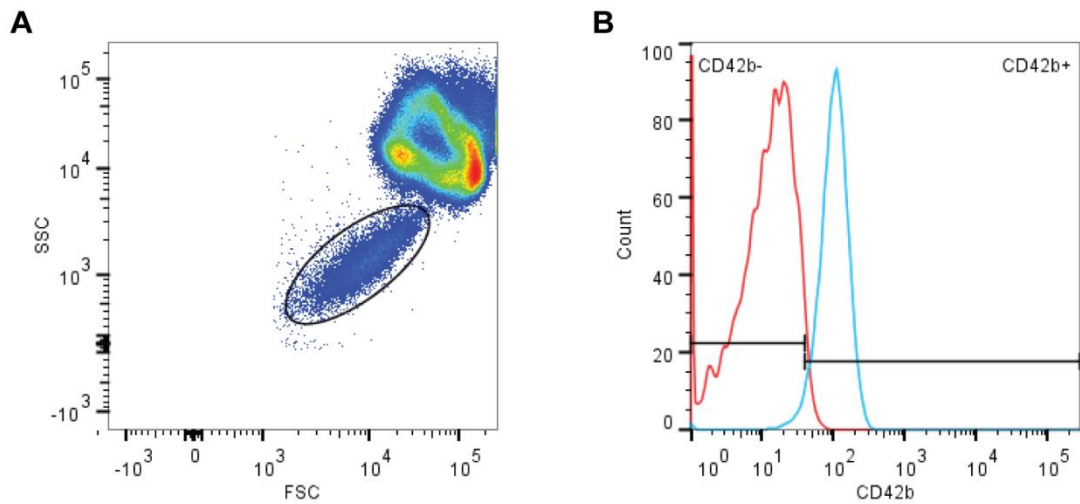
Figure 2.2. Flow cytometric identification of platelets in whole blood.
(**A**) Platelets were gated on their scatter properties. (**B**) Cells within the gate were positive for the platelet-specific marker CD42b (blue trace) above an appropriate negative threshold (red trace).

For platelet-leukocyte aggregates, monocyte and neutrophil subpopulations were identified based on measures of light scatter and CD45 expression (Figure 2.3). To determine the percentage of leukocytes binding platelets, these subpopulations were analysed for the platelet-specific antigen CD42a (Li et al., 1999). Data were analysed with FlowJo (TreeStar, Ashland, OR).
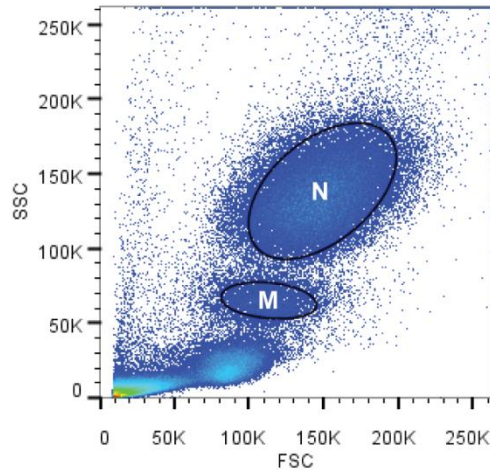
Figure 2.3. Flow cytometric identification of leukocyte subpopulations in whole blood. Monocytes (M) and neutrophils (N) were gated on measures of forward- and side scatter.

2.6 Phosphoflow cytometry

Flow cytometry is often used to examine the expression of cell surface markers, the expression of which is the result of complex intracellular signalling events. As flow cytometry protocols have developed in scope and complexity, it has become possible to measure intracellular signalling events such as protein phosphorylation. Since phosphorylation-based signalling events are reversible, this application requires the fixation of stimulated intact cells whose membranes must be permeabilised so that fluorescent-labelled phosphospecific antibodies can access their intracellular epitopes. As samples pass through the cytometer, they emit fluorescence that is proportional to the level of phosphorylation inside the cell. This rapid and convenient technique is suitable for routine laboratory use and correlates with immunoblotting. As part of this project, we developed a flow cytometric

method for the analysis of signalling events in washed platelets and those in whole blood.

2.6.1 Sample preparation for phosphoflow cytometry

We tested various fixation, permeabilisation, and staining techniques to determine the optimal conditions for sample preparation (see Chapter 4, section 2). Washed platelets (1×10^8 platelets/mL, 10^7 cells, 100 µL) were stimulated at 37°C in 96-well polypropylene plates containing the appropriate agonists, antagonists or inhibitors. After stimulation, platelets were fixed for 10 min with paraformaldehyde (PFA) solution (1.5% final concentration, 100 µL). Platelets were then pelleted ($1000g$, 4°C, 10 min), supernatants were aspirated, and platelets were permeabilised for 10 min with Triton X-100 (0.1%) in phosphate buffered saline (PBS, 1.8 mM KH_2PO_4, 10 mM Na_2HPO_4, 2.7 mM KCl, 137 mM NaCl, pH 7.4) (200 µL). Permeabilised platelets were pelleted, washed with PBS, pelleted again and then resuspended in PBS (100 µL) containing the indicated phosphospecific antibodies (2 µg/mL). Platelets were stained on ice for 30 min, washed with PBS (200 µL), pelleted and then resuspended in PBS (100 µL) containing Alexa Fluor 647 (1 µg/mL). We used Alexa Fluor 647-labeled secondary antibodies to generate fluorescent signals because our phosphospecific antibodies were not available as fluorophore-labelled conjugates. Platelets were stained on ice in the dark for 45 min, washed with PBS (200 µL), pelleted, resuspended in PBS (200 µL), and then transferred to FACS tubes for flow cytometric analyses using a BD LSRFortessa. Whole blood analyses

were performed using 15 µL of citrated blood and followed the same procedure except that samples were fixed with BD Phosflow Lyse/Fix Buffer (300 µL) according to the manufacturer's protocol.

2.6.2 Fluorescent cell barcoding

In fluorescent cell barcoding (FCB), samples are labelled (or barcoded) with amine-reactive fluorophores, which bind covalently to the primary amine groups (R-NH$_2$) of cellular proteins. These fluorophores can be combined in different ratios to create unique fluorescent signatures for individual samples (Krutzik and Nolan, 2006). Since reacted fluorophores covalently attach to cells, unbound fluorophores can be washed away, allowing multiple barcoded samples to be combined in a single well for staining and acquisition in a single analytical run, increasing throughput and decreasing acquisition time. FCB was incorporated into the standard protocol described in section 2.6.1 (Figure 2.4) where fixed and permeabilised platelets were washed, resuspended in PBS (200 µL) and then transferred to a 96-well plate containing appropriate dilutions of the indicated fluorophores.
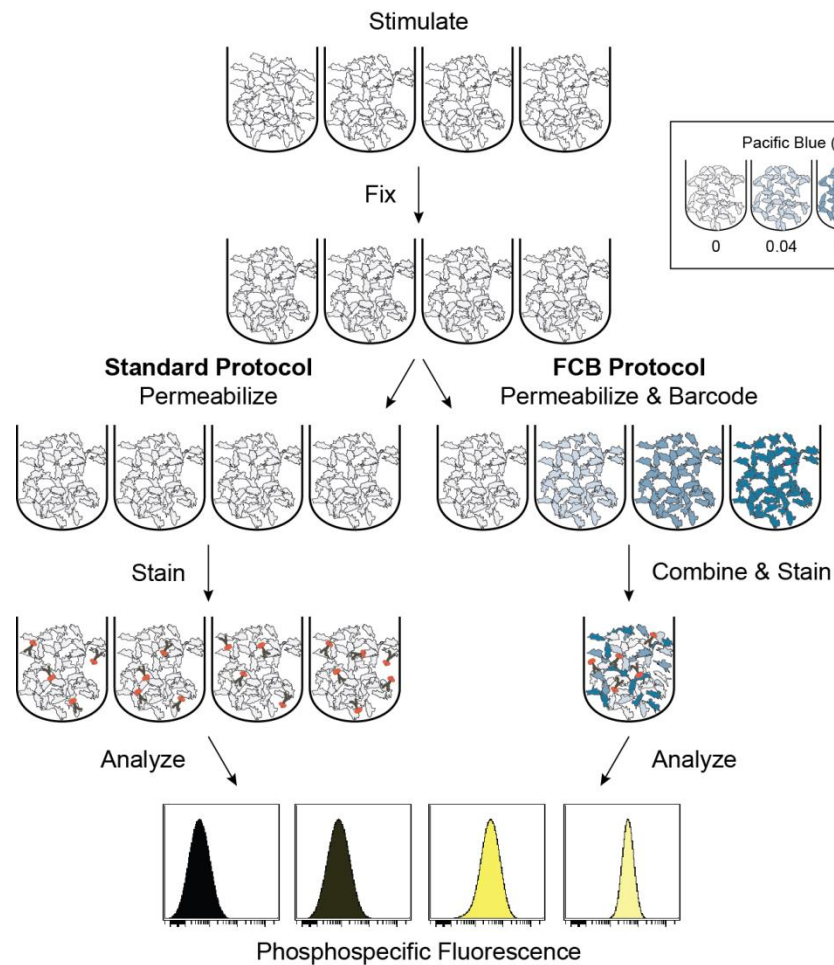
Figure 2.4. Fluorescent cell barcoding. Samples are stimulated, fixed, and then permeabilised. In standard phosphoflow, these samples are stained with phosphospecific antibodies and analysed individually. In FCB, permeabilised samples are barcoded with different intensities of amine-reactive fluorophores (e.g., Pacific Blue), combined into a single well, and then stained with phosphospecific antibodies. During analysis, combined barcoded samples are deconvoluted according to the unique fluorescent signatures of the original samples yielding the same robust signalling data as the standard protocol (Krutzik and Nolan, 2006).

Fluorophores were prepared at 40× concentrations in PBS and equal volumes (5 µL) were pipetted into the wells of a fresh 96-well plate according to the matrices shown in Figures A1-A5. The final volume in each well was brought up to 200 µL by addition of platelet suspensions from the original plate in which samples were stimulated, fixed, and permeabilised. Samples were thoroughly mixed with fluorophores by pipetting up and down. Samples were barcoded on ice in the dark for 30 min before unbound fluorophores were removed by two washes in PBS (200 µL). Barcoded samples were combined into a single well and pelleted (1000g, 4°C, 10 min) if the resulting volume was greater than 100 µL. The combined barcoded sample (100 µL) was stained with primary and secondary antibodies as described in section 2.6.1 and then transferred to a single FACS tube for flow cytometric analysis.

Platelets were barcoded with a number of different fluorophores, including Alexa Fluor 488, Alexa Fluor 750, DyLight 800, and Pacific Blue (for examples see Figures A1-A5), allowing us to create up to 96 distinct fluorescent signatures. Automatic compensation was applied using unstained samples as negative controls and single-colour highly-barcoded samples (those stained with the highest concentration of one particular fluorophore but no others) as positive controls. Small volumes of unmixed barcoded samples were set aside at the sample combination step for use as compensation controls. Fluorophores with distinct emission profiles were selected to minimise spillover into adjacent channels so that the median fluorescence intensity (MFI) of the parameter of interest did not fluctuate in a pattern reflecting the FCB matrix. To check the accuracy of compensation, we set aside a small volume of the combined barcoded sample prior to

antibody staining. This sample was acquired and barcoded populations were gated and analysed for Alexa Fluor 647 fluorescence. If fluorescence fluctuated between barcoded populations, the compensation matrix was adjusted until spillover was eliminated. Thus, we could be certain that variations in Alexa Fluor 647 fluorescence represented variations in protein phosphorylation and not variations in the intensity of barcoding markers.

Platelets were gated on their scatter properties and 10,000 events were analysed per sample for median fluorescence. Unlike the standard protocol, FCB experiments require an additional step where barcoded populations are deconvoluted (or separated by gating) into the individual samples they represent. Here, samples were deconvoluted from two-dimensional plots of scatter versus fluorescence as previously described (Figure 2.5) (Krutzik et al., 2011). Fold change was calculated by dividing the MFI of the stimulated sample by that of the unstimulated sample. It is important to recognise that unstimulated samples represent basal levels of phosphorylation and that these levels may change as soon as blood is drawn from the body and platelets are removed from physiological systems that can modulate their signalling activity such as the vascular endothelium, which actively secretes PGI_2 and NO. To minimise data variation due to delays between sampling and analysis, blood samples were processed as soon as possible after venepuncture. Data were presented either as histograms, where a shift along the *x*-axis and a transition to brighter colours represents an increase in phosphorylation; or as heatmaps, where brighter squares represent an increase in phosphorylation. Data were analysed with Cytobank (Kotecha et al., 2010).
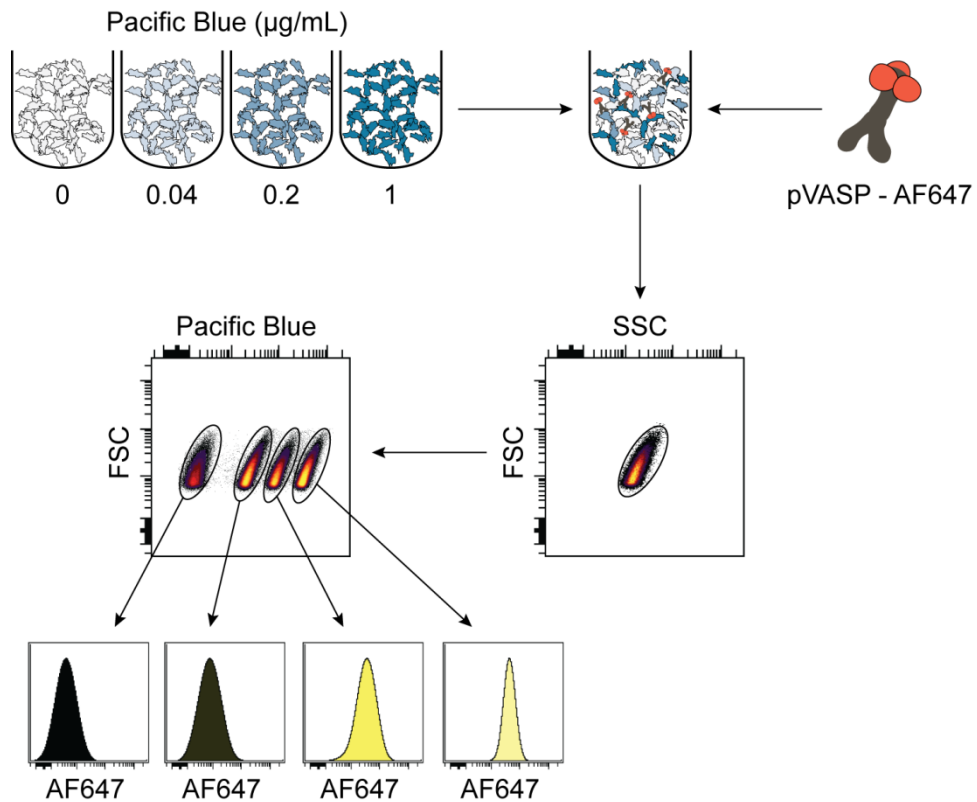
Figure 2.5. Deconvolution method for fluorescent cell barcoding. Stimulated, fixed, and permeabilised platelets were barcoded with Pacific Blue (0, 0.04, 0.2, and 1 µg/mL), combined into a single well, and then stained with Alexa Fluor 647 (AF647)-conjugated phosphospecific antibodies. During sample acquisition, platelets were gated on their scatter properties (FSC versus SSC). Plotting FSC versus Pacific Blue reveals four distinct populations that correspond to the original four samples. Once gated, these populations can be analysed as individual samples for phosphospecific fluorescence (AF647).

2.7 Measurement of platelet aggregation *in vitro*

Platelet aggregation plays an important role in thrombosis (Ruggeri, 2002) and is the end result of a series of complex signalling processes. Platelet aggregation is commonly measured by optical aggregometry using the method developed by Born (Born, 1962) where the extent of aggregate formation is proportional to the transmission of light through a platelet suspension. Unstimulated platelets form a turbid suspension of cells that impede light transmission. Following agonist stimulation, the formation of aggregates reduces the turbidity of the suspension and increases the transmission of light through the platelet suspension. Aggregation was expressed as a percentage and measured in real-time (Figure 2.6).

In this study, washed platelets (2.5×10^8 platelets/mL) were pre-incubated at 37°C with the indicated prostaglandin analogues in the presence or absence of antagonists for 2 min prior to stimulation with collagen (5 µg/mL), and aggregation was measured for 3 min under continuous stirring (1000 rpm) using a Chrono-log optical aggregometer. Calibration was performed using unstimulated platelets (0% aggregation) and modified Tyrode's buffer (100% aggregation).
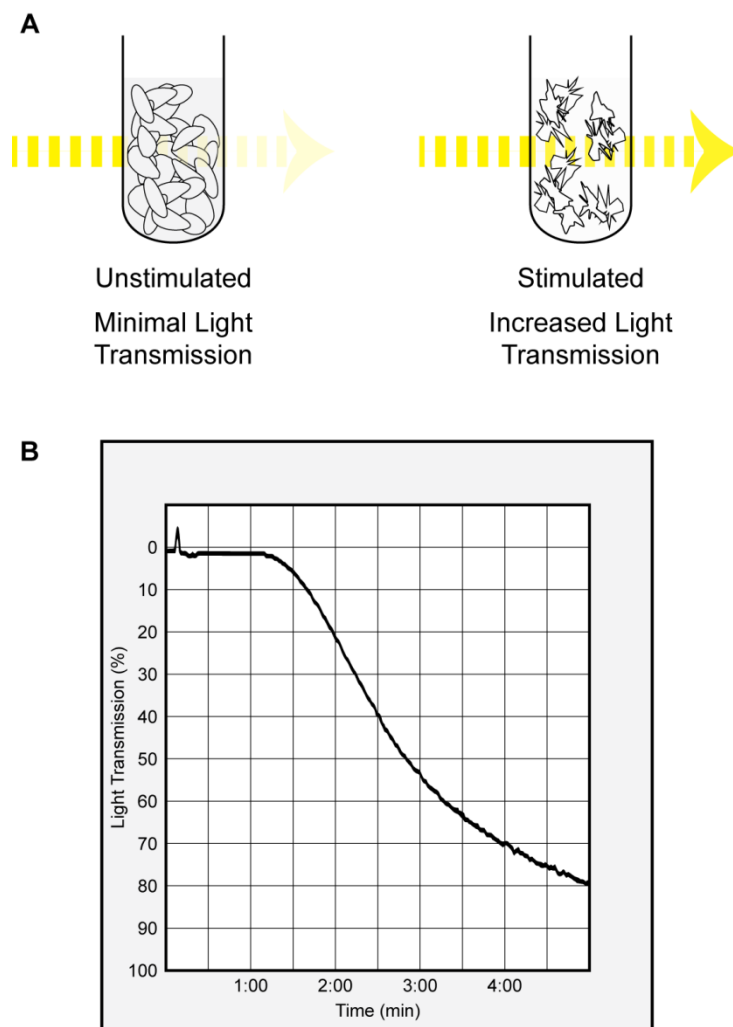
Figure 2.6. Optical measurement of platelet aggregation. (**A**) Unstimulated platelets form a turbid suspension of cells that impede light transmission (yellow arrow). After stimulation, the formation of aggregates reduces turbidity and increases the transmission of light through the platelet suspension. (**B**) Light transmission is expressed as a percentage (0-100%) and measured in real time as the platelets aggregate.

2.8 Measurement of platelet cAMP

cAMP levels were determined using a well-established enzyme immunoassay (EIA) kit according to the manufacturer's protocol. The assay is based on the competition between free cAMP and an acetylcholinesterase-conjugated cAMP (cAMP tracer) to occupy a limited number of cAMP binding sites on a cAMP-specific rabbit antibody. The amount of free cAMP is variable while the amount of cAMP tracer is constant in every assay. Therefore, the amount of cAMP tracer bound to the cAMP rabbit antibody is inversely proportional to the amount of free cAMP in the sample.

2.8.1 Sample preparation for the measurement of platelet cAMP

Washed platelets ($2x10^8$ platelets/mL) were treated with prostaglandins (1 µM) for 2 minutes at 37°C. Reactions were terminated by addition of lysis buffer containing 0.1 M HCl to inhibit endogenous phosphodiesterase activity. Samples were then centrifuged ($1000g$, 4°C, 10 min), and supernatants were diluted (1:4) with EIA buffer. To improve assay sensitivity, standards and diluted supernatants were acetylated by addition of potassium hydroxide and acetic anhydride according to the manufacturer's protocol. Since cAMP antibodies are raised against cAMP-acetylcholinesterase (cAMP tracers), they have a low affinity for free cAMP. Acetylation induces a structural change that enhances the immunogenicity of free cAMP, allowing it to bind antibodies with a greater affinity.

Standards, samples, cAMP tracer, and a cAMP-specific rabbit antibody were added to an anti-rabbit IgG-coated assay plate and incubated for 18 hr at 4°C. The plate was then washed and filled with Ellman's reagent, which contained an acetylcholinesterase substrate. The resultant enzyme-substrate reaction yielded a yellow-coloured product that was measured at 405 nm using a microplate spectrophotometer (Thermo Scientific Multiskan GO, Loughborough, UK). The intensity of the colour was proportional to the amount of cAMP tracer bound to the well, which was inversely proportional to the amount of free cAMP in the sample.

Data were analysed with the Cayman Chemical EIA Analysis Tool. All assays were carried out in triplicate with independent donors and cAMP was expressed as fmol/10^6 platelets.

2.9 Statistical Analysis

Results, expressed as means ± SEM, underwent one-way ANOVA with Tukey HSD using GraphPad Prism 6 (GraphPad Software, La Jolla, CA). Significance was accepted at $P < 0.05$.

Analysis of Platelet Function

3.1 Introduction

Blood platelets are central to thrombosis, haemorrhage, and inflammation (Wagner and Burger, 2003). Under normal physiological conditions, platelets are maintained in a resting state by the endothelial-derived inhibitors, prostacyclin (PGI_2) and nitric oxide (NO). To prevent haemorrhage, platelets aggregate to form a primary haemostatic plug and stimulate the coagulation cascade at sites of vascular injury. The formation of a stable haemostatic plug requires the degranulation of activated platelets and the binding of fibrinogen to integrin αIIbβ3. Antibodies against fibrinogen and granule-specific proteins such as P-selectin (CD62P) have emerged as powerful tools for the detection and quantification of activated platelets (Michelson et al., 2000). While P-selectin and αIIbβ3 are important mediators of platelet-platelet aggregation, they also mediate the adhesion of activated platelets to leukocytes. Platelet-leukocyte aggregates are thought to be sensitive markers of platelet activation (Michelson et al., 2001), but little is known about the pathways that are capable of inducing interactions between these cells. Platelets can be activated by multiple pathways. Key among these are the ADP, collagen, and thrombin-mediated pathways. Here, we show that these pathways have distinct effects on the aggregation of platelets with important leukocyte subpopulations (monocytes and neutrophils).

A major aim of this study is to demonstrate that PGI_2 inhibits platelet function and that its inhibitory properties can be detected by flow cytometry in whole blood. CD62P expression and fibrinogen binding are regulated through

different mechanisms and represent different aspects of the platelet activation process. Here, we show that PGI_2 inhibits CD62P expression and fibrinogen binding downstream of several different receptor systems. This suggests that PGI_2 regulates multiple signalling pathways and multiple aspects of platelet function.

3.2 PGI_2 inhibits platelet aggregation

Platelet function is commonly examined by light transmission aggregometry (LTA). Although LTA is considered the gold standard for platelet function testing (Harrison, 2009), it lacks physiological relevance because whole blood samples must be manipulated to obtain washed platelet suspensions. In initial experiments, we used LTA to show that the physiological inhibitor PGI_2 could inhibit collagen-induced platelet aggregation (Figure 3.1). Here, washed platelets were pre-incubated with PGI_2 (0-100 nM) prior to stimulation with collagen (5 µg/mL). Collagen alone induced a maximal aggregation response that was inhibited in a dose-dependent manner by PGI_2 (Figure 3.1A). PGI_2 produced potent inhibition of platelet aggregation with an IC_{50} value of 12 nM (Figure 3.1B). In the following sections, we show that flow cytometry can be used to examine the effects of PGI_2 on different aspects of platelet function (CD62P expression and fibrinogen binding) both rapidly and conveniently in whole blood.
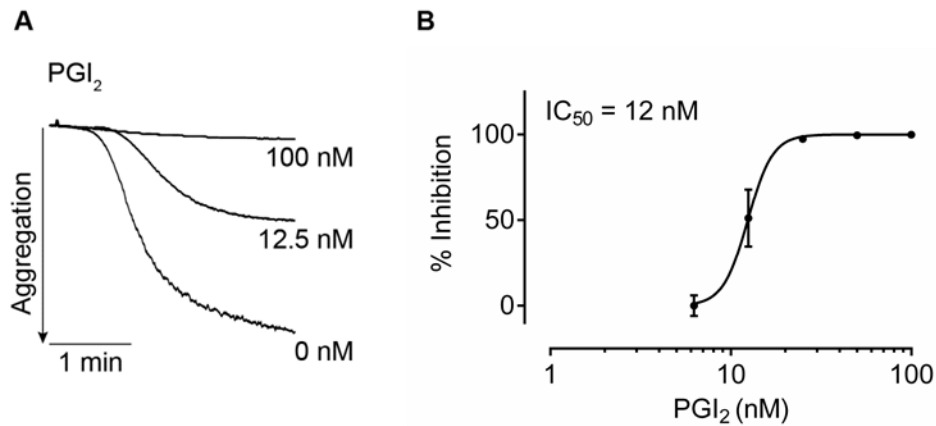
Figure 3.1. PGI$_2$ inhibits platelet aggregation. (**A**) Traces, representative of three independent experiments, show that PGI$_2$ inhibits collagen-induced platelet aggregation in a concentration-dependent manner. (**B**) Dose-response curve reveals the potency of PGI$_2$, where data points represent the mean ± SEM from three independent experiments. Platelets were stimulated with collagen (5 µg/mL) following pre-incubation (2 min) with PGI$_2$.

3.3 Analysis of platelets in whole blood

Whole blood flow cytometry can be performed either by single-colour analysis in which the platelet population is identified by forward- and side scatter or by two-colour analysis in which the sample is colabelled with an antibody raised against a platelet-specific antigen such as CD42b (Goodall and Appleby, 2004). Single-colour methods are simple and economic but often exclude platelets whose scatter properties fall outside the normal range. Two-colour methods are therefore preferred for the analysis of samples from patients with giant platelet syndromes or storage pool disorders. Antibody binding can be expressed either as median fluorescence intensity (MFI) or as the percentage of platelets staining positive for a particular antibody. Percentage positive data better represent the expression

of antigens that are not normally present on the platelet surface (such as CD62P and fibrinogen) while MFI better represents the expression of antigens that are constitutively expressed. Unlike MFI, percentage positive data are not affected by variations in signal intensity that may result from photobleaching or variations in reagent lots.

In the first part of the study, we performed multiparameter analyses of CD62P expression and fibrinogen binding in response to a number of distinct platelet agonists and then evaluated whether these responses were sensitive to inhibition by PGI$_2$. Platelets were gated on forward- and side scatter characteristics and the accuracy of gating was confirmed in a separate sample using the platelet-specific marker CD42b (see section 2.5.2).

3.3.1 ADP-induced platelet activation

To assess *in* vitro platelet activation, we measured both CD62P expression and fibrinogen binding in whole blood samples incubated with ADP (0.1-10 µM) (Figure 3.2A and B). Submicromolar ADP (0.1 µM) did not induce CD62P expression when compared with unstimulated platelets but significant increases were observed in response to 1 µM ADP (39 ± 6%) and 10 µM ADP (71 ± 5%) (Figure 3.2C). Submicromolar ADP (0.1 µM) failed to induce fibrinogen binding but significant increases were detected on platelets stimulated with 1 µM ADP (40 ± 8%) and 10 µM ADP (68 ± 6%) (Figure 3.2C).

Figure 3.2. Flow cytometric analysis of ADP-induced platelet activation.
(**A**) CD62P expression and (**B**) fibrinogen (FGN) binding in unstimulated platelets (red trace), those stimulated with ADP (10 µM) (blue trace), and those stimulated with ADP (10 µM) after pre-incubation with PGI_2 (10 nM) (orange trace). (**C**) ADP-induced CD62P expression and fibrinogen binding is concentration-dependent. (**D**) PGI_2 inhibits ADP-induced CD62P expression and fibrinogen binding in a concentration-dependent manner. Data from four independent experiments are expressed as means ± SEM (*P <0.05).

3.3.2 The effect of PGI$_2$ on ADP-induced platelet activation

To determine the *in vitro* effects of PGI$_2$ on ADP-induced CD62P expression and fibrinogen binding, whole blood samples were pre-incubated with PGI$_2$ (0.1-10 nM, 2 min) before stimulation with ADP (10 µM). Consistent with previous observations (Figure 3.2C), ADP induced substantial CD62P expression (71 ± 5%) and fibrinogen binding (68 ± 6%). CD62P expression was significantly inhibited (48%) by 0.1 nM PGI$_2$ with further inhibition (67%) at 1 nM PGI$_2$ (P <0.05). CD62P expression on platelets incubated with 10 nM PGI$_2$ was not significantly different from that on unstimulated platelets indicating complete inhibition of degranulation (Figure 3.2D). Fibrinogen binding was significantly inhibited (39- and 61%) by 0.1- and 1 nM PGI$_2$ with complete inhibition at 10 nM PGI$_2$ (Figure 3.2D). These data confirm the concentration-dependent ability of PGI$_2$ to inhibit ADP-induced platelet activation.

3.3.3 CRP-XL-induced platelet activation

Having examined ADP-induced platelet activation, we next measured CD62P expression and fibrinogen binding on platelets stimulated with the GPVI-selective agonist CRP-XL (Morton et al., 1995). While the physiologic GPVI agonist collagen cross-links and aggregates platelets, CRP-XL can be used without hindrance in flow cytometric analyses of platelet activation (Kehrel et al., 1998). CRP-XL (0.1 µg/mL) did not induce platelet activation under the conditions used here but higher concentrations (1- and 10 µg/mL) of the peptide induced significant CD62P expression and fibrinogen binding (P

<0.05). CD62P expression increased significantly in response to 1 μg/mL CRP-XL (48 ± 12%) and 10 μg/mL CRP-XL (95 ± 2%) while fibrinogen binding increased on platelets stimulated with 1 μg/mL CRP-XL (49 ± 14%) and 10 μg/mL CRP-XL (96 ± 2%) (Figure 3.3A, B and C).
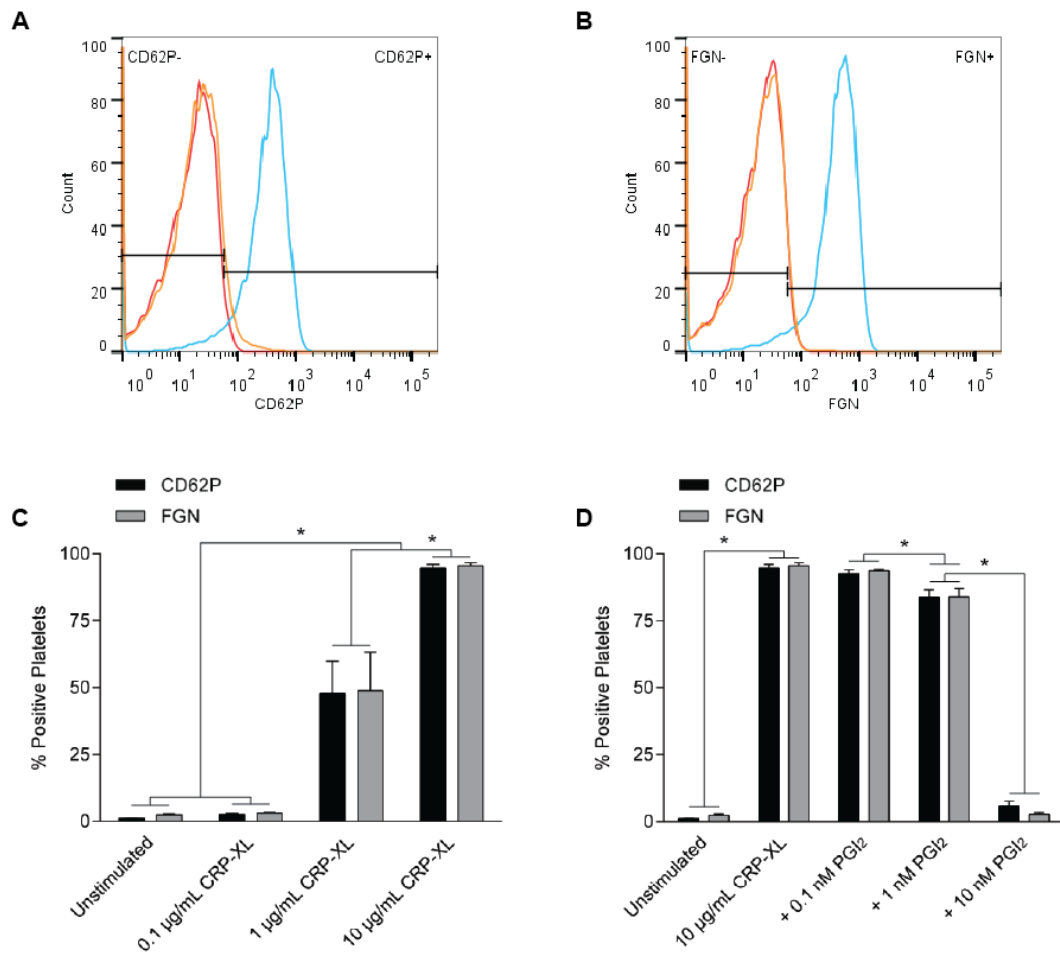
Figure 3.3. Flow cytometric analysis of CRP-XL-induced platelet activation. (**A**) CD62P expression and (**B**) fibrinogen (FGN) binding in unstimulated platelets (red trace), those stimulated with CRP-XL (10 µg/mL) (blue trace), and those stimulated with CRP-XL (10 µg/mL) after pre-incubation with PGI$_2$ (10 nM) (orange trace). (**C**) CRP-XL-induced CD62P expression and fibrinogen binding is concentration-dependent. (**D**) PGI$_2$ inhibits CRP-XL-induced CD62P expression and fibrinogen binding in a concentration-dependent manner. Data from three independent experiments are expressed as means ± SEM (*P <0.05).

3.3.4 The effect of PGI$_2$ on CRP-XL-induced platelet activation

Having demonstrated that PGI$_2$ could inhibit ADP-induced platelet activation, we sought to determine whether PGI$_2$ could inhibit GPVI-mediated platelet activation. Subnanomolar PGI$_2$ (0.1 nM) did not affect CD62P expression or fibrinogen binding on platelets stimulated with CRP-XL (10 µg/mL) but significant inhibition was observed at 1- and 10 nM PGI$_2$ ($P <0.05$) (Figure 3.3D). CD62P expression was significantly inhibited (11%) by 1 nM PGI$_2$ with further inhibition (94%) at 10 nM PGI$_2$. Fibrinogen binding was significantly inhibited (12%) by 1 nM PGI$_2$ with complete inhibition at 10 nM PGI$_2$ (Figure 3.3D). These data reveal that PGI$_2$ can inhibit GPVI-mediated platelet activation.

3.3.5 TRAP-induced platelet activation

We next measured CD62P expression and fibrinogen binding through G protein-coupled PAR receptors, which are responsible for thrombin-mediated platelet activation. Thrombin-mediated platelet activation occurs predominantly through PAR-1, which is activated when thrombin cleaves an amino-terminal extension unmasking a self-activating tethered ligand (Andersen et al., 1999). While the physiologic PAR agonist thrombin cross-links fibrin and causes clotting in whole blood samples, the PAR-1 activating peptide SFLLRN (TRAP) can be used without hindrance in flow cytometric analyses of platelet activation (Goodall and Appleby, 2004). TRAP (1 µM) did not significantly induce platelet activation under the conditions used here but near-maximal CD62P expression and fibrinogen binding were observed in

response to 5- and 10 µM TRAP (Figure 3.5A, B and C). CD62P expression

increased significantly on platelets stimulated with 5 µM TRAP (96 ± 2%) and

10 µM TRAP (98 ± 1%) while fibrinogen binding increased in response to 5

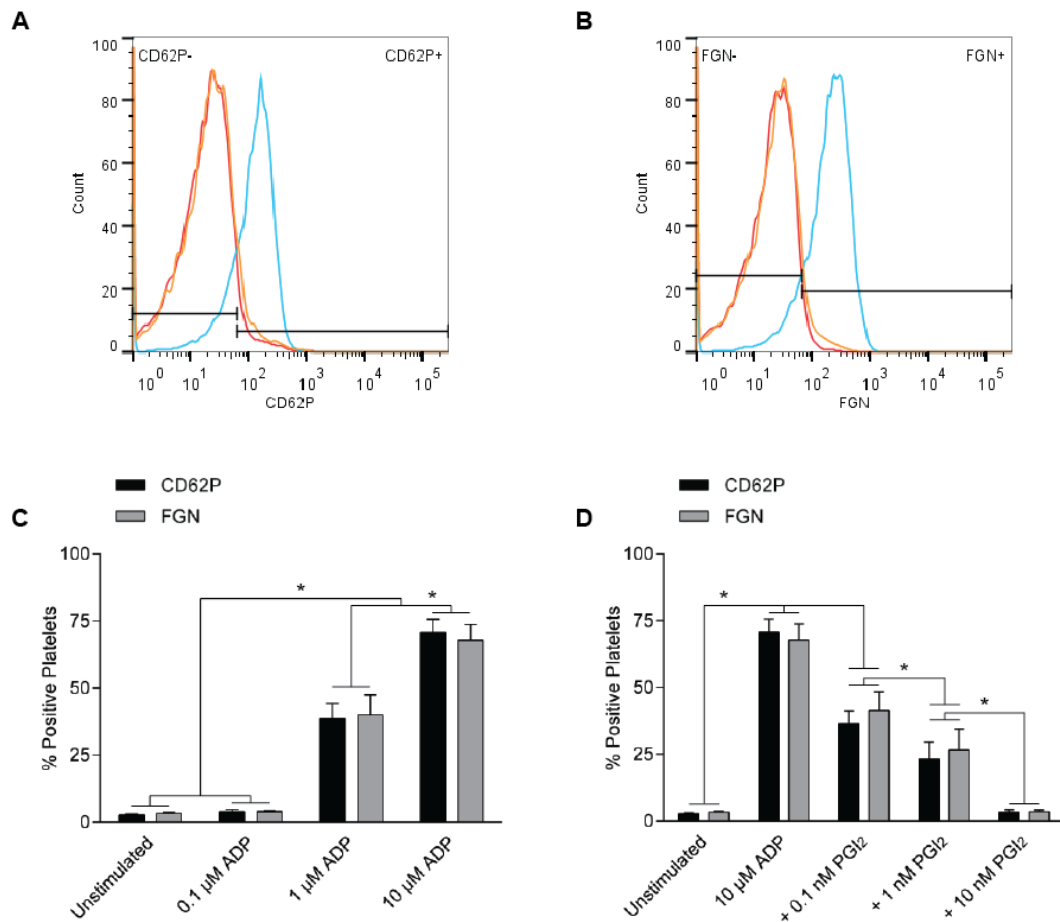µM TRAP (92 ± 3%) and 10 µM TRAP (93 ± 1%) ($P < 0.05$).
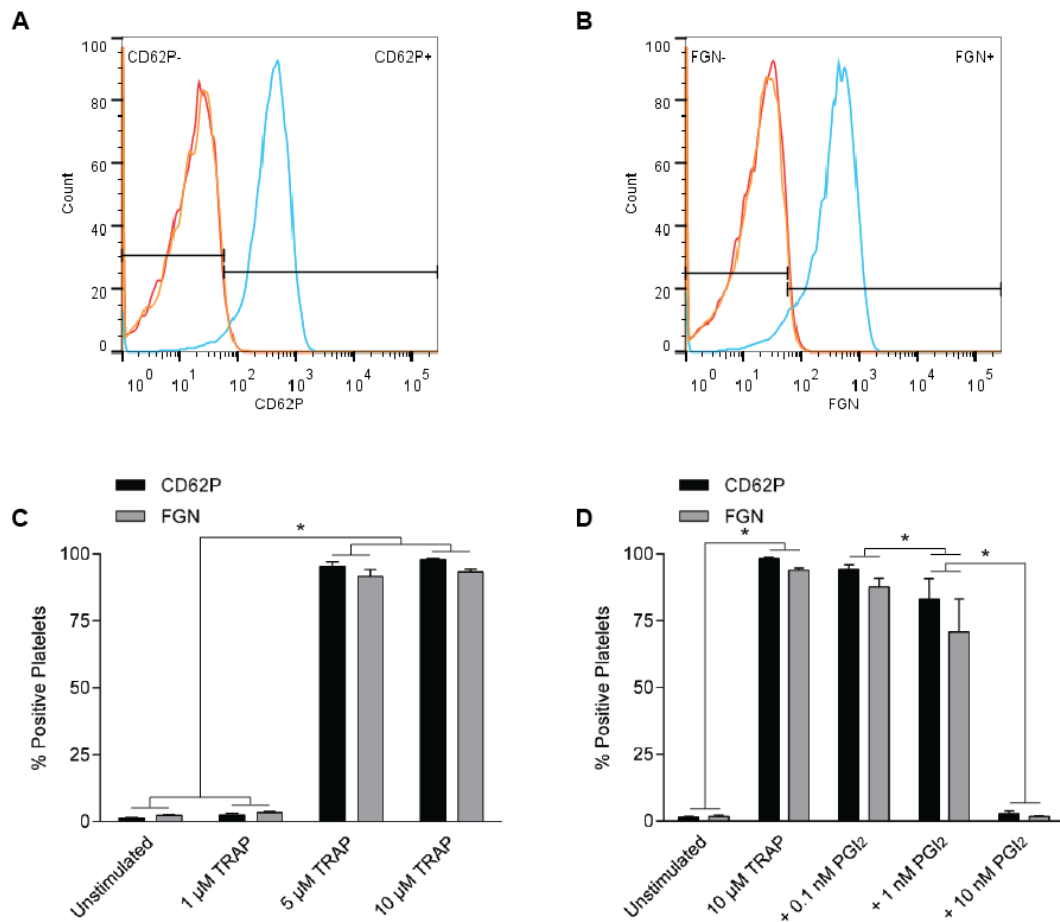
Figure 3.4. Flow cytometric analysis of TRAP-induced platelet activation. (**A**) CD62P expression and (**B**) fibrinogen (FGN) binding in unstimulated platelets (red trace), those stimulated with TRAP (10 µM) (blue trace), and those stimulated with TRAP (10 µM) after pre-incubation with PGI$_2$ (10 nM) (orange trace). (**C**) TRAP-induced CD62P expression and fibrinogen binding is concentration-dependent. (**D**) PGI$_2$ inhibits TRAP-induced CD62P expression and fibrinogen binding in a concentration-dependent manner. Data from five independent experiments are expressed as means ± SEM (*P <0.05).

3.3.6 The effect of PGI$_2$ on TRAP-induced platelet activation

Consistent with previous observations for ADP and CRP-XL (Figures 3.2D and 3.3D), PGI$_2$ inhibited TRAP-induced platelet activation in a concentration-dependent manner (Figure 3.4A, B and D). Subnanomolar PGI$_2$ (0.1 nM) failed to inhibit CD62P expression and fibrinogen binding on platelets stimulated with TRAP (10 µM) but significant inhibition was observed at 1 nM PGI$_2$ where CD62P expression and fibrinogen binding were inhibited by 15- and 25% respectively (P <0.05). Further inhibition was observed at 10 nM PGI$_2$ where TRAP-induced platelet activation was completely abolished (P <0.05) (Figure 3.4D). Together, these data show that PGI$_2$ can inhibit ADP, CRP-XL, and TRAP-induced platelet activation suggesting that PGI$_2$ targets aspects of platelet function that are common to P2Y$_{12}$, GPVI, and PAR receptor systems.

3.4 Platelet-leukocyte aggregation in whole blood

It has been suggested that platelet-leukocyte aggregates are sensitive markers of platelet activation *ex vivo*. Here, platelet-leukocyte aggregates were detected by two-colour flow cytometry in which leukocytes were first identified as CD45 positive cells and then discriminated into monocyte and neutrophil subpopulations according to measures of forward- and side scatter. To determine the percentage of leukocytes binding platelets, these subpopulations were analysed for the platelet-specific antigen CD42a (Goodall and Appleby, 2004). We avoided antibodies against CD42b

because its epitope is often masked in platelet-leukocyte aggregates (McEver, 2007).

Our data show that monocytes (5%) and neutrophils (4%) associate with platelets in untreated whole blood (Figure 3.5). After stimulation with ADP (10 μM), the monocyte population binding platelets increased from 5- to 16% while the percentage of neutrophils binding platelets increased from 4- to 5%. CRP-XL (10 μg/mL) induced a higher percentage of platelet-monocyte (59%) than platelet-neutrophil (16%) aggregation while TRAP (10 μM) induced 64% platelet-monocyte versus 46% platelet-neutrophil aggregation. These data show that different agonists induce varying degrees of platelet-leukocyte aggregation in whole blood.
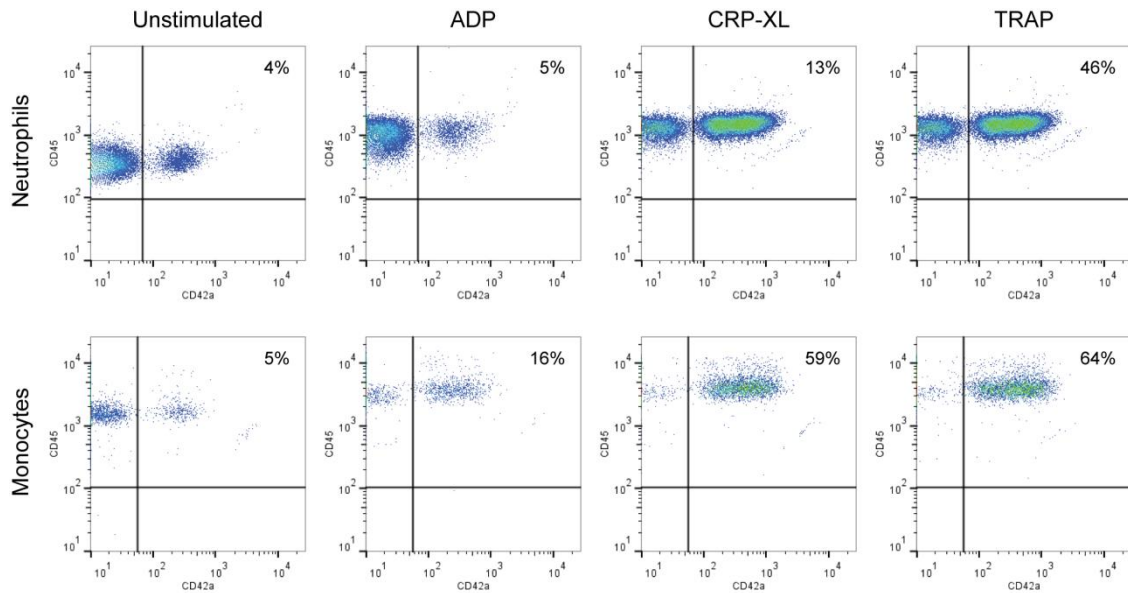
Figure 3.5. Flow cytometric analysis of agonist-induced platelet-leukocyte aggregation. Platelet-leukocyte aggregation in untreated whole blood samples and those incubated with ADP (10 µM), CRP-XL (10 µg/mL), and TRAP (10 µM). Representative data from three independent experiments.

3.5 Discussion

Over the past three decades, the flow cytometric analysis of platelet function has become increasingly popular. In the 1980s, whole blood assays were developed for the measurement of platelet activation *in vivo*. When whole blood was incubated with exogenous agonists, these assays could predict the reactivity of circulating platelets *in vitro* (Shattil et al., 1987). Whole blood flow cytometry provides physiologic relevance while assays of platelet-rich plasma or washed platelets suffer from artifactual activation resulting from obligatory cell isolation procedures (Ejim et al., 1990, Wehmeier et al., 1991). Moreover; whole blood assays require only microliters of blood, making it possible to study neonates and individuals with thrombocytopenias (Michelson, 1996).

Flow cytometric assays of platelet activation normally employ antibodies against P-selectin (CD62P) and human fibrinogen, which represent different aspects of the platelet activation process. In this chapter, our aim was to establish basic methodology for the flow cytometric analysis of platelet activation and to determine whether we could detect inhibition by PGI_2. We used antibodies against CD62P and human fibrinogen that were coupled to fluorophores with different emission properties, enabling the simultaneous detection of both antigens. We demonstrated significant increases in CD62P expression and fibrinogen binding after stimulation with ADP, CRP-XL, and TRAP. These agonists induced platelet activation with varying degrees of potency. Goodall and Appleby (2004) found that TRAP (0.1-5 µM) induced >90% CD62P expression and fibrinogen binding while ADP (10 µM) induced 20-25% CD62P expression and 70-80% fibrinogen binding. We detected

more CD62P expression (71%) on ADP-stimulated platelets but our incubation times were shorter, which could explain greater retention of CD62P on the platelet surface. Indeed, activated platelets shed >60% of surface P-selectin within 2 hours when incubated at room temperature in whole blood (Berger et al., 1998). CRP-XL (10 µg/mL) induced >90% CD62P expression and fibrinogen binding consistent with previous observations (Jones et al., 2009, Joutsi-Korhonen et al., 2003).

While the immediate signalling mechanisms of different receptor systems are likely to differ, most agonists converge on a set of common intracellular targets (Varga-Szabo et al., 2009). Degranulation and P-selectin expression is a common response to all agonists. Platelet degranulation is a signalling amplification mechanism that serves to enhance platelet activation, encourage aggregation, and stabilise the growing thrombus. Binding of fibrinogen to $\alpha IIb\beta 3$ is common on agonist-stimulated platelets and facilitates homotypic (platelet-platelet) and heterotypic (platelet-leukocyte) aggregation (Gawaz et al., 1991). Both granule secretion and the activation of $\alpha IIb\beta 3$ are dependent on calcium mobilisation (Siess, 1989). ADP, CRP-XL, and TRAP activate distinct signalling pathways that converge on phospholipase C (PLC), which mediates the release of intracellular calcium through IP_3 receptors (Li et al., 2010). We identified TRAP as the most potent agonist, suggesting that PAR-1 is more efficiently coupled to PLC than $P2Y_{12}$ or GPVI. Indeed, TRAP stimulates more substantial calcium responses than ADP or collagen (Chatterjee et al., 2010). The PLC signalling node is likely targeted by PGI_2, which inhibits CD62P expression and fibrinogen binding on platelets stimulated with ADP, CRP-XL, and TRAP.

A major aim of this study is to use flow cytometry to examine platelet cyclic nucleotide signalling. With this in mind we first wished to demonstrate that PGI$_2$, which stimulates cAMP production and activates cAMP-dependent protein kinase (Haslam et al., 1999a), was active under our assay conditions. In platelets and megakaryocytes, this kinase phosphorylates and inactivates IP$_3$ receptors causing substantial inhibition of calcium release (Quinton and Dean, 1992, Tertyshnikova and Fein, 1998). However, it is unlikely that the inhibitory properties of PGI$_2$ are entirely dependent on the inhibition of calcium mobilisation. Indeed, the downstream cAMP-dependent protein kinase phosphorylates a number of targets that regulate platelet function through different mechanisms (Schwarz et al., 2001). PGI$_2$ inhibited CD62P expression and fibrinogen binding in response to ADP consistent with previous observations (Aye et al., 2014). For the first time, we demonstrated that PGI$_2$ inhibits CD62P expression and fibrinogen binding on platelets stimulated with CRP-XL and TRAP. However, PGI$_2$ was only effective against these agonists at high concentrations (10 nM). The lack of potent inhibition might result from minimal convergence between GPVI/PAR-1 and cAMP signalling pathways.

Flow cytometric assays of platelet function are frequently used to assess the efficacy of antiplatelet therapies in clinical disorders. Fibrinogen binding assays are normally performed to monitor the efficacy of αIIbβ3 antagonists. These anti-integrin agents are prescribed to reduce the risk of ischemic complications following percutaneous coronary intervention (Coller, 1997). Assays have also been developed that can measure, either directly or indirectly, the percentage of αIIbβ3 receptor occupancy (Jennings and White,

1998, Konstantopoulos et al., 1995). Platelet surface P-selectin is widely-regarded as the gold standard marker of platelet activation (Michelson and Furman, 1999). Because this adhesion molecule is expressed only on activated cells, it has achieved popularity as an independent predictor of future cardiovascular risk (Blake and Ridker, 2001). While P-selectin expression is irreversible *in vitro*, circulating degranulated platelets rapidly lose their surface P-selectin *in vivo* (Michelson et al., 1996). Since the *in vivo* half-life of detectable platelet-leukocyte aggregates is significantly longer than the *in vivo* half-life of platelet surface P-selectin, it has been suggested that these aggregates are more sensitive markers of platelet activation than P-selectin positive cells (Michelson et al., 2001). Nonetheless, the measurement of platelet-leukocyte aggregates has, perhaps owing to increased technical demands, failed to displace the P-selectin assay as the method of choice for measuring the activation state of circulating platelets.

We have shown that ADP, CRP-XL, and TRAP induce the aggregation of platelets with monocytes and neutrophils. These agonists induce CD62P expression and fibrinogen binding to αIIbβ3. Both of these antigens interact with leukocyte counter-receptors, including PSGL-1, Mac-1, and LFA-1 (McEver, 2007). The leukocyte glycoprotein PSGL-1 binds CD62P, facilitating the adhesion of activated platelets to circulating leukocytes and the rolling and arrest of circulating leukocytes on surface-adherent activated platelets (Fernandes et al., 2003, Smyth et al., 2001). Leukocyte integrin Mac-1 then binds αIIbβ3-bound fibrinogen to stabilise platelet-leukocyte aggregates (Lishko et al., 2004). To enhance adhesion, Mac-1 also binds CD42b and JAM-3 on the platelet surface membrane (Simon et al., 2000,

Santoso et al., 2002). Mac-1 activation is mediated by Src family kinases and results from the binding of PSGL-1 to CD62P (Evangelista et al., 2007). The cytoplasmic domain of PSGL-1 associates with the integral membrane protein Naf-1. PSGL-1 engagement induces the tyrosine phosphorylation of Naf-1, the recruitment of PI3K, and the functional upregulation and activation of Mac-1 (Wang et al., 2007). PSGL-1 signalling also mediates the activation of leukocyte integrin LFA-1, which binds fibrinogen and ICAM-2 on activated platelets (McEver, 2007). Chemokines, released from degranulated platelets, play an important role in leukocyte recruitment *in vivo* (von Hundelshausen et al., 2007). Binding of leukocytes to activated platelets is thought to accelerate thrombus formation. Indeed, leukocytes deliver tissue factor-bearing microparticles to developing thrombi (Falati et al., 2003). Moreover, the presence of leukocytes promotes fibrin deposition at sites of vascular injury (Palabrica et al., 1992). While platelet-leukocyte interactions are considered beneficial to natural clotting and wound healing processes, in various disease states these interactions correlate with unfavourable clinical outcomes. For example, platelet-leukocyte interactions have been shown to exacerbate rheumatoid arthritis (Gasparyan et al., 2011), predispose asthmaticus (Pitchford et al., 2003), and enhance tumour metastasis (Kim et al., 1998). Platelet-leukocyte interactions have also been implicated in the pathogenesis of bowel, kidney, lung, and skin diseases (Totani and Evangelista, 2010). Given their important role in a variety of clinical conditions, platelets and the molecular determinants of platelet-leukocyte interactions could represent attractive targets for therapeutic intervention.

This chapter has described the analysis of platelet function by multicolour flow cytometry. We have demonstrated increased CD62P expression and fibrinogen binding on platelets stimulated with ADP, CRP-XL, and TRAP and shown that these agonists have distinct effects on platelet-leukocyte interactions. We have also demonstrated the significant and reproducible inhibition of platelet activation by PGI_2. Having demonstrated that whole blood flow cytometry is sensitive to low concentrations of this inhibitor, we will next develop methodology to assess the impact of PGI_2 on cyclic nucleotide signalling, which regulates platelet function at the intracellular level. Like traditional assays of platelet function, platelet signalling is commonly measured in washed platelets and therefore lacks physiological relevance. Having shown that flow cytometry can be used to analyse platelets in the complex milieu of whole blood, the major question posed by this thesis is "why not look at platelet signalling events in whole blood too?"

Flow Cytometric Analysis of Platelet Signalling Events

4.1 Introduction

The activation of blood platelets at sites of vascular injury is a critical step in the haemostatic response preventing haemorrhage. Uncontrolled platelet activation is associated with arterial thrombosis (Ruggeri, 2002), which can predispose to serious clinical events such as myocardial infarction and stroke. Endogenous inhibitor mechanisms have evolved to regulate platelet activation and prevent vascular thrombosis. These are mediated by the vascular endothelium and include CD39 and the endothelial-derived inhibitors prostacyclin (PGI_2) and nitric oxide (NO). Shear stress drives platelets to the periphery of blood vessels where they are ideally positioned to encounter PGI_2 and NO, which maintain platelets in a resting state. These endogenous inhibitors stimulate adenylyl cyclase (AC) and soluble guanylyl cyclase (sGC) respectively, leading to the activation of cAMP- and cGMP-dependent signalling cascades. cAMP- and cGMP-dependent protein kinases phosphorylate a multitude of target proteins, including vasodilator-stimulated phosphoprotein (VASP) (Butt et al., 1994), actin-binding protein (ABP) (Chen and Stracher, 1989), and the IP_3 receptor (Cavallini et al., 1996) to prevent platelet activation, while phosphodiesterases (PDEs) hydrolyse cyclic nucleotides to terminate signalling. cAMP- and cGMP-dependent protein kinases have unique target specificities but also synergise to create diversity in target selection (Butt et al., 1994). Transgenic animal studies show that these kinases cannot compensate for each other since cAMP signalling is normal in platelets lacking cGMP-dependent protein kinase but NO/cGMP-mediated VASP phosphorylation and platelet inhibition

is impaired, indicating that both kinases are required for the coordinated regulation of platelet function (Massberg et al., 1999). A number of antiplatelet therapies including iloprost, dipyridamole, cilostazol, and clopidogrel attempt to harness the inhibitory potential of cyclic nucleotide signalling. Rapid measurement of cyclic nucleotide-dependent phosphorylation events, particularly in high risk patient populations, could facilitate a better understanding of the molecular mechanisms underlying thrombosis, compliance with and effectiveness of current therapies, and facilitate the identification of novel antiplatelet compounds.

The activity of cyclic nucleotide signalling is normally assessed by measuring the phosphorylation status of established substrate proteins such as VASP whose phosphorylation state is regulated by cAMP- and cGMP-dependent protein kinases (Butt et al., 1994). In many research laboratories, the phosphorylation states of intraplatelet proteins are measured through immunoblotting. While this approach is reproducible, it has a number of limitations in that it requires large numbers of cells and is incompatible with whole blood. Thus; while immunoblotting is useful for examining signalling events in cell biology studies, it is not conducive to large-scale signalling profiling or drug screening. As an alternative, the flow cytometric measurement of protein phosphorylation can overcome some of these limitations. This approach relies on well-characterised phosphospecific antibodies and can provide rapid information on intracellular phosphorylation events in complex mixtures of cells such as those present in whole blood. To facilitate the detection of short-lived intracellular phospho-epitopes, cells must be fixed and permeabilised prior to staining. The development of

innovative fluorescent cell barcoding (FCB) protocols by the Nolan laboratory enables multiplexing of samples for flow cytometry experiments. This provides the possibility of developing high-throughput flow cytometric assays to facilitate the generation of large signalling datasets and rapid screening of entire compound libraries (Krutzik and Nolan, 2006, Krutzik et al., 2007). Despite the potential power of this technology, its full potential has not been realised because it has not yet been applied to primary human cells. In this chapter, our aim was to validate a reproducible phosphoflow protocol that could use FCB to provide a high-throughput flow cytometric platform for the measurement of intraplatelet protein phosphorylation. To achieve this, we used VASP phosphorylation as a marker of cyclic nucleotide signalling (Walter et al., 1993). The outline of this approach is highlighted in Figure 4.1
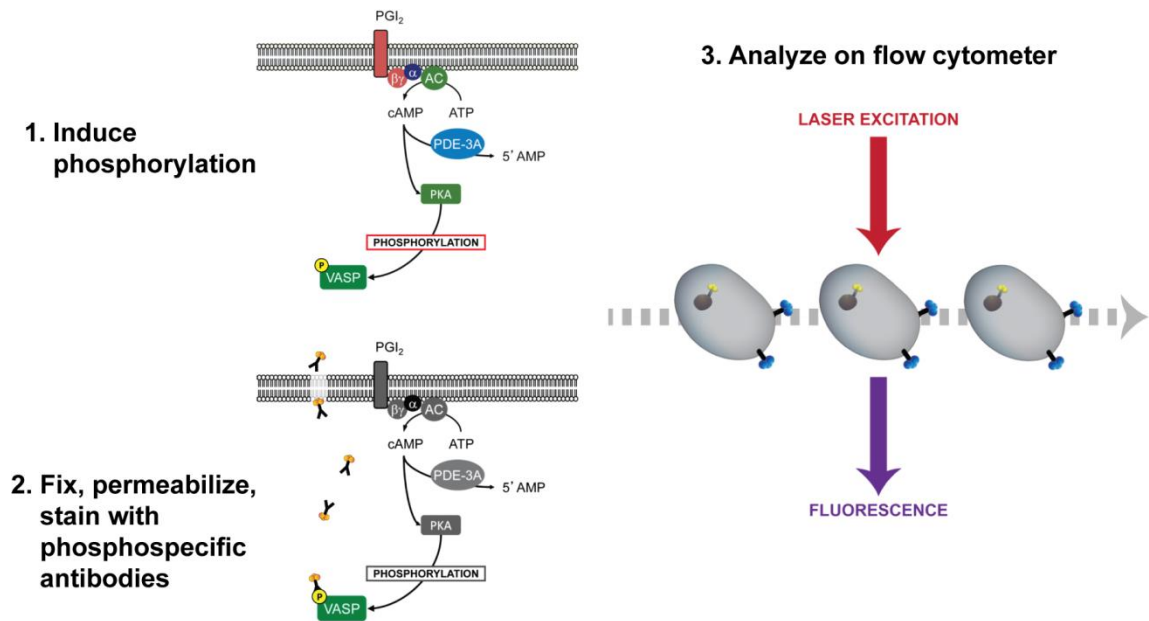
Figure 4.1. General staining protocol for phosphoflow cytometry. First, platelets are stimulated to induce intracellular signalling and the phosphorylation of a target protein. Next, platelets are fixed, permeabilised, and stained with fluorophore-labelled phosphospecific antibodies against the target protein. Finally, platelets are analysed on a flow cytometer, where an increase in fluorescence correlates with an increase in phosphorylation.

4.2 Optimisation of fixation, permeabilisation, and staining techniques

Our major aim was to optimise and validate a flow cytometric method for large-scale analyses of phosphorylation-based signalling events in human platelets. Figure 4.1 illustrates a general protocol, where stimulated platelets are fixed, permeabilised, and then stained with fluorophore-labelled phospho-antibodies that emit fluorescence that is directly proportional to the level of intracellular protein phosphorylation. The success of phosphoflow cytometry is dependent on several variables including (a) fixation, which preserves the phosphorylation states of intracellular proteins by immobilising

kinase and phosphatase activity, (b) permeabilisation, which facilitates the passage of antibodies into the cell by creating pores in lipid bilayers, and (c) antibody staining time, which affects antigen saturation and the intensity of fluorescent signals. Given the importance of these variables, we performed a series of experiments to determine the optimal conditions for fixation, permeabilisation, and staining. These experiments were performed using antibodies against phosphoVASP-ser[157], which are accepted as being robust and specific, having been used in numerous immunoblotting and flow cytometry studies (Oberprieler et al., 2010, Iyú et al., 2011, Halbrügge et al., 1990).

4.2.1 Cellular fixation

Using constant staining times, we first examined a number of different fixation conditions for their ability to maximise the fold change in fluorescence between unstimulated and PGI_2 (100 nM)-stimulated samples. Platelets were stimulated with PGI_2 and then fixed with either 1.5, 2, or 3% paraformaldehyde (PFA) for 10 min. PFA is a common fixative and concentrations between 1.5- and 3% have been effective in various cell types (Krutzik and Nolan, 2003). PFA penetrates cell membranes and forms irreversible methylene cross-links with amino, imino, amido, guanidyl, hydroxyl, carboxyl, and aromatic groups on proteins, thereby immobilising biological activity (Melan, 1999). PFA is particularly useful because platelets fixed with this agent do not retain their propensity for nonspecific binding, thus obviating the need for blocking agents (Buchwalow et al., 2011). The

variations in fixative concentration used here did not affect PGI_2-induced phosphoVASP-ser[157] (Figure 4.2) since all concentrations provided an approximate 8-fold increase in fluorescence. For economy, we selected the lowest effective concentration (1.5% PFA) as optimal. Varying fixation time at the optimal concentration (5-30 min) altered quantitative measures of phosphorylation (Figure 4.3). While there were no significant changes in VASP phosphorylation between 5 and 10 min, longer fixation times resulted in significantly lower staining intensities (14.3 ± 0.2, 5 min; 14.9 ± 0.5, 10 min; 12.1 ± 0.1, 20 min; 10.2 ± 0.8, 30 min; P <0.05), potentially due to excessive PFA-induced cross-linking. Based on these data, we decided that optimal fixation could be achieved using 1.5% PFA for 10 min.
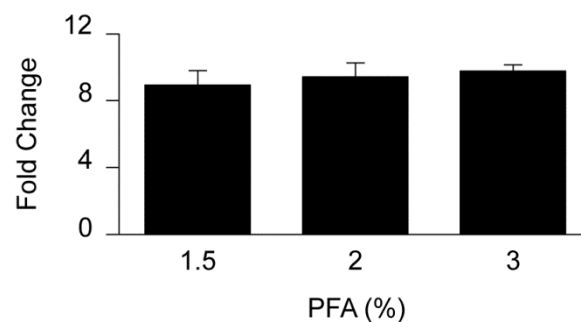
Figure 4.2. Optimisation of fixative concentration. Washed platelets were treated with PGI_2 (100 nM, 1 min) and then fixed with varying concentrations of PFA (10 min), permeabilised with 0.1% Triton X-100 (10 min), and stained with phosphoVASP-ser[157] (2 µg/mL, 30 min) and Alexa Fluor 647 (1 µg/mL, 30 min). Data represents the mean ± SEM from three independent experiments.
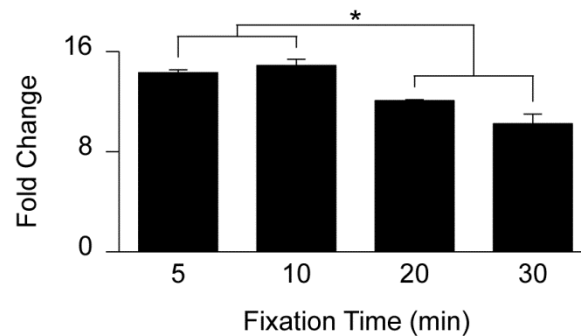
Figure 4.3. Optimisation of fixation time. Washed platelets were treated with PGI$_2$ (100 nM, 1 min) and then fixed with 1.5% PFA for varying times, permeabilised with 0.1% Triton X-100 (10 min), and stained with phosphoVASP-ser[157] (2 µg/mL, 30 min) and Alexa Fluor 647 (1 µg/mL, 30 min). Data represents the mean ± SEM from three independent experiments (*P <0.05).

4.2.2 Phosphoprotein staining

PhosphoVASP-ser[157] antibodies were not available as fluorophore-labelled conjugates so Alexa Fluor 647-labelled secondary antibodies were employed to generate fluorescence. Alexa Fluor 647 is an extremely bright and photostable small-molecule fluorophore that is suitable for intracellular staining (Krutzik and Nolan, 2003). A series of experiments were performed to determine the optimal conditions for staining in terms of antibody concentrations and incubation times. In the first instance, antibody incubation times were examined. Incubation with phosphoVASP-ser[157] (2 µg/mL) from 15-60 min led to a time-dependent increase in fluorescence that was optimal at 30 min (Figure 4.4). Incubation with Alexa Fluor 647 (1 µg/mL) from 15-60 min also led to a time-dependent increase in fluorescence but optimal

staining was observed at 45 min (Figure 4.5). Optimal concentrations for the primary phosphospecific- and fluorophore-labelled secondary antibodies, determined by titration, were 2- and 1 µg/mL respectively.
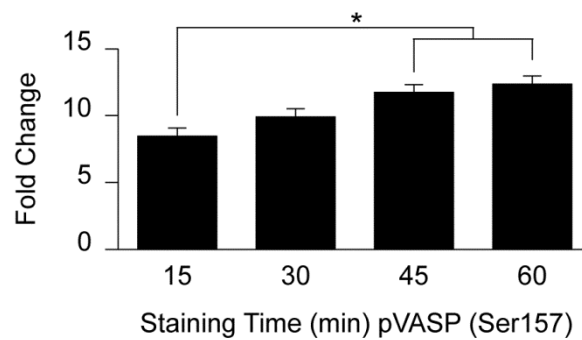
Figure 4.4. Optimisation of phosphospecific antibody staining time. Washed platelets were treated with PGI_2 (100 nM, 1 min), fixed with 1.5% PFA (10 min), permeabilised with 0.1% Triton X-100 (10 min), and then stained with phosphoVASP-ser[157] (2 µg/mL) for varying times and Alexa Fluor 647 (1 µg/mL, 30 min). Data represents the mean ± SEM from three independent experiments (*P <0.05).
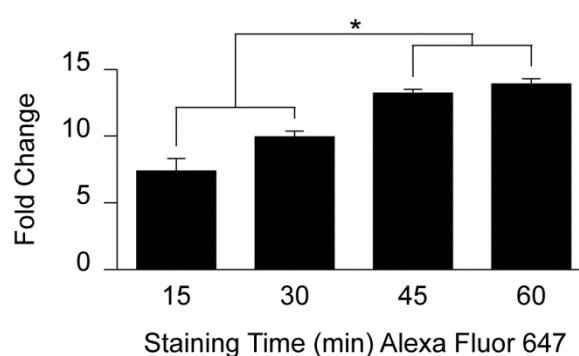
Figure 4.5. Optimisation of Alexa Fluor 647 staining time. Washed platelets were treated with PGI_2 (100 nM, 1 min), fixed with 1.5% PFA (10 min), permeabilised with 0.1% Triton X-100 (10 min), and then stained with phosphoVASP-ser[157] (2 μg/mL, 30 min) and Alexa Fluor 647 (1 μg/mL) for varying times. Data represents the mean ± SEM from three independent experiments (*P <0.05).

4.2.3 Cell membrane permeabilisation

Permeabilisation of the cell membrane is a critical requirement for the entry of primary and secondary antibodies into PFA-fixed cells. Using the optimal conditions for fixation and staining (sections 4.21 and 4.2.2), we compared a number of detergent- and alcohol-based permeabilisation reagents for their abilities to stain phosphoVASP-ser[157], phosphoGSK-3α-ser[21], and phosphoPKA substrates (RRXS/T). Reagents included Triton X-100, the saponin-containing BD Perm/Wash Buffer, and the methanol-containing BD Perm Buffers II & III. Triton X-100 has previously been used to permeabilise platelets for intracellular staining (Schwarz et al., 1999b). At concentrations of 0.1-0.5%, this detergent efficiently solvates all lipid bilayers and yields irreversible permeabilisation. Saponin is a mild detergent that intercalates

93

with cell membranes and solvates cholesterol (Jamur and Oliver, 2010). Because intercalation is reversible, the saponin-containing buffer was used in all washing and staining steps. Alcohol-based permeabilisation is a common intracellular staining technique. Alcohols, such as methanol, dissolve membrane lipids and render cells irreversibly permeable (Jamur and Oliver, 2010). The choice of permeabilisation reagent had the largest impact on staining levels, with fold changes showing significant variation depending on the protein of interest and the reagent used (Figure 4.6). Permeabilisation with 0.1% (10.1 ± 0.4) and 0.5% (10.0 ± 0.8) Triton X-100 produced significantly higher phosphoVASP-ser[157] staining than BD Perm/Wash Buffer (5.6 ± 0.8) (P <0.05). Triton X-100 also provided better phosphoVASP-ser[157] staining than BD Perm Buffers II & III (8.6 ± 0.7 & 8.9 ± 1.5) but this was not significant. While no significant differences were detected between phosphoGSK-3α-ser[21] and phosphoPKA substrate (RRXS/T), the data suggested that permeabilisation with 0.1% Triton X-100 could provide consistently high fluorescence and this reagent was therefore used in future experiments.
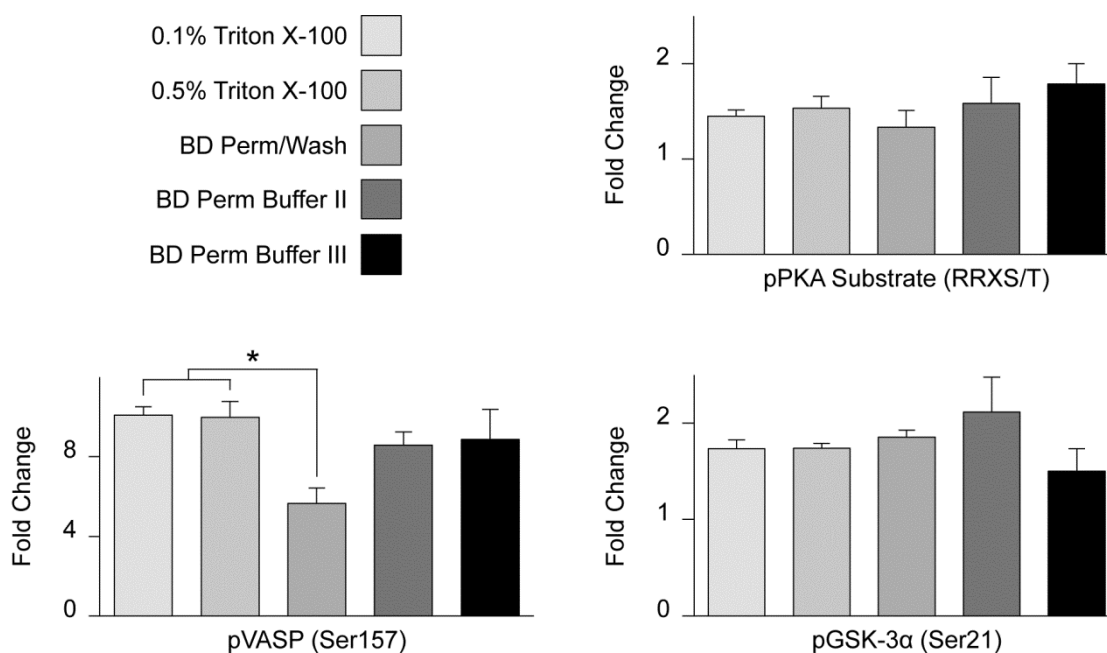
Figure 4.6. Optimisation of permeabilisation reagent. Washed platelets were treated with PGI_2 (100 nM, 1 min), fixed with 1.5% PFA (10 min), permeabilised with different reagents, and then stained with the indicated phospho-antibodies (2 µg/mL, 30 min) and Alexa Fluor 647 (1 µg/mL, 30 min). Data represents the mean ± SEM from three independent experiments (*P <0.05).

4.3 Validation of antibodies for phosphoflow cytometry

Having developed an optimised flow cytometry protocol (section 4.2), we compared its performance to immunoblotting, which is regarded as the gold standard method for analysing phosphorylation-based signalling events. Washed platelets were treated with PGI_2 or the NO donor GSNO, and then divided into two aliquots for either immunoblotting or phosphoflow cytometry analysis. PGI_2 (50 nM) induced substantial phosphorylation of VASP on ser[157] and ser[239] with the former being a more robust response (Figures 4.7A

and B). By contrast, GSNO (20 µM) induced significant phosphorylation on ser^{239} (Figure 4.7B) with only minor effects on ser^{157} consistent with reports that ser^{239} is preferentially phosphorylated by PKG (Butt et al., 1994). These signalling events lay downstream of PKA and cGMP because PGI$_2$-induced phosphorylation events were diminished in the presence of the PKA inhibitor H89 (10 µM) (Chijiwa et al., 1990) (Figure 4.7A) while GSNO-induced phosphorylation events were abolished after pretreatment with the sGC inhibitor ODQ (20 µM) (Garthwaite et al., 1995) (Figure 4.7B). Changes in phosphorylation were detectable by both immunoblotting and flow cytometry. In all cases, increases in band density were mirrored by rightward shifts along the horizontal axes of histogram overlays and brighter coloured squares on heatmaps, which indicate increases in fluorescence and phosphorylation.
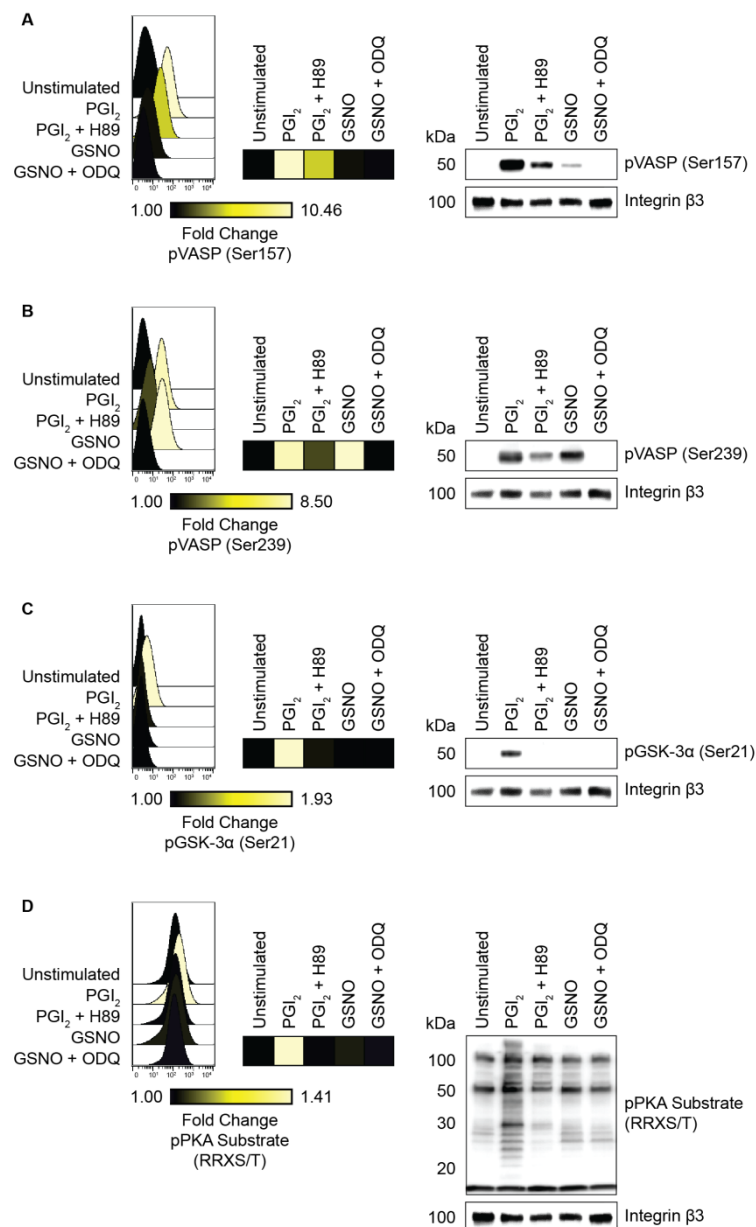
Figure 4.7. Flow cytometric measurement of intraplatelet protein phosphorylation mirrors immunoblotting. Platelets were either unstimulated or stimulated with PGI$_2$ (50 nM, 1 min) or GSNO (20 µM, 2 min) in the presence or absence of the PKA- and sGC inhibitors H89 (10 µM, 20 min) and ODQ (20 µM, 20 min). Thereafter, platelets underwent lysis for immunoblotting or fixation and permeabilisation for phosphoflow cytometry. Blots and histograms are representative of five independent experiments.

To demonstrate that the method had the capacity to measure other cyclic nucleotide-mediated signalling events, we examined phosphoGSK-3α-ser[21], which has been identified as a PKA substrate in leukocytes (Oberprieler et al., 2010) (Figure 4.7C), and the phosphorylation of other PKA substrates using an antibody that recognises proteins with a consensus sequence (RRXS/T) for PKA phosphorylation (Figure 4.7D). GSK-3α underwent phosphorylation on ser[21] after stimulation with PGI_2. Consistent with its designation as a PKA substrate, we found no evidence of GSK-3α phosphorylation in platelets stimulated with GSNO, but observed complete ablation of phosphorylation by H89 (Figure 4.2C). In flow cytometry analyses, the maximal fold change values for phosphoGSK-3α-ser[21] and phosphoPKA substrate (RRXS/T) were lower than those for phosphoVASP, possibly owing to subcellular localisation and/or differences in the abundance of target proteins. In immunoblotting, signal strength (band density) is the product of an HRP-catalysed reaction that can be enhanced by longer exposure of the membrane to light-sensitive film. In standard flow cytometry protocols, signal strength (fluorescence) is not the product of enzymatic amplification but it is limited by the abundance of the protein of interest. Indeed, cells that contain phosphoproteins of low abundance will bind fewer antibodies and emit less fluorescence than cells that contain phosphoproteins of high abundance. Thus, fold change values for less abundant targets will be lower than those for more abundant targets. Proteomics studies have shown that VASP is more abundant than GSK-3α in human platelets (Burkhart et al., 2012). It is therefore not surprising that our phosphoVASP-ser[157] (10.5) and ser[239] (8.5) values were higher than those for phosphoGSK-3α (1.9) (Figure 4.7). This

concept is further complicated by subcellular localisation. In immunoblotting, cells are lysed and protein complexes are denatured, separated, and then transferred to a solid-phase membrane that facilitates binding between antibodies and their phosphoprotein targets. By contrast, flow cytometry is performed on intact cells in which protein-protein complexes are fixed and often buried in subcellular compartments. Unlike immunoblotting, these phospho-epitopes may be inaccessible to antibodies resulting in weak fluorescent signals such as those obtained for phosphoPKA substrate (RRXS/T). While the immunoblot shows an abundance of bands, the maximal fold change values (1.4) for phosphoPKA substrate (RRXS/T) were relatively low (Figure 4.7D). While these values may be confounded by high levels of basal phosphorylation (Figure 4.7D), it is possible that antibody binding was restricted by the subcellular localisation of PKA substrates. Indeed, these substrates often form multiprotein signalling complexes in distinct subcellular compartments (Taskén and Aandahl, 2004). As a result, their phospho-epitopes may be masked within protein interfaces making them difficult to detect by flow cytometry. Despite between-target differences in fluorescence intensity, our data show close consistencies between immunoblotting and flow cytometry with changes in band density mirrored by changes in fluorescence, confirming previous reports that the latter is a valid method for measuring intracellular protein phosphorylation (Krutzik and Nolan, 2003).
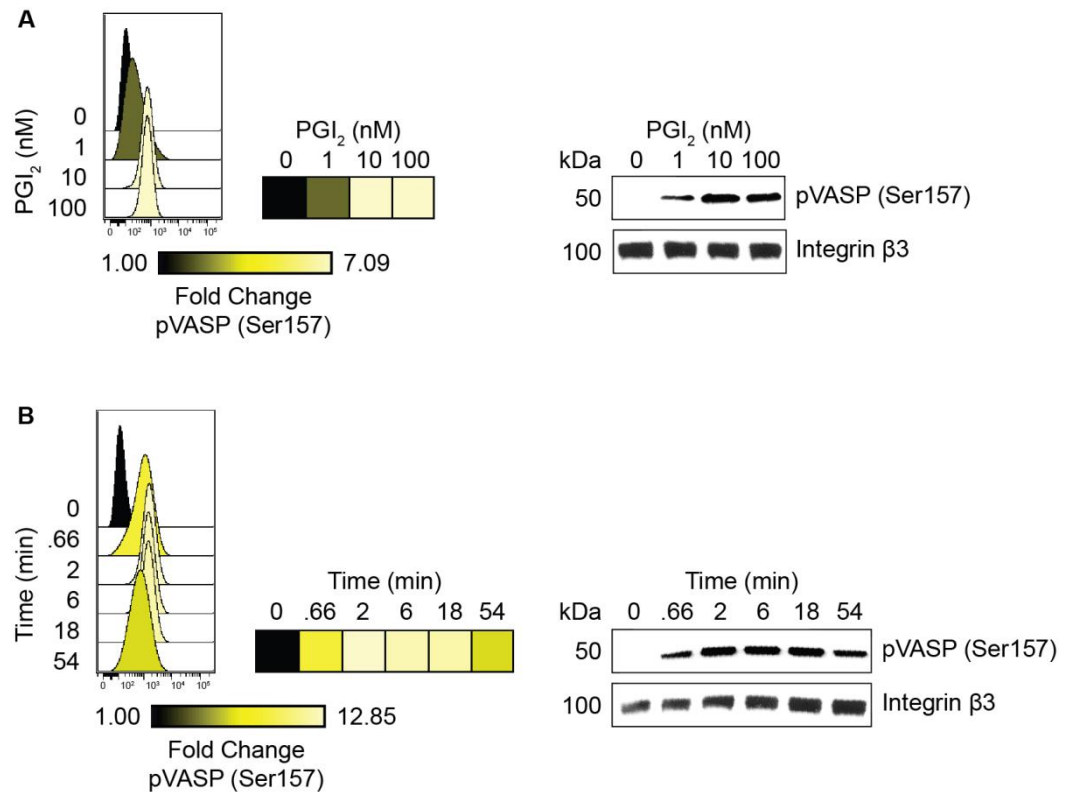
Figure 4.8. Phosphoflow cytometry can detect dose- and time-dependent changes in phosphorylation. Washed platelets were stimulated with PGI_2 (0, 1, 10, or 100 nM) for 2 min, or stimulated with PGI_2 (10 nM) for the indicated times. Thereafter, platelets underwent lysis for immunoblotting or fixation and permeabilisation for phosphoflow cytometry. Data are representative of five independent experiments.

4.4 Fluorescent cell barcoding enables large-scale signalling profiling

Having established an optimised protocol for the flow cytometric measurement of intraplatelet protein phosphorylation, we next examined whether the method could be used to quantify the kinetics of VASP phosphorylation and its sensitivity to several cAMP elevating agents. Both immunoblotting and flow cytometry could detect subtle changes in phosphoVASP-ser[157] at 1 nM PGI_2 (Figure 4.8A). PhosphoVASP-ser[157] peaked at 10 nM PGI_2 where immunoblot bands were dense and histograms

and heatmaps were bright. No further increases in phosphorylation were detected at 100 nM PGI_2 (Figure 4.8A). Flow cytometry could also detect time-dependent changes in phosphoVASP-ser[157] that were mirrored by immunoblotting (Figure 4.8B). Here, PGI_2 (10 nM) stimulated a moderate increase in phosphoVASP-ser[157] at 0.66 min. Band densities and fluorescence reached maximal levels between 2 and 18 min but decreased thereafter (Figure 4.8B) reflecting the action of protein phosphatases.

Despite the sensitivity of our optimised protocol, its application to large-scale analyses would encounter limitations relating to antibody reagent expense, staining variability, and sample acquisition throughput. To overcome these limitations, we developed a multiplexing protocol where fixed and permeabilised platelets are labelled (or barcoded) with different concentrations of multiple amine-reactive fluorophores to create unique fluorescent signatures for individual samples. Barcoded samples are combined into a single well for simultaneous antibody staining and acquisition. This approach eliminates between-sample variability that may result from inconsistencies in staining volume and antibody concentration. In addition, since many samples are combined into a single tube, data acquisition times are reduced. For example, an experiment that requires 24 samples can be combined into a single tube and stained as a single sample (Figure 4.9). Only one tube is run on the cytometer, eliminating the need to load and unload 24 separate samples. During analysis, the original samples can be traced (or deconvoluted) according to their differentiable fluorescent barcodes (Kotecha et al., 2010).
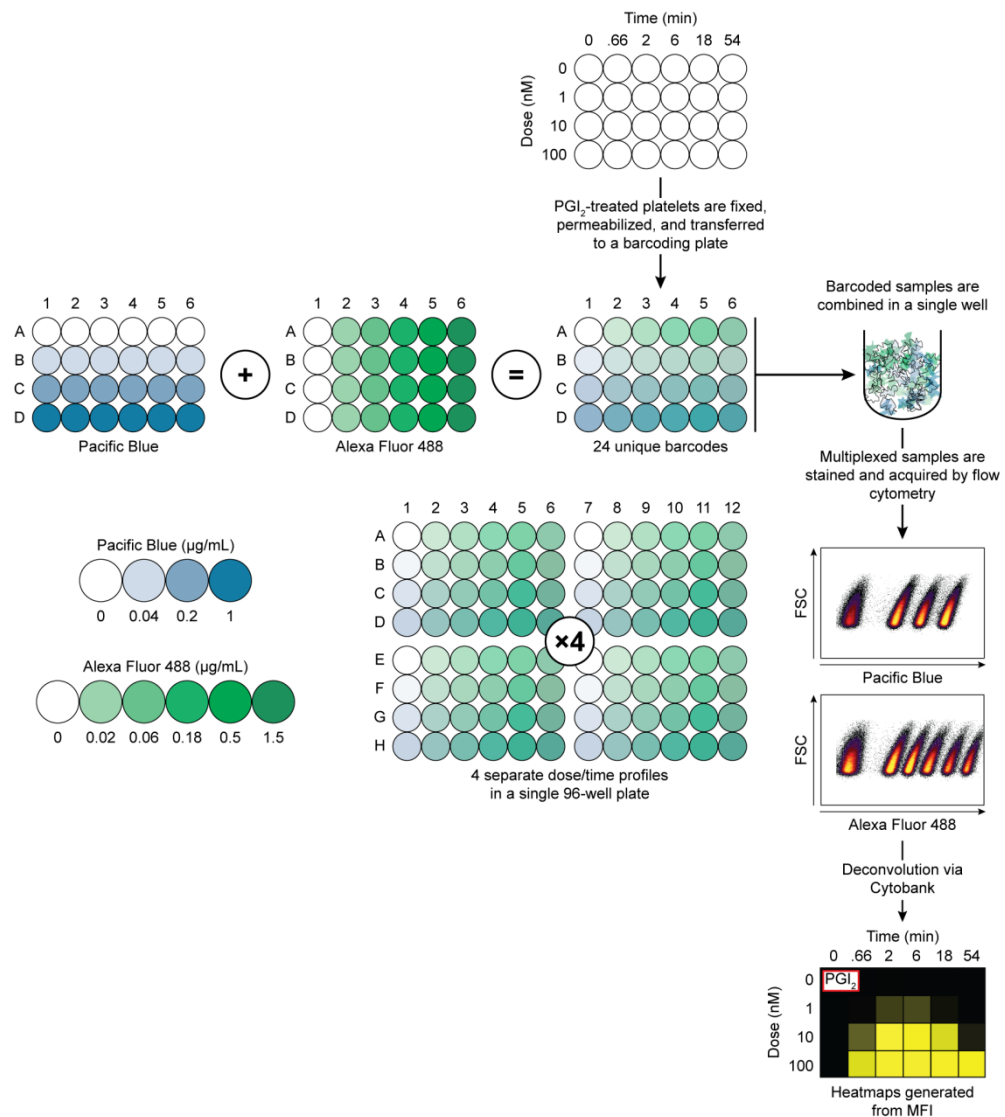
Figure 4.9. Workflow for FCB, deconvolution and data presentation. Various concentrations of Pacific Blue and Alexa Fluor 488 dyes were added to the wells of a 96-well plate. The addition of stimulated, fixed, and permeabilised platelets to these wells created 24 samples with unique fluorescent signatures. After barcoding, all 24 samples were combined into a single tube and labelled with the appropriate antibodies. After acquisition, each set of multiplexed samples were deconvoluted into individual samples by their distinct fluorescent barcodes. Antibody-specific fluorescence was then determined for each of the groups and presented as a heat map.

Initially, we labelled platelets with Alexa Fluor 488 and Pacific Blue (Figure 4.9) to examine the kinetics of VASP phosphorylation across six time points and four concentrations of various cAMP-elevating agents. Samples were stimulated, fixed and permeabilised in a 96-well plate according to the standard protocol (section 4.2). Samples were then transferred to a fresh 96-well plate containing different concentrations of Alexa Fluor 488 and Pacific Blue to create 24 samples with unique fluorescent signatures. After labelling, these samples were combined into one well, stained with primary and secondary antibodies, and analysed by flow cytometry. Using specialist software, the original 24 samples were identified by gating the different intensities of Alexa Fluor 488 and Pacific Blue in a process termed deconvolution. After deconvolution of 24 barcoded samples, we generated heatmaps, where brighter colours indicate greater degrees of phosphorylation, to enable the direct visualisation of signalling trends at each dose and time point.

As highlighted in Figure 4.10B, VASP underwent rapid time- and concentration-dependent phosphorylation on both ser^{157} and ser^{239} in PGI_2-stimulated platelets. While ser^{157} underwent substantial and prolonged phosphorylation, ser^{239} underwent transient phosphorylation that decreased at earlier time points. Minor increases in phosphoVASP-ser^{157} were detected at 1 nM PGI_2 but substantial increases were detected at 10 nM PGI_2 (Figures 4.11 and 4.12). At this concentration, significant phosphorylation occurred at 0.66 min (11.9 ± 3.2), peaked at 18 min (19.6 ± 3.8), and decreased at 54 min (6.8 ± 1.8) ($P < 0.05$). By contrast, PGI_2 (10 nM)-induced phosphoVASP-ser^{239} reached significance at later time points (14.1 ± 2.9, 2 min) and

peaked earlier (18.9 ± 3.7, 6 min). PGI_2 (100 nM) caused significant phosphoVASP-ser^{157} at 0.66 min (15.5 ± 2.1) and peaked at 54 min (26.2 ± 2.9) while phosphoVASP-ser^{239} peaked at 18 min (21.1 ± 3.9) and decreased at 54 min (17.1 ± 2.2). PGI_2 was more potent than PGE_1, which failed to induce significant phosphorylation on either ser^{157} or ser^{239} at concentrations below 100 nM (Figure 4.13). PGE_1 (100 nM) caused significant phosphoVASP-ser^{157} at 0.66 min (16.8 ± 1.7) and peaked at 54 min (21.6 ± 1.3). PGE_1 (100 nM)-induced phosphoVASP-ser^{239} also reached significance at 0.66 min (4.7 ± 0.6) and peaked at 54 min (8.6 ± 0.9). Forskolin, the cell-permeable activator of AC (Seamon and Daly, 1980), induced gradual increases in phosphorylation at both serine residues (Figures 4.15 and 4.16). However; unlike the receptor-mediated agonists PGI_2 and PGE_1, significant increases in phosphorylation were not detected until 2 min since additional time is required for forskolin to traverse the cell membrane and bind its intracellular target. Forskolin (1 µM) caused significant phosphorylation on ser^{157} (15.3 ± 2.1) but not ser^{239} (P <0.05) indicating that ser^{157} is more sensitive to this agent (Figure 4.15). Forskolin (10 µM) induced significant phosphoVASP-ser^{157} at 2 min (4.5 ± 2.0) but required 6 min (9.6 ± 0.6) to induce significant phosphorylation on ser^{239} (P <0.05). By contrast, 100 µM forskolin induced significant phosphoVASP-ser^{239} at 2 min (5.2 ± 1.0). In all cases, forskolin was optimal at 54 min when maximal phosphorylation on ser^{157} (29.3 ± 3.5) and ser^{239} (22.0 ± 3.8) was observed (Figure 4.16). Adenosine induced weak phosphorylation of phosphoVASP-ser^{157} and had little effect on phosphoVASP-ser^{239} (Figures 4.17 and 4.18). Adenosine (1 µM) induced significant phosphoVASP-ser^{157} at 6 min (3.0 ± 0.7) but required

18 min to induce significant phosphoVASP-ser^{239} (1.9 ± 0.1) (P <0.05). Higher concentrations of adenosine (10- and 100 μM) induced rapid and robust phosphorylations but these did not exceed 6.9 ± 0.7 for ser^{157} or 2.7 ± 0.2 for ser^{239} (Figures 4.17 and 4.18). VASP underwent more robust phosphorylation on ser^{157} than ser^{239} in response to the cAMP-elevating agents used here consistent with reports that ser^{157} is the preferential phosphorylation site for PKA (Butt et al., 1994). We observed different responses to each agonist, suggesting that the receptors for PGI$_2$, PGE$_1$, and adenosine have different cAMP-generating abilities, which may reflect the involvement of different AC isoforms or differences in the localisation of downstream effector molecules.
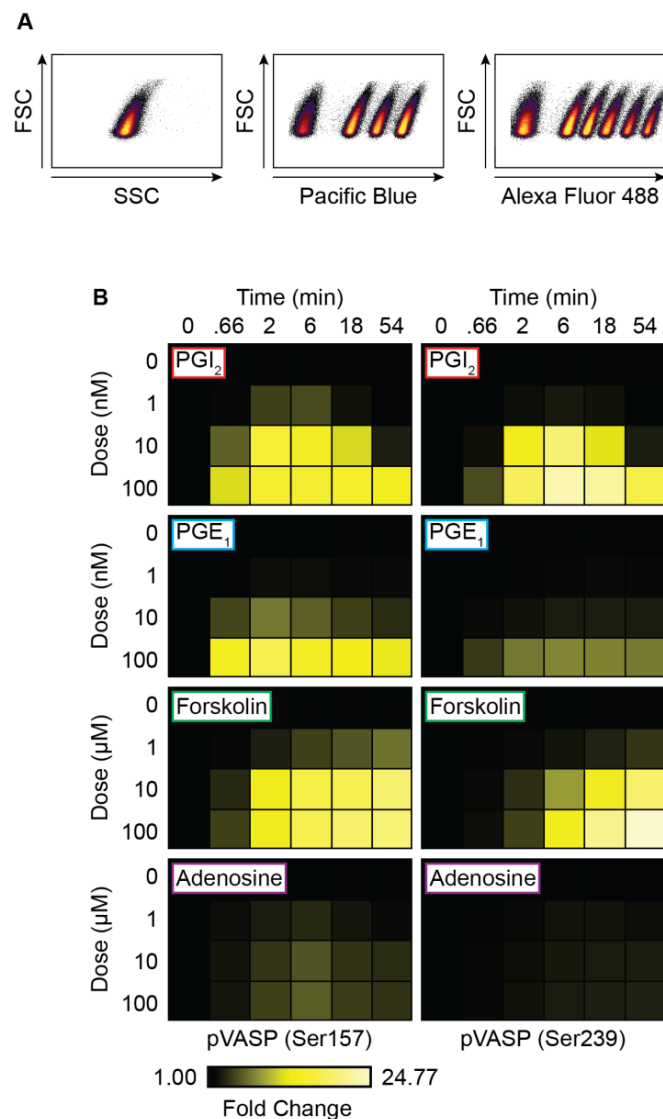
Figure 4.10. Two-dimensional FCB enables large-scale signalling profiling. (**A**) Washed platelets were barcoded with Pacific Blue and Alexa Fluor 488. (**B**) Prior to FCB, platelets were stimulated with PGI$_2$ (0, 1, 10, or 100 nM), PGE$_1$ (0, 1, 10, or 100 nM), forskolin (0, 1, 10, or 100 µM), or adenosine (0, 1, 10, or 100 µM) for the indicated times. Heatmap data are representative of four independent experiments.
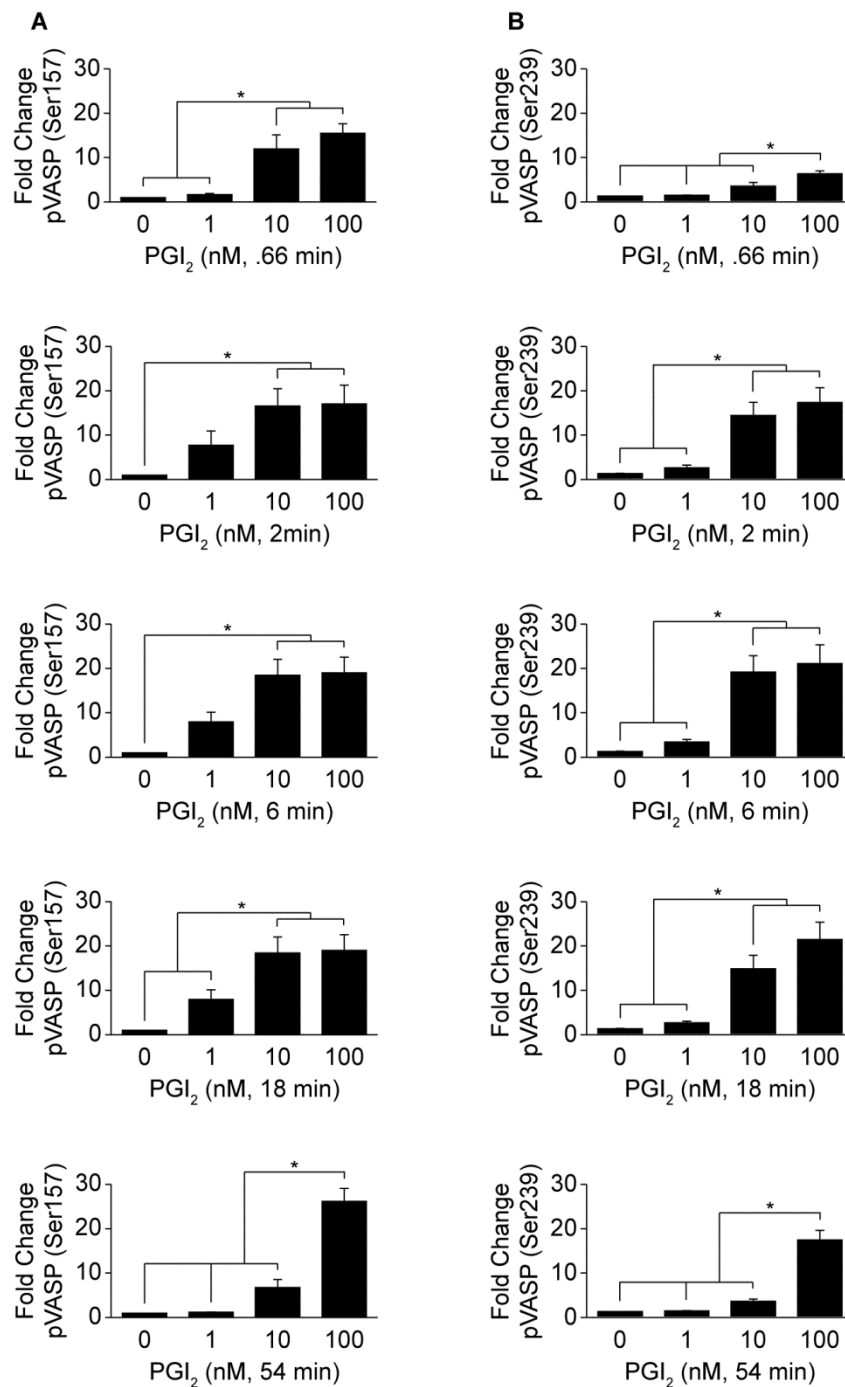
Figure 4.11. Statistical analysis of phosphoVASP-ser[157] and ser[239] in response to PGI₂. Quantitative dose-response data were exported and then analysed at five different timepoints for (**A**) ser[157] and (**B**) ser[239]. Data represents the mean ± SEM from four independent experiments (*P <0.05).
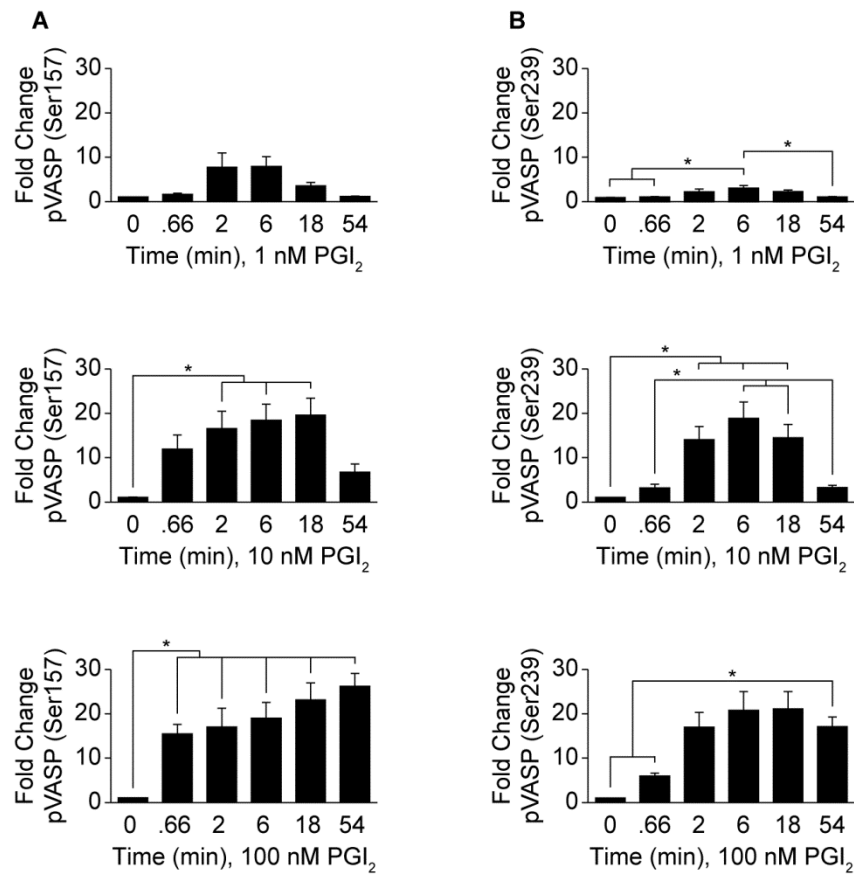
Figure 4.12. Statistical analysis of phosphoVASP-ser[157] and ser[239] in response to PGI₂. Quantitative time-response data were exported and then analysed at three different concentrations for (**A**) ser[157] and (**B**) ser[239]. Data represents the mean ± SEM from four independent experiments (*$P < 0.05$).
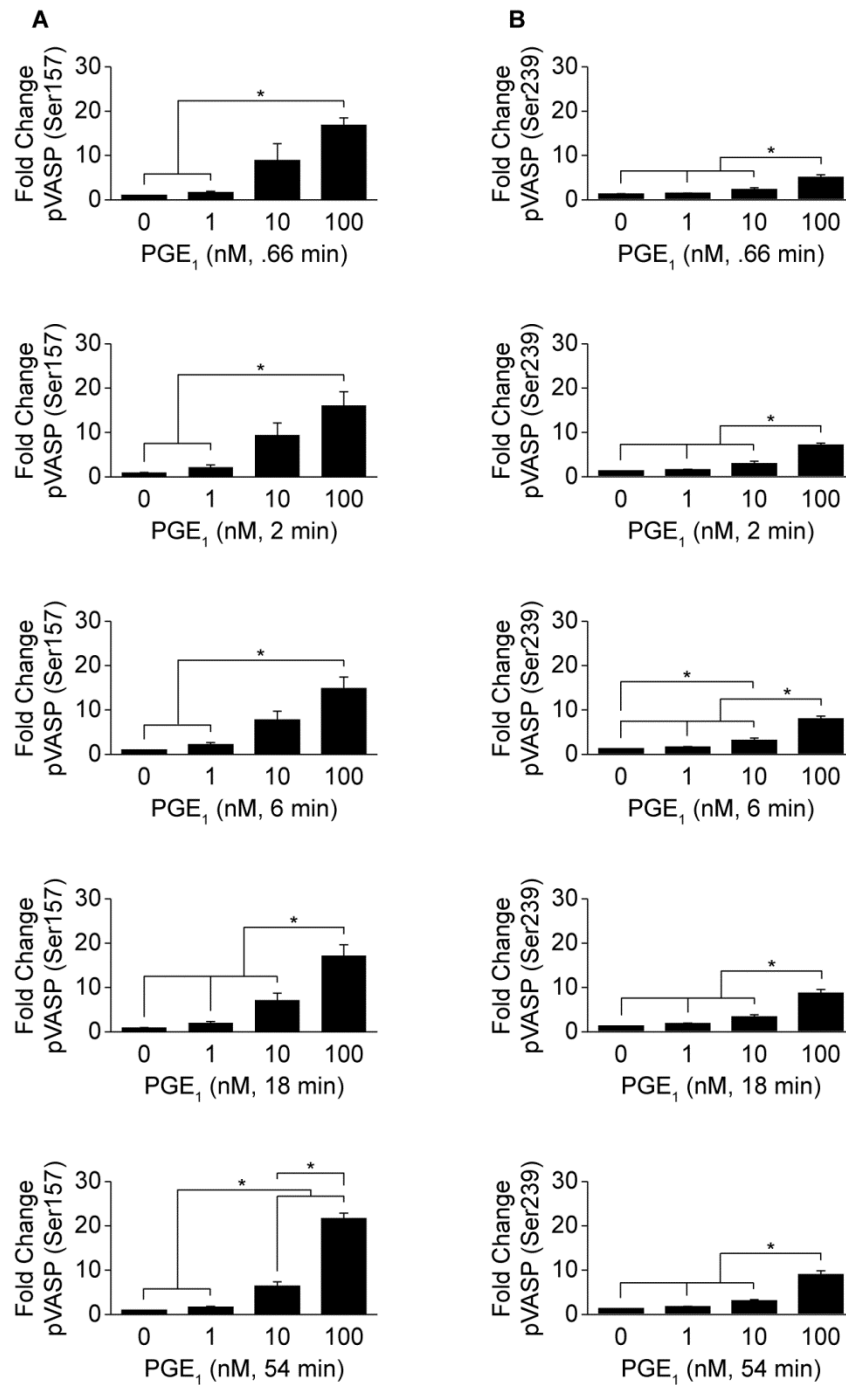
Figure 4.13. Statistical analysis of phosphoVASP-ser[157] and ser[239] in response to PGE₁. Quantitative dose-response data were exported and then analysed at five different timepoints for (**A**) ser[157] and (**B**) ser[239]. Data represents the mean ± SEM from four independent experiments (*P <0.05).
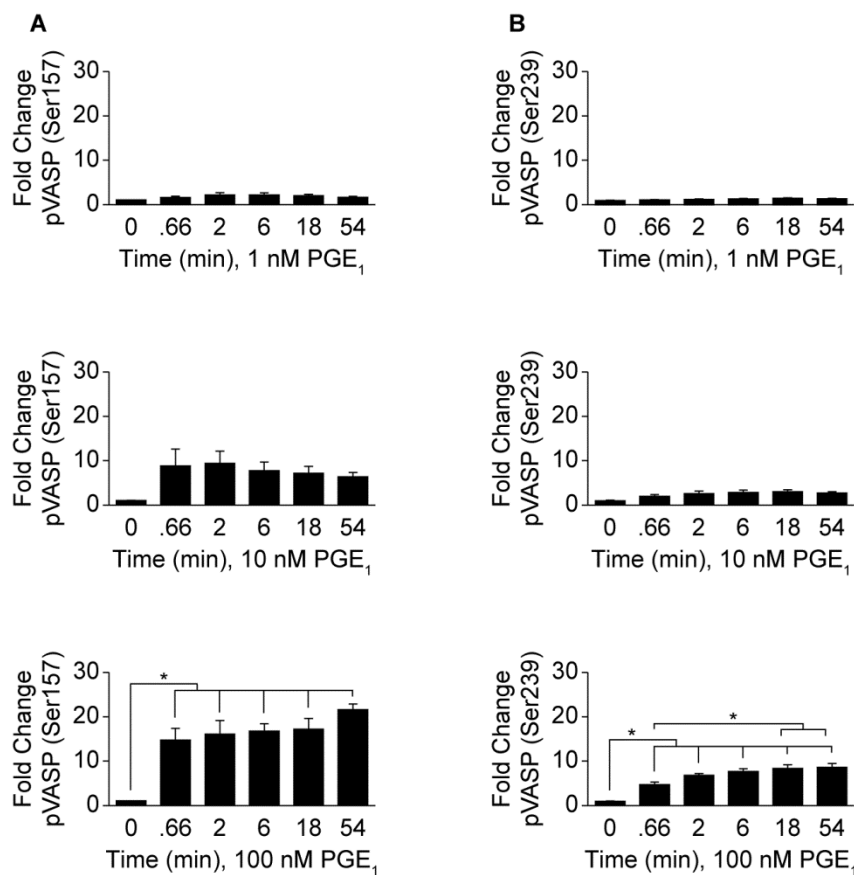
Figure 4.14. Statistical analysis of phosphoVASP-ser[157] and ser[239] in response to PGE₁. Quantitative time-response data were exported and then analysed at three different concentrations for (**A**) ser[157] and (**B**) ser[239]. Data represents the mean ± SEM from four independent experiments (*P <0.05).
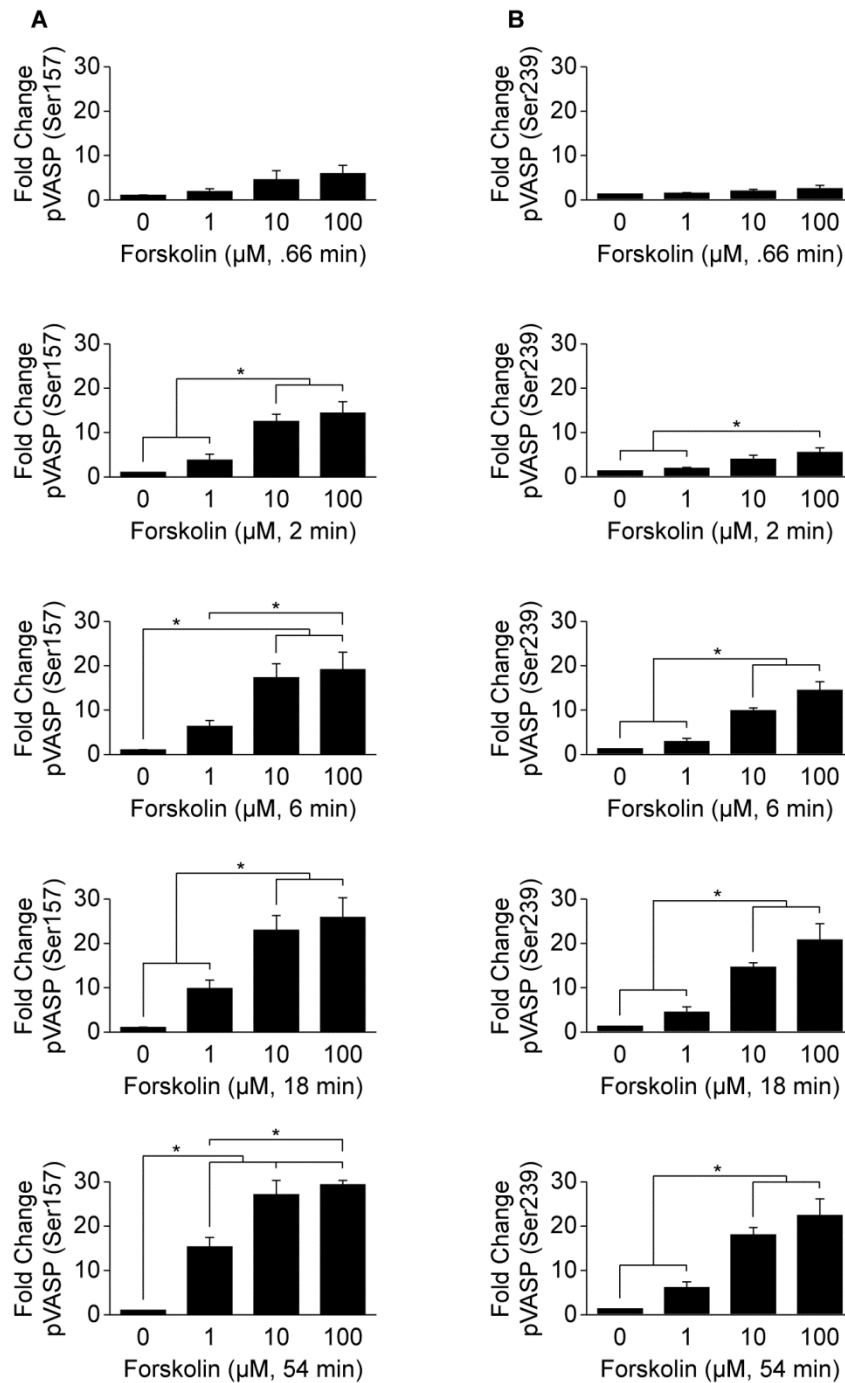
Figure 4.15. Statistical analysis of phosphoVASP-ser[157] and ser[239] in response to forskolin. Quantitative dose-response data were exported and then analysed at five different timepoints for (**A**) ser[157] and (**B**) ser[239]. Data represents the mean ± SEM from four independent experiments (*P<0.05).
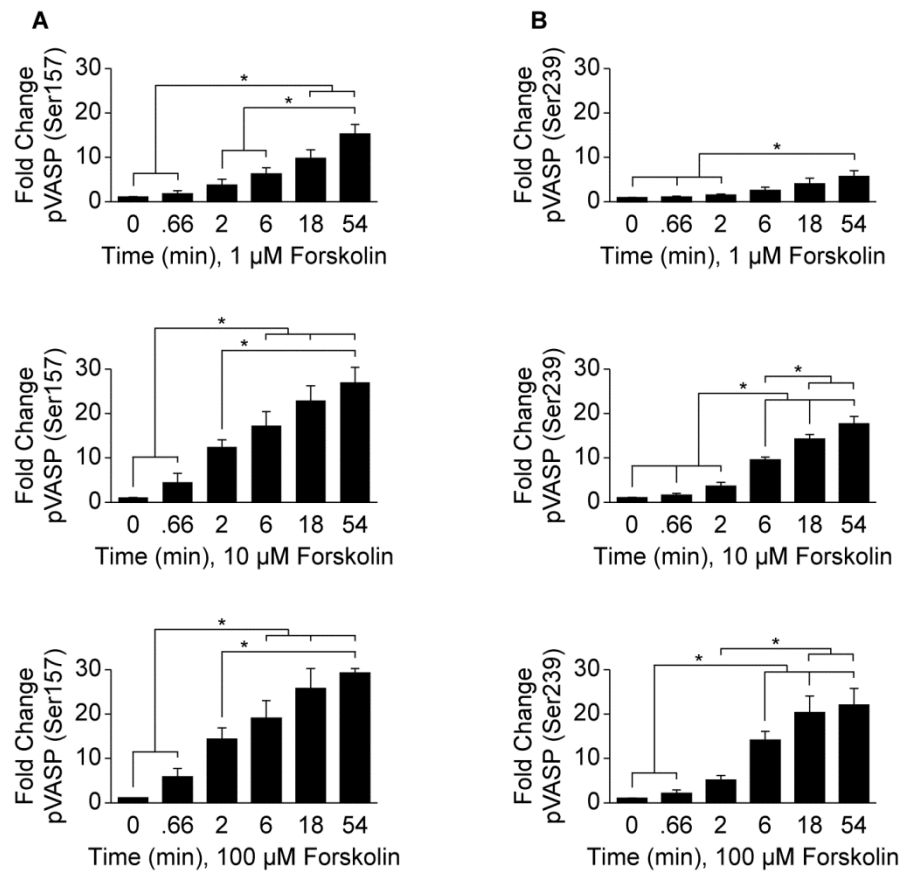
Figure 4.16. Statistical analysis of phosphoVASP-ser[157] and ser[239] in response to forskolin. Quantitative time-response data were exported and then analysed at three different concentrations for (**A**) ser[157] and (**B**) ser[239]. Data represents the mean ± SEM from four independent experiments (*P <0.05).
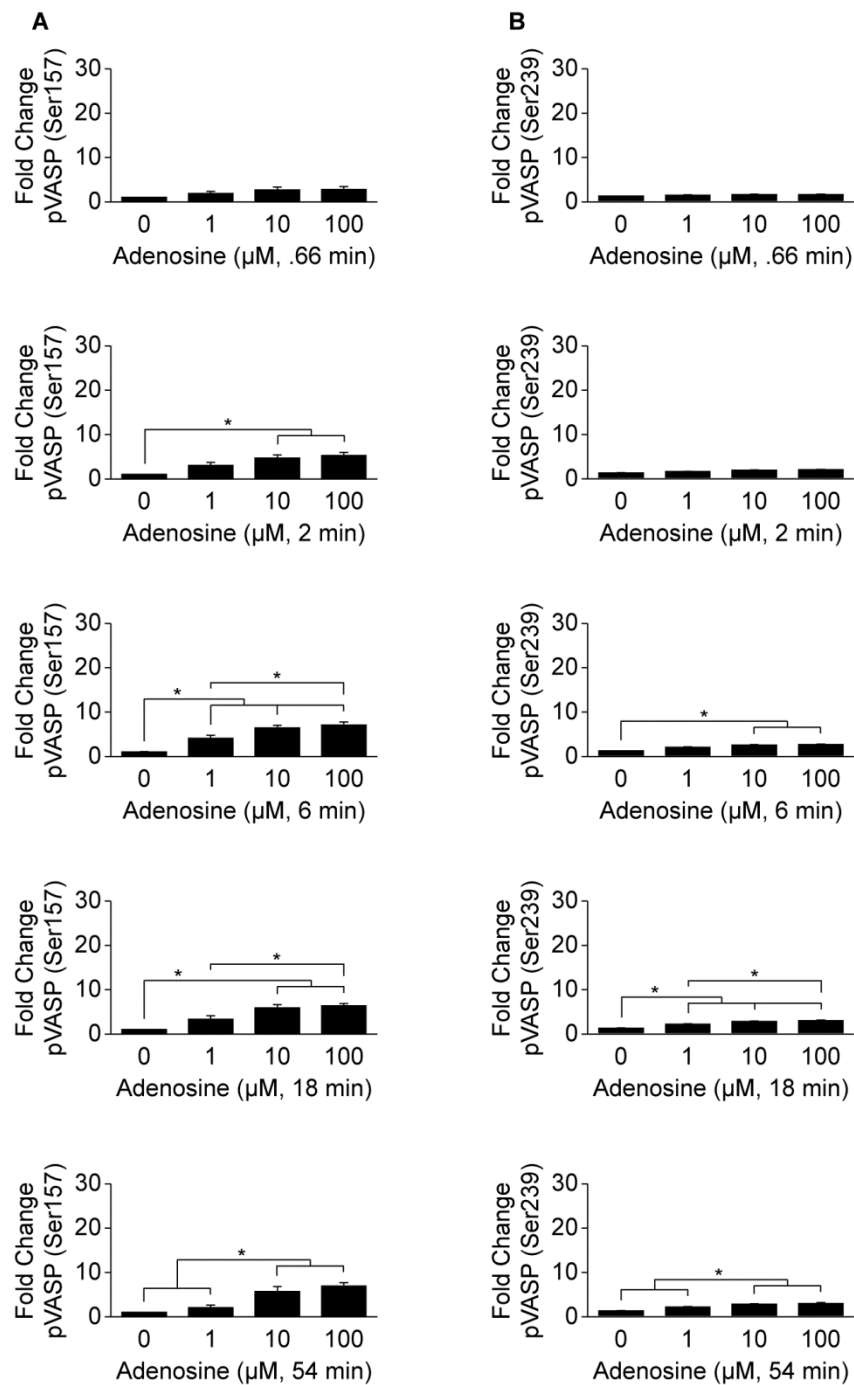
Figure 4.17. Statistical analysis of phosphoVASP-ser[157] and ser[239] in response to adenosine. Quantitative dose-response data were exported and then analysed at five different timepoints for (**A**) ser[157] and (**B**) ser[239]. Data represents the mean ± SEM from four independent experiments (*P <0.05).
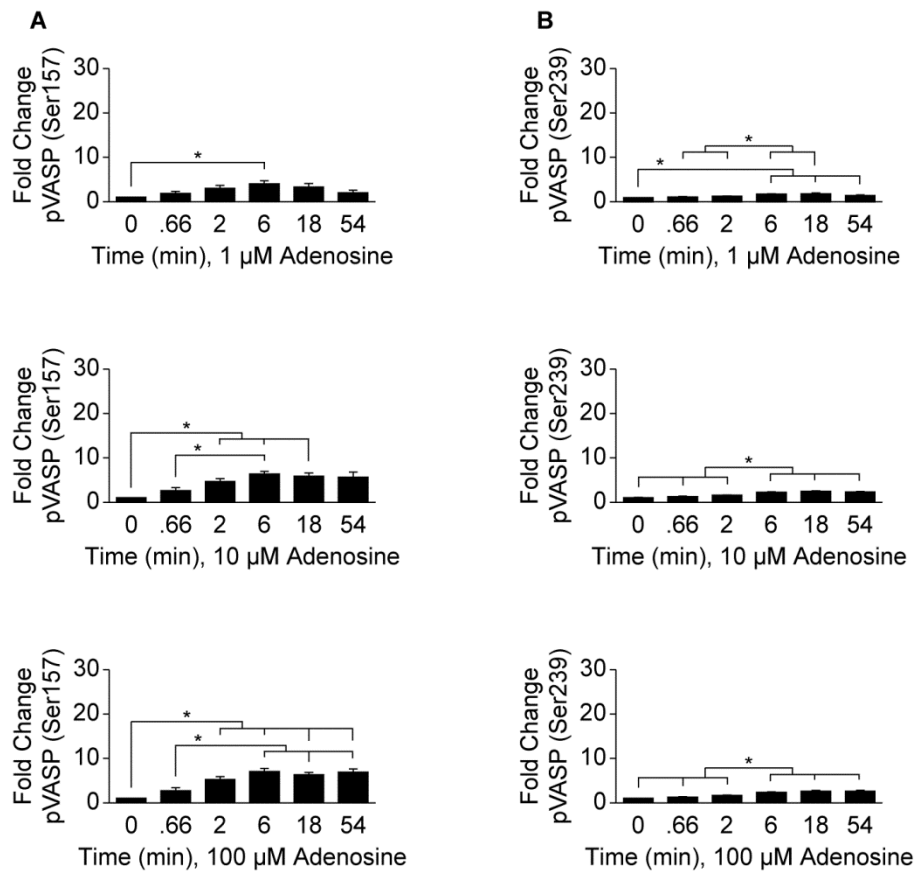
Figure 4.18. Statistical analysis of phosphoVASP-ser[157] and ser[239] in response to adenosine. Quantitative time-response data were exported and then analysed at three different concentrations for (**A**) ser[157] and (**B**) ser[239]. Data represents the mean ± SEM from four independent experiments (*P <0.05).

4.5. Fluorescent cell barcoding enables the detailed interrogation of cyclic nucleotide signalling events

We next used three barcoding dyes to examine a number of agents that have been shown to modulate cyclic nucleotide signalling, thereby demonstrating the sensitivity of the assay to established modulators (Figure 4.19A). We first used the IP receptor antagonist RO1138452 (Jones et al., 2006) to confirm receptor-dependent and independent signalling. PGI_2- and PGE_1-induced phosphoVASP-ser[157] was completely abolished in the presence of RO1138452, indicating that these agents signal through the IP receptor (Figure 4.18B). By contrast, this receptor antagonist had no effect on phosphorylation in platelets incubated with forskolin consistent with its receptor-independent mechanism. Using ADP, we next tackled the effects of Gi-mediated signalling on cAMP-dependent phosphorylation events. ADP is known to induce $P2Y_{12}$ receptor-mediated inhibition of AC (Hollopeter et al., 2001) (Figure 4.18B). ADP inhibited AC agonist-induced phosphoVASP-ser[157] indicating that it exerts its effects downstream of multiple AC-coupled receptor systems and on the multiple AC isoforms that forskolin is known to activate (Seamon and Daly, 1980). Using caffeine, we then tested whether the assay was sensitive enough to detect the distinct effects of a chemical inhibitor. Caffeine is an adenosine receptor antagonist and a nonselective PDE inhibitor (Fredholm, 1985). Caffeine blocked adenosine-induced phosphoVASP-ser[157] but potentiated phosphorylation induced by other AC agonists (Figure 4.18B) consistent with its dual effects. Finally, we examined the effects of other PDE inhibitors on cyclic nucleotide signalling. The nonselective PDE inhibitor IBMX (Beavo et al., 1970) potentiated

phosphoVASP-ser[157] in stimulated but not unstimulated platelets (Figure 4.18B) while the PDE3A-selective inhibitor milrinone (Mary Tang et al., 1994) was found to increase both basal and all agonist-induced phosphoVASP-ser[157] (Figure 4.18B). Importantly, the PDE2-specific inhibitor EHNA (Podzuweit et al., 1995) and the PDE5-specific inhibitor zaprinast (Corbin and Francis, 2001) did not affect basal levels of phosphorylation (Figure 4.18B). However, these inhibitors potentiated phosphoVASP-ser[157] in stimulated platelets consistent with reported cross-talk between cyclic nucleotide signalling cascades (Haslam et al., 1999b). Thus, our assay was sensitive enough to accurately detect the effects of known modulators of cyclic nucleotide signalling.
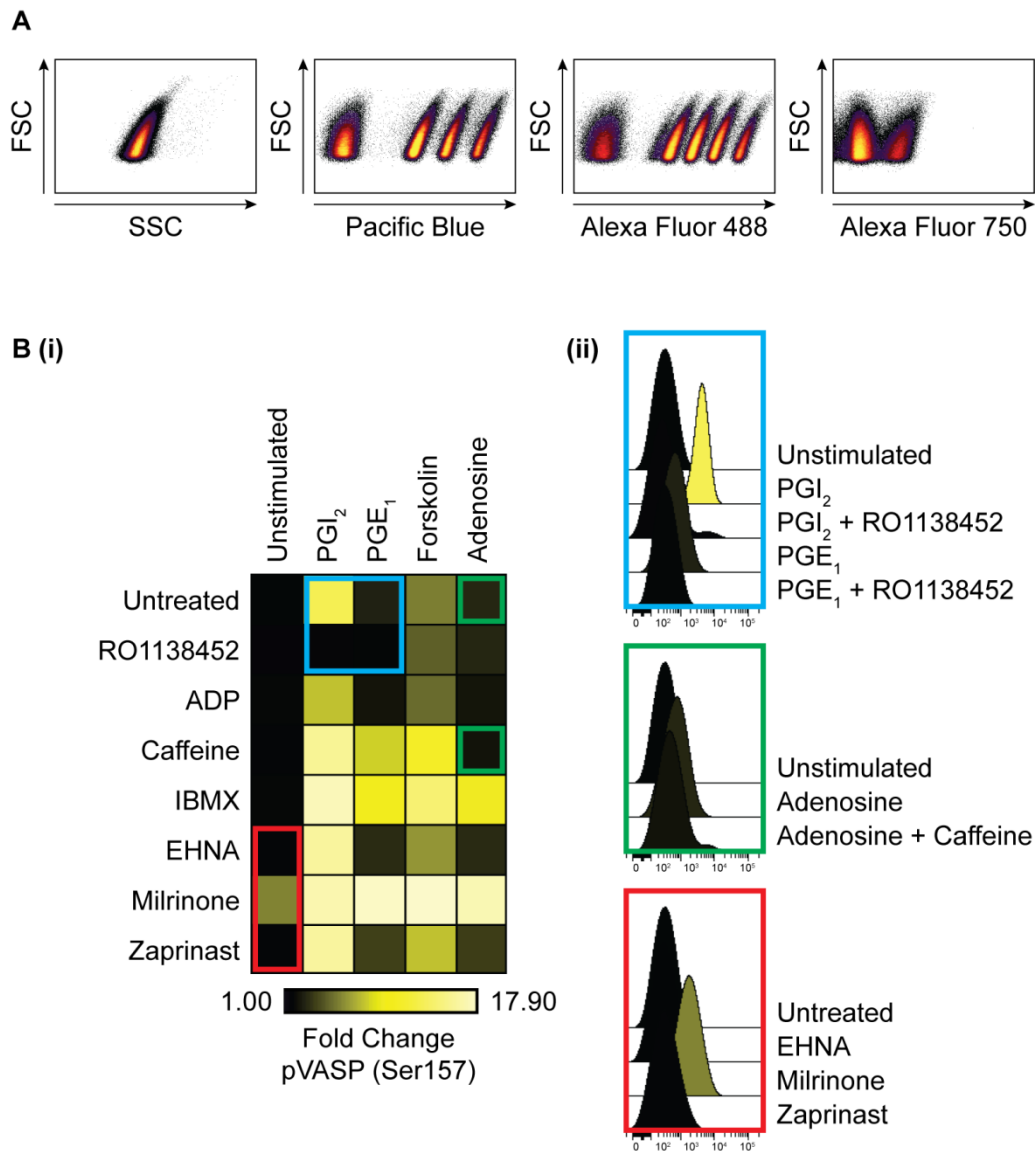
Figure 4.19. Three-dimensional FCB facilitates interrogation of cyclic nucleotide signalling. (**A**) Washed platelets were barcoded with Pacific Blue, Alexa Fluor 488, and Alexa Fluor 750. (**B**) Prior to FCB, platelets were either unstimulated or stimulated with PGI_2 (10 nM, 2 min), PGE_1 (10 nM, 2 min), adenosine (10 µM, 2 min), or forskolin (10 µM, 2 min) after pretreatment with either RO1138452 (10 µM, 20 min), caffeine (1 mM, 20 min), ADP (10 µM, 10 min), IBMX (10 µM, 20 min), EHNA (10 µM, 20 min), milrinone (10 µM, 20 min), or zaprinast (10 µM, 20 min). Data are representative of four independent experiments.

4.6 Fluorescent cell barcoding facilitates the analysis of platelet signalling events in whole blood

The analysis of platelet function in whole blood is critical for the evaluation of both novel and established platelet inhibitors. We thus adapted our method for whole blood analyses and harnessed the ability of the cytometer to discern specific cell populations from heterogeneous mixtures based on their distinct light scatter properties. To simplify whole blood analyses, BD Phosflow Lyse/Fix buffer was used to lyse red blood cells and fix platelets in a single step. Red cell lysis enables better resolution of the platelet population, which can overlap with small erythrocytes on plots of forward versus side scatter. The change in fixative did not affect the scatter properties of whole-blood platelets when compared to washed platelets (Figure 4.20Ai and Bi). We applied the FCB protocol to whole blood samples by examining the signalling kinetics of phosphoVASP-ser^{157} and ser^{239} in response to PGI$_2$. The time- and concentration- dependent phosphorylation of VASP in response to PGI$_2$ could be detected in washed platelets and those present in whole blood, indicating that the methodology could be used to examine platelet signalling events under (patho)physiological conditions (Figure 4.20Aii and Bii).
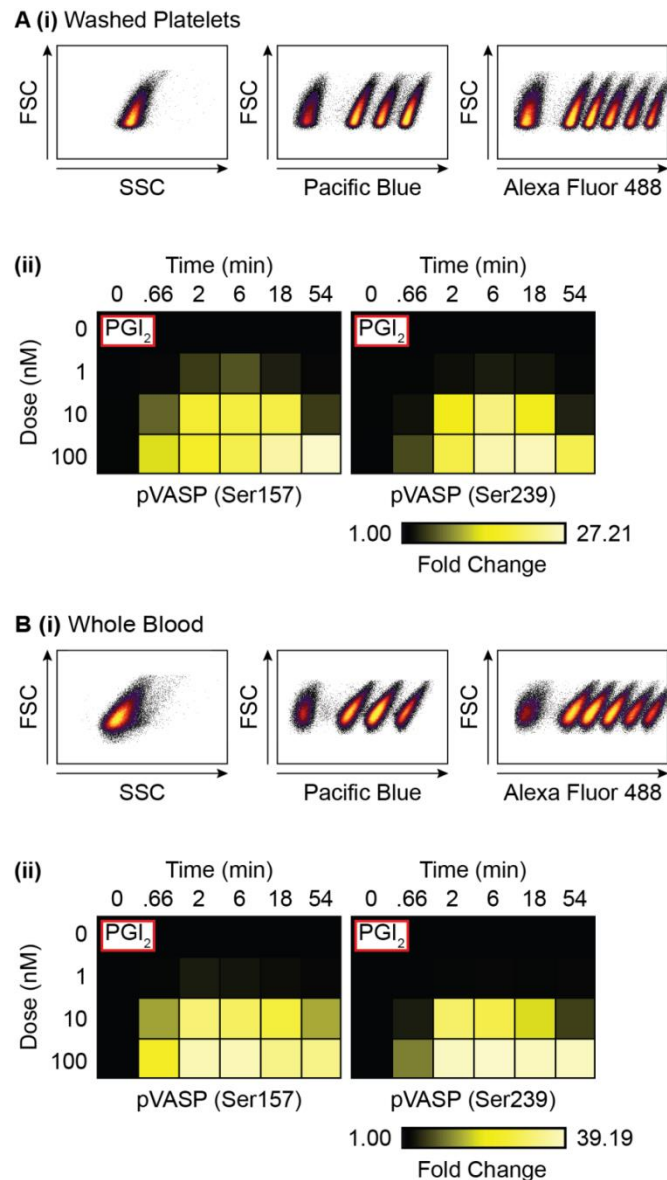
Figure 4.20. Application of FCB to examine platelet signalling in whole blood. Fixed and permeabilised (**Ai**) washed platelets or (**Bi**) whole-blood platelets were barcoded with Pacific Blue and Alexa Fluor 488 after treatment with PGI_2 (0, 1, 10, and 100 nM) for the indicated times. Barcoded samples were combined and stained with phosphoVASP-ser[157] or phosphoVASP-ser[239] and Alexa Fluor 647. Heatmaps were comparable between (**Aii**) washed platelets and (**Bii**) whole-blood platelets. Data are representative of three independent experiments.

4.7 Examination of sample storage conditions on phosphorylation

We wished to determine whether fixed whole blood samples could withstand freezing and therefore undergo processing at a later time. Whole blood samples were treated with PGI_2 (10 or 100 nM) before fixation, and then either permeabilised and stained immediately or stored at $4^{\circ}C$ or $-20^{\circ}C$ overnight before permeabilisation and staining with phosphoVASP-ser[157]. Samples that were stored at $4^{\circ}C$ overnight showed reduced phosphoVASP-ser[157] staining compared to those processed immediately. Samples stored at $-20°C$ were the most stable, where staining was reduced from 15.5- to 10.5-fold and from 18.6- to 13.0-fold for 10 and 100 nM PGI_2 respectively. Thus, while there were small reductions in staining, the samples were still sufficiently stable to provide meaningful readouts on signalling events (Figure 4.21).
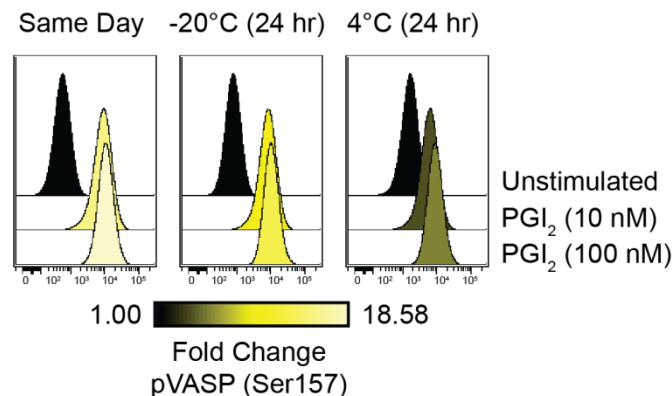
Figure 4.21. Fixed whole blood samples can be stored overnight with minor losses in signal intensity. Prior to fixation, whole blood samples were either untreated or treated with PGI_2 (10 or 100 nM) for 2 min. Samples underwent either immediate analysis or next day analysis after storage at -20°C or 4°C.

4.8 Discussion

Understanding the signal transduction mechanisms that drive platelet function may allow the identification of new targets or therapeutic agents. Cyclic nucleotide signalling cascades are potent global modulators of platelet function and may therefore present targets for antithrombotic agents. The activity of cyclic nucleotide signalling can be determined by measuring the phosphorylation status of VASP, which is sensitive to modification by both PKA and PKG (Butt et al., 1994). Traditional phosphoproteomic approaches have several drawbacks that do not lend themselves to high-throughput analyses. The flow cytometric assay developed here facilitates large-scale analyses of compounds that modulate cAMP- and potentially cGMP-dependent signalling in platelets.

Phosphoflow has been widely applied in the field of immune signalling (Table 4.1) but its application to platelets has not achieved wide use or popularity. Schwarz and colleagues first demonstrated that phosphoVASP could be measured in platelets by whole blood flow cytometry but their approach has never been fully exploited (Schwarz et al., 1999b). To develop methodology for the flow cytometric analysis of platelet signalling events, we applied a series of general phosphoprotein staining techniques to washed platelets and those in whole blood. Our flow cytometric method could detect subtle time- and concentration-dependent changes in phosphorylation, was sensitive to kinase inhibition, and showed comparable results with immunoblotting. Immunoblotting has been used to cross-validate phosphoflow protocols in cell lines (Krutzik and Nolan, 2003) and murine splenocytes (Krutzik et al., 2007). In all cases, flow cytometry analyses

correlated closely with immunoblot analyses over a wide range of conditions. While flow cytometry has many advantages over immunoblotting, it is not well-suited to the analysis of low-abundance signalling proteins and/or those buried in subcellular compartments. Through enzymatic amplification, immunoblotting is capable of detecting very small amounts of protein with large signal-to-noise ratios and since immunoblotting is performed on cell lysates (as opposed to intact cells) there are no concerns about antigen accessibility.

Having established a standard protocol, the key innovations were to apply FCB first to washed platelets and then to whole-blood platelets. Evaluating platelets in whole blood more accurately reflects the complex *in vivo* environment and is technically less demanding than immune cell analyses because platelets possess distinct scatter properties and can therefore be identified without surface markers. To the best of our knowledge, this is the first time FCB has been applied to primary human cells. Indeed, previous applications have been confined to cell lines (Krutzik and Nolan, 2006) and primary murine cells (Krutzik et al., 2007). FCB offers significant advantages over traditional phosphoproteomic approaches. The multiplexing step allows large-scale analyses to be completed in only a few hours while reducing reagent consumption and eliminating pipetting error and staining variability. Using two fluorophores, we showed that 24 samples could be multiplexed to resolve dose- and time-response relationships for multiple AC agonists. These analyses spanned six timepoints and four concentrations of various cAMP-elevating agents and were equivalent to 48 separate dose-response or 32 separate time-response immunoblots. While these analyses could be

completed in only a few hours using FCB flow cytometry, they would take several weeks using standard immunoblot techniques. Moreover, samples could be frozen overnight without significantly affecting assay performance, which could facilitate use of the assay in laboratories that are remote for the flow cytometry platform. Using three fluorophores, we then multiplexed 40 samples to examine known modulators of cAMP signalling. The assay was sensitive enough to detect changes in phosphoVASP-ser[157] both in response to multiple cAMP-elevating stimuli and to compounds that have been shown to influence cAMP signalling including receptor antagonists, kinase inhibitors, and PDE inhibitors. Since FCB labelling intensity correlates with cell size and the abundance of amines within the cell, smaller cells such as platelets label less intensely than larger cells (Krutzik et al., 2011). At the same time, fluorophores that are excited optimally by a laser require lower concentrations than fluorophores that are not optimally excited (Krutzik et al., 2011). We selected fluorophores for optimal excitation, allowing intense fluorescent signals to be obtained from the platelet population. It is recommended to label cells with no more than 1 µg/mL (Krutzik et al., 2011) but we achieved optimal labelling at 1.5 µg/mL. This concentration has successfully been used to label murine splenocytes, which are similar in size to human platelets (Krutzik and Nolan, 2006). This concentration was diluted fivefold to produce differentially labelled populations that did not bleed into one another, thus enabling clear identification and deconvolution of multiplexed samples.

To fully exploit potential applications of our method, it will be important to characterise entire signalling cascades by analysing multiple targets within

the same sample. In the present study, we were unable to perform multiparameter analyses due to the absence of directly-labelled primary antibodies. We used fluorophore-labelled secondary antibodies to determine the extent of protein phosphorylation but these reagents are not conducive to multiparameter analyses because they can cross-react with different primary antibodies and generate false positive signals. Reagents aside, the maximum number of phosphoproteins that can be analysed in any given cell type is limited by hardware specifications. While three laser cytometers can detect up to ten separate parameters, sophisticated five laser machines can detect around twenty. Preliminary data shows that directly-labelled antibodies raised against kinases that mediate platelet activation are fully conducive to multiparameter analyses. This raises the possibility that multiple components of one or more platelet signalling cascades could be analysed simultaneously. These antibodies have successfully enabled the simultaneous analysis of multiple phosphoproteins in cell lines (Shachaf et al., 2007), primary murine splenocytes (O'Gorman et al., 2010), and isolated human peripheral blood cells (Irish et al., 2010). Since numerous signalling cascades are ubiquitous and since kinase inhibitors are an important and emerging class of targeted therapeutic agents (Cohen, 2002) our whole blood assay for platelets could serve as a model system for quantifying the *in vivo* effects of novel kinase and phosphatase inhibitors that are intended for therapeutic application in other cell types. Our flow cytometric method could therefore be applied across a broad range of therapeutic areas.

Table 4.1. Published applications of phosphoflow cytometry.

Phosphoproteins	Specimen	Fixation	Permeabilisation	FCB	Reference
PhosphoERK-thr^{202}/tyr^{204} PhosphoJNK-thr^{183}/tyr^{185}	Jurkat	1.6% PFA	100% Methanol	N/A	(Kinoshita et al., 2012)
PhosphoSTAT1-tyr^{701} PhosphoSTAT3-tyr^{705} PhosphoSTAT4-tyr^{693} PhosphoSTAT5-tyr^{694}	Leukocytes in human whole blood	BD Phosflow Lyse/Fix Buffer	100% Methanol	≤36 samples	(Thomas et al., 2011)
PhosphoERK-thr^{202}/tyr^{204} PhosphoSTAT3-tyr^{705} PhosphoSTAT5-tyr^{694}	Hematopoietic stem and progenitor cells	1.6% PFA	90% Ethanol	N/A	(Gibbs et al., 2011)
PhosphoAKT-ser^{473} PhosphoSTAT5-tyr^{694}	Hematopoietic stem cells	2% PFA	90% Ethanol	N/A	(Heffner et al., 2011)
PhosphoBTK/ITK-tyr^{551} Phospho-p38-thr^{180}/tyr^{182} PhosphoERK-thr^{202}/tyr^{204} PhosphoSFK/LCK-tyr^{505} PhosphoSYK/ZAP70-tyr^{352}/tyr^{319} Phospho-NFκB-p65-ser^{529} PhosphoSTAT1-tyr^{701} PhosphoSTAT3-tyr^{705} PhosphoSTAT5-tyr^{694} PhosphoSTAT6-tyr^{641} PhosphoCBL-tyr^{700} PhosphoPLCγ2-tyr^{759} PhosphoBLNK-tyr^{84} PhosphoAKT-ser^{473} PhosphoS6-ser^{235}/ser^{236}	Peripheral blood mononuclear cells	1.6% PFA	100% Methanol	9-27 samples	(Irish et al., 2010)
PhosphoSTAT1-tyr^{701} PhosphoSTAT3-tyr^{705} PhosphoSTAT4-tyr^{693} PhosphoSTAT5-tyr^{694} PhosphoSTAT6-tyr^{641}	Murine splenocytes	1.5% PFA	100% Methanol		(O'Gorman et al., 2010)
PhosphoSTAT5-tyr^{694}	Murine splenocytes	1.5% PFA	100% Methanol	N/A	(O'Gorman et al., 2009)

PhosphoSTAT1-tyr[701] PhosphoSTAT3-tyr[705] PhosphoSTAT5-tyr[694] PhosphoSTAT6-tyr[641]	Murine splenocytes	1.5% PFA	100% Methanol	N/A	(Hale et al., 2009)
PhosphoERK-thr[202]/tyr[204] PhosphoSTAT5-tyr[694] PhosphoS6-ser[235]/ser[236]	Peripheral blood mononuclear cells U937	1.6% PFA	95% Methanol	N/A	(Kotecha et al., 2008)
Phospho-p38-thr[180]/tyr[182] PhosphoERK-thr[202]/tyr[204] PhosphoJNK-thr[183]/tyr[185] PhosphoIκBα-ser[32]/ser[36] PhosphoIKKα-ser[176]/ser[180] Phospho-cRAF-ser[259] Phospho-cRAF-ser[338] Phospho-cRAF-ser[621] PhosphoELK-ser[338] Phospho-cJUN-ser[73] PhosphoBAD-ser[112] PhosphoBAD-ser[136] PhosphoMEK-thr[394] PhosphoMEK-ser[298] PhosphoVAV1-tyr[160] Phospho-NFκB-p65-ser[529] PhosphoSTAT1-tyr[701] PhosphoSTAT3-tyr[705] PhosphoSTAT5-tyr[694] PhosphoPLCγ1-tyr[783] PhosphoAKT-ser[473] PhosphoAKT-thr[305]	ST486	2% PFA	100% Methanol	N/A	(Shachaf et al., 2007)
Phospho-p53-ser[15] Phospho-p53-ser[20] Phospho-p53-ser[37] Phospho-p53-ser[46] Phospho-p53-ser[392]	Acute myeloid leukemia	1.6% PFA	100% Methanol	N/A	(Irish et al., 2007)
Phospho-p38-thr[180]/tyr[182] PhosphoSTAT1-tyr[701] PhosphoSTAT3-tyr[705] PhosphoSTAT5-tyr[694] PhosphoSTAT6-tyr[641]	U937 Murine splenocytes	1.6% PFA BD Phosflow Lyse/Fix Buffer	100% Methanol	24 samples	(Krutzik et al., 2007)

PhosphoERK-thr^{202}/tyr^{204} PhosphoSTAT5-tyr^{694} PhosphoS6-ser^{235}/ser^{236}	Hematopoietic stem and progenitor cells	2% PFA	95% Methanol	N/A	(Van Meter et al., 2007)
PhosphoBTK/ITK-tyr^{551} Phospho-p38-thr^{180}/tyr^{182} PhosphoERK-thr^{202}/tyr^{204} PhosphoSYK/ZAP70-tyr^{352}/tyr^{319}	Peripheral blood mononuclear cells	1.6% PFA	100% Methanol	N/A	(Irish et al., 2006)
PhosphoERK-thr^{202}/tyr^{204} PhosphoSTAT1-tyr^{701} PhosphoSTAT3-tyr^{705} PhosphoSTAT5-tyr^{694} PhosphoSTAT6-tyr^{641}	U937 Jurkat Murine splenocytes	1.6% PFA	100% Methanol	4-96 samples	(Krutzik and Nolan, 2006)
PhosphoSTAT3-tyr^{705} PhosphoSTAT5-tyr^{694}	Murine splenocytes	1.6% PFA	100% Methanol	N/A	(Krutzik et al., 2005a)
Phospho-p38-thr^{180}/tyr^{182} PhosphoSTAT1-tyr^{701} PhosphoSTAT3-tyr^{705} PhosphoSTAT5-tyr^{694}	Murine splenocytes	1.5% PFA	100% Methanol	N/A	(Krutzik et al., 2005b)
PhosphoSTAT1-tyr^{701}	U937	1.6% PFA	100% Methanol	N/A	(Stitz et al., 2005)
Phospho-p38-thr^{180}/tyr^{182} PhosphoERK-thr^{202}/tyr^{204} PhosphoSTAT1-tyr^{701} PhosphoSTAT3-tyr^{705} PhosphoSTAT5-tyr^{694} PhosphoSTAT6-tyr^{641}	Acute myeloid leukemia	1.6% PFA	100% Methanol	N/A	(Irish et al., 2004)
Phospho-p38-thr^{180}/tyr^{182} PhosphoERK-thr^{202}/tyr^{204} PhosphoJNK-thr^{183}/tyr^{185} PhosphoSTAT1-tyr^{701} PhosphoSTAT5-tyr^{694} PhosphoSTAT6-tyr^{641}	U937 Jurkat	1.5% PFA	100% Methanol	N/A	(Krutzik and Nolan, 2003)

Pharmacological and Clinical Applications of Phosphoflow Cytometry

5.1 Introduction

Atherothrombosis is the leading cause of morbidity and mortality worldwide, and will become increasingly prevalent in Western countries (Mathers and Loncar, 2006). To alleviate the continued burden of atherothrombotic-related disease, there are clinical and pharmacological requirements for the (a) identification of high risk patients, (b) monitoring of therapies in patients with established disease, and (c) identification of novel targets and therapies. Thrombotic complications accompany a wide range of clinical conditions including insulin resistance. The procoagulant state associated with insulin resistance is thought to be partly associated with platelet hyperactivity (Tschoepe et al., 1990). In healthy blood vessels, platelet activation is counterbalanced by inhibitory signalling cascades that are activated by endothelial-derived prostacyclin (PGI_2) and nitric oxide (NO). These inhibitors stimulate cAMP- and cGMP-dependent protein kinases, which phosphorylate downstream target proteins such as vasodilator-stimulated phosphoprotein (VASP) to prevent excessive platelet activation (Horstrup et al., 1994). However, there is potential for platelet resistance to these inhibitors in certain disease states. Such resistance has been identified in type 2 diabetes, an insulin resistant state associated with premature cardiovascular mortality (Davi et al., 1982, Modesti et al., 1991). Insulin resistance is also a feature of polycystic ovary syndrome (PCOS), an endocrine disorder affecting 5-7% of premenopausal women (Franks, 1995). Women with PCOS are phenotypically similar to diabetics since 80% are obese and 33% are hyperlipidemic (Ehrmann et al., 2006). Platelet hyperactivity has been

observed in PCOS (Dereli et al., 2003) and the condition is associated with an increased risk of atherothrombosis. However, the molecular mechanisms underpinning platelet dysfunction in PCOS have not been determined.

Flow cytometry is an indispensable platform for the assessment of platelet function in atherothrombotic-related disease but the majority of applications have been confined to the quantification of surface antigens such as P-selectin or $\alpha IIb\beta 3$ (Linden et al., 2004). Since platelet function is regulated by the activation or inhibition of kinase signalling cascades, the analysis of phosphorylation-based signalling events could allow for a more sensitive and specific characterisation of disease status. Additionally, these analyses could facilitate the identification of defective signalling cascades and aid in the identification of compounds that can favourably modulate these cascades to improve clinical outcomes. Using phosphoVASP as a marker of cyclic nucleotide signalling, we demonstrate how phosphoflow can be applied in the context of drug screening, identifying three novel agents that inhibit platelet aggregation through cAMP-dependent mechanisms. We then demonstrate how the method can be used to assess platelet function and PGI_2 sensitivity in PCOS.

5.2 Fluorescent cell barcoding facilitates the identification of cAMP-mediated platelet inhibitors in whole blood

Since VASP phosphorylation correlates with the inhibition of platelet aggregation (Horstrup et al., 1994), we reasoned that phosphoVASP-ser^{157} could serve as a marker for identifying potential antiplatelet agents. To this end, we designed a three-dimensional FCB scheme to screen a library of 70 prostaglandins (96 multiplexed samples) for their ability to induce phosphoVASP-ser^{157} in whole-blood platelets (Figure A3). PGI_2-induced phosphoVASP-ser^{157} was used as a positive control and a hit threshold was drawn 3 SD from the mean MFI of PGI_2-stimulated controls. Six screening library compounds induced phosphoVASP-ser^{157} above the hit threshold (Figures 5.1A and B). Two of these compounds, 16-phenyl tetranor PGE_1 and 16,16-dimethyl-6-keto PGE_1, referred to as C5 and D5 according to their respective coordinates in the screening plate (Figure 5.2A), induced 26.9 and 26.6 fold increases in phosphoVASP-ser^{157}. Since C5 and D5 had previously undetermined biological activity, they underwent further characterisation. A third compound, 5-*trans* PGD_2 (D2), also underwent follow-up analyses (Figure 5.2A). This compound, which induced a moderate level of phosphoVASP-ser^{157} (16.4), was selected because its biological activity was, like compounds C5 and D5, completely unknown. We obtained similar data using washed platelets, confirming the accuracy of the screen (Figure 5.3).
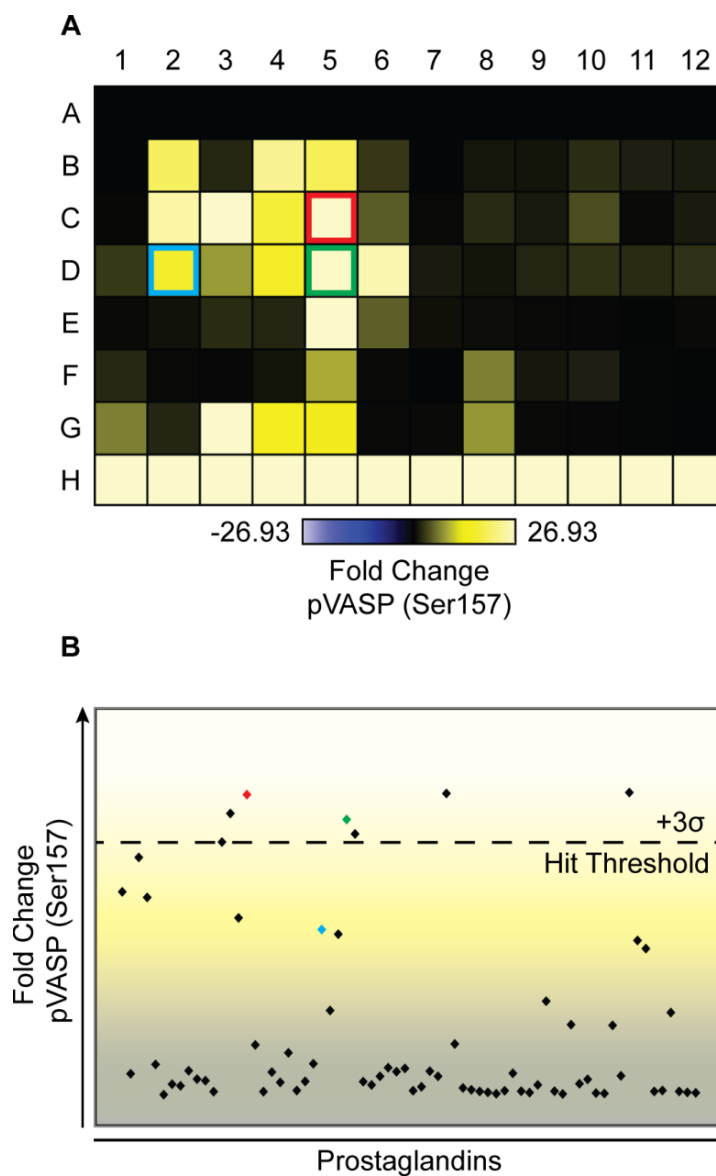
Figure 5.1. Three-dimensional FCB facilitates whole blood screening and identification of antiplatelet compounds. (**A**) Heatmap visualisation of the screen, where coloured squares indicate novel hits. (**B**) PhosphoVASP-ser[157] plot, where coloured data points represent novel hits.

Table 5.1. Statistical values from the prostaglandin library screen.

Control	Number of wells	Mean MFI	Standard deviation	Z'
Negative	12	448.1	31.3	
Positive	12	18992.8	1002.3	0.84

To evaluate the quality of our cell-based screen, we calculated the Z'-factor from control samples (Table 5.1). The Z'-factor, a screening window coefficient reflecting the dynamic range and variability of control measurements, was 0.84 indicating excellent assay performance (Zhang et al., 1999). In follow-up analyses, all three compounds induced phosphoVASP-ser[157] and ser[239], confirming the results of our initial screen. These compounds induced phosphorylation with a potency order of C5>D5>D2. The ability of these compounds to induce phosphoVASP-ser[157] was reflected by their ability to stimulate intraplatelet cAMP production (Figure 5.4), where the same order of potency was observed. The signalling activities of these compounds were validated at five doses across six time points (30 multiplexed samples) with a two-dimensional FCB scheme with Alexa Fluor 488 and Pacific Blue (Figure A4). As highlighted in Figures 5.2 and 5.3, VASP underwent time- and concentration-dependent phosphorylation on both ser[157] and ser[239] in response to C5. Ser[157] underwent rapid phosphorylation while ser[239] peaked at later time points. PhosphoVASP-ser[157] was more sensitive to lower concentrations (1- and 10 nM) of C5 than ser[239] (Figures 5.2 and 5.3). C5 induced higher levels of phosphorylation at all concentrations and time points tested than D2 or D5.

Compound C5 (100 nM) induced significant phosphoVASP-ser^{157} at 40 sec (25.4 ± 6.2) and this was maintained over 54 min (P <0.05). By contrast, C5 (100 nM) did not induce significant phosphoVASP-ser^{239} until 6 min (17.1 ± 5.3) (P <0.05). C5 (1000 nM) caused significant phosphorylation on ser^{157} (29.0 ± 6.4) and ser^{239} (19.1 ± 3.8) within 40 sec and peaked at 54 min (P <0.05). Compound D2 induced substantial phosphorylation on ser^{157} and ser^{239} at 1000 nM and peaked at 18 min (Figures 5.2 and 5.3). Ser^{157} was more sensitive to D2 (1000 nM) than ser^{239}. Low concentrations (1-100 nM) of D2 had modest effects on phosphoVASP-ser^{157} and minimal effects on ser^{239}. Compound D5 caused significant phosphoVASP-ser^{157} and ser^{239} at 100 nM (P <0.05). D5 (100 nM)-induced phosphoVASP-ser^{157} and ser^{239} peaked at 6 min and decreased thereafter. The kinetics of phosphorylation were similar in D5 (1000 nM)-stimulated platelets (Figures 5.2 and 5.3). The time- and concentration-dependent changes in phosphoVASP-ser^{157} and ser^{239} confirmed the results of our initial screen.
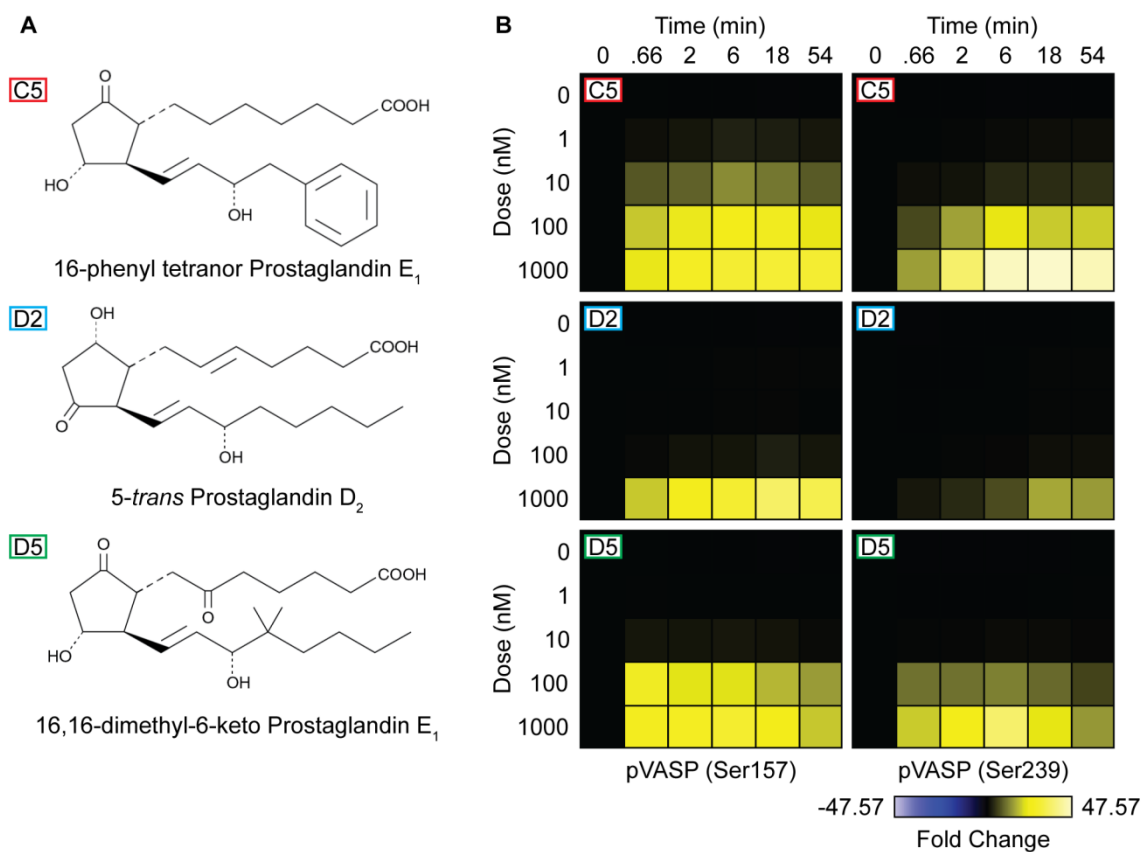
Figure 5.2. Two-dimensional FCB facilitates validation of antiplatelet compounds in whole blood. (**A**) Chemical structures of compounds C5, D2, and D5. (**B**) Hit validation. Prior to FCB, whole blood samples were treated with compound C5, D2, or D5 (0, 1, 10, 100, and 1000 nM) for the indicated times.
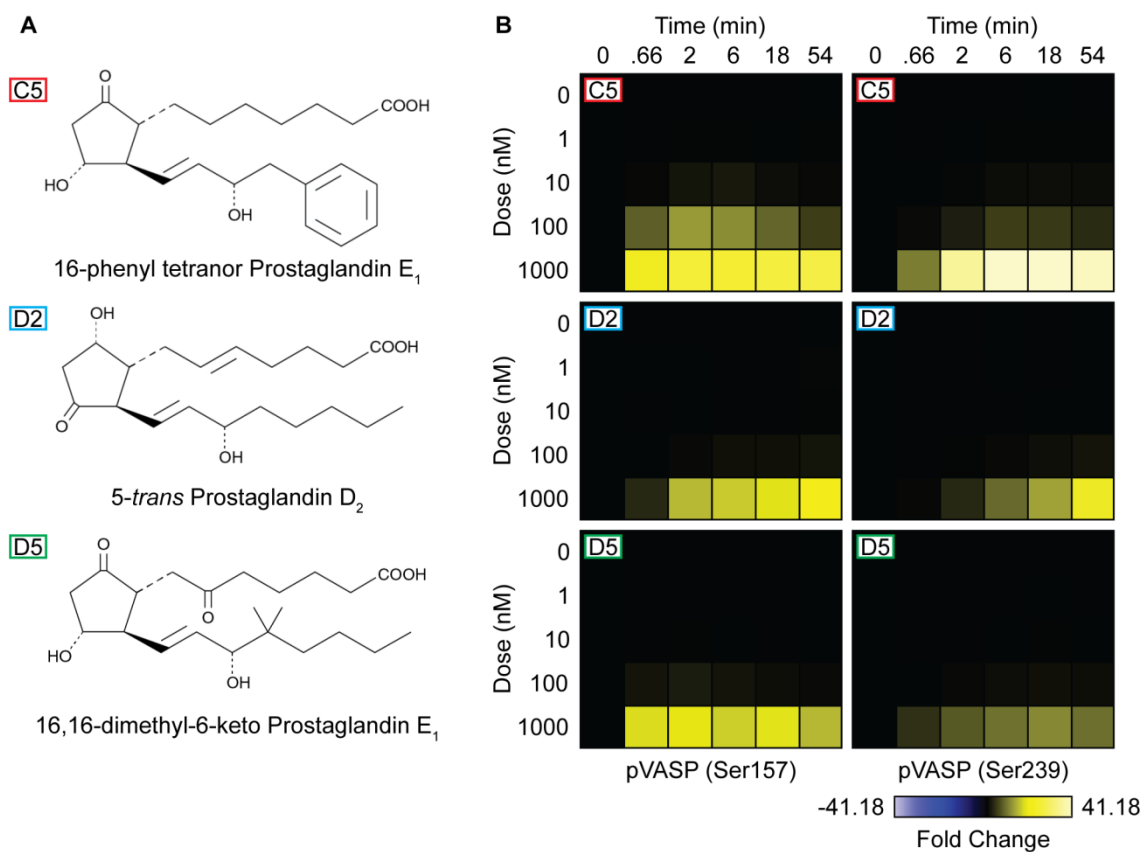
Figure 5.3. Two-dimensional FCB facilitates validation of antiplatelet compounds in washed platelets. (**A**) Chemical structures of compounds C5, D2, and D5. (**B**) Hit validation. Prior to FCB, washed platelets were treated with compound C5, D2, or D5 (0, 1, 10, 100, and 1000 nM) for the indicated times.
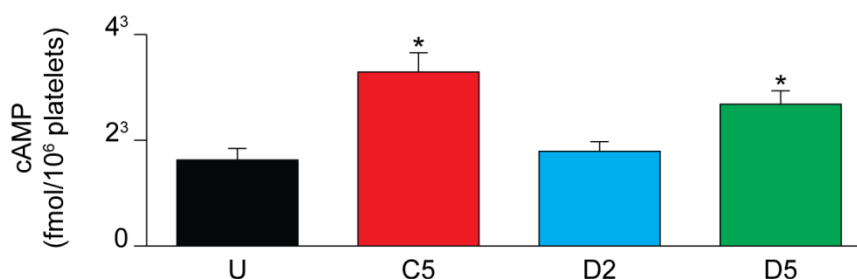
Figure 5.4. Hit compounds elevate intraplatelet cAMP. Stimulation with compounds C5 (1 µM, 2 min), D2 (1 µM, 2 min), or D5 (1 µM, 2 min) elevates cAMP in washed platelets. Data represents the mean ± SEM from three independent experiments (*P <0.05).

5.3 Hit compounds inhibit platelet aggregation

Having identified novel agents that activate cAMP signalling, we next determined their effects on platelet function. Compounds C5, D2, and D5 inhibited collagen-induced platelet aggregation in a concentration-dependent manner (Figure 5.5A) with respective IC_{50} values of 330 nM, 488 nM and 881 nM (Figure 5.5B). The antiplatelet properties of compound D2, but not compounds C5 or D5, were completely abolished in the presence of BW A868C, suggesting that D2 signals exclusively through the DP receptor (Figure 5.6A). The anti-aggregatory effects of compounds C5 and D5, but not compound D2, were largely but not completely abolished in the presence of RO1138452, suggesting that compounds C5 and D5 signal through the IP receptor (Figure 5.6B).
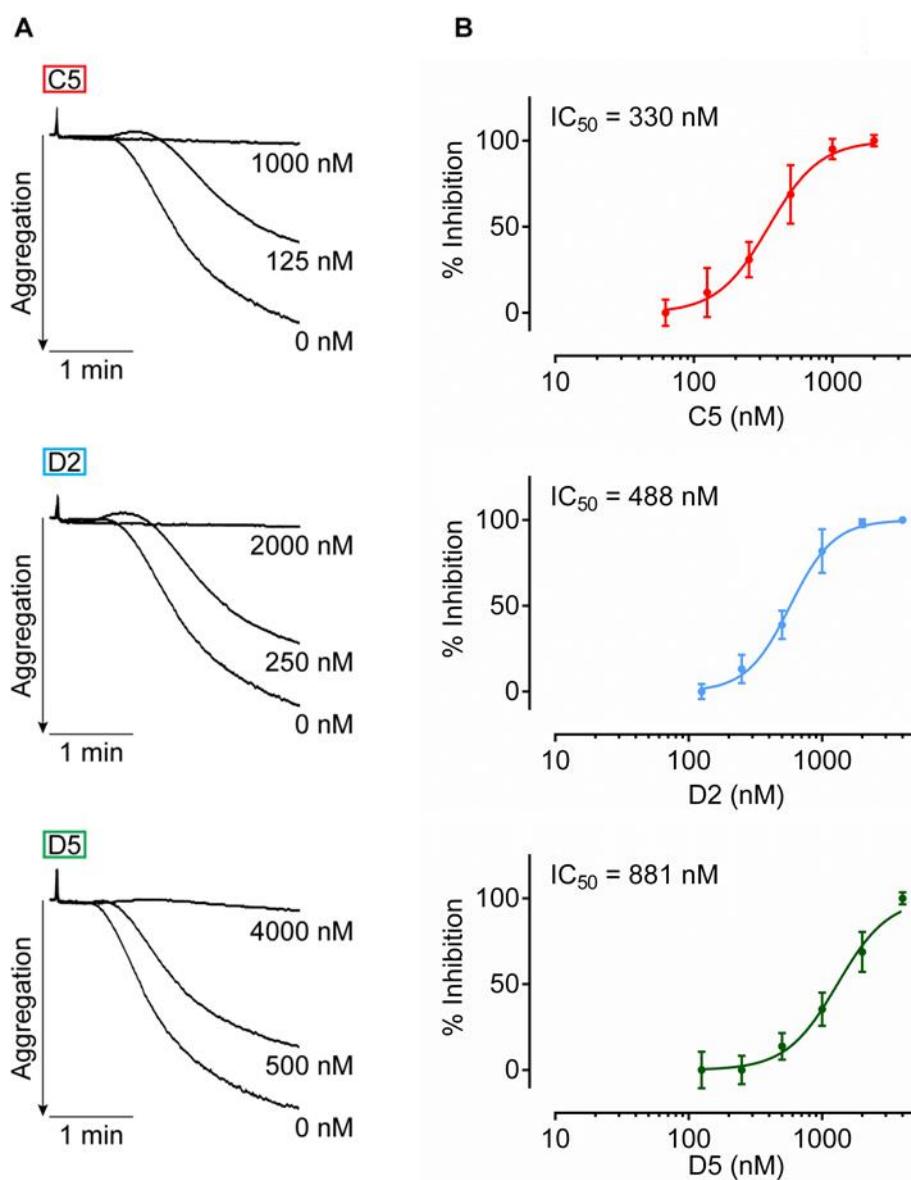
Figure 5.5. Hit compounds demonstrate antiplatelet properties. (**A**) Traces, representative of three independent experiments, show that hit compounds inhibit collagen-induced platelet aggregation in a concentration-dependent manner. (**B**) Dose-response curves reveal the respective potencies of the hit compounds, where data points represent mean values from three independent experiments. Platelets were stimulated with collagen (5 µg/mL) following pre-incubation (2 min) with each compound.
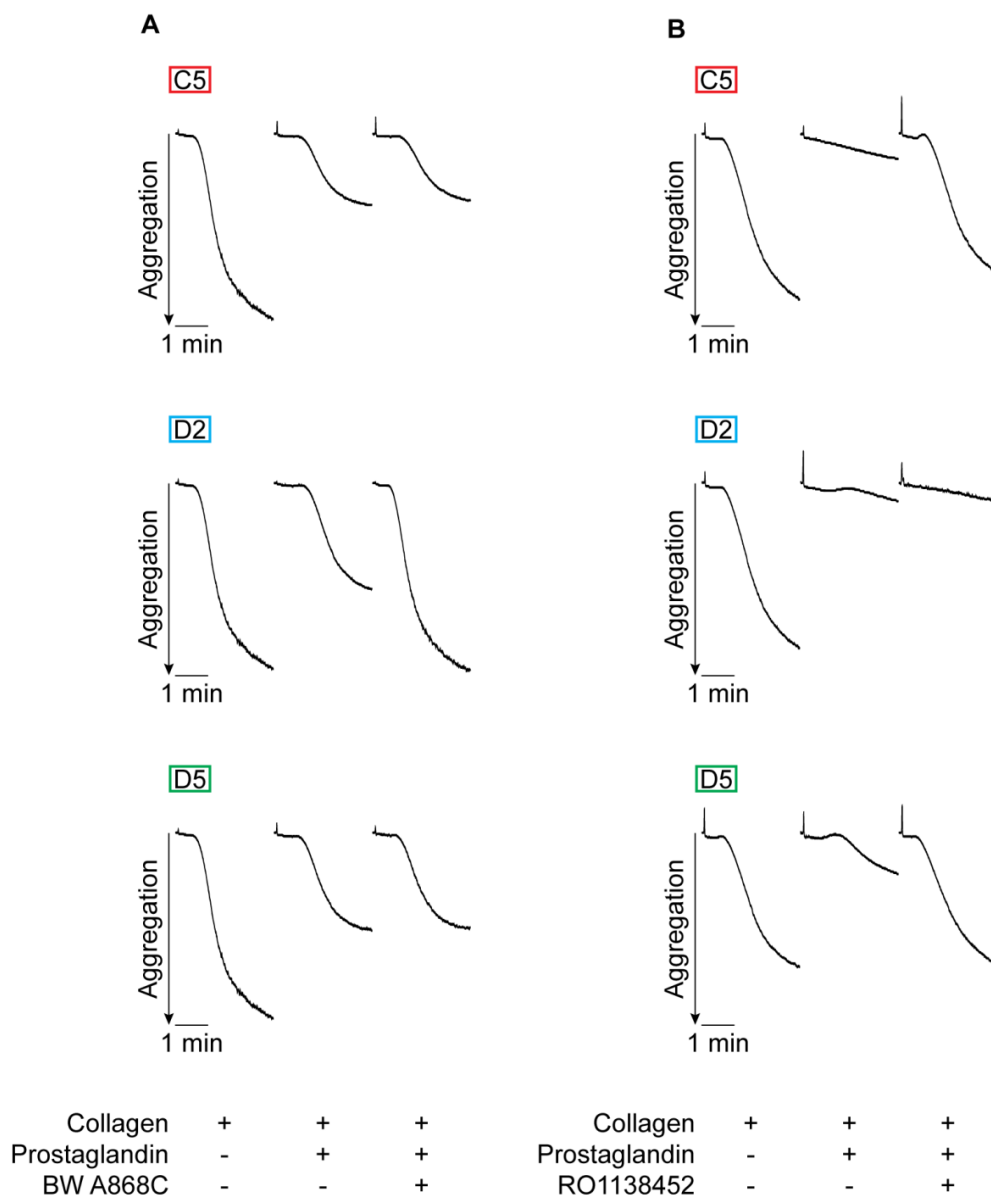
Figure 5.6. Hit compounds signal through prostanoid receptors. (**A**) The DP-receptor antagonist, BW A868C (1 µM, 10 min), blocks the anti-aggregatory effects of compound D2 (1 µM, 2 min), but not compounds C5 (1 µM, 2 min) or D5 (2 µM, 2 min). (**B**) The IP-receptor antagonist, RO1138452 (1 µM, 10 min), blocks the anti-aggregatory effects of compounds C5 (1 µM, 2 min) and D5 (2 µM, 2 min), but not compound D2 (1 µM, 2 min). Washed platelets were stimulated with collagen (5 µg/mL) following pre-incubation first with the receptor antagonist and then with the hit compound.

5.4 Fluorescent cell barcoding facilitates signalling profiling in PCOS

Whole blood flow cytometry is a valuable clinical tool that enables the (patho)physiological assessment of platelet function (Michelson et al., 2000). Insulin resistant states such as PCOS are associated with platelet hyperactivity and PGI_2 resistance (Modesti et al., 1991, Dereli et al., 2003). To try and elucidate the mechanism(s) for platelet dysfunction in PCOS, we explored the possibility that cyclic nucleotide signalling cascades were compromised. To this end, we designed a two-dimensional FCB scheme to measure prostaglandin-induced phosphoVASP-ser[157] and ser[239] in nine PCOS patients versus nine healthy controls (Figures 5.7 and A5). PCOS was diagnosed by the presence of two of three characteristics including oligomenorrhea, clinical and/or biochemical hyperandrogenism, and polycystic ovaries on ultrasound as per the Rotterdam diagnostic criteria (Rotterdam ESHRE/ASRM-sponsored PCOS Consensus Workshop Group, 2004). PCOS subjects were clinically obese (BMI≥30) and had higher blood pressure than controls (Table 5.2).

Table 5.2. Anthropometric parameters and biochemical markers for study participants.

	CON ($N = 9$)	PCOS ($N = 9$)
Height (cm)	167.1 ± 2.4	167.7 ± 2.8
Weight (kg)	66.2 ± 2.9	88.3 ± 5.0*
BMI (kg/m^2)	23.8 ± 0.9	31.0 ± 1.4*
Systolic BP (mmHg)	109.8 ± 5.3	121.0 ± 2.7
Diastolic BP (mmHg)	68.8 ± 3.2	81.2 ± 3.9*
Cholesterol (mmol/L)	5.7 ± 0.2	4.9 ± 0.4
LDL (mmol/L)	3.8 ± 0.3	3.0 ± 0.3
HDL (mmol/L)	1.5 ± 0.1	1.2 ± 0.1*
Triglycerides (mmol/L)	1.1 ± 0.2	1.1 ± 0.2
Cholesterol/HDL	3.7 ± 0.3	3.7 ± 0.4

Note. BMI, body mass index; BP, blood pressure; LDL, low-density lipoprotein; HDL, high-density lipoprotein. Data are presented as means ± SEM (*$P<0.05$).
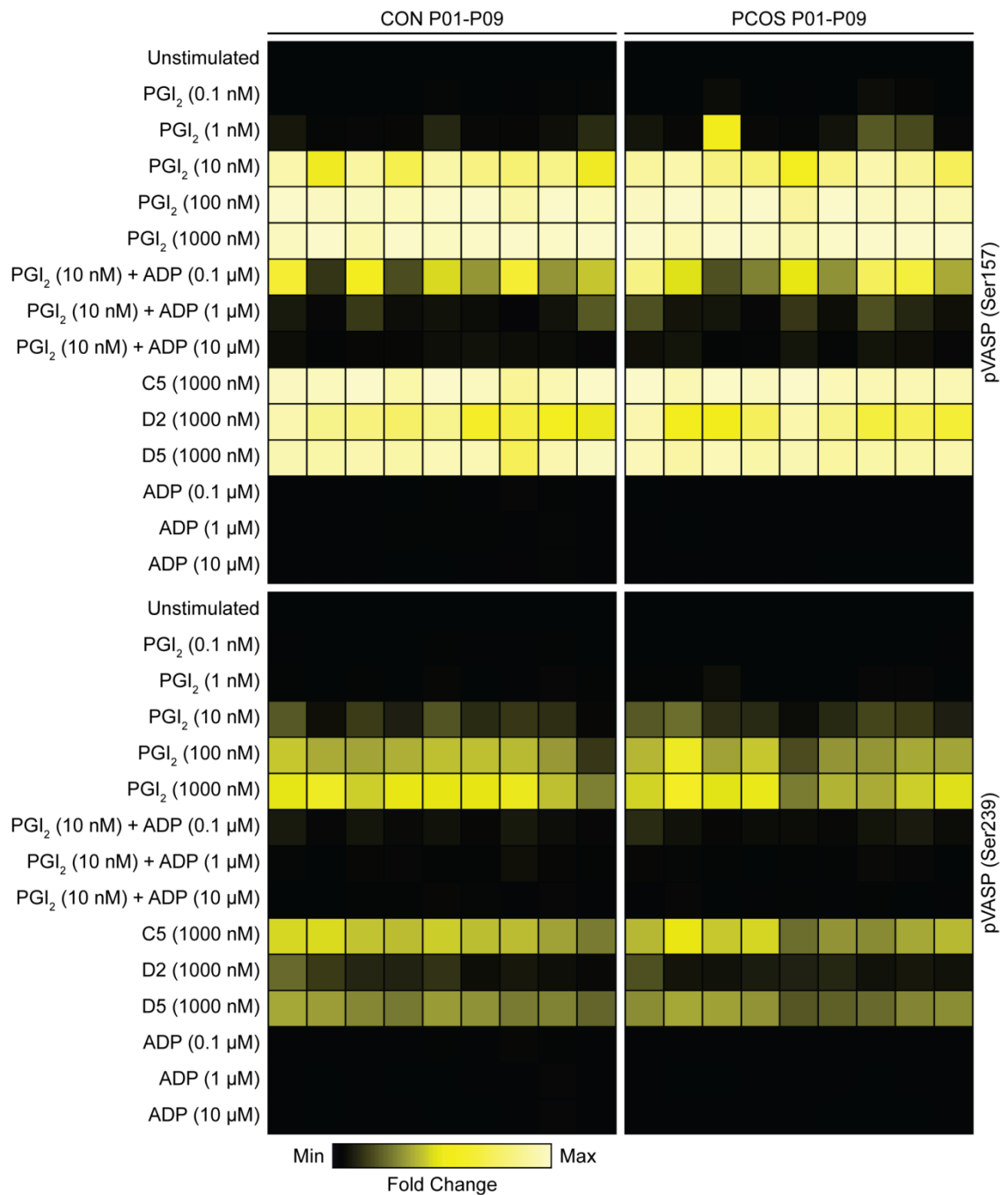
Figure 5.7. FCB facilitates large-scale profiling of cyclic nucleotide signalling in PCOS patients. Heatmap representation of signalling profiles from nine control (CON P01-P09) and nine PCOS (PCOS P01-P09) patients. Data were normalised to the maximal level of phosphorylation for each individual patient.

5.4.1 PGI$_2$-induced VASP phosphorylation is not diminished in PCOS

To determine platelet sensitivity to PGI$_2$, our multiplexed analyses incorporated a six-point dose-response from which EC$_{50}$ values were calculated. In brief, quantitative phosphoflow data were normalised to span the range from 0-100% and plotted against the logarithm of PGI$_2$ concentration (Figures 5.8 and 5.9). Normalisation was required for statistical comparisons between groups. PCOS and control EC$_{50}$ values were not significantly different for either phosphoVASP-ser[157] (PCOS = 4.6 nM, CON = 5.5 nM, P >0.05) or phosphoVASP-ser[239] (PCOS = 28.3 nM, CON = 33.7 nM, P >0.05). However, EC$_{50}$ values were lower for phosphoVASP-ser[157] than for ser[239] indicating that PGI$_2$ preferentially targeted ser[157]. These data suggest that the cyclic nucleotide signalling response to PGI$_2$ is not diminished in PCOS.
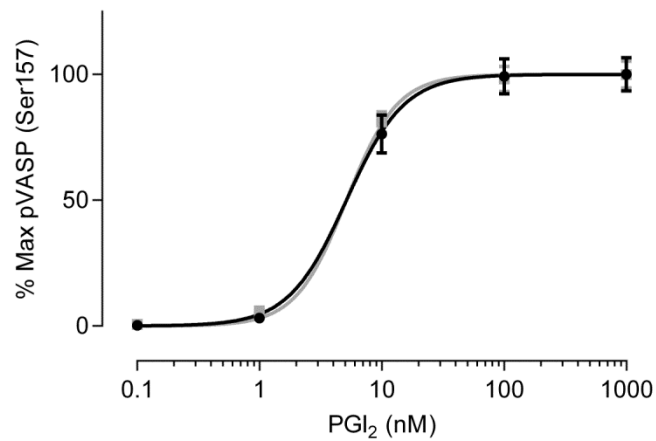
Figure 5.8. Dose-response curves of PGI$_2$ on phosphoVASP-ser[157] in PCOS versus controls. Dose-response curves derived from phosphoflow analyses reveal PGI$_2$ sensitivity in PCOS patients (grey curve) versus healthy controls (black curve). Data were normalised to the maximum response for each patient and expressed as means ± SEM.
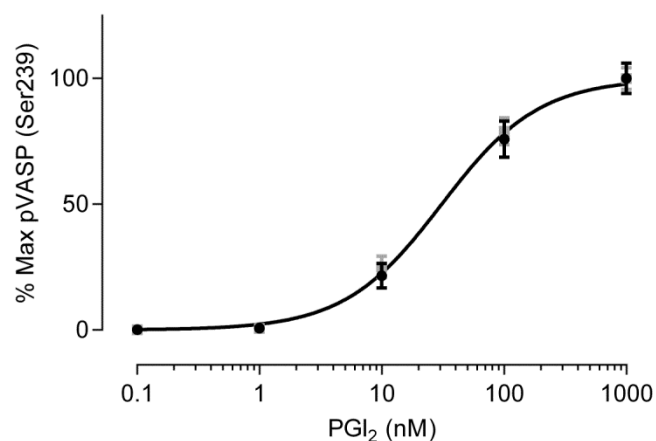
Figure 5.9. Dose-response curves of PGI$_2$ on phosphoVASP-ser[239] in PCOS versus controls. Dose-response curves derived from phosphoflow analyses reveal PGI$_2$ sensitivity in PCOS patients (grey curve) versus healthy controls (black curve). Data were normalised to the maximum response for each patient and expressed as means ± SEM.

5.4.2 ADP-mediated inhibition of PGI$_2$-induced VASP phosphorylation is not enhanced in PCOS

Next, our multiplexed analyses examined the ability of ADP to inhibit PGI$_2$-induced phosphoVASP-ser[157] and ser[239]. ADP inhibits cyclic nucleotide signalling and promotes platelet activation through its ability to induce P2Y$_{12}$ receptor-mediated inhibition of adenylyl cyclase (Hollopeter et al., 2001). Compared to PGI$_2$ alone (10 nM, 2 min), co-stimulation with ADP (0.1-10 μM, 2 min) and PGI$_2$ (10 nM, 2 min) diminished VASP phosphorylation on both ser[157] and ser[239]. Submicromolar ADP (0.1 μM) caused significant inhibition of VASP phosphorylation (Figures 5.10 and 5.11) but this was not significantly different between groups. Greater levels of inhibition were observed at 1- and 10 μM ADP but again these were not significantly different between groups. As a negative control, ADP alone (0.1-10 μM, 2 min) had no effect on phosphoVASP-ser[157] or ser[239] (Figure 5.7). These data suggest that the propensity for ADP to inhibit cyclic nucleotide signalling is not enhanced in PCOS.
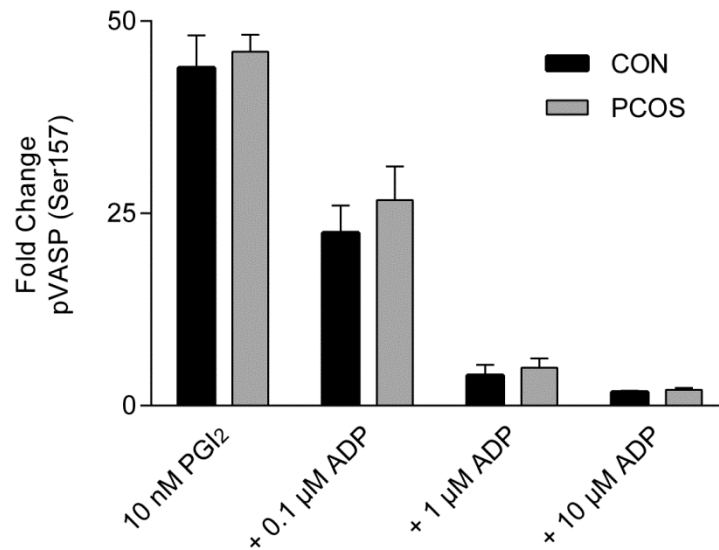
Figure 5.10. ADP-mediated inhibition of PGI$_2$-induced phosphoVASP-ser^{157} in PCOS and controls. ADP inhibits PGI$_2$-induced phosphoVASP-ser^{157} in a concentration-dependent manner. Data are expressed as means ± SEM.
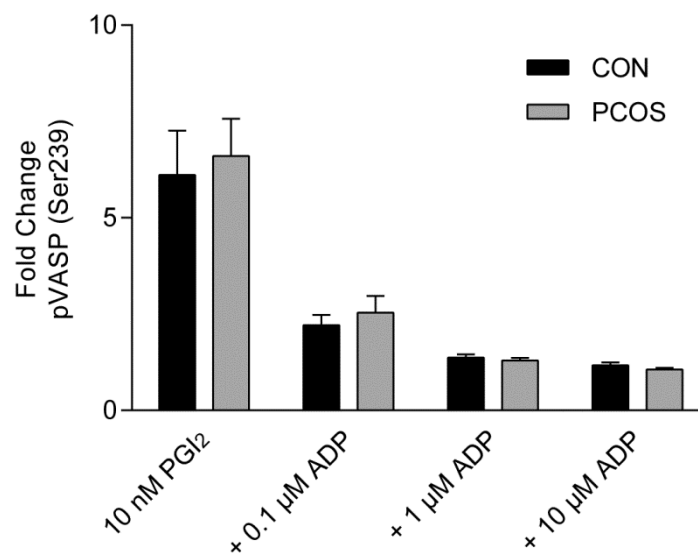
Figure 5.11. ADP-mediated inhibition of PGI$_2$-induced phosphoVASP-ser^{239} in PCOS and controls. ADP inhibits PGI$_2$-induced phosphoVASP-ser^{239} in a concentration-dependent manner. Data are expressed as means ± SEM.

5.4.3 Novel inhibitors induce VASP phosphorylation in PCOS

Having identified three novel modulators of cyclic nucleotide signalling, we examined their ability to induce phosphoVASP-ser[157] and ser[239] in PCOS subjects (Figures 5.12 and 5.13). After stimulation with either C5 (1 µM, 2 min), D2 (1 µM, 2 min), or D5 (1 µM, 2 min), phosphoVASP-ser[157] and ser[239] were not significantly different between PCOS or controls. Only D2 induced significantly less phosphoVASP-ser[157] than PGI_2 (1 µM, 2 min). By contrast, all three compounds induced significantly less phosphoVASP-ser[239] than PGI_2 while C5 induced more robust phosphorylation on ser[239] than compounds D2 and D5. These data suggest that our novel platelet inhibitors can modulate cyclic nucleotide signalling in clinical populations.
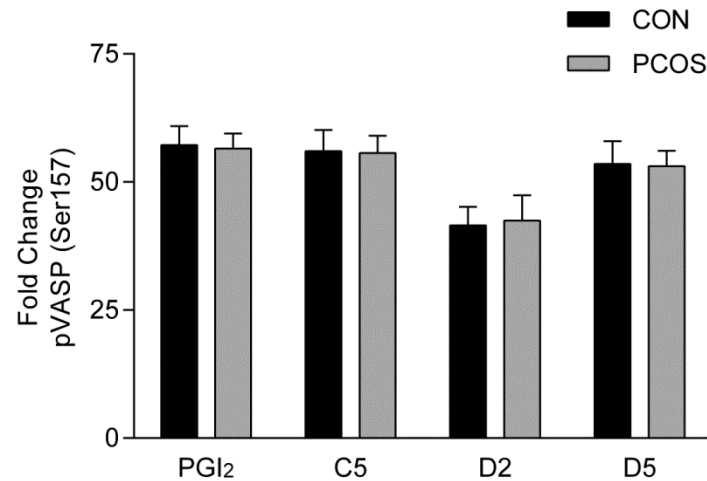
Figure 5.12. Novel agents induce phosphoVASP-ser[157] in PCOS and controls. Stimulation with PGI_2 (1 μM, 2 min), C5 (1 μM, 2 min), D2 (1 μM, 2 min), or D5 (1 μM, 2 min) induced phosphoVASP-ser[157]. Data represents the mean ± SEM.
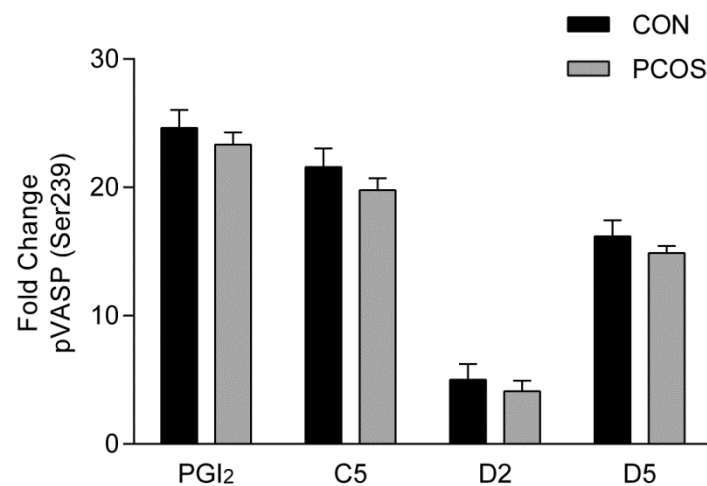
Figure 5.13. Novel agents induce phosphoVASP-ser[239] in PCOS and controls. Stimulation with PGI_2 (1 μM, 2 min), C5 (1 μM, 2 min), D2 (1 μM, 2 min), or D5 (1 μM, 2 min) induced phosphoVASP-ser[239]. Data represents the mean ± SEM.

5.5 Discussion

Identifying and monitoring high risk patients and developing new antiplatelet drugs is critical to alleviating the continued burden of atherothrombotic-related diseases. Cyclic nucleotide signalling cascades are potent regulators of platelet function and may therefore present targets for antithrombotic agents. The activity of cyclic nucleotide signalling can be determined by measuring the phosphorylation status of VASP. In this chapter, we used our phosphoflow assay to measure cyclic nucleotide signalling in PCOS, an endocrine disorder associated with high thrombotic risk (Carmina and Lobo, 1999). In addition, we demonstrated application of our assay to drug screening against freshly-obtained human cells in the complex milieu of whole blood. Using this approach, we identified three structurally-novel prostaglandins that signal through cAMP-dependent mechanisms and inhibit platelet aggregation.

The relevance of our assay for clinical or pharmacological application, such as the evaluation of drug efficacy or identification of novel antiplatelet agents, would have been limited by the use of washed platelets. Indeed, manipulation of whole blood may lead to artifactual platelet activation and there is limited value screening drugs in the absence of plasma lipids and proteins. To overcome these limitations, we adapted our method for whole blood analyses (see section 4.6). Since flow cytometric analyses of protein phosphorylation can be applied throughout the drug development process, we used our method to screen a library of prostaglandins against human platelets in the physiological milieu of whole blood. Since platelets are abundant in the blood, we could readily obtain sufficient numbers of cells

(from <1.5 mL whole blood) to screen entire 96-well plates. We anticipated that our cell-based screen, designed to detect phosphoVASP-ser[157], would uncover efficacious antiplatelet agents. Using a prostaglandin screening library (Table A1), we identified three previously uncharacterised lipids that stimulated VASP phosphorylation. In follow-up assays, these lipids of no known biological effect were shown to interact with prostanoid receptors, elevate intraplatelet cAMP, and inhibit platelet aggregation. These lipids stimulated phosphoVASP-ser[157] and ser[239] with varying degrees of potency. Using the IP receptor antagonist RO1138452, we demonstrated that compounds C5 and D5 signalled through the same receptor as PGI_2 (Jones et al., 2006) but inhibited collagen-induced platelet aggregation at much higher concentrations. While compound D2 signalled through a different receptor, it was also a less potent inhibitor than PGI_2. It is possible that the different compounds have different receptor binding affinities and/or they activate different adenylyl cyclase isoforms to induce the varied inhibitory responses seen here.

Aside from its role in drug development, flow cytometry has emerged as a powerful tool for the analysis of phosphorylation-based signalling cascades in clinical populations. Studies have shown that potentiated signalling responses can predict clinical outcomes in acute leukemias (Irish et al., 2004) and the immune response to chronic infections such as HIV (Schweneker et al., 2008) and HCV (Franceschini et al., 2009). Phosphoflow has also enabled researchers to identify the aberrant kinase activity that drives the progression of these diseases (Irish et al., 2010). Platelet cyclic nucleotide signalling is sometimes compromised in cardiovascular conditions

(Chirkov and Horowitz, 2007, Van Geet et al., 2009) and insulin resistant states such as diabetes mellitus (Davi et al., 1982, Modesti et al., 1991). PCOS is an insulin resistant state associated with platelet hyperactivity (Dereli et al., 2003) but the signalling mechanism(s) driving platelet dysfunction have not been determined. To try and elucidate the mechanism(s) underpinning platelet dysfunction in PCOS, we stimulated whole blood samples with known modulators of cyclic nucleotide signalling and measured intraplatelet VASP phosphorylation. We found that PGI_2-induced VASP phosphorylation was not diminished in PCOS, suggesting that impaired cyclic nucleotide signalling is not a mechanism for platelet dysfunction in these subjects. Reduced PGI_2 sensitivity has been observed in hyperlipidemic women with PCOS (Aye et al., 2014). However, no such defects were observed in our PCOS subjects whose lipid levels were not significantly different from normolipidemic controls (Table 5.2) suggesting that hyperlipidemia itself could be a major cause of PGI_2 resistance. Indeed, given that the IP receptor naturally binds lipid mediators (Jones et al., 2006), it is conceivable that excess plasma lipids or their derivatives could occupy its binding site and block the effects of PGI_2 in hyperlipidemic individuals. The negative effects of hyperlipidemia on platelet function appear to exert themselves mainly on platelet inhibitory pathways since there have been no reported differences in baseline P-selectin expression or fibrinogen binding in patients with primary hypertriglyceridemia compared to age- and sex-matched controls (De Man et al., 2000). Like hyperlipidemia, obesity is thought to induce platelet resistance to PGI_2 (Russo et al., 2009). Although

our PCOS subjects were significantly more overweight than controls, their obesity did not affect PGI_2-induced VASP phosphorylation.

The platelet agonist ADP can modulate platelet sensitivity to cAMP-elevating agents such as PGI_2. Insulin resistance, a common feature of PCOS, is associated with increased platelet reactivity to ADP (Kreutz et al., 2011). ADP induces shape change, $\alpha IIb\beta 3$ activation and platelet aggregation through two distinct pathways: $P2Y_1$, coupled to PLC activation and calcium mobilisation; and $P2Y_{12}$, coupled to the inhibition of adenylyl cyclase (Jin and Kunapuli, 1998). We found that the ability of ADP to inhibit cyclic nucleotide signalling was not enhanced in PCOS. Hence, the increased reactivity to ADP that is commonly reported in insulin resistant states likely occurs through the $P2Y_1$ pathway; independent of $P2Y_{12}$, adenylyl cyclase inhibition, and downstream effects on cyclic nucleotide signalling.

This chapter has described potential pharmacological and clinical applications of phosphoflow. We have shown that VASP can be used as a reliable marker for the identification of antiplatelet agents. We adapted our multiplexed assay to screen an entire library of prostaglandins for their ability to induce intraplatelet VASP phosphorylation in whole blood. Screening revealed three novel prostaglandins that inhibited platelet aggregation through cAMP-dependent mechanisms. We then demonstrated the application of phosphoflow to profile cyclic nucleotide signalling in women with PCOS, an endocrine disorder associated with platelet dysfunction. While our results were somewhat negative, they provide important additional insights into the underlying platelet biochemistry that accompanies PCOS.

General Discussion

6.1 Discussion

Platelets play an important role in haemostasis and thrombosis. To prevent haemorrhage, activated platelets interact with endothelial cells, leukocytes, and one another at sites of vascular injury to form stable haemostatic plugs (Libby and Simon, 2001). Platelet activation is regulated in part through a plethora of phosphorylation-based signalling events. Our major challenge is to understand how the phosphorylation of intracellular proteins regulates different aspects of platelet function. The phosphorylation of intraplatelet proteins is commonly measured through immunoblot techniques. However, these techniques have numerous limitations including the requirement for large numbers of cells, incompatibility with whole blood samples, and they are not conducive to large-scale signalling analyses. The flow cytometric measurement of protein phosphorylation can potentially overcome these limitations by providing rapid information on the activities of kinase signalling cascades in single cells.

In this thesis, we have reported the development of a high-throughput flow cytometric assay for the measurement of intracellular protein phosphorylation in washed platelets and its application in the complex milieu of whole blood. This assay could examine up to 96 samples in a single FACS tube, thereby reducing several weeks' work to a single flow cytometry run. To develop the assay, we used phosphorylation of the cytoskeletal-associated vasodilator-stimulated phosphoprotein (VASP) as readout. VASP was chosen because its phosphorylation is an important marker for (i) analysis of prostacyclin

(PGI_2) and nitric oxide (NO)-mediated signalling events that inhibit platelets, (ii) monitoring a number of antiplatelet therapies including iloprost, dipyridamole, and cilostazol, that attempt to harness the inhibitory potential of cyclic nucleotide signalling, and (iii) clinical assessment of antagonists of the ADP receptor, $P2Y_{12}$.

We believe that this assay will be a valuable tool for basic scientists investigating platelet signalling, pharmacologists seeking novel therapies, and clinicians wishing to evaluate the efficacy of antiplatelet drugs for which there are currently 46 million annual prescriptions (Allender et al., 2012). With a growing, ageing population, the demand for these drugs will continue to increase. To alleviate the future burden of cardiovascular disease, there are clinical requirements for better monitoring of antiplatelet drugs. An effective monitoring system could enhance compliance with particular therapies and improve clinical outcomes through the identification of drug-resistant individuals. However, the cost associated with monitoring these increasingly-prescribed drugs is likely to place a significant financial burden on the healthcare system. There is thus a requirement for cost-effective tests that can reliably determine the efficacy of antiplatelet therapies.

This work has focused on the cAMP and cGMP signalling pathways because of their potential importance in the regulation of platelet function. One of the most commonly studied substrates of these signalling pathways, VASP, is currently being used as a marker in effective tests evaluating the efficacy of thienopyridines ($P2Y_{12}$ antagonists), which are a cornerstone of antiplatelet therapy (Aleil et al., 2005). Unlike other tests of platelet function, the VASP/$P2Y_{12}$ assay is not affected by platelet count, vWF level, aspirin, or

αIIbβ3 inhibitors. The assay measures the level of intraplatelet VASP phosphorylation in whole blood, which provides clinically relevant information about *in vivo* endothelial function and the *in* vivo effects of antiplatelet therapies. In its first clinical application, the assay could detect subtle changes in VASP phosphorylation in volunteers receiving the thienopyridines, ticlopidine and clopidogrel (Schwarz et al., 1999a). The assay results proved to be a reliable predictor of subacute thrombosis in patients treated with thienopyridines after coronary stent implantation (Barragan et al., 2003). In these studies, a platelet reactivity index was calculated from the median fluorescence intensity of whole blood samples incubated with either PGE_1 alone or PGE_1 plus ADP. An inverse relation was found between platelet reactivity and thienopyridine efficacy. Moreover, there was a marked interindividual variability in platelet reactivity following treatment, suggesting either poor compliance or thienopyridine resistance. Similar results were obtained in patients with ischemic cardiovascular disease (Aleil et al., 2005). Thus, it became clear that the VASP/$P2Y_{12}$ assay would allow clinicians to discriminate between "good responders" to thienopyridines and "poor responders". Recognition of these benefits, together with widespread interest from clinical and scientific communities, led to the manufacture of a standardised commercial kit for the flow cytometric determination of intraplatelet VASP phosphorylation. The VASP/$P2Y_{12}$ assay, which yields quantitative results in <1 hr, is currently the gold standard for monitoring $P2Y_{12}$ antagonists.

Despite its accolades, the VASP/$P2Y_{12}$ assay has a number of limitations. First, the assay uses phosphoVASP-ser[239] which is only weakly stimulated

by PGE_1. The assay window, and therefore assay quality, could be improved by using phosphoVASP-ser[157], which undergoes more substantial phosphorylation in response to PGE_1. Alternatively, PGE_1 could be replaced by the physiologic inhibitor PGI_2. Second, time-efficiency of the assay could be improved by using directly-labelled phosphoVASP antibodies, which are now commercially available and being used in cytometric bead assays (Glenn et al., 2012). Third, staining is susceptible to interference from plasma lipids and proteins because antibodies are added directly to whole blood. Fourth, the assay is considerably more expensive than existing tests of platelet function; and, fifth, its concentrations of PGE_1 and ADP are relatively high and do not span the physiologic range. In this context, the high-throughput nature of our multiplexed assay could allow for a more detailed characterisation of drug efficacy and potential resistance by measuring VASP phosphorylation across a range of different agonist concentrations that more accurately reflect those found in the bloodstream. Additionally, we could generate multiple readouts from a single analysis tube while the VASP/$P2Y_{12}$ assay generates only a single readout from three separate tubes. Multiplexing would eliminate between-sample variability and facilitate a threefold reduction in antibody consumption compared to the VASP/$P2Y_{12}$ assay, which requires a fixed amount of antibody to be delivered to each separate tube. By reducing antibody consumption, our assay could enable a more cost-effective evaluation of drug efficacy.

While flow cytometric analyses of VASP phosphorylation can be used to monitor antiplatelet agents such as clopidogrel, they can also be used to discover alternative therapies for those resistant to thienopyridines. VASP

phosphorylation correlates with the inhibition of platelet aggregation (Horstrup et al., 1994), and is sensitive to the effects of antiplatelets including phosphodiesterase inhibitors and prostaglandin analogs that target cyclic nucleotide signalling cascades (Schwarz et al., 2001). For these reasons, phosphoVASP can be used as a reliable marker for the identification of potential antiplatelet agents. Since phosphoflow enables the rapid analysis of up to 96 samples in a single tube, we screened a library of prostaglandins for their ability to induce intraplatelet VASP phosphorylation in the physiologic milieu of whole blood. Our cell-based screen revealed three previously uncharacterised lipids that inhibited platelet aggregation through cAMP-dependent mechanisms. These novel agents were structurally similar to established antiplatelets such as iloprost and epoprostenol, which have been approved for the treatment of numerous cardiovascular indications (Michelson, 2010). Our screening assay is valuable from a pharmacologic standpoint because it can evaluate drug efficacy in the presence of plasma lipids and proteins as well as other cell types. Screening against freshly-obtained human cells is a major advancement because previous applications have been limited to screening against immortalised cell lines or primary murine cells, neither of which are aptly representative of a working human system (Krutzik and Nolan, 2006, Krutzik et al., 2007). Screening against physiologically relevant targets, such as human cells, better predicts the activities of compounds *in vivo*.

Developing a new drug is a complex process that can take 10-15 years (Hughes et al., 2011). The first step in the drug discovery process requires the identification of druggable targets such as cell surface receptors,

intracellular proteins, or signalling cascades, together with evidence that the activation or inhibition of these targets will produce a therapeutic effect in a disease state. Insulin resistant states, such as polycystic ovary syndrome (PCOS), are associated with platelet hyperactivity, PGI_2 resistance, and premature cardiovascular mortality (Davi et al., 1982). Based on these observations, we hypothesised that cyclic nucleotide signalling cascades were compromised in PCOS. While our data did not support this notion, we demonstrated the successful application of our assay in a clinical setting. Blood samples were drawn, stimulated, and fixed at the point of care. Since the clinic was not equipped with a flow cytometer, these samples were transported to a core facility for multiplexing, staining, and acquisition. Even after transit, we could obtain robust signalling data for each sample, thereby eliminating the need for specialised equipment and technical expertise at the point of care. Thus, our assay could be applied in remote locations provided that blood can be drawn and mixed with two solutions: an agonist solution and a fixative solution. Fixed samples could then be sent to our laboratory for analysis. There is great interest in remote tests of platelet function, and efforts have already been made to monitor clopidogrel and aspirin based on measurements of P-selectin in samples that were obtained at remote sites (Fox et al., 2009).

6.2 Future directions

Having established a robust method for the flow cytometric measurement of intraplatelet protein phosphorylation, further optimisation should be undertaken to advance its capabilities. To date, we have examined cyclic nucleotide signalling cascades using antibodies against phosphoVASP-ser[157] and ser[239], phosphoGSK-3α-ser[21], and phosphoPKA substrate (RRXS/T), which are well-validated for this purpose (Oberprieler et al., 2010). Alternative signalling proteins such as phosphoAkt-ser[473], phosphoERK-thr[202]/tyr[204], phosphoPLCγ2-tyr[759], and phosphoSYK/ZAP70-tyr[352]/thr[319] are involved in platelet activation (Gibbins, 2004) and have been successfully analysed in a variety of other cell types (Irish et al., 2010). The flow cytometric analysis of these intraplatelet proteins would be useful, but would pose a number of problems. First, the scatter properties of activated platelets are broad and variable due to shape change. On two-dimensional plots of scatter versus fluorescence, barcoded populations would therefore bleed into one another making it difficult to deconvolute multiplexed samples. Collecting data over a broader dynamic range (10^7 log decades) could allow for greater separation of barcoded populations, but this would be possible only on certain instruments. Second, activation results in the loss of normally scattered platelets as they form aggregates with leukocytes. While these cells can be identified retrospectively with a platelet-specific marker, data would reflect the sum of phosphorylation in both the platelet and the leukocyte because cell-cell aggregates are recognised as a single entity. However, this problem could be avoided by using leukocyte-free washed platelet preparations. Third, unlike VASP, many intraplatelet proteins are

present at low levels (Burkhart et al., 2012). Thus, it may be difficult to obtain intense fluorescent signals and robust Z'-factors (>0.5) when screening for kinase and/or phosphatase inhibitors. Newly-developed signal amplification techniques could improve the measurement resolution of low abundance phosphoproteins, but these have not yet been applied in primary cells (Clutter et al., 2010).

Future applications should also exploit the multiparameter capabilities of flow cytometry to facilitate high-content analyses of several signalling cascades or several components of one particular cascade. Thus, we could determine the selectivity of agonists and/or inhibitors for one cascade over another; or correlate phosphorylation events across multiple parallel, convergent, and/or divergent signalling cascades. However, these analyses would be limited by the availability of directly-labelled phospho-antibodies and the variety of fluorophore labels available.

Appendix

Table A1. Prostaglandin screening library.

Well	Contents
A1	Empty
A2	Empty
A3	Empty
A4	Empty
A5	Empty
A6	Empty
A7	Empty
A8	Empty
A9	Empty
A10	Empty
A11	Empty
A12	Empty
B1	Empty
B2	Prostaglandin D_2 Ethanolamide
B3	17-phenyl trinor Prostaglandin D_2
B4	13,14-dihydro Prostaglandin E_1
B5	16,16-dimethyl Prostaglandin E_1
B6	Prostaglandin E_2 *p*-acetamidophenyl ester
B7	15-keto Prostaglandin E_2
B8	tetranor-PGEM
B9	Prostaglandin E_2-biotin
B10	Prostaglandin D_1 Alcohol
B11	Prostaglandin D_2
B12	16-phenyl tetranor Prostaglandin E_2
C1	15(R)-Prostaglandin D_2
C2	Prostaglandin D_2-1-glyceryl ester
C3	Prostaglandin E_1
C4	13,14-dihydro-15-(R)-Prostaglandin E_1
C5	16-phenyl tetranor Prostaglandin E_1
C6	Prostaglandin E_2 p-benzamidophenyl ester
C7	15(R)-15-methyl Prostaglandin E_2
C8	19(R)-hydroxy Prostaglandin E_2
C9	*ent*-Prostaglandin E_2
C10	15(R)-15-methyl Prostaglandin D_2
C11	15(S)-15-methyl Prostaglandin D_2
C12	11-keto Fluprostenol
D1	Prostaglandin E_2-1-glyceryl ester
D2	5-*trans* Prostaglandin D_2
D3	Prostaglandin E_1 Ethanolamide
D4	13,14-dihydro-15-keto Prostaglandin E_1
D5	16,16-dimethyl-6-keto Prostaglandin E_1
D6	5-*trans* Prostaglandin E_2
D7	15(S)-15-methyl Prostaglandin E_2
D8	20-ethyl Prostaglandin E_2
D9	Prostaglandin D_2 methyl ester

D10	8-*iso* Prostaglandin E_1
D11	11β-Prostaglandin E_1
D12	17-phenyl trinor Prostaglandin E_2
E1	Prostaglandin D_2 serinol amide
E2	11-deoxy-11-methylene Prostaglandin D_2
E3	Prostaglandin E_1 Alcohol
E4	15-keto Prostaglandin E_1
E5	Limaprost
E6	8-*iso* Prostaglandin E_2
E7	16,16-dimethyl Prostaglandin E_2
E8	20-hydroxy Prostaglandin E_2
E9	3-methoxy Limaprost
E10	(R)-Butaprost
E11	CAY10408
E12	(R)-Butaprost (free acid)
F1	Prostaglandin E_2 serinol amide
F2	13,14-dihydro-15-keto Prostaglandin D_2
F3	1a,1b-dihomo Prostaglandin E_1
F4	15(R)-Prostaglandin E_1
F5	Misoprostol
F6	8-*iso* Prostaglandin E_2
F7	16,16-dimethyl Prostaglandin E_2 *p*-(*p*-acetamidobenzamido) phenyl ester
F8	Prostaglandin E_3
F9	8-*iso*-16-cyclohexyl-tetranor Prostaglandin E_2
F10	Prostaglandin E_2 methyl ester
F11	Prostaglandin E_2 ethanolamide
F12	8-*iso* Misoprostol
G1	Prostaglandin D_1
G2	Δ^{12}-Prostaglandin D_2
G3	6-keto Prostaglandin E_1
G4	15(S)-15-methyl Prostaglandin E_1
G5	Prostaglandin E_2
G6	11β-Prostaglandin E_2
G7	Sulprostone
G8	17-*trans* Prostaglandin E_3
G9	13,14-dihydro-15-keto Prostaglandin D_1
G10	13,14-dihydro-15-keto Prostaglandin E_2
G11	15(R)-Prostaglandin E_2
G12	Empty
H1	Prostaglandin I_2
H2	Prostaglandin I_2
H3	Prostaglandin I_2
H4	Prostaglandin I_2
H5	Prostaglandin I_2
H6	Prostaglandin I_2
H7	Prostaglandin I_2
H8	Prostaglandin I_2
H9	Prostaglandin I_2
H10	Prostaglandin I_2
H11	Prostaglandin I_2
H12	Prostaglandin I_2

Figure A1. Two-dimensional fluorescent cell barcoding. Two dyes were used to barcode 24 samples. Fivefold dilutions of Pacific Blue were used across rows while threefold dilutions of Alexa Fluor 488 were used across columns. Four such matrices could occupy a single 96-well plate.
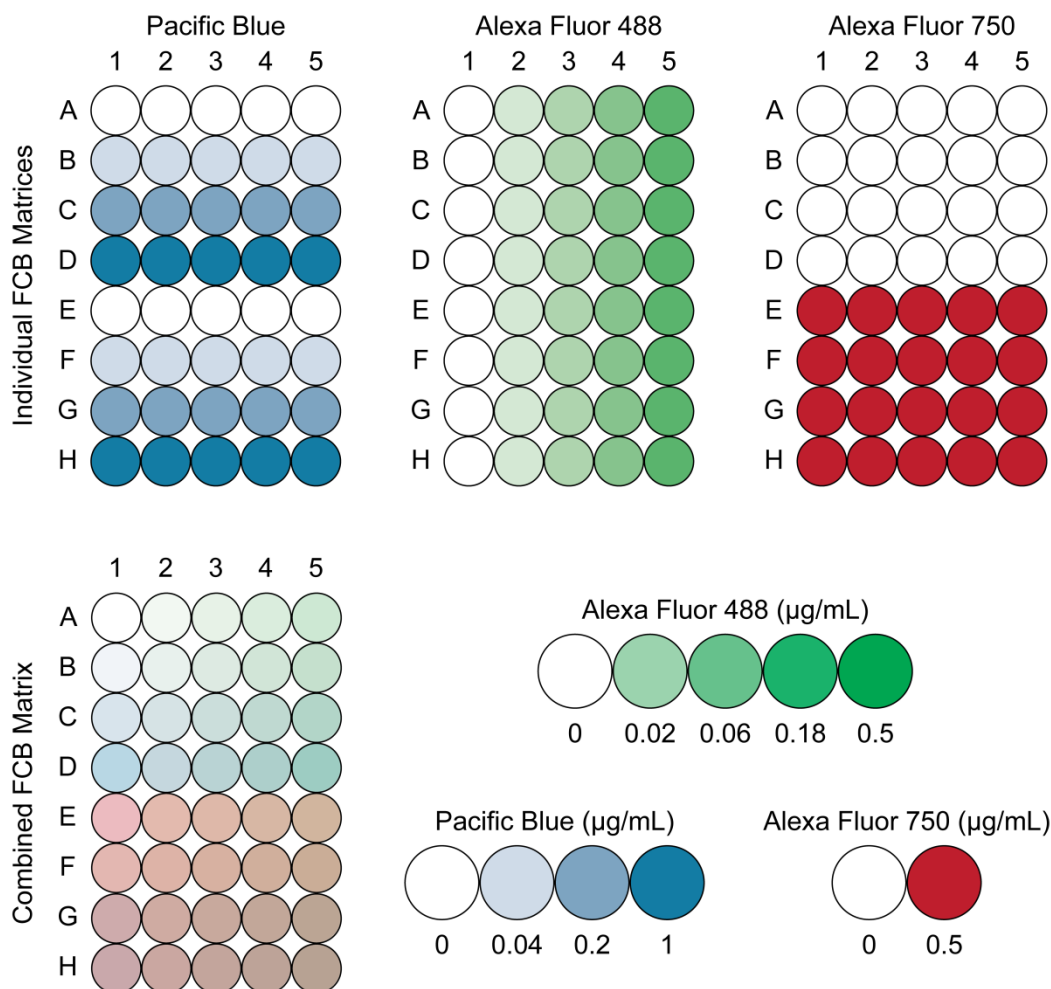
Figure A2. Three-dimensional fluorescent cell barcoding. Three dyes were used to barcode 40 samples. Fivefold dilutions of Pacific Blue were used across rows while threefold dilutions of Alexa Fluor 488 were used across columns. Different concentrations of Alexa Fluor 750 were used to discriminate between samples that contained the same concentrations of Pacific Blue and Alexa Fluor 488.
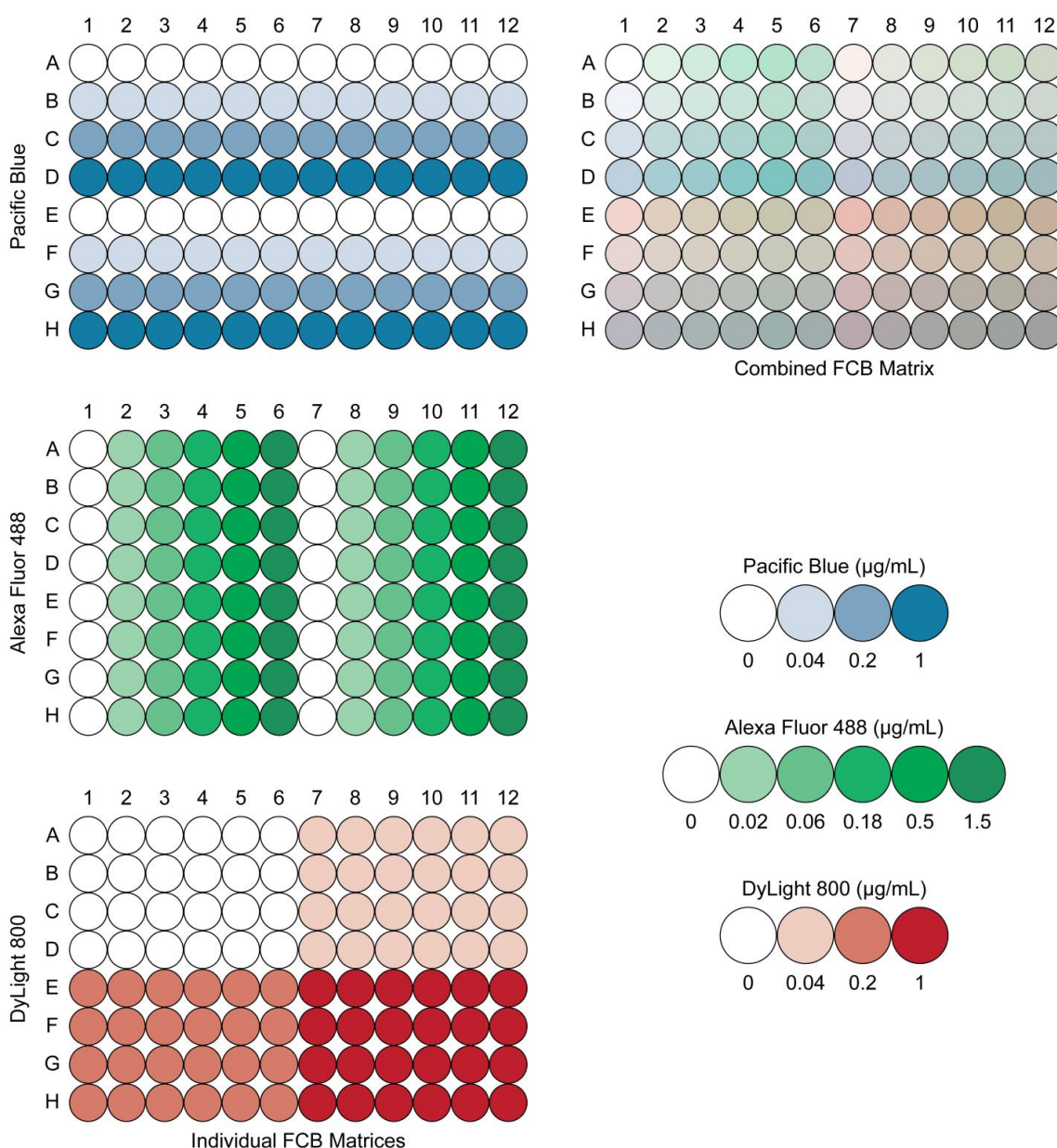
Figure A3. Three-dimensional barcoding of an entire 96-well plate. Three dyes were used to barcode 96 samples. Four concentrations of Pacific Blue were used across rows and six concentrations of Alexa Fluor 488 were used across columns. Four concentrations of DyLight 800 were used to discriminate between rows and columns that contained the same concentrations of Pacific Blue and Alexa Fluor 488.

Figure A4. Two-dimensional barcoding of 30 samples. Two dyes were used to barcode 30 samples. Threefold dilutions of Pacific Blue were used across rows, whereas threefold dilutions of Alexa Fluor 488 were used across columns.
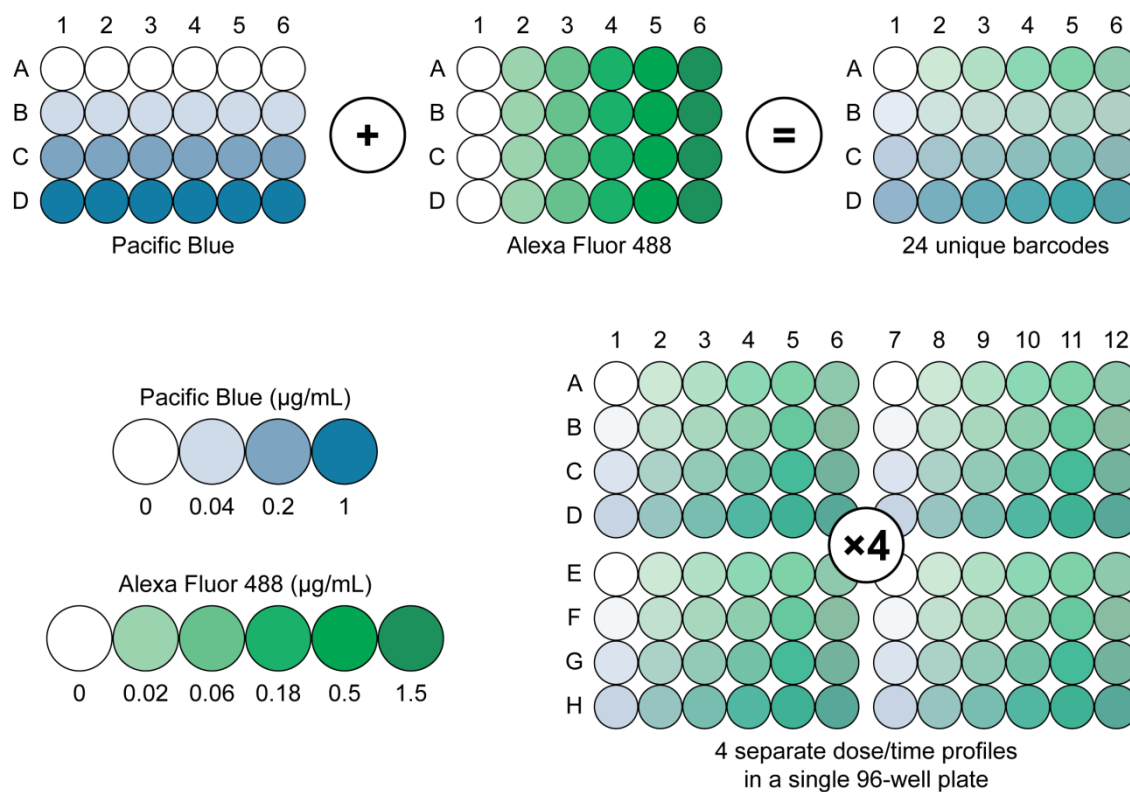
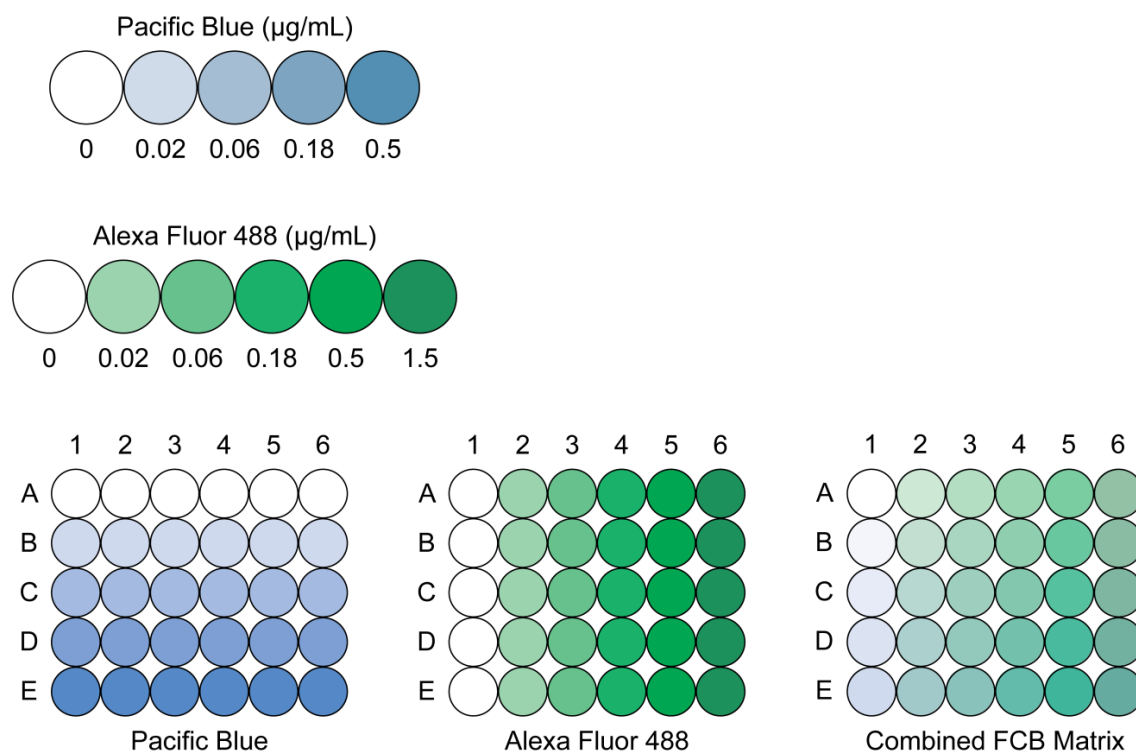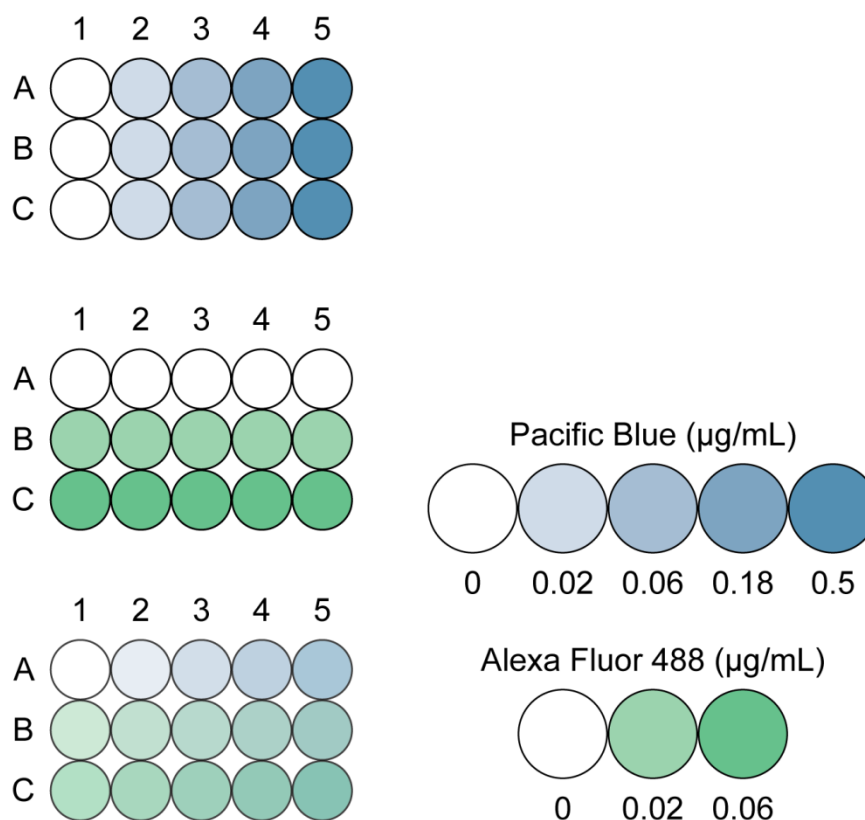**Figure A5. Two-dimensional barcoding of 15 samples.** Two dyes were used to barcode 15 samples. Fivefold dilutions of Pacific Blue were used across columns while threefold dilutions of Alexa Fluor 488 were used across rows.

References

ABURIMA, A., WRAITH, K. S., RASLAN, Z., LAW, R., MAGWENZI, S. & NASEEM, K. M. 2013. cAMP signaling regulates platelet myosin light chain (MLC) phosphorylation and shape change through targeting the RhoA-Rho kinase-MLC phosphatase signaling pathway. *Blood,* 122**,** 3533-3545.

ALEIL, B., RAVANAT, C., CAZENAVE, J., ROCHOUX, G., HEITZ, A. & GACHET, C. 2005. Flow cytometric analysis of intraplatelet VASP phosphorylation for the detection of clopidogrel resistance in patients with ischemic cardiovascular diseases. *Journal of Thrombosis and Haemostasis,* 3**,** 85-92.

ALLENDER, S., PETO, V., SCARBOROUGH, P., BOXER, A. & RAYNER, M. 2012. Coronary Heart Disease Statistics. *British Heart Foundation*.

ANDERSEN, H., GREENBERG, D. L., FUJIKAWA, K., XU, W., CHUNG, D. W. & DAVIE, E. W. 1999. Protease-activated receptor 1 is the primary mediator of thrombin-stimulated platelet procoagulant activity. *Proceedings of the National Academy of Sciences,* 96**,** 11189-11193.

ANTL, M., VON BRÜHL, M.-L., EIGLSPERGER, C., WERNER, M., KONRAD, I., KOCHER, T., WILM, M., HOFMANN, F., MASSBERG, S. & SCHLOSSMANN, J. 2007. IRAG mediates NO/cGMP-dependent inhibition of platelet aggregation and thrombus formation. *Blood,* 109**,** 552-559.

ARIAS-SALGADO, E. G., LIZANO, S., SARKAR, S., BRUGGE, J. S., GINSBERG, M. H. & SHATTIL, S. J. 2003. Src kinase activation by direct interaction with the integrin β cytoplasmic domain. *Proceedings of the National Academy of Sciences,* 100**,** 13298-13302.

ARIMURA, N. & KAIBUCHI, K. 2007. Neuronal polarity: from extracellular signals to intracellular mechanisms. *Nature Reviews Neuroscience,* 8**,** 194-205.

ARMSTRONG, R. A. 1996. Platelet prostanoid receptors. *Pharmacology & therapeutics,* 72**,** 171-191.

ASAZUMA, N., OZAKI, Y., SATOH, K., YATOMI, Y., HANDA, M., FUJIMURA, Y., MIURA, S. & KUME, S. 1997. Glycoprotein Ib-von Willebrand factor interactions activate tyrosine kinases in human platelets. *Blood,* 90**,** 4789-4798.

ASAZUMA, N., WILDE, J. I., BERLANGA, O., LEDUC, M., LEO, A., SCHWEIGHOFFER, E., TYBULEWICZ, V., BON, C., LIU, S. K. & MCGLADE, C. J. 2000. Interaction of linker for activation of T cells with multiple adapter proteins in platelets activated by the glycoprotein VI-selective ligand, convulxin. *Journal of Biological Chemistry,* 275**,** 33427-33434.

ASIRVATHAM, A. L., GALLIGAN, S. G., SCHILLACE, R. V., DAVEY, M. P., VASTA, V., BEAVO, J. A. & CARR, D. W. 2004. A-kinase anchoring proteins interact with phosphodiesterases in T lymphocyte cell lines. *The Journal of Immunology,* 173**,** 4806-4814.

AYE, M. M., KILPATRICK, E. S., ABURIMA, A., WRAITH, K. S., MAGWENZI, S., SPURGEON, B., RIGBY, A. S., SANDEMAN, D., NASEEM, K. M. & ATKIN, S. L. 2014. Acute Hypertriglyceridemia Induces Platelet Hyperactivity That is Not Attenuated by Insulin in Polycystic Ovary Syndrome. *Journal of the American Heart Association,* 3**,** e000706.

BARRAGAN, P., BOUVIER, J. L., ROQUEBERT, P. O., MACALUSO, G., COMMEAU, P., COMET, B., LAFONT, A., CAMOIN, L., WALTER, U. & EIGENTHALER, M. 2003. Resistance to thienopyridines: Clinical detection of coronary stent thrombosis by monitoring of vasodilator-stimulated phosphoprotein phosphorylation. *Catheterization and Cardiovascular interventions,* 59**,** 295-302.

BARRY, F. A., GRAHAM, G. J., FRY, M. J. & GIBBINS, J. M. 2003. Regulation of glycogen synthase kinase 3 in human platelets: a possible role in platelet function? *FEBS letters,* 553**,** 173-178.

BEAVO, J., ROGERS, N., CROFFORD, O., HARDMAN, J., SUTHERLAND, E. & NEWMAN, E. 1970. Effects of xanthine derivatives on lipolysis and on adenosine 3', 5'-monophosphate phosphodiesterase activity. *Molecular pharmacology,* 6**,** 597-603.

BECK, F., GEIGER, J., GAMBARYAN, S., VEIT, J., VAUDEL, M., NOLLAU, P., KOHLBACHER, O., MARTENS, L., WALTER, U. & SICKMANN, A. 2014. Time-resolved characterization of cAMP/PKA-dependent signaling reveals that platelet inhibition is a concerted process involving multiple signaling pathways. *Blood,* 123**,** e1-e10.

BELLAMY, T. C., WOOD, J., GOODWIN, D. A. & GARTHWAITE, J. 2000. Rapid desensitization of the nitric oxide receptor, soluble guanylyl cyclase, underlies diversity of cellular cGMP responses. *Proceedings of the National Academy of Sciences,* 97**,** 2928-2933.

BENDER, A. T. & BEAVO, J. A. 2006. Cyclic nucleotide phosphodiesterases: molecular regulation to clinical use. *Pharmacological reviews,* 58**,** 488-520.

BENNETT, J. & VILAIRE, G. 1979. Exposure of platelet fibrinogen receptors by ADP and epinephrine. *Journal of Clinical Investigation,* 64**,** 1393.

BENNETT, J. S., ZIGMOND, S., VILAIRE, G., CUNNINGHAM, M. E. & BEDNAR, B. 1999. The platelet cytoskeleton regulates the affinity of the integrin αIIbβ3 for fibrinogen. *Journal of Biological Chemistry,* 274**,** 25301-25307.

BERGER, G., HARTWELL, D. W. & WAGNER, D. D. 1998. P-Selectin and platelet clearance. *Blood,* 92**,** 4446-4452.

BLAKE, G. J. & RIDKER, P. M. 2001. Novel clinical markers of vascular wall inflammation. *Circulation research,* 89**,** 763-771.

BODNAR, R. J., XI, X., LI, Z., BERNDT, M. C. & DU, X. 2002. Regulation of glycoprotein Ib-IX-von Willebrand factor interaction by cAMP-dependent protein kinase-mediated phosphorylation at Ser 166 of glycoprotein Ibβ. *Journal of Biological Chemistry,* 277**,** 47080-47087.

BORN, G. 1962. Aggregation of blood platelets by adenosine diphosphate and its reversal. *Nature,* 194**,** 927-929.

BUCHWALOW, I., SAMOILOVA, V., BOECKER, W. & TIEMANN, M. 2011. Non-specific binding of antibodies in immunohistochemistry: fallacies and facts. *Scientific reports,* 1.

BUENSUCESO, C. S., OBERGFELL, A., SORIANI, A., ETO, K., KIOSSES, W. B., ARIAS-SALGADO, E. G., KAWAKAMI, T. & SHATTIL, S. J. 2005. Regulation of outside-in signaling in platelets by integrin-associated protein kinase Cβ. *Journal of Biological Chemistry,* 280**,** 644-653.

BURKHART, J. M., VAUDEL, M., GAMBARYAN, S., RADAU, S., WALTER, U., MARTENS, L., GEIGER, J., SICKMANN, A. & ZAHEDI, R. P. 2012. The first comprehensive and quantitative analysis of human platelet protein composition allows the comparative analysis of structural and functional pathways. *Blood,* 120**,** e73-e82.

BUTT, E., ABEL, K., KRIEGER, M., PALM, D., HOPPE, V., HOPPE, J. & WALTER, U. 1994. cAMP- and cGMP-dependent protein kinase phosphorylation sites of the focal adhesion vasodilator-stimulated phosphoprotein (VASP) in vitro and in intact human platelets. *Journal of Biological Chemistry,* 269**,** 14509-14517.

BUTT, E., IMMLER, D., MEYER, H., KOTLYAROV, A., LAASS, K. & GAESTEL, M. 2001. Heat shock protein 27 is a substrate of cGMP-dependent protein kinase in intact human platelets: phosphorylation-induced actin polymerization caused by HSP27 mutants. *The Journal of biological chemistry,* 276**,** 7108.

CARMINA, E. & LOBO, R. A. 1999. Polycystic ovary syndrome (PCOS): arguably the most common endocrinopathy is associated with significant morbidity in women. *Journal of Clinical Endocrinology & Metabolism,* 84**,** 1897-1899.

CARNEGIE, G. K., MEANS, C. K. & SCOTT, J. D. 2009. A-kinase anchoring proteins: From protein complexes to physiology and disease. *IUBMB life,* 61**,** 394-406.

CASTEEL, D. E., SCHWAPPACHER, R., RANGASWAMI, H. & SU-YUO, J. 2013. cGMP-dependent protein kinase Iβ phosphorylates and regulates the function of the actin/myosin-associated protein caldesmon. *BMC Pharmacology and Toxicology,* 14**,** P13.

CASTEEL, D. E., ZHUANG, S., GUDI, T., TANG, J., VUICA, M., DESIDERIO, S. & PILZ, R. B. 2002. cGMP-dependent protein kinase Iβ physically and functionally interacts with the transcriptional regulator TFII-I. *Journal of Biological Chemistry,* 277**,** 32003-32014.

CAVALLINI, L., COASSIN, M., BOREAN, A. & ALEXANDRE, A. 1996. Prostacyclin and sodium nitroprusside inhibit the activity of the platelet inositol 1, 4, 5-trisphosphate receptor and promote its phosphorylation. *Journal of Biological Chemistry,* 271**,** 5545-5551.

CHATTERJEE, M. S., PURVIS, J. E., BRASS, L. F. & DIAMOND, S. L. 2010. Pairwise agonist scanning predicts cellular signaling responses to combinatorial stimuli. *Nature biotechnology,* 28**,** 727-732.

CHEN, J., DIACOVO, T. G., GRENACHE, D. G., SANTORO, S. A. & ZUTTER, M. M. 2002. The α2 Integrin Subunit-Deficient Mouse: A Multifaceted Phenotype Including Defects of Branching Morphogenesis and Hemostasis. *The American journal of pathology,* 161**,** 337-344.

CHEN, M. & STRACHER, A. 1989. In situ phosphorylation of platelet actin-binding protein by cAMP-dependent protein kinase stabilizes it against proteolysis by calpain. *Journal of Biological Chemistry,* 264**,** 14282-14289.

CHEN, Y., HARRY, A., LI, J., SMIT, M. J., BAI, X., MAGNUSSON, R., PIERONI, J. P., WENG, G. & IYENGAR, R. 1997. Adenylyl cyclase 6 is selectively regulated by protein kinase A phosphorylation in a region involved in Gαs stimulation. *Proceedings of the National Academy of Sciences,* 94**,** 14100-14104.

CHIJIWA, T., MISHIMA, A., HAGIWARA, M., SANO, M., HAYASHI, K., INOUE, T., NAITO, K., TOSHIOKA, T. & HIDAKA, H. 1990. Inhibition of forskolin-induced neurite outgrowth and protein phosphorylation by a newly synthesized selective inhibitor of cyclic AMP-dependent protein kinase, N-[2-(p-bromocinnamylamino) ethyl]-5-isoquinolinesulfonamide (H-89), of PC12D pheochromocytoma cells. *Journal of Biological Chemistry,* 265**,** 5267-5272.

CHIRKOV, Y. Y. & HOROWITZ, J. D. 2007. Impaired tissue responsiveness to organic nitrates and nitric oxide: a new therapeutic frontier? *Pharmacology & therapeutics,* 116**,** 287-305.

CLUTTER, M. R., HEFFNER, G. C., KRUTZIK, P. O., SACHEN, K. L. & NOLAN, G. P. 2010. Tyramide signal amplification for analysis of kinase activity by intracellular flow cytometry. *Cytometry Part A,* 77**,** 1020-1031.

COHEN, P. 2002. Protein kinases—the major drug targets of the twenty-first century? *Nature Reviews Drug Discovery,* 1**,** 309-315.

COLLER, B. S. 1997. Platelet GPIIb/IIIa antagonists: the first anti-integrin receptor therapeutics. *Journal of Clinical Investigation,* 99**,** 1467.

COOPER, D. 2003. Regulation and organization of adenylyl cyclases and cAMP. *Biochem. J,* 375**,** 517-529.

COOPER, D. M., MONS, N. & KARPEN, J. W. 1995. Adenylyl cyclases and the interaction between calcium and cAMP signalling.

CORBIN, J. & FRANCIS, S. 2001. Pharmacology of phosphodiesterase-5 inhibitors. *International journal of clinical practice,* 56**,** 453-459.

COUGHLIN, S. R. 2005. Protease-activated receptors in hemostasis, thrombosis and vascular biology. *Journal of Thrombosis and Haemostasis,* 3**,** 1800-1814.

CRANMER, S. L., ASHWORTH, K. J., YAO, Y., BERNDT, M. C., RUGGERI, Z. M., ANDREWS, R. K. & JACKSON, S. P. 2011. High shear–dependent loss of membrane integrity and defective platelet adhesion following disruption of the GPIbα-filamin interaction. *Blood,* 117**,** 2718-2727.

DANIEL, J. L., DANGELMAIER, C., JIN, J., ASHBY, B., SMITH, J. B. & KUNAPULI, S. P. 1998. Molecular basis for ADP-induced platelet activation I. Evidence for three distinct ADP receptors on human platelets. *Journal of Biological Chemistry,* 273**,** 2024-2029.

DAVI, G., RINI, G., AVERNA, M., NOVO, S., DI FEDE, G., PINTO, A., NOTARBARTOLO, A. & STRANO, A. 1982. Thromboxane B$_2$ formation and platelet sensitivity to prostacyclin in insulin-dependent and insulin-independent diabetics. *Thrombosis research,* 26**,** 359-370.

DE MAN, F. H., NIEUWLAND, R., VAN DER LAARSE, A., ROMIJN, F., SMELT, A. H., GEVERS LEUVEN, J. A. & STURK, A. 2000. Activated platelets in patients with severe hypertriglyceridemia: effects of triglyceride-lowering therapy. *Atherosclerosis,* 152**,** 407-414.

DEBILI, N., KIEFFER, N., NAKAZAWA, M., GUICHARD, J., TITEUX, M., CRAMER, E., BRETON-GORIUS, J. & VAINCHENKER, W. 1990. Expression of platelet glycoprotein Ib by cultured human megakaryocytes: ultrastructural localization and biosynthesis. *Blood,* 76**,** 368-376.

DERELI, D., OZGEN, G., BUYUKKECECI, F., GUNEY, E. & YILMAZ, C. 2003. Platelet dysfunction in lean women with polycystic ovary syndrome and association with insulin sensitivity. *Journal of Clinical Endocrinology & Metabolism,* 88**,** 2263-2268.

DESSAUER, C. W., TESMER, J. J., SPRANG, S. R. & GILMAN, A. G. 1998. Identification of a Giα binding site on type V adenylyl cyclase. *Journal of Biological Chemistry,* 273**,** 25831-25839.

DIMMELER, S., ASSMUS, B., HERMANN, C., HAENDELER, J. & ZEIHER, A. M. 1998. Fluid shear stress stimulates phosphorylation of Akt in human endothelial cells involvement in suppression of apoptosis. *Circulation research,* 83**,** 334-341.

DIVIANI, D. & SCOTT, J. D. 2001. AKAP signaling complexes at the cytoskeleton. *Journal of Cell Science,* 114**,** 1431-1437.

DODGE, K. L., KHOUANGSATHIENE, S., KAPILOFF, M. S., MOUTON, R., HILL, E. V., HOUSLAY, M. D., LANGEBERG, L. K. & SCOTT, J. D. 2001. mAKAP assembles a protein kinase A/PDE4 phosphodiesterase cAMP signaling module. *The EMBO Journal,* 20**,** 1921-1930.

DUNKERN, T. R. & HATZELMANN, A. 2005. The effect of Sildenafil on human platelet secretory function is controlled by a complex interplay between phosphodiesterases 2, 3 and 5. *Cellular signalling,* 17**,** 331-339.

EDWARDS, H. V., SCOTT, J. D. & BAILLIE, G. S. 2012. PKA phosphorylation of the small heat-shock protein Hsp20 enhances its cardioprotective effects. *Biochemical Society transactions,* 40**,** 210.

EHRMANN, D. A., LILJENQUIST, D. R., KASZA, K., AZZIZ, R., LEGRO, R. S. & GHAZZI, M. N. 2006. Prevalence and predictors of the metabolic syndrome in women with polycystic ovary syndrome. *Journal of Clinical Endocrinology & Metabolism,* 91**,** 48-53.

EIGENTHALER, M., NOLTE, C., HALBRUGGE, M. & WALTER, U. 1992. Concentration and regulation of cyclic nucleotides, cyclic-nucleotide-dependent protein kinases and one of their major substrates in human platelets. *European Journal of Biochemistry,* 205**,** 471-481.

EJIM, O., POWLING, M., DANDONA, P., KERNOFF, P. & GOODALL, A. 1990. A flow cytometric analysis of fibronectin binding to platelets from patients with peripheral vascular disease. *Thrombosis research,* 58**,** 519-524.

EL-DAHER, S., EIGENTHALER, M., WALTER, U., FURUICHI, T., MIYAWAKI, A., MIKOSHIBA, K., KAKKAR, V. & AUTHI, K. 1996. Distribution and activation of cAMP-and cGMP-dependent protein kinases in highly purified human platelet plasma and intracellular membranes. *Thrombosis and Haemostasis,* 76**,** 1063-1071.

ENG, C. H., HUCKABA, T. M. & GUNDERSEN, G. G. 2006. The formin mDia regulates GSK3β through novel PKCs to promote microtubule stabilization but not MTOC reorientation in migrating fibroblasts. *Molecular biology of the cell,* 17**,** 5004-5016.

ETIENNE-MANNEVILLE, S. & HALL, A. 2003. Cdc42 regulates GSK-3β and adenomatous polyposis coli to control cell polarity. *Nature,* 421**,** 753-756.

EVANGELISTA, V., PAMUKLAR, Z., PICCOLI, A., MANARINI, S., DELL'ELBA, G., PECCE, R., MARTELLI, N., FEDERICO, L., ROJAS, M. & BERTON, G. 2007. Src family kinases mediate neutrophil adhesion to adherent platelets. *Blood,* 109**,** 2461-2469.

FAGAN, K. A., MAHEY, R. & COOPER, D. M. 1996. Functional co-localization of transfected Ca2+-stimulable adenylyl cyclases with capacitative Ca2+ entry sites. *Journal of Biological Chemistry,* 271**,** 12438-12444.

FALATI, S., LIU, Q., GROSS, P., MERRILL-SKOLOFF, G., CHOU, J., VANDENDRIES, E., CELI, A., CROCE, K., FURIE, B. C. & FURIE, B. 2003. Accumulation of tissue factor into developing thrombi in vivo is dependent upon microparticle P-selectin glycoprotein ligand 1 and platelet P-selectin. *The Journal of experimental medicine,* 197**,** 1585-1598.

FANG, X., YU, S. X., LU, Y., BAST, R. C., WOODGETT, J. R. & MILLS, G. B. 2000. Phosphorylation and inactivation of glycogen synthase kinase 3 by protein kinase A. *Proceedings of the National Academy of Sciences,* 97**,** 11960-11965.

FARNDALE, R., SIXMA, J., BARNES, M. & DE GROOT, P. 2004. The role of collagen in thrombosis and hemostasis. *Journal of Thrombosis and Haemostasis,* 2**,** 561-573.

FEINSTEIN, M., HALENDA, S. & ZAVOICO, G. 1985. Calcium and platelet function. *Calcium and Cell Physiology.* Springer.

FENG, S., RESÉNDIZ, J. C., LU, X. & KROLL, M. H. 2003. Filamin A binding to the cytoplasmic tail of glycoprotein Ibα regulates von Willebrand factor–induced platelet activation. *Blood,* 102**,** 2122-2129.

FERNANDES, L. S., CONDE, I. D., WAYNE SMITH, C., KANSAS, G. S., SNAPP, K. R., BENNET, N., BALLANTYNE, C., MCINTIRE, L. V., O'BRIAN SMITH, E. & KLEM, J. A. 2003. Platelet–monocyte complex formation: effect of blocking PSGL-1 alone, and in combination with αIIbβ3 and αMβ2, in coronary stenting. *Thrombosis research,* 111**,** 171-177.

FLAUMENHAFT, R. 2003. Molecular basis of platelet granule secretion. *Arteriosclerosis, thrombosis, and vascular biology,* 23**,** 1152-1160.

FLAUMENHAFT, R., DILKS, J. R., ROZENVAYN, N., MONAHAN-EARLEY, R. A., FENG, D. & DVORAK, A. M. 2005. The actin cytoskeleton differentially regulates platelet α-granule and dense-granule secretion. *Blood,* 105**,** 3879-3887.

FORCE, T. & WOODGETT, J. R. 2009. Unique and overlapping functions of GSK-3 isoforms in cell differentiation and proliferation and cardiovascular development. *Journal of Biological Chemistry,* 284**,** 9643-9647.

FOX, J. & BERNDT, M. 1989. Cyclic AMP-dependent phosphorylation of glycoprotein Ib inhibits collagen-induced polymerization of actin in platelets. *Journal of Biological Chemistry,* 264**,** 9520-9526.

FOX, J. E., SHATTIL, S. J., KINLOUGH-RATHBONE, R. L., RICHARDSON, M., PACKHAM, M. A. & SANAN, D. A. 1996. The Platelet Cytoskeleton Stabilizes the Interaction between and Its Ligand and Induces Selective Movements of Ligand-occupied Integrin. *Journal of Biological Chemistry,* 271**,** 7004-7011.

FOX, S., MAY, J., SHAH, A., NEUBERT, U. & HEPTINSTALL, S. 2009. Measurement of platelet P-selectin for remote testing of platelet function during treatment with clopidogrel and/or aspirin. *Platelets,* 20**,** 250-259.

FRAME, S. & COHEN, P. 2001. GSK3 takes centre stage more than 20 years after its discovery. *Biochemical Journal,* 359**,** 1-16.

FRANCESCHINI, D., PAROLI, M., FRANCAVILLA, V., VIDETTA, M., MORRONE, S., LABBADIA, G., CERINO, A., MONDELLI, M. U. & BARNABA, V. 2009. PD-L1 negatively regulates CD4+ CD25+ Foxp3+ Tregs by limiting STAT-5 phosphorylation in patients chronically infected with HCV. *The Journal of clinical investigation,* 119**,** 551-564.

FRANCIS, S. H., BUSCH, J. L. & CORBIN, J. D. 2010. cGMP-dependent protein kinases and cGMP phosphodiesterases in nitric oxide and cGMP action. *Pharmacological reviews,* 62**,** 525-563.

FRANGOS, J. A., ESKIN, S. G., MCINTIRE, L. V. & IVES, C. 1985. Flow effects on prostacyclin production by cultured human endothelial cells. *Science,* 227**,** 1477-1479.

FRANKS, S. 1995. Polycystic ovary syndrome. *New England Journal of Medicine,* 333**,** 853-861.

FREDHOLM, B. B. 1985. On the mechanism of action of theophylline and caffeine. *Acta Medica Scandinavica,* 217**,** 149-153.

FRIEBE, A. & KOESLING, D. 2003. Regulation of nitric oxide-sensitive guanylyl cyclase. *Circulation research,* 93**,** 96-105.

FUKAMI, K., ENDO, T., IMAMURA, M. & TAKENAWA, T. 1994. alpha-Actinin and vinculin are PIP2-binding proteins involved in signaling by tyrosine kinase. *Journal of Biological Chemistry,* 269**,** 1518-1522.

FULTON, D., GRATTON, J.-P., MCCABE, T. J., FONTANA, J., FUJIO, Y., WALSH, K., FRANKE, T. F., PAPAPETROPOULOS, A. & SESSA, W. C. 1999. Regulation of endothelium-derived nitric oxide production by the protein kinase Akt. *Nature,* 399**,** 597-601.

FUNG, C. E., JONES, S., NTRAKWAH, A., NASEEM, K. M., FARNDALE, R. W. & MAHAUT-SMITH, M. P. 2012. Platelet Ca2+ responses coupled to glycoprotein VI and Toll-like receptors persist in the presence of endothelial-derived inhibitors: roles for secondary activation of P2X1 receptors and release from intracellular Ca2+ stores. *Blood,* 119**,** 3613-3621.

GAMBARYAN, S., KOBSAR, A., HARTMANN, S., BIRSCHMANN, I., KUHLENCORDT, P., MÜLLER-ESTERL, W., LOHMANN, S. & WALTER, U. 2008. NO-synthase-/NO-independent regulation of human and murine platelet soluble guanylyl cyclase activity. *Journal of Thrombosis and Haemostasis,* 6**,** 1376-1384.

GARBERS, D. 1979. Purification of soluble guanylate cyclase from rat lung. *Journal of Biological Chemistry,* 254**,** 240-243.

GARTHWAITE, J., SOUTHAM, E., BOULTON, C. L., NIELSEN, E. B., SCHMIDT, K. & MAYER, B. 1995. Potent and selective inhibition of nitric oxide-sensitive guanylyl cyclase by 1H-[1, 2, 4] oxadiazolo [4, 3-a] quinoxalin-1-one. *Molecular pharmacology,* 48**,** 184-188.

GASPARYAN, A. Y., STAVROPOULOS-KALINOGLOU, A., MIKHAILIDIS, D. P., DOUGLAS, K. M. & KITAS, G. D. 2011. Platelet function in rheumatoid arthritis: arthritic and cardiovascular implications. *Rheumatology international,* 31**,** 153-164.

GAWAZ, M. P., LOFTUS, J., BAJT, M., FROJMOVIC, M., PLOW, E. & GINSBERG, M. 1991. Ligand bridging mediates integrin alpha IIb beta 3 (platelet GPIIB-IIIA) dependent homotypic and heterotypic cell-cell interactions. *Journal of Clinical Investigation,* 88**,** 1128.

GAYLE, R., MALISZEWSKI, C. R., GIMPEL, S. D., SCHOENBORN, M. A., CASPARY, R. G., RICHARDS, C., BRASEL, K., PRICE, V., DROSOPOULOS, J. & ISLAM, N. 1998. Inhibition

of platelet function by recombinant soluble ecto-ADPase/CD39. *Journal of Clinical Investigation,* 101**,** 1851.

GEIGER, J., NOLTE, C. & WALTER, U. 1994. Regulation of calcium mobilization and entry in human platelets by endothelium-derived factors. *American Journal of Physiology-Cell Physiology,* 36**,** C236.

GIBBINS, J., ASSELIN, J., FARNDALE, R., BARNES, M., LAW, C.-L. & WATSON, S. P. 1996. Tyrosine phosphorylation of the Fc receptor γ-chain in collagen-stimulated platelets. *Journal of Biological Chemistry,* 271**,** 18095-18099.

GIBBINS, J. M. 2004. Platelet adhesion signalling and the regulation of thrombus formation. *Journal of Cell Science,* 117**,** 3415-3425.

GIBBINS, J. M. & MAHAUT-SMITH, M. P. 2004. *Platelets and megakaryocytes*, Springer.

GIBBS, K. D., GILBERT, P. M., SACHS, K., ZHAO, F., BLAU, H. M., WEISSMAN, I. L., NOLAN, G. P. & MAJETI, R. 2011. Single-cell phospho-specific flow cytometric analysis demonstrates biochemical and functional heterogeneity in human hematopoietic stem and progenitor compartments. *Blood,* 117**,** 4226-4233.

GLENN, J., DOVLATOVA, N., WHITE, A., DHILLON, K., HEPTINSTALL, S. & FOX, S. 2012. 'VASPFix'for measurement of VASP phosphorylation in platelets and for monitoring effects of P2Y12 antagonists. *Thromb Haemost,* 108**,** 955-962.

GLENN, J., DOVLATOVA, N., WHITE, A., DHILLON, K., HEPTINSTALL, S. & FOX, S. 2014. 'VASPFix' for measurement of VASP phosphorylation in platelets and for monitoring effects of P2Y12 antagonists. *Thrombosis and Haemostasis,* 111**,** 539-48.

GOODALL, A. H. & APPLEBY, J. 2004. Flow-cytometric analysis of platelet-membrane glycoprotein expression and platelet activation. *Platelets and megakaryocytes.* Springer.

GORMAN, R., BUNTING, S. & MILLER, O. 1977. Modulation of human platelet adenylate cyclase by prostacyclin (PGX). *Prostaglandins,* 13**,** 377-388.

GROSS, B. S., MELFORD, S. K. & WATSON, S. P. 1999. Evidence that phospholipase C-γ2 interacts with SLP-76, Syk, Lyn, LAT and the Fc receptor γ-chain after stimulation of the collagen receptor glycoprotein VI in human platelets. *European Journal of Biochemistry,* 263**,** 612-623.

HALBRÜGGE, M., FRIEDRICH, C., EIGENTHALER, M., SCHANZENBÄCHER, P. & WALTER, U. 1990. Stoichiometric and reversible phosphorylation of a 46-kDa protein in human platelets in response to cGMP-and cAMP-elevating vasodilators. *Journal of Biological Chemistry,* 265**,** 3088-3093.

HALE, M. B., KRUTZIK, P. O., SAMRA, S. S., CRANE, J. M. & NOLAN, G. P. 2009. Stage dependent aberrant regulation of cytokine-STAT signaling in murine systemic lupus erythematosus. *PLoS One,* 4**,** e6756.

HALLS, M. L. & COOPER, D. M. 2011. Regulation by Ca2+-signaling pathways of adenylyl cyclases. *Cold Spring Harbor perspectives in biology,* 3**,** a004143.

HANDAGAMA, P. J., GEORGE, J. N., SHUMAN, M. A., MCEVER, R. P. & BAINTON, D. F. 1987. Incorporation of a circulating protein into megakaryocyte and platelet granules. *Proceedings of the National Academy of Sciences,* 84**,** 861-865.

HARBECK, B., HÜTTELMAIER, S., SCHLÜTER, K., JOCKUSCH, B. M. & ILLENBERGER, S. 2000. Phosphorylation of the vasodilator-stimulated phosphoprotein regulates its interaction with actin. *Journal of Biological Chemistry,* 275**,** 30817-30825.

HARRISON, P. 2009. Assessment of platelet function in the laboratory. *Hamostaseologie,* 29**,** 25-31.

HARTENECK, C., KOESLING, D., SÖLING, A., SCHULTZ, G. & BÖHME, E. 1990. Expression of soluble guanylyl cyclase: catalytic activity requires two enzyme subunits. *FEBS letters,* 272**,** 221-223.

HARTWIG, J. H. 2002. Platelet structure. *Platelets,* 1**,** 37-52.

HARTWIG, J. H. Year. The platelet: form and function. *In:* Seminars in hematology, 2006. Elsevier, S94-S100.

HARTWIG, J. H. 2012. The Platelet Cytoskeleton. *Platelets***,** 145.

HARTWIG, J. H., BOKOCH, G. M., CARPENTER, C. L., JANMEY, P. A., TAYLOR, L. A., TOKER, A. & STOSSEL, T. P. 1995. Thrombin receptor ligation and activated Rac uncap actin filament barbed ends through phosphoinositide synthesis in permeabilized human platelets. *Cell,* 82**,** 643-653.

HARTWIG, J. H. & DESISTO, M. 1991. The cytoskeleton of the resting human blood platelet: structure of the membrane skeleton and its attachment to actin filaments. *The Journal of cell biology,* 112**,** 407-425.

HASLAM, R. J., DICKINSON, N. T. & JANG, E. K. 1999a. Cyclic nucleotides and phosphodiesterases in platelets. *THROMBOSIS AND HAEMOSTASIS-STUTTGART-,* 82**,** 412-423.

HASLAM, R. J., DICKINSON, N. T. & JANG, E. K. 1999b. Cyclic nucleotides and phosphodiesterases in platelets. *Thrombosis and haemostasis,* 82**,** 412-23.

HASSOCK, S. R., ZHU, M. X., TROST, C., FLOCKERZI, V. & AUTHI, K. S. 2002. Expression and role of TRPC proteins in human platelets: evidence that TRPC6 forms the store-independent calcium entry channel. *Blood,* 100**,** 2801-2811.

HEEMSKERK, J., BEVERS, E. & LINDHOUT, T. 2002. Platelet activation and blood coagulation. *Thrombosis and Haemostasis,* 88**,** 186.

HEFFNER, G. C., CLUTTER, M. R., NOLAN, G. P. & WEISSMAN, I. L. 2011. Novel hematopoietic progenitor populations revealed by direct assessment of GATA1 protein expression and cMPL signaling events. *Stem Cells,* 29**,** 1774-1782.

HEIJNEN, H. F., DEBILI, N., VAINCHENCKER, W., BRETON-GORIUS, J., GEUZE, H. J. & SIXMA, J. J. 1998. Multivesicular bodies are an intermediate stage in the formation of platelet α-granules. *Blood,* 91**,** 2313-2325.

HERAUD, J.-M., RACAUD-SULTAN, C., GIRONCEL, D., ALBIGÈS-RIZO, C., GIACOMINI, T., ROQUES, S., MARTEL, V., BRETON-DOUILLON, M., PERRET, B. & CHAP, H. 1998. Lipid products of phosphoinositide 3-kinase and phosphatidylinositol 4′, 5′-bisphosphate are both required for ADP-dependent platelet spreading. *Journal of Biological Chemistry,* 273**,** 17817-17823.

HETTASCH, J. & SELLERS, J. 1991. Caldesmon phosphorylation in intact human platelets by cAMP-dependent protein kinase and protein kinase C. *Journal of Biological Chemistry,* 266**,** 11876-11881.

HOBBS, A. J. 1997. Soluble guanylate cyclase: the forgotten sibling. *Trends in pharmacological sciences,* 18**,** 484-491.

HOFMANN, F., AMMENDOLA, A. & SCHLOSSMANN, J. 2000. Rising behind NO: cGMP-dependent protein kinases. *Journal of Cell Science,* 113**,** 1671-1676.

HOLLOPETER, G., JANTZEN, H.-M., VINCENT, D., LI, G., ENGLAND, L., RAMAKRISHNAN, V., YANG, R.-B., NURDEN, P., NURDEN, A. & JULIUS, D. 2001. Identification of the platelet ADP receptor targeted by antithrombotic drugs. *Nature,* 409**,** 202-207.

HORSTRUP, K., JABLONKA, B., HÖNIG-LIEDL, P., JUST, M., KOCHSIEK, K. & WALTER, U. 1994. Phosphorylation of Focal Adhesion Vasodilator-Stimulated Phosphoprotein at Ser157 in Intact Human Platelets Correlates with Fibrinogen Receptor Inhibition. *European Journal of Biochemistry,* 225**,** 21-27.

HUGHES, J., REES, S., KALINDJIAN, S. & PHILPOTT, K. 2011. Principles of early drug discovery. *British journal of pharmacology,* 162**,** 1239-1249.

HUNTER, R. W., MACKINTOSH, C. & HERS, I. 2009. Protein kinase C-mediated phosphorylation and activation of PDE3A regulate cAMP levels in human platelets. *Journal of Biological Chemistry,* 284**,** 12339-12348.

HURLEY, J. H. 1999. Structure, mechanism, and regulation of mammalian adenylyl cyclase. *Journal of Biological Chemistry,* 274**,** 7599-7602.

INOUE, O., SUZUKI-INOUE, K., DEAN, W. L., FRAMPTON, J. & WATSON, S. P. 2003. Integrin α2β1 mediates outside-in regulation of platelet spreading on collagen through activation of Src kinases and PLCγ2. *The Journal of cell biology,* 160**,** 769-780.

IRISH, J. M., ÅNENSEN, N., HOVLAND, R., SKAVLAND, J., BØRRESEN-DALE, A.-L., BRUSERUD, Ø., NOLAN, G. P. & GJERTSEN, B. T. 2007. Flt3 Y591 duplication and Bcl-2 overexpression are detected in acute myeloid leukemia cells with high levels of phosphorylated wild-type p53. *Blood,* 109**,** 2589-2596.

IRISH, J. M., CZERWINSKI, D. K., NOLAN, G. P. & LEVY, R. 2006. Kinetics of B cell receptor signaling in human B cell subsets mapped by phosphospecific flow cytometry. *The Journal of Immunology,* 177**,** 1581-1589.

IRISH, J. M., HOVLAND, R., KRUTZIK, P. O., PEREZ, O. D., BRUSERUD, Ø., GJERTSEN, B. T. & NOLAN, G. P. 2004. Single cell profiling of potentiated phospho-protein networks in cancer cells. *Cell,* 118**,** 217-228.

IRISH, J. M., MYKLEBUST, J. H., ALIZADEH, A. A., HOUOT, R., SHARMAN, J. P., CZERWINSKI, D. K., NOLAN, G. P. & LEVY, R. 2010. B-cell signaling networks reveal a negative prognostic human lymphoma cell subset that emerges during tumor progression. *Proceedings of the National Academy of Sciences,* 107**,** 12747-12754.

IYÚ, D., GLENN, J. R., WHITE, A. E., FOX, S. C., DOVLATOVA, N. & HEPTINSTALL, S. 2011. P2Y12 and EP3 antagonists promote the inhibitory effects of natural modulators of platelet aggregation that act via cAMP. *Platelets,* 22**,** 504-515.

JACKSON, S. P. 2007. The growing complexity of platelet aggregation. *Blood,* 109**,** 5087-5095.

JAMES, N., HARRISON, D. & NEREM, R. 1995. Effects of shear on endothelial cell calcium in the presence and absence of ATP. *The FASEB journal,* 9**,** 968-973.

JAMUR, M. C. & OLIVER, C. 2010. Permeabilization of cell membranes. *Immunocytochemical methods and protocols.* Springer.

JANTZEN, H.-M., MILSTONE, D. S., GOUSSET, L., CONLEY, P. B. & MORTENSEN, R. M. 2001. Impaired activation of murine platelets lacking Gαi2. *Journal of Clinical Investigation,* 108**,** 477-483.

JENNINGS, L. K. & WHITE, M. M. 1998. Expression of ligand-induced binding sites on glycoprotein IIb/IIIa complexes and the effect of various inhibitors. *American heart journal,* 135**,** S179-S183.

JENSEN, B. O., SELHEIM, F., DØSKELAND, S. O., GEAR, A. R. & HOLMSEN, H. 2004. Protein kinase A mediates inhibition of the thrombin-induced platelet shape change by nitric oxide. *Blood,* 104**,** 2775-2782.

JIANG, H., COLBRAN, J., FRANCIS, S. & CORBIN, J. 1992. Direct evidence for cross-activation of cGMP-dependent protein kinase by cAMP in pig coronary arteries. *Journal of Biological Chemistry,* 267**,** 1015-1019.

JIN, J. & KUNAPULI, S. P. 1998. Coactivation of two different G protein-coupled receptors is essential for ADP-induced platelet aggregation. *Proceedings of the National Academy of Sciences,* 95**,** 8070-8074.

JONES, C. I., GARNER, S. F., MORAES, L. A., KAISER, W. J., RANKIN, A., OUWEHAND, W. H., GOODALL, A. H. & GIBBINS, J. M. 2009. PECAM-1 expression and activity negatively regulate multiple platelet signaling pathways. *FEBS letters,* 583**,** 3618-3624.

JONES, R., WISE, H., CLARK, R., WHITING, R. & BLEY, K. 2006. Investigation of the prostacyclin (IP) receptor antagonist RO1138452 on isolated blood vessel and platelet preparations. *British journal of pharmacology,* 149**,** 110-120.

JOUTSI-KORHONEN, L., SMETHURST, P. A., RANKIN, A., GRAY, E., IJSSELDIJK, M., ONLEY, C. M., WATKINS, N. A., WILLIAMSON, L. M., GOODALL, A. H. & DE GROOT, P. G. 2003.

The low-frequency allele of the platelet collagen signaling receptor glycoprotein VI is associated with reduced functional responses and expression. *Blood,* 101**,** 4372-4379.

KARNIK, S. S., GOGONEA, C., PATIL, S., SAAD, Y. & TAKEZAKO, T. 2003. Activation of G-protein-coupled receptors: a common molecular mechanism. *Trends in Endocrinology & Metabolism,* 14**,** 431-437.

KAUSHANSKY, K. 1995. Thrombopoietin: the primary regulator of megakaryocyte and platelet production. *Thrombosis and Haemostasis,* 74**,** 521-525.

KAUSHANSKY, K. 2005. The molecular mechanisms that control thrombopoiesis. *The Journal of clinical investigation,* 115, 3339-3347.

KEHREL, B., WIERWILLE, S., CLEMETSON, K. J., ANDERS, O., STEINER, M., KNIGHT, C. G., FARNDALE, R. W., OKUMA, M. & BARNES, M. J. 1998. Glycoprotein VI is a major collagen receptor for platelet activation: it recognizes the platelet-activating quaternary structure of collagen, whereas CD36, glycoprotein IIb/IIIa, and von Willebrand factor do not. *Blood,* 91**,** 491-499.

KIM, Y. J., BORSIG, L., VARKI, N. M. & VARKI, A. 1998. P-selectin deficiency attenuates tumor growth and metastasis. *Proceedings of the National Academy of Sciences,* 95**,** 9325-9330.

KINOSHITA, S. M., KRUTZIK, P. O. & NOLAN, G. P. 2012. COP9 Signalosome Component JAB1/CSN5 Is Necessary for T Cell Signaling through LFA-1 and HIV-1 Replication. *PLoS One,* 7**,** e41725.

KLAGES, B., BRANDT, U., SIMON, M. I., SCHULTZ, G. & OFFERMANNS, S. 1999. Activation of G12/G13 results in shape change and Rho/Rho-kinase–mediated myosin light chain phosphorylation in mouse platelets. *The Journal of cell biology,* 144**,** 745-754.

KNEZEVIC, I., BORG, C. & LE BRETON, G. C. 1993. Identification of Gq as one of the G-proteins which copurify with human platelet thromboxane A2/prostaglandin H2 receptors. *Journal of Biological Chemistry,* 268**,** 26011-26017.

KOGLIN, M. & BEHRENDS, S. 2003. A functional domain of the α1 subunit of soluble guanylyl cyclase is necessary for activation of the enzyme by nitric oxide and YC-1 but is not involved in heme binding. *Journal of Biological Chemistry,* 278**,** 12590-12597.

KOLCH, W. 2005. Coordinating ERK/MAPK signalling through scaffolds and inhibitors. *Nature reviews Molecular cell biology,* 6**,** 827-837.

KONSTANTOPOULOS, K., KAMAT, S. G., SCHAFER, A. I., BAÑEZ, E. I., JORDAN, R., KLEIMAN, N. S. & HELLUMS, J. D. 1995. Shear-induced platelet aggregation is inhibited by in vivo infusion of an anti–glycoprotein IIb/IIIa antibody fragment, c7E3 Fab, in patients undergoing coronary angioplasty. *Circulation,* 91**,** 1427-1431.

KOTECHA, N., FLORES, N. J., IRISH, J. M., SIMONDS, E. F., SAKAI, D. S., ARCHAMBEAULT, S., DIAZ-FLORES, E., CORAM, M., SHANNON, K. M. & NOLAN, G. P. 2008. Single-cell profiling identifies aberrant STAT5 activation in myeloid malignancies with specific clinical and biologic correlates. *Cancer cell,* 14**,** 335-343.

KOTECHA, N., KRUTZIK, P. O. & IRISH, J. M. 2010. Web-based analysis and publication of flow cytometry experiments. *Curr Protoc Cytom,* 10.

KOZASA, T., JIANG, X., HART, M. J., STERNWEIS, P. M., SINGER, W. D., GILMAN, A. G., BOLLAG, G. & STERNWEIS, P. C. 1998. p115 RhoGEF, a GTPase activating protein for Gα12 and Gα13. *Science,* 280**,** 2109-2111.

KREUTZ, R. P., ALLOOSH, M., MANSOUR, K., NEEB, Z., KREUTZ, Y., FLOCKHART, D. A. & STUREK, M. 2011. Morbid obesity and metabolic syndrome in Ossabaw miniature swine are associated with increased platelet reactivity. *Diabetes, metabolic syndrome and obesity: targets and therapy,* 4**,** 99.

KRUTZIK, P. O., CLUTTER, M. R. & NOLAN, G. P. 2005a. Coordinate analysis of murine immune cell surface markers and intracellular phosphoproteins by flow cytometry. *The Journal of Immunology,* 175**,** 2357-2365.

KRUTZIK, P. O., CLUTTER, M. R., TREJO, A. & NOLAN, G. P. 2011. Fluorescent cell barcoding for multiplex flow cytometry. *Current Protocols in Cytometry***,** 6.31. 1-6.31. 15.

KRUTZIK, P. O., CRANE, J. M., CLUTTER, M. R. & NOLAN, G. P. 2007. High-content single-cell drug screening with phosphospecific flow cytometry. *Nature chemical biology,* 4**,** 132-142.

KRUTZIK, P. O., HALE, M. B. & NOLAN, G. P. 2005b. Characterization of the murine immunological signaling network with phosphospecific flow cytometry. *The Journal of Immunology,* 175**,** 2366-2373.

KRUTZIK, P. O. & NOLAN, G. P. 2003. Intracellular phospho-protein staining techniques for flow cytometry: Monitoring single cell signaling events. *Cytometry Part A,* 55**,** 61-70.

KRUTZIK, P. O. & NOLAN, G. P. 2006. Fluorescent cell barcoding in flow cytometry allows high-throughput drug screening and signaling profiling. *Nature methods,* 3**,** 361-368.

LAI, H.-L., YANG, T.-H., MESSING, R. O., CHING, Y.-H., LIN, S.-C. & CHERN, Y. 1997. Protein kinase C inhibits adenylyl cyclase type VI activity during desensitization of the A2a-adenosine receptor-mediated cAMP response. *Journal of Biological Chemistry,* 272**,** 4970-4977.

LAPETINA, E. G., LACAL, J. C., REEP, B. R. & Y VEDIA, L. M. 1989. A ras-related protein is phosphorylated and translocated by agonists that increase cAMP levels in human platelets. *Proceedings of the National Academy of Sciences,* 86**,** 3131-3134.

LEE, H.-S., LIM, C. J., PUZON-MCLAUGHLIN, W., SHATTIL, S. J. & GINSBERG, M. H. 2009. RIAM activates integrins by linking talin to ras GTPase membrane-targeting sequences. *Journal of Biological Chemistry,* 284**,** 5119-5127.

LESLIE, C. C. 1997. Properties and regulation of cytosolic phospholipase A2. *Journal of Biological Chemistry,* 272**,** 16709-16712.

LEVY, F. O., RASMUSSEN, A. M., TASKÉN, K., SKÅLHEGG, B. S., HUITFELDT, H. S., FUNDERUD, S., SMELAND, E. B. & HANSSON, V. 1996. Cyclic AMP-dependent protein kinase (cAK) in human B cells: co-localization of type I cAK (RIα2C2) with the antigen receptor during anti-immunoglobulin-induced B cell activation. *European journal of immunology,* 26**,** 1290-1296.

LI, D., AUGUST, S. & WOULFE, D. S. 2008. GSK3β is a negative regulator of platelet function and thrombosis. *Blood,* 111**,** 3522-3530.

LI, N., GOODALL, A. H. & HJEMDAHL, P. 1999. Efficient flow cytometric assay for platelet-leukocyte aggregates in whole blood using fluorescence signal triggering. *Cytometry,* 35**,** 154-161.

LI, Z., DELANEY, M. K., O'BRIEN, K. A. & DU, X. 2010. Signaling during platelet adhesion and activation. *Arteriosclerosis, thrombosis, and vascular biology,* 30**,** 2341-2349.

LIBBY, P. & SIMON, D. I. 2001. Inflammation and thrombosis the clot thickens. *Circulation,* 103**,** 1718-1720.

LINDEN, M. D., FRELINGER III, A. L., BARNARD, M. R., PRZYKLENK, K., FURMAN, M. I. & MICHELSON, A. D. Year. Application of flow cytometry to platelet disorders. *In:* Seminars in thrombosis and hemostasis, 2004. Copyright© 2004 by Thieme Medical Publishers, Inc., 333 Seventh Avenue, New York, NY 10001, USA., 501-511.

LISHKO, V. K., PODOLNIKOVA, N. P., YAKUBENKO, V. P., YAKOVLEV, S., MEDVED, L., YADAV, S. P. & UGAROVA, T. P. 2004. Multiple binding sites in fibrinogen for integrin αMβ2 (Mac-1). *Journal of Biological Chemistry,* 279**,** 44897-44906.

MACPHEE, C., REIFSNYDER, D., MOORE, T., LEREA, K. & BEAVO, J. 1988. Phosphorylation results in activation of a cAMP phosphodiesterase in human platelets. *Journal of Biological Chemistry,* 263**,** 10353-10358.

MANGANELLO, J. M., DJELLAS, Y., BORG, C., ANTONAKIS, K. & LE BRETON, G. C. 1999. Cyclic AMP-dependent phosphorylation of thromboxane A2 receptor-associated Gα13. *Journal of Biological Chemistry,* 274**,** 28003-28010.

MANGIN, P., YUAN, Y., GONCALVES, I., ECKLY, A., FREUND, M., CAZENAVE, J., GACHET, C., JACKSON, S. & LANZA, F. 2003. Signaling role for phospholipase C gamma 2 in platelet glycoprotein Ib alpha calcium flux and cytoskeletal reorganization. Involvement of a pathway distinct from FcR gamma chain and Fc gamma RIIA. *The Journal of biological chemistry,* 278**,** 32880-32891.

MANNS, J., BRENNAN, K., COLMAN, R. & SHETH, S. 2002. Differential regulation of human platelet responses by cGMP inhibited and stimulated cAMP phosphodiesterases. *THROMBOSIS AND HAEMOSTASIS-STUTTGART-,* 87**,** 873-879.

MARY TANG, K., JANG, E. K. & HASLAM, R. J. 1994. Photoaffinity labelling of cyclic GMP-inhibited phosphodiesterase (PDE III) in human and rat platelets and rat tissues: effects of phosphodiesterase inhibitors. *European Journal of Pharmacology: Molecular Pharmacology,* 268**,** 105-114.

MASSBERG, S., GRÜNER, S., KONRAD, I., ARGUINZONIS, M. I. G., EIGENTHALER, M., HEMLER, K., KERSTING, J., SCHULZ, C., MÜLLER, I. & BESTA, F. 2004. Enhanced in vivo platelet adhesion in vasodilator-stimulated phosphoprotein (VASP)–deficient mice. *Blood,* 103**,** 136-142.

MASSBERG, S., SAUSBIER, M., KLATT, P., BAUER, M., PFEIFER, A., SIESS, W., FASSLER, R., RUTH, P., KROMBACH, F. & HOFMANN, F. 1999. Increased adhesion and aggregation of platelets lacking cyclic guanosine 3',5'-monophosphate kinase I. *J Exp Med,* 189**,** 1255-64.

MATHERS, C. D. & LONCAR, D. 2006. Projections of global mortality and burden of disease from 2002 to 2030. *PLoS medicine,* 3**,** e442.

MCEVER, R. P. 2007. P-Selectin/PSGL-1 and other interactions between platelets, leukocytes, and endothelium. *Platelets,* 2007**,** 231-249.

MEINKOTH, J. L., JI, Y., TAYLOR, S. S. & FERAMISCO, J. R. 1990. Dynamics of the distribution of cyclic AMP-dependent protein kinase in living cells. *Proceedings of the National Academy of Sciences,* 87**,** 9595-9599.

MELAN, M. A. 1999. Overview of cell fixatives and cell membrane permeants. *Immunocytochemical Methods and Protocols.* Springer.

METCALFE, P., WILLIAMSON, L. M., REUTELINGSPERGER, C. P., SWANN, I., OUWEHAND, W. H. & GOODALL, A. H. 1997. Activation during preparation of therapeutic platelets affects deterioration during storage: a comparative flow cytometric study of different production methods. *British journal of haematology,* 98**,** 86-95.

MICHELSON, A. D. 1996. Flow cytometry: a clinical test of platelet function. *Open Access Articles***,** 290.

MICHELSON, A. D. 2010. Antiplatelet therapies for the treatment of cardiovascular disease. *Nature Reviews Drug Discovery,* 9**,** 154-169.

MICHELSON, A. D., BARNARD, M. R., HECHTMAN, H. B., MACGREGOR, H., CONNOLLY, R. J., LOSCALZO, J. & VALERI, C. R. 1996. In vivo tracking of platelets: circulating degranulated platelets rapidly lose surface P-selectin but continue to circulate and function. *Proceedings of the National Academy of Sciences,* 93**,** 11877-11882.

MICHELSON, A. D., BARNARD, M. R., KRUEGER, L. A., FRELINGER III, A. L. & FURMAN, M. I. 2000. Evaluation of platelet function by flow cytometry. *Methods,* 21**,** 259-270.

MICHELSON, A. D., BARNARD, M. R., KRUEGER, L. A., VALERI, C. R. & FURMAN, M. I. 2001. Circulating monocyte-platelet aggregates are a more sensitive marker of in vivo

platelet activation than platelet surface P-selectin studies in baboons, human coronary intervention, and human acute myocardial infarction. *Circulation,* 104**,** 1533-1537.

MICHELSON, A. D. & FURMAN, M. I. 1999. Laboratory markers of platelet activation and their clinical significance. *Current opinion in hematology,* 6**,** 342-348.

MODESTI, P., FORTINI, A., GENSINI, G. F., VANNI, D., PRISCO, D. & ABBATE, R. 1991. Human prostacyclin platelet receptors in diabetes mellitus. *Thrombosis research,* 63**,** 541-548.

MONCADA, S., GRYGLEWSKI, R., BUNTING, S. & VANE, J. 1976. An enzyme isolated from arteries transforms prostaglandin endoperoxides to an unstable substance that inhibits platelet aggregation.

MORTON, L., HARGREAVES, P., FARNDALE, R., YOUNG, R. & BARNES, M. 1995. Integrin alpha 2 beta 1-independent activation of platelets by simple collagen-like peptides: collagen tertiary (triple-helical) and quaternary (polymeric) structures are sufficient alone for alpha 2 beta 1-independent platelet reactivity. *Biochem. J,* 306**,** 337-344.

MOSER, M., NIESWANDT, B., USSAR, S., POZGAJOVA, M. & FÄSSLER, R. 2008. Kindlin-3 is essential for integrin activation and platelet aggregation. *Nature medicine,* 14**,** 325-330.

MOUNT, P. F., KEMP, B. E. & POWER, D. A. 2007. Regulation of endothelial and myocardial NO synthesis by multi-site eNOS phosphorylation. *Journal of molecular and cellular cardiology,* 42**,** 271-279.

MULLERSHAUSEN, F., RUSSWURM, M., THOMPSON, W. J., LIU, L., KOESLING, D. & FRIEBE, A. 2001. Rapid nitric oxide–induced desensitization of the cGMP response is caused by increased activity of phosphodiesterase type 5 paralleled by phosphorylation of the enzyme. *The Journal of cell biology,* 155**,** 271-278.

MURRAY, A. J. 2008. Pharmacological PKA inhibition: all may not be what it seems. *Science signaling,* 1**,** re4.

MUSTARD, J., KINLOUGH-RATHBONE, R. & PACKHAM, M. 1989. Isolation of human platelets from plasma by centrifugation and washing. *Methods in enzymology,* 169**,** 3.

NAKAMURA, M., ICHIKAWA, K., ITO, M., YAMAMORI, B., OKINAKA, T., ISAKA, N., YOSHIDA, Y., FUJITA, S. & NAKANO, T. 1999. Effects of the phosphorylation of myosin phosphatase by cyclic GMP-dependent protein kinase. *Cellular signalling,* 11**,** 671-676.

NESBITT, W. S., KULKARNI, S., GIULIANO, S., GONCALVES, I., DOPHEIDE, S. M., YAP, C. L., HARPER, I. S., SALEM, H. H. & JACKSON, S. P. 2002. Distinct glycoprotein Ib/V/IX and integrin αIIbβ3-dependent calcium signals cooperatively regulate platelet adhesion under flow. *Journal of Biological Chemistry,* 277**,** 2965-2972.

NIESWANDT, B., SCHULTE, V., BERGMEIER, W., MOKHTARI-NEJAD, R., RACKEBRANDT, K., CAZENAVE, J.-P., OHLMANN, P., GACHET, C. & ZIRNGIBL, H. 2001. Long-term antithrombotic protection by in vivo depletion of platelet glycoprotein VI in mice. *The Journal of experimental medicine,* 193**,** 459-470.

NIESWANDT, B. & WATSON, S. P. 2003. Platelet-collagen interaction: is GPVI the central receptor? *Blood,* 102**,** 449-461.

NOÉ, L., DI MICHELE, M., GIETS, E., THYS, C., WITTEVRONGEL, C., DE VOS, R., OVERBERGH, L., WAELKENS, E., JAEKEN, J. & VAN GEET, C. 2010. Platelet Gs hypofunction and abnormal morphology resulting from a heterozygous RGS2 mutation. *Journal of Thrombosis and Haemostasis,* 8**,** 1594-1603.

O'GORMAN, W. E., DOOMS, H., THORNE, S. H., KUSWANTO, W. F., SIMONDS, E. F., KRUTZIK, P. O., NOLAN, G. P. & ABBAS, A. K. 2009. The initial phase of an immune

response functions to activate regulatory T cells. *The Journal of Immunology,* 183**,** 332-339.

O'GORMAN, W. E., SAMPATH, P., SIMONDS, E. F., SIKORSKI, R., O'MALLEY, M., KRUTZIK, P. O., CHEN, H., PANCHANATHAN, V., CHAUDHRI, G. & KARUPIAH, G. 2010. Alternate mechanisms of initial pattern recognition drive differential immune responses to related poxviruses. *Cell host & microbe,* 8**,** 174-185.

OBERGFELL, A., JUDD, B. A., DEL POZO, M. A., SCHWARTZ, M. A., KORETZKY, G. A. & SHATTIL, S. J. 2001. The molecular adapter SLP-76 relays signals from platelet integrin αIIbβ3 to the actin cytoskeleton. *Journal of Biological Chemistry,* 276**,** 5916-5923.

OBERPRIELER, N. G., LEMEER, S., KALLAND, M. E., TORGERSEN, K. M., HECK, A. J. & TASKÉN, K. 2010. High-resolution mapping of prostaglandin E2–dependent signaling networks identifies a constitutively active PKA signaling node in CD8+ CD45RO+ T cells. *Blood,* 116**,** 2253-2265.

OFFERMANNS, S. 2006. Activation of platelet function through G protein–coupled receptors. *Circulation research,* 99**,** 1293-1304.

OFFERMANNS, S., LAUGWITZ, K.-L., SPICHER, K. & SCHULTZ, G. 1994. G proteins of the G12 family are activated via thromboxane A2 and thrombin receptors in human platelets. *Proceedings of the National Academy of Sciences,* 91**,** 504-508.

OFFERMANNS, S., TOOMBS, C. F., HU, Y.-H. & SIMON, M. I. 1997. Defective platelet activation in Gαq-deficient mice. *Nature,* 389**,** 183-186.

OHLMANN, P., LAUGWITZ, K., NURNBERG, B., SPICHER, K., SCHULTZ, G., CAZENAVE, J. & GACHET, C. 1995. The human platelet ADP receptor activates Gi2 proteins. *Biochem. J,* 312**,** 775-779.

PALABRICA, T., LOBB, R., FURIE, B. C., ARONOVITZ, M., BENJAMIN, C., HSU, Y.-M., SAJER, S. A. & FURIE, B. 1992. Leukocyte accumulation promoting fibrin deposition is mediated in vivo by P-selectin on adherent platelets.

PASQUET, J., BOBE, R., GROSS, B., GRATACAP, M., TOMLINSON, M., PAYRASTRE, B. & WATSON, S. 1999. A collagen-related peptide regulates phospholipase Cγ2 via phosphatidylinositol 3-kinase in human platelets. *Biochem. J,* 342**,** 171-177.

PATEL, S. R., HARTWIG, J. H. & ITALIANO, J. E. 2005. The biogenesis of platelets from megakaryocyte proplatelets. *The Journal of clinical investigation,* 115**,** 3348-3354.

PEARCE, A. C., SENIS, Y. A., BILLADEAU, D. D., TURNER, M., WATSON, S. P. & VIGORITO, E. 2004. Vav1 and vav3 have critical but redundant roles in mediating platelet activation by collagen. *Journal of Biological Chemistry,* 279**,** 53955-53962.

PEARSON, R. & KEMP, B. 1991. Protein kinase phosphorylation site sequences and consensus specificity motifs: tabulations. *Methods in enzymology,* 200**,** 62.

PFEIFER, A., RUTH, P., DOSTMANN, W., SAUSBIER, M., KLATT, P. & HOFMANN, F. 1999. Structure and function of cGMP-dependent protein kinases. *Reviews of Physiology, Biochemistry and Pharmacology, Volume 135.* Springer.

PHILLIPS, D. R., PRASAD, K. S., MANGANELLO, J., BAO, M. & NANNIZZI-ALAIMO, L. 2001. Integrin tyrosine phosphorylation in platelet signaling. *Current opinion in cell biology,* 13**,** 546-554.

PIGAZZI, A., HEYDRICK, S., FOLLI, F., BENOIT, S., MICHELSON, A. & LOSCALZO, J. 1999. Nitric oxide inhibits thrombin receptor-activating peptide-induced phosphoinositide 3-kinase activity in human platelets. *Journal of Biological Chemistry,* 274**,** 14368-14375.

PITCHFORD, S. C., YANO, H., LEVER, R., RIFFO-VASQUEZ, Y., CIFERRI, S., ROSE, M. J., GIANNINI, S., MOMI, S., SPINA, D. & O'CONNOR, B. 2003. Platelets are essential for leukocyte recruitment in allergic inflammation. *Journal of allergy and clinical immunology,* 112**,** 109-118.

PODZUWEIT, T., NENNSTIEL, P. & MÜLLER, A. 1995. Isozyme selective inhibition of cGMP-stimulated cyclic nucleotide phosphodiesterases by erythro-9-(2-hydroxy-3-nonyl) adenine. *Cellular signalling,* 7**,** 733-738.

POLLARD, T. D., BLANCHOIN, L. & MULLINS, R. D. 2000. Molecular mechanisms controlling actin filament dynamics in nonmuscle cells. *Annual review of biophysics and biomolecular structure,* 29**,** 545-576.

POOLE, A., GIBBINS, J., TURNER, M., VAN VUGT, M., VAN DE WINKEL, J., SAITO, T., TYBULEWICZ, V. & WATSON, S. 1997. The Fc receptor γ-chain and the tyrosine kinase Syk are essential for activation of mouse platelets by collagen. *The EMBO Journal,* 16**,** 2333-2341.

QUEK, L. S., PASQUET, J.-M., HERS, I., CORNALL, R., KNIGHT, G., BARNES, M., HIBBS, M. L., DUNN, A. R., LOWELL, C. A. & WATSON, S. P. 2000. Fyn and Lyn phosphorylate the Fc receptor γ chain downstream of glycoprotein VI in murine platelets, and Lyn regulates a novel feedback pathway. *Blood,* 96**,** 4246-4253.

QUINTON, T. M. & DEAN, W. L. 1992. Cyclic AMP-dependent phosphorylation of the inositol-1, 4, 5-trisphosphate receptor inhibits Ca< sup> 2+</sup> release from platelet membranes. *Biochemical and biophysical research communications,* 184**,** 893-899.

RASLAN, Z. & NASEEM, K. M. 2014. The control of blood platelets by cAMP signalling. *Biochemical Society transactions,* 42**,** 289-294.

REID, H. M. & KINSELLA, B. T. 2003. The α, but Not the β, Isoform of the Human Thromboxane A2 Receptor Is a Target for Nitric Oxide-mediated Desensitization INDEPENDENT MODULATION OF TPα SIGNALING BY NITRIC OXIDE AND PROSTACYCLIN. *Journal of Biological Chemistry,* 278**,** 51190-51202.

REINHARD, M., JARCHAU, T. & WALTER, U. 2001. Actin-based motility: stop and go with Ena/VASP proteins. *Trends in biochemical sciences,* 26**,** 243-249.

RIBA, R., PATEL, B., ABURIMA, A. & NASEEM, K. 2008. Globular adiponectin increases cGMP formation in blood platelets independently of nitric oxide. *Journal of Thrombosis and Haemostasis,* 6**,** 2121-2131.

RICHARDSON, J. L., SHIVDASANI, R. A., BOERS, C., HARTWIG, J. H. & ITALIANO, J. E. 2005. Mechanisms of organelle transport and capture along proplatelets during platelet production. *Blood,* 106**,** 4066-4075.

RITTENHOUSE, S. E. 1996. Phosphoinositide 3-kinase activation and platelet function. *Blood,* 88**,** 4401-4414.

RIZZO, V., MCINTOSH, D. P., OH, P. & SCHNITZER, J. E. 1998. In situ flow activates endothelial nitric oxide synthase in luminal caveolae of endothelium with rapid caveolin dissociation and calmodulin association. *Journal of Biological Chemistry,* 273**,** 34724-34729.

ROTTERDAM ESHRE/ASRM-SPONSORED PCOS CONSENSUS WORKSHOP GROUP, T. 2004. Revised 2003 consensus on diagnostic criteria and long-term health risks related to polycystic ovary syndrome (PCOS). *Human reproduction (Oxford, England),* 19**,** 41.

ROWLEY, J. W., OLER, A. J., TOLLEY, N. D., HUNTER, B. N., LOW, E. N., NIX, D. A., YOST, C. C., ZIMMERMAN, G. A. & WEYRICH, A. S. 2011. Genome-wide RNA-seq analysis of human and mouse platelet transcriptomes. *Blood,* 118**,** e101-e111.

RUGGERI, Z. M. 2002. Platelets in atherothrombosis. *Nature medicine,* 8**,** 1227-1234.

RUGGERI, Z. M. & MENDOLICCHIO, G. L. 2007. Adhesion mechanisms in platelet function. *Circulation research,* 100**,** 1673-1685.

RUSSO, I., TRAVERSA, M., BONOMO, K., DE SALVE, A., MATTIELLO, L., DEL MESE, P., DORONZO, G., CAVALOT, F., TROVATI, M. & ANFOSSI, G. 2009. In central obesity, weight loss restores platelet sensitivity to nitric oxide and prostacyclin. *Obesity,* 18**,** 788-797.

SACHS, U. J. & NIESWANDT, B. 2007. In vivo thrombus formation in murine models. *Circulation research,* 100**,** 979-991.

SANTORO, S. A. 1986. Identification of a 160,000 dalton platelet membrane protein that mediates the initial divalent cation-dependent adhesion of platelets to collagen. *Cell,* 46**,** 913-920.

SANTOSO, S., SACHS, U. J., KROLL, H., LINDER, M., RUF, A., PREISSNER, K. T. & CHAVAKIS, T. 2002. The junctional adhesion molecule 3 (JAM-3) on human platelets is a counterreceptor for the leukocyte integrin Mac-1. *The Journal of experimental medicine,* 196**,** 679-691.

SAVAGE, B., GINSBERG, M. H. & RUGGERI, Z. M. 1999. Influence of fibrillar collagen structure on the mechanisms of platelet thrombus formation under flow. *Blood,* 94**,** 2704-2715.

SAVI, P., PFLIEGER, A. & HERBERT, J. 1996. cAMP is not an important messenger for ADP-induced platelet aggregation. *Blood coagulation & fibrinolysis,* 7**,** 249-252.

SCHÄFER, A., WIESMANN, F., NEUBAUER, S., EIGENTHALER, M., BAUERSACHS, J. & CHANNON, K. M. 2004. Rapid regulation of platelet activation in vivo by nitric oxide. *Circulation,* 109**,** 1819-1822.

SCHWAPPACHER, R., RANGASWAMI, H., SU-YUO, J., HASSAD, A., SPITLER, R. & CASTEEL, D. E. 2013. cGMP-dependent protein kinase Iβ regulates breast cancer cell migration and invasion via interaction with the actin/myosin-associated protein caldesmon. *Journal of Cell Science,* 126**,** 1626-1636.

SCHWARZ, U. R., GEIGER, J., WALTER, U. & EIGENTHALER, M. 1999a. Flow cytometry analysis of intracellular VASP phosphorylation for the assessment of activating and inhibitory signal transduction pathways in human platelets-definition and detection of ticlopidine/clopidogrel effects. *THROMBOSIS AND HAEMOSTASIS-STUTTGART-,* 82**,** 1145-1152.

SCHWARZ, U. R., GEIGER, J., WALTER, U. & EIGENTHALER, M. 1999b. Flow cytometry analysis of intracellular VASP phosphorylation for the assessment of activating and inhibitory signal transduction pathways in human platelets-definition and detection of ticlopidine/clopidogrel effects. *Thrombosis and Haemostasis,* 82**,** 1145-1152.

SCHWARZ, U. R., WALTER, U. & EIGENTHALER, M. 2001. Taming platelets with cyclic nucleotides. *Biochemical pharmacology,* 62**,** 1153-1161.

SCHWENEKER, M., FAVRE, D., MARTIN, J. N., DEEKS, S. G. & MCCUNE, J. M. 2008. HIV-induced changes in T cell signaling pathways. *The Journal of Immunology,* 180**,** 6490-6500.

SEAMON, K. & DALY, J. 1980. Forskolin: a unique diterpene activator of cyclic AMP-generating systems. *Journal of cyclic nucleotide research,* 7**,** 201-224.

SESSA, W. C. 2004. eNOS at a glance. *Journal of Cell Science,* 117**,** 2427-2429.

SETTE, C. & CONTI, M. 1996. Phosphorylation and Activation of a cAMP-specific Phosphodiesterase by the cAMP-dependent Protein Kinase INVOLVEMENT OF SERINE 54 IN THE ENZYME ACTIVATION. *Journal of Biological Chemistry,* 271**,** 16526-16534.

SHACHAF, C. M., PEREZ, O. D., YOUSSEF, S., FAN, A. C., ELCHURI, S., GOLDSTEIN, M. J., SHIRER, A. E., SHARPE, O., CHEN, J. & MITCHELL, D. J. 2007. Inhibition of HMGcoA reductase by atorvastatin prevents and reverses MYC-induced lymphomagenesis. *Blood,* 110**,** 2674-2684.

SHATTIL, S. J., CUNNINGHAM, M. & HOXIE, J. A. 1987. Detection of activated platelets in whole blood using activation-dependent monoclonal antibodies and flow cytometry. *Blood,* 70**,** 307-315.

SIESS, W. 1989. Molecular mechanisms of platelet activation. *Physiological Reviews,* 69**,** 58-178.

SIESS, W., WINEGAR, D. A. & LAPETINA, E. G. 1990. Rap1-B is phosphorylated by protein kinase A in intact human platelets. *Biochemical and biophysical research communications,* 170**,** 944-950.

SIMON, D. I., CHEN, Z., XU, H., LI, C. Q., DONG, J.-F., MCINTIRE, L. V., BALLANTYNE, C. M., ZHANG, L., FURMAN, M. I. & BERNDT, M. C. 2000. Platelet glycoprotein Ibα is a counterreceptor for the leukocyte integrin Mac-1 (CD11b/CD18). *The Journal of experimental medicine,* 192**,** 193-204.

SKÅLHEGG, B. & TASKEN, K. 2000. Specificity in the cAMP/PKA signaling pathway. Differential expression, regulation, and subcellular localization of subunits of PKA. *Front Biosci,* 5**,** D678-D693.

SKÅLHEGG, B. S., TASKEN, K., HANSSON, V., HUITFELDT, H. S., JAHNSEN, T. & LEA, T. 1994. Location of cAMP-dependent protein kinase type I with the TCR-CD3 complex. *Science,* 263**,** 84-87.

SMYTH, S. S., REIS, E. D., ZHANG, W., FALLON, J. T., GORDON, R. E. & COLLER, B. S. 2001. β3-Integrin–Deficient Mice but Not P-Selectin–Deficient Mice Develop Intimal Hyperplasia After Vascular Injury Correlation With Leukocyte Recruitment to Adherent Platelets 1 Hour After Injury. *Circulation,* 103**,** 2501-2507.

STAATZ, W. D., RAJPARA, S. M., WAYNER, E. A., CARTER, W. G. & SANTORO, S. A. 1989. The membrane glycoprotein Ia-IIa (VLA-2) complex mediates the Mg++-dependent adhesion of platelets to collagen. *The Journal of cell biology,* 108**,** 1917-1924.

STASCH, J.-P., PACHER, P. & EVGENOV, O. V. 2011. Soluble guanylate cyclase as an emerging therapeutic target in cardiopulmonary disease. *Circulation,* 123**,** 2263-2273.

STENBERG, P. E., SHUMAN, M. A., LEVINE, S. P. & BAINTON, D. F. 1984. Redistribution of alpha-granules and their contents in thrombin-stimulated platelets. *The Journal of cell biology,* 98**,** 748-760.

STITZ, J., KRUTZIK, P. & NOLAN, G. 2005. Screening of retroviral cDNA libraries for factors involved in protein phosphorylation in signaling cascades. *Nucleic acids research,* 33**,** e39-e39.

SUN, G., RAMDAS, L., WANG, W., VINCI, J., MCMURRAY, J. & BUDDE, R. J. 2002. Effect of autophosphorylation on the catalytic and regulatory properties of protein tyrosine kinase Src. *Archives of biochemistry and biophysics,* 397**,** 11-17.

SUN, T., RODRIGUEZ, M. & KIM, L. 2009. Glycogen synthase kinase 3 in the world of cell migration. *Development, growth & differentiation,* 51**,** 735-742.

SURKS, H. K., MOCHIZUKI, N., KASAI, Y., GEORGESCU, S. P., TANG, K. M., ITO, M., LINCOLN, T. M. & MENDELSOHN, M. E. 1999. Regulation of myosin phosphatase by a specific interaction with cGMP-dependent protein kinase Iα. *Science,* 286**,** 1583-1587.

SUZUKI-INOUE, K., TULASNE, D., SHEN, Y., BORI-SANZ, T., INOUE, O., JUNG, S. M., MOROI, M., ANDREWS, R. K., BERNDT, M. C. & WATSON, S. P. 2002. Association of Fyn and Lyn with the proline-rich domain of glycoprotein VI regulates intracellular signaling. *Journal of Biological Chemistry,* 277**,** 21561-21566.

TANG, W.-J. & HURLEY, J. H. 1998. Catalytic mechanism and regulation of mammalian adenylyl cyclases. *Molecular pharmacology,* 54**,** 231-240.

TANG, W., ZHANG, Y., XU, W., HARDEN, T. K., SONDEK, J., SUN, L., LI, L. & WU, D. 2011. A PLCβ/PI3Kγ-GSK3 signaling pathway regulates cofilin phosphatase slingshot2 and neutrophil polarization and chemotaxis. *Developmental cell,* 21**,** 1038-1050.

TASKÉN, K. & AANDAHL, E. M. 2004. Localized effects of cAMP mediated by distinct routes of protein kinase A. *Physiological Reviews,* 84**,** 137-167.

TASKÉN, K. A., COLLAS, P., KEMMNER, W. A., WITCZAK, O., CONTI, M. & TASKÉN, K. 2001. Phosphodiesterase 4D and protein kinase a type II constitute a signaling unit in the centrosomal area. *Journal of Biological Chemistry,* 276**,** 21999-22002.

TATESON, J., MONCADA, S. & VANE, J. 1977. Effects of prostacyclin (PGX) on cyclic AMP concentrations in human platelets. *Prostaglandins,* 13**,** 389-397.

TAUSSIG, R., TANG, W.-J., HEPLER, J. R. & GILMAN, A. G. 1994. Distinct patterns of bidirectional regulation of mammalian adenylyl cyclases. *Journal of Biological Chemistry,* 269**,** 6093-6100.

TERTYSHNIKOVA, S. & FEIN, A. 1998. Inhibition of inositol 1, 4, 5-trisphosphate-induced Ca2+ release by cAMP-dependent protein kinase in a living cell. *Proceedings of the National Academy of Sciences,* 95**,** 1613-1617.

THAULOW, E., ERIKSSEN, J., SANDVIK, L., STORMORKEN, H. & COHN, P. F. 1991. Blood platelet count and function are related to total and cardiovascular death in apparently healthy men. *Circulation,* 84**,** 613-617.

THOMAS, C., MORAGA, I., LEVIN, D., KRUTZIK, P. O., PODOPLELOVA, Y., TREJO, A., LEE, C., YARDEN, G., VLECK, S. E. & GLENN, J. S. 2011. Structural linkage between ligand discrimination and receptor activation by type I interferons. *Cell,* 146**,** 621-632.

TILNEY, L. G., BONDER, E. M. & DEROSIER, D. J. 1981. Actin filaments elongate from their membrane-associated ends. *The Journal of cell biology,* 90**,** 485-494.

TOTANI, L. & EVANGELISTA, V. 2010. Platelet–leukocyte interactions in cardiovascular disease and beyond. *Arteriosclerosis, thrombosis, and vascular biology,* 30**,** 2357-2361.

TSAI, A.-L., HSU, M.-J., PATSCH, W. & WU, K. K. 1991. Regulation of PGI2 activity by serum proteins: serum albumin but not high density lipoprotein is the PGI2 binding and stabilizing protein in human blood. *Biochimica et Biophysica Acta (BBA)-General Subjects,* 1115**,** 131-140.

TSCHOEPE, D., ROESEN, P., KAUFMANN, L., SCHAUSEIL, S., KEHREL, B., OSTERMANN, H. & GRIES, F. 1990. Evidence for abnormal platelet glycoprotein expression in diabetes mellitus. *European journal of clinical investigation,* 20**,** 166-170.

TURKO, I., FRANCIS, S. & CORBIN, J. 1998. Binding of cGMP to both allosteric sites of cGMP-binding cGMP-specific phosphodiesterase (PDE5) is required for its phosphorylation. *The Biochemical journal,* 329**,** 505-510.

VAN GEET, C., IZZI, B., LABARQUE, V. & FRESON, K. 2009. Human platelet pathology related to defects in the G-protein signaling cascade. *Journal of Thrombosis and Haemostasis,* 7**,** 282-286.

VAN METER, M. E., DÍAZ-FLORES, E., ARCHARD, J. A., PASSEGUÉ, E., IRISH, J. M., KOTECHA, N., NOLAN, G. P., SHANNON, K. & BRAUN, B. S. 2007. K-RasG12D expression induces hyperproliferation and aberrant signaling in primary hematopoietic stem/progenitor cells. *Blood,* 109**,** 3945-3952.

VARGA-SZABO, D., BRAUN, A. & NIESWANDT, B. 2009. Calcium signaling in platelets. *Journal of Thrombosis and Haemostasis,* 7**,** 1057-1066.

VON HUNDELSHAUSEN, P., PETERSEN, F. & BRANDT, E. 2007. Platelet-derived chemokines in vascular biology. *THROMBOSIS AND HAEMOSTASIS-STUTTGART-,* 97**,** 704.

VU, T.-K. H., HUNG, D. T., WHEATON, V. I. & COUGHLIN, S. R. 1991. Molecular cloning of a functional thrombin receptor reveals a novel proteolytic mechanism of receptor activation. *Cell,* 64**,** 1057-1068.

WAGNER, D. D. & BURGER, P. C. 2003. Platelets in inflammation and thrombosis. *Arteriosclerosis, thrombosis, and vascular biology,* 23**,** 2131-2137.

WALL, M. E., FRANCIS, S. H., CORBIN, J. D., GRIMES, K., RICHIE-JANNETTA, R., KOTERA, J., MACDONALD, B. A., GIBSON, R. R. & TREWHELLA, J. 2003. Mechanisms associated with cGMP binding and activation of cGMP-dependent protein kinase. *Proceedings of the National Academy of Sciences,* 100**,** 2380-2385.

WALTER, U., EIGENTHALER, M., GEIGER, J. & REINHARD, M. 1993. Role of cyclic nucleotide-dependent protein kinases and their common substrate VASP in the regulation of human platelets. *Mechanisms of Platelet Activation and Control.* Springer.

WANG, H.-B., WANG, J.-T., ZHANG, L., GENG, Z. H., XU, W.-L., XU, T., HUO, Y., ZHU, X., PLOW, E. F. & CHEN, M. 2007. P-selectin primes leukocyte integrin activation during inflammation. *Nature immunology,* 8**,** 882-892.

WARDELL, M. R., REYNOLDS, C., BERNDT, M., WALLACE, R. & FOX, J. 1989. Platelet glycoprotein Ib beta is phosphorylated on serine 166 by cyclic AMP-dependent protein kinase. *Journal of Biological Chemistry,* 264**,** 15656-15661.

WATSON, S., AUGER, J., MCCARTY, O. & PEARCE, A. 2005. GPVI and integrin αIIbβ3 signaling in platelets. *Journal of Thrombosis and Haemostasis,* 3**,** 1752-1762.

WAYMAN, G. A., IMPEY, S. & STORM, D. R. 1995. Ca2+ inhibition of type III adenylyl cyclase in vivo. *Journal of Biological Chemistry,* 270**,** 21480-21486.

WEDEL, B., HARTENECK, C., FOERSTER, J., FRIEBE, A., SCHULTZ, G. & KOESLING, D. 1995. Functional domains of soluble guanylyl cyclase. *Journal of Biological Chemistry,* 270**,** 24871-24875.

WEDEL, B., HUMBERT, P., HARTENECK, C., FOERSTER, J., MALKEWITZ, J., BÖHME, E., SCHULTZ, G. & KOESLING, D. 1994. Mutation of His-105 in the beta 1 subunit yields a nitric oxide-insensitive form of soluble guanylyl cyclase. *Proceedings of the National Academy of Sciences,* 91**,** 2592-2596.

WEHMEIER, A., TSCHÖPE, D., ESSER, J., MENZEL, C., NIEUWENHUIS, H. & SCHNEIDER, W. 1991. Circulating activated platelets in myeloproliferative disorders. *Thrombosis research,* 61**,** 271-278.

WEI, J., WAYMAN, G. & STORM, D. R. 1996. Phosphorylation and inhibition of type III adenylyl cyclase by calmodulin-dependent protein kinase II in vivo. *Journal of Biological Chemistry,* 271**,** 24231-24235.

WEKSLER, B. B., MARCUS, A. J. & JAFFE, E. A. 1977. Synthesis of prostaglandin I2 (prostacyclin) by cultured human and bovine endothelial cells. *Proceedings of the National Academy of Sciences,* 74**,** 3922-3926.

WHITE, J. G. 1970. A search for the platelet secretory pathway using electron dense tracers. *The American journal of pathology,* 58**,** 31.

WHITE, J. G. 2012. Platelet Structure. *Platelets***,** 117.

WILLOUGHBY, D. & COOPER, D. M. 2007. Organization and Ca2+ regulation of adenylyl cyclases in cAMP microdomains. *Physiological Reviews,* 87**,** 965-1010.

WILSON, L. S., ELBATARNY, H. S., CRAWLEY, S. W., BENNETT, B. M. & MAURICE, D. H. 2008. Compartmentation and compartment-specific regulation of PDE5 by protein kinase G allows selective cGMP-mediated regulation of platelet functions. *Proceedings of the National Academy of Sciences,* 105**,** 13650-13655.

WONEROW, P., OBERGFELL, A., WILDE, J., BOBE, R., ASAZUMA, N., BRDICKA, T., LEO, A., SCHRAVEN, B., HOREJSÍ, V. & SHATTIL, S. 2002. Differential role of glycolipid-enriched membrane domains in glycoprotein VI-and integrin-mediated phospholipase Cγ2 regulation in platelets. *Biochem. J,* 364**,** 755-765.

WONEROW, P., PEARCE, A. C., VAUX, D. J. & WATSON, S. P. 2003. A critical role for phospholipase Cγ2 in αIIbβ3-mediated platelet spreading. *Journal of Biological Chemistry,* 278**,** 37520-37529.

WONG, W. & SCOTT, J. D. 2004. AKAP signalling complexes: focal points in space and time. *Nature reviews Molecular cell biology,* 5**,** 959-970.

WOODSIDE, D. G., OBERGFELL, A., LENG, L., WILSBACHER, J. L., MIRANTI, C. K., BRUGGE, J. S., SHATTIL, S. J. & GINSBERG, M. H. 2001. Activation of Syk protein tyrosine kinase through interaction with integrin β cytoplasmic domains. *Current biology,* 11**,** 1799-1804.

WU, Y., ASAZUMA, N., SATOH, K., YATOMI, Y., TAKAFUTA, T., BERNDT, M. C. & OZAKI, Y. 2003. Interaction between von Willebrand factor and glycoprotein Ib activates Src kinase in human platelets: role of phosphoinositide 3–kinase. *Blood,* 101**,** 3469-3476.

WU, Z., WONG, S. T. & STORMS, D. 1993. Modification of the calcium and calmodulin sensitivity of the type I adenylyl cyclase by mutagenesis of its calmodulin binding domain. *Journal of Biological Chemistry,* 268**,** 23766-23768.

YAN, S.-Z., HUANG, Z.-H., RAO, V. D., HURLEY, J. H. & TANG, W.-J. 1997. Three discrete regions of mammalian adenylyl cyclase form a site for Gsα activation. *Journal of Biological Chemistry,* 272**,** 18849-18854.

YOSHIMURA, M. & COOPER, D. 1992. Cloning and expression of a Ca (2+)-inhibitable adenylyl cyclase from NCB-20 cells. *Proceedings of the National Academy of Sciences,* 89**,** 6716-6720.

YOSHIOKA, A., SHIRAKAWA, R., NISHIOKA, H., TABUCHI, A., HIGASHI, T., OZAKI, H., YAMAMOTO, A., KITA, T. & HORIUCHI, H. 2001. Identification of protein kinase Cα as an essential, but not sufficient, cytosolic factor for Ca2+-induced α-and dense-core granule secretion in platelets. *Journal of Biological Chemistry,* 276**,** 39379-39385.

YUAN, Y., KULKARNI, S., ULSEMER, P., CRANMER, S. L., YAP, C. L., NESBITT, W. S., HARPER, I., MISTRY, N., DOPHEIDE, S. M. & HUGHAN, S. C. 1999. The von Willebrand factor-glycoprotein Ib/V/IX interaction induces actin polymerization and cytoskeletal reorganization in rolling platelets and glycoprotein Ib/V/IX-transfected cells. *Journal of Biological Chemistry,* 274**,** 36241-36251.

ZABEL, U., KLEINSCHNITZ, C., OH, P., NEDVETSKY, P., SMOLENSKI, A., MÜLLER, H., KRONICH, P., KUGLER, P., WALTER, U. & SCHNITZER, J. E. 2002. Calcium-dependent membrane association sensitizes soluble guanylyl cyclase to nitric oxide. *Nature cell biology,* 4**,** 307-311.

ZAHEDI, R. P., LEWANDROWSKI, U., WIESNER, J., WORTELKAMP, S., MOEBIUS, J., SCHÜTZ, C., WALTER, U., GAMBARYAN, S. & SICKMANN, A. 2007. Phosphoproteome of resting human platelets. *Journal of proteome research,* 7**,** 526-534.

ZHANG, J., CHUNG, T. & OLDENBURG, K. 1999. A Simple Statistical Parameter for Use in Evaluation and Validation of High Throughput Screening Assays. *Journal of biomolecular screening,* 4**,** 67.

ZHANG, W. & COLMAN, R. W. 2007. Thrombin regulates intracellular cyclic AMP concentration in human platelets through phosphorylation/activation of phosphodiesterase 3A. *Blood,* 110**,** 1475-1482.

ZHU, Y., O'NEILL, S., SAKLATVALA, J., TASSI, L. & MENDELSOHN, M. E. 1994. Phosphorylated HSP27 associates with the activation-dependent cytoskeleton in human platelets. *Blood,* 84**,** 3715-3723.